SUPRAMOLECULAR SELF-ASSEMBLED NANOSTRUCTURES BASED ON STAR POLYMERS FOR DRUG AND GENE DELIVERY

LI JIAJING

(*B.Eng., Sichuan University of China*)

A THESIS SUBMITTED

FOR THE DEGREE OF DOCTOR OF PHILOSOPHY

DEPARTMENT OF BIOENGINEERING

NATIONAL UNIVERSITY OF SINGAPORE

2012

ACKNOWLEDGEMENTS

First and foremost I would like to express my utmost gratitude and appreciation to my supervisor, Professor Li Jun, for his constant guidance, motivation, encouragement and patience given to me throughout my whole research. His insight, genius and passion to research, which impressed me deeply, has been my greatest motivation in my research and will be always influence in my future life. His critical comments have promoted and enriched my research ability, and also triggered and nourished my intellectual maturity. Without his consistent, patient and invaluable guiding, the completion of my research could not be possible. I am really grateful to his directions.

I would like to thank Dr. Evelyn Yim and Dr. Huang Zhiwei, who served as my oral qualification examiners and provided me useful comments on my research. Moreover, I would like to thank the National University of Singapore and the Department of Bioengineering for offering a Research Scholarship to me, so that I could successfully complete my research and gain overseas research experience.

I would also like to express my sincere appreciation to all the members in Supramolecular Biomaterials Laboratory, past and present, for their friendship,

continuous kind help and useful advices throughout my research. With all of them, I have experienced a wonderful and memorable post-graduate life. Thanks go in particular to the members in our group: Dr. Wu Yunlong, Ping Yuan, Yin Hui, Zhu Jingling, Liu Chengde, She Zhen, Zhao Feng, Li Zibiao, and Wen Yuting who gave me great helps in my research. And I also appratiate the seniors in IMRE: Dr. Loh Xian Jun, Dr. Zhang Zhong-Xing, Dr. Liu Kerh Li and Ms Ni Xiping for their kind help. Thank you very much!

Last, but no least, my deepest appreciation goes to my family, my parents and my boyfriend, Kelei, for their expectation, understanding, encouragement, and warm support during my academic career. I would not have been able to complete this without them. Thank you!

TABLE OF CONTENTS

SUMMARY

Cyclodextrins (CDs) are a series of cyclic oligosaccharides composed of 6, 7, or 8 D (+)-gluCOSe units linked by α-1,4-linkages and named α-, β-, or γ-CD, respectively. Since the first synthesis of polyrotaxane with multiple α-CD rings threaded around a polymer chain, CD-based polypseudorotaxanes and polyrotaxanes have been receiving increasing attention due to their intriguing supramolecular architecture of sliding/dethreading and promising bio-applications. The objective of this research was to develop a novel core-shell nanostructures self-assembled from star polyrotaxanes, based on star PEG, α-CD, end blocking group with biodegradable linkage and cationic polymers, and to investigate the feasibility of their applications to biomedical areas such as drug delivery and gene delivery.

This thesis is divided into five parts. In the first part, we present a literature review of drug and gene delivery systems, their developments and challenges, followed by a brief summary of recent promising structures as delivery vectors, such as core-shell nanostructure (e.g. polymeric micelles), CD-based supramolecular structures and environmentally sensitive vectors.

Summary

In the second part, we demonstrate a supramolecular approach for creating biodegradable star polyrotaxane (SPR) by controlled threading of α-CD onto star PEG and end blocked with enzyme-triggered degradable linkage. The resulting polyrotaxane could further self-assembled into nanoparticles with hydrophilic PEG shell and polyrotaxane core. The core-shell nanoaggregates showed high capacity for DOX loading with sustained *in vitro* release for more than 2 months. Furthermore, owning to the CD dethreading nature and biodegradable linkage, the SPR nanostructure showed enzyme-responsible release properties, which would be beneficial to controlled drug delivery.

In order to meet the conflicting requirements of an ideal drug delivery system, disulfide-linkage was introduced on above SPR core-shell nanostructure for reduction-sensitive drug delivery. The reduction sensitive properties of the polyrotaxanes were confirmed. Furthermore, DOX loaded nano-particles exhibited sustained *in vitro* release profile within 30 days even in the presence of DTT, which could be important for intravenous delivery to prolong therapeutic effect and reduce cardiotoxicity. In the intracellular study, the biodegradable SPR accomplished much faster internalization, rapid release of DOX inside cells and higher anticancer efficacy as compared to the reduction insensitive control and free DOX.

Besides drug delivery, we also developed a series of disulfide-containing cationic polyrotaxanes as reduction-sensitive gene carriers and investigated their applications in gene delivery. Multiple OEI arms with different chain length were conjugated onto α-CD rings in the polyrotaxane, which is end blocked with disulfide linkage. The degradability and DNA release capability in response to DTT was confirmed. Due to the introduction of disulfide linkage, significant lower *in vitro*

cytotoxicity and higher gene transfection were achieved in contrast to reduction insensitive control and polyethylenimine (PEI) 25k. Furthermore, the hindrance effect of PEG shell allows the system to be stable in salt and protein solution, and thus improve their serum stability.

In the final part, aiming to increase the serum stability and improve the transfection efficiency of PDMAEMA systems with optimal DNA release and decreasing cytotoxicity, another reduction-sensitive gene delivery system was successfully developed based on star polyrotaxanes, which consists of partially threaded α-CD, star PEG and low molecular weight PDMAEMA segments linked to the end of PEG arms with disulfide linkage. This research may be helpful as it creates a new approach to design a reduction-sensitive delivery system, which achieves rapid intracellular release, effective unpacking ability, low cytotoxicity, high transfection efficiency and high stability in biological fluids. Moreover, by taking the advantage of the core-shell nanostructure, we encapsulated DOX into the center of the star cationic polyrotaxane nanoaggregates which could be very promising for the applications in the co-delivery of DNA and anti-cancer drugs by achieving a synergistic effect in suppressing the proliferation of cancer cells.

In sum, a series of supramolecular self-assembled nanostructures were developed and they can be promising in drug and gene delivery due to many advantages, including reduction sensitive degradability, high cell uptake, efficient anti-cancer ability, serum stability and high transfection efficiency with low cytotoxicity and DNA release ability.

LIST OF TABLES

LIST OF FIGURES

LIST OF ABBREVIATIONS

ATRP	Atom Transfer Radical Polymerization
BSA	Bovine Serum Albumin
BSO	D,L-Buthionine sulfoxamine
CD	Cyclodextrin
CDI	1,1′-Carbonyldiimidazole
CAC	Critical Micellization Concentration
DCC	1,3-N,N'-Dicyclohexylcarbodiimide
DCM	Dichloromethane
DDS	Drug Delivery Systems
DLS	Dynamic light scattering
DMAE	2-Dimethyl- aminoethanol
DMAEC	Dimethylaminoethyl
DMAEMA	2-(Dimethylamino) ethyl methacrylate
DMAP	4-(Dimethylamino) pyridine
DMEM	Dulbecco's Modified Eagle's Medium
DMF	Dimethylformamide

List of Abbreviations

DMSO	Dimethyl Sulfoxide
DNA	Deoxyribonucleic Acid
DOX	Doxorubicin
DPH	1,6-diphenyl-1,3,4-hexatriene
DSC	Differntial Scanning Calorimetry
DTT	Dithiothreitol
EDTA	Ethylenediaminetetraacetic acid
EPR	Enhanced Permeability and Retention
FBS	Fetal Bovine Serum
GFP	Green Fluorescence Protein
GSH	Glutathione tripeptide
HMTETA	Hexamethyltriethylenetetramine
IC	Inclusion Complex
IC_{50}	Half maximal inhibitory concentration
MTT	3-(4,5-Dimethylthiazol-2-yl)-2,5-diphenyl Tetrazolium Bromide
MTX	Methotrexate
NaOH	Solution of sodium hydroxide
NHS	Hydroxysuccinimide
NMR	Nuclear Magnetic Resonance
OEI	Oligoethylenimine
PBS	Phosphate Buffered Saline
PCL	Polycaprolactone
PDMAEMA	Poly [(2-dimethylamino) ethyl methacrylate]
PEG	Poly (ethylene glycol)

List of Abbreviations

PEGMA	Poly (ethylene glycol) methyl ether methacrylate
PEI	Poly (ethylene imine)
PEO	Poly (ethylene oxide)
PHB	Poly [(R)-3-hydroxybutyrate]
PLA	Polylactic acid
PLGA	Poly (lactic acid-co-glycolic acid)
PMPC	Poly (methacryloxyloxyethyl phosphorylcholine)
PPA	Polyphosphoramidate
PPO	Poly (propylene oxide)
PPR	Polypseudorotaxanes
PR	Polyrotaxane
RES	Reticuloendothelium system
RLU	Relative luciferase activity
SEC	Size Exclusion Chromatogram
TEA	Triethylamine
TEM	Tranmission Electron Microscopy
TGA	Thermal Gravimetric Analysis
THF	Tetrahydrofuran
TNBS	2,4,6-Trinitrobenzene Sulfonic Acid
Z-L-Phe	N-carbobenzyloxy-L-phenylalanine

CHAPTER 1   INTRODUCTION

This thesis is concerned with some supramolecular self-assembled core-shell nanostructures based on star polyethylene glycol (PEG) and α-cyclodextrin (α-CD) with their promising applications in drug and gene delivery. In this introductory chapter, some background information will be provided, followed by a brief introduction to core-shell systems (e.g. micelle), polyrotaxane and bioreductive systems as a useful tool for the design of functional nanomaterials for biomedical applications, such as drug and gene delivery. Then we will give the scope and objective of our research. Finally, a summary of the contents and organization of this thesis will be presented.

1.1 BACKGROUND INFORMATION

Over the past few decades, drug delivery systems (DDSs) have been developed and studied in great depth to improve the curative effect of drugs [1-3]. In this method, the administered drug is encapsulated within a material that releases the therapeutic in a controlled manner that optimizes the dosage for a specified period of time. DDS can ameliorate the problems of conventional administration by enhancing

drug solubility, prolonging duration time, reducing side effect, retaining drug bioactivity, and so on [4, 5]. For localized treatments, the delivery vehicle is acutely retained at the site of delivery, ensuring the local administration of the therapeutic. For therapeutics that is delivered through the vasculature, the delivery vehicle increases the circulation half-life, and in some cases, targets the therapeutic to a desired tissue. A variety of systems have been used as DDSs, such as vesicles [6-8] , nanoparticles [9, 10], micelles [11, 12], polymer gels [13], alipids [14], etc. At present, stimuli sensitive DDSs have been an attractive theme for controlled release. The release behaviors of drugs can be easily controlled by surrounding properties, such as pH [15] , temperature [16, 17], ionic strength [18] and electric field [19].

In addition to DDS, gene delivery systems are also very attractive as a major concern component of gene therapy. Gene therapy is the insertion of genes into a patient's cells and tissues to treat a disease, such as a hereditary disease in which a deleterious mutant allele is replaced with a functional one [20]. It has drawn a lot of attentions in the field of medicine, pharmaceutical sciences and biotechnology due to the potentials for treating chronic diseases and genetic disorders such as severe combined immunodeficiency [21], cystic fibrosis, and Parkinson's disease [22]. Gene therapy has also been considered as a suitable substitute for conventional protein therapy [23] and chemotherapy [24].

Although many clinical studies were carried out during the last 20 years, the issue of delivery systems has yet to be satisfied. Drug delivery poses great challenges to clinicians everywhere. For example, drugs that are administered by the oral route suffer from losses resulting from first-pass metabolism, reducing the bioavailability of the drug. In these cases, an alternative method of administration is daily intravenous

(IV) infusion. This method, however, increases the risk of infections at the site of administration and could lead to systemic toxicity, as in the case of chemotherapeutic drugs for the treatment of cancer. In the field of gene delivery, the lack of a safe and efficient delivery system is a fundamental obstacle to successful clinical application of gene therapy. Although viral vectors show excellent transfection efficiencies, their association with safety issues such as insertional mutagenesis, immunogenic and inflammatory responses has limited their applications in clinical trials. Because of these concerns, non-viral vectors especially cationic polymers (polycations) have been extensively investigated in the last twenty years, as they can spontaneously condense plasmid DNA (pDNA) into structures small enough to enter cells via endocytosis [25]. However, the main disadvantages of these polycations are their poor transfection efficiency, high toxicity, non-selectivity and *in vivo* instability.

Among various designs on the encapsulation structures, core-shell nanostructures (e.g. polymeric micelles) with smaller sizes (20-100nm) have shown great promise as nanocarriers for efficient drug and gene delivery.[26, 27] Polymeric micelles, which are self-assembled from amphiphilic block copolymers, show distinct stability in solution. The core-shell structure of the micelle can improve solubility of hydrophobic drugs, and protect the incorporated drug from premature degradation [11, 28, 29]. As a nanosize carrier, micelle can easily permeate into the tumor and induce its passive accumulation due to the vascular leakiness and impaired lymphatic drainage in solid tumors, which have been known as the enhanced permeability and retention (EPR) [30, 31]. So the core-shell nanostructures offer the advantages of decreased side effects and improved drug availability. Furthermore, when environmentally sensitive (pH, temperature, enzyme, etc) functional groups are

introduced into these amphiphilic copolymers, "smart" micelles are formed, and they can be used as environmentally controlled drug release system [32-34].

Since the first synthesis of polyrotaxanes with multiple α-CD rings threaded on a polymer [35-37], tremendous interest has been attracted on the studies of these series inclusion complexes and their applications on biomaterials [36-40]. Cyclodextrins (CDs), also known as cycloamyloses, and cyclomaltoses, are a series of natural cyclic oligosaccharides composed of 6, 7, and 8 D (+)-gluCOSe units linked by α-1,4-linkages, and named with α-, β-, and γ-CD, respectively (Fig. 1.1). Polyrotaxane is composed of three elements: the macrocycle wheels, the appropriate axle, and the bulky end-caps on the terminal of axle. According to the fascinating capability of macrocyclic CD rings as host molecules, various guest molecules have been investigated to form inclusion complexes with enhanced physical and biological properties for drug delivery, and to thread into their cavities to create polypseudorotaxanes and polyrotaxanes with controllable size and structure for various functional nanomaterials [37-39, 41-46]

	n	Cavity Size (nm)	Height (nm)
α-CD	6	0.47-0.53	
β-CD	7	0.60-0.65	0.78
γ-CD	8	0.75-0.83	
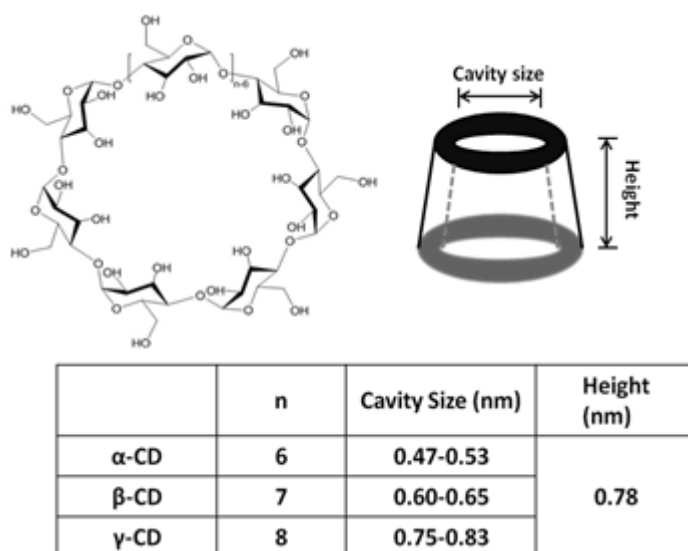
Fig. 1.1 Chemical structure of cyclodextrins with different cavity and height

Because of the properties of the low toxicity, sliding, dethreading and easy to modification, cyclodextrin-based polyrotaxanes and polypseudorotaxanes have inspired interesting and rapid exploitation in life science and biotechnology over the past two decades, including drug delivery and gene delivery [40, 47-49]. Specifically, cyclodextrin-based biodegradable polypseudorotaxane hydrogels could be promising as injectable drug delivery systems for sustained and controlled drug release [50-52]. Polyrotaxanes with drug/ligand-conjugated CDs threaded on a polymer chain with biodegradable end group could be useful for controlled and multivalent targeting delivery due to the mobility of CDs [53, 54]. This kind of polyrotaxane is fascinating and very promising for drug-conjugating delivery due to several unique structural characteristics. Firstly, CDs bear many hydroxyl groups that could be easily modified by chemical reactions, allowing for the conjugation of bioactive agent on the CD rings; Secondly, self-assembled polyrotaxanes display the highly mobility of CDs as a result of the CD rotating around the polymer chain. This flexibility is expected to enhance multivalent ligand-receptor interaction, and is promising for applications such as targeting drugs, drug-mediated drug delivery and tissue engineering [55]. Thirdly, CDs can dethread through the polymer chain when the end is capped through biodegradable linkage, which insures the release of drug into the cell [47].

In the field of gene delivery, based on the design of CD containing polymer with low cytotoxicity [56, 57], a new class of CD-containing gene carriers was developed based on cationic polyrotaxanes where multiple cationic CDs are threaded onto a polymer chain and capped by bulky ends [58-61]. By taking advantage of the CD's ability to slide and rotate along the polymer axle, this system might be able to generate well-matched DNA complexes, and thus accomplish the gene transfection

with a minimum amount of cationic polyrotaxanes. As a result, the cationic supramolecular gene delivery vectors showed good DNA binding ability, low cytotoxicity, and high gene transfection efficacy that is similar to PEI (25K) at the optimized N/P ratio and molecular weight.

In the past decades, reduction-sensitive biodegradable polymers have emerged as an attractive class of biomedical materials as the delivery systems for both biotherapeutics (pDNA, siRNA, peptides and pharmaceutical proteins) as well as low molecular weight drugs. Usually, bio-reducible disulfide linkage was introduced to these materials in the main chain, side chain, or in the cross-linker. The disulfide bonds are subject to rapid degradation under a reductive environment via thiol-disulfide exchange reactions [62]. In eukaryotic cells, glutathione tripeptide (GSH) is the major redox [63]. Under different intracellular environment, GSH maintain distinct and non-equilibrium level [64]. For example, in cell surface or blood fluids, the concentration of GSH is low (approximately 2-20 μM). So the disulfide linkage is sufficiently stable under the conditions in the circulation as well as in extracellular matrices. However, in the cytosol, the disulfide bond may be prone to rapid degradation in minutes to hours due to the high concentration of GSH (0.5-10mM) [65]. Therefore, reduction-sensitive gene carriers in principle could meet the conflicting requirements of an ideal delivery system, i.e. high stability in circulation while rapid degradation inside targeted cells [66].

Therefore, disulfide-containing systems are very attractive for the development of drug and gene delivery. In the cancer therapy, it is often more desirable to accomplish rapid drug release after vectors arriving at the pathological site, which may enhance the therapeutic efficacy as well as reduce the probability of

drug resistance in cells. Due to the stimuli-responsive properties of disulfide linkage, reduction-sensitive polymers have received a tremendous amount of interest for intracellular drug delivery. In gene therapy, the rapid degradation due to the disulfide linkage on the one hand could lead to polyplex dissociation and efficient intracellular release of DNA or siRNA, on the other hand, they may result in low toxicity by avoiding accumulation of high molecular weight polycations inside cells, and finally increasing the transfection efficiency [67].

1.2 OBJECTIVE AND SCOPE OF STUDY

In view of the above review, in spite of many studies on the formation of polypseudorotaxanes and polyrotaxanes reported so far, the application of supramolecular self-assembled core-shell nanostructures in drug and gene delivery system has not been developed sufficiently till now:

(1) Although supramolecular hydrogels and drug-conjugated polyrotaxane have been developed for drug delivery, little is known about the dual self-assembly behavior of polyrotaxane and their application to sustained and reduction-sensitive intracellular drug release;

(2) Non-vial gene carriers are challenged with a set of obstacles before and after entering cells, including stability in biological fluids, stimuli DNA release inside cells, low cytotoxicity and high gene transfection efficiency [68]. Recently, CD-containing gene carriers have been synthesized for gene delivery. However, little research has been done on introduction of disulfide bond and PEG shell with their related supramolecular structures for bioreducible and shell sheddable intracellular gene delivery to improve DNA release ability and

serum tolerance ability, to decrease cytotoxicity and to enhance gene transfection efficiency.

(3) In spite of many studies on poly(2-dimethylamino) ethyl methacrylate) (pDMAEMA) based gene vectors reported so far, there are few studies on bioreducible and shell detachable star polyrotaxane with pDMAEMA, not to mention their self-assembly behaviors and their applications to reduction-sensitive intracellular gene delivery, drug delivery and gene/drug codelivery.

The main aim of this research was to develop a novel core-shell biodegradable nanostructure self-assembled from supramolecular architectures based on star PEG, α-CD and biodegradable linkage, and to investigate the feasibility of their application to biomedical areas such as drug delivery and gene delivery. The specific objectives of the study were:

- To synthesize a novel star polyrotaxane derived from controlled threading of α-CD onto star PEG and to study their dual supramolecular self-assembly behavior, which leads to the formation of core-shell nanostructures, and to explore its potential as a candidate in sustained, stimuli-responsive and efficient anti-cancer drug delivery.

- To design a series of core-shell nanostructures self-assembled from star polyrotaxanes with reduction-sensitive end group, which should be helpful to meet the conflicting requirements of an ideal drug delivery system, i.e. high stability in circulation while rapid degradation inside targeted cells;

- To develop a series of disulfide-containing cationic polyrotaxanes as reduction-sensitive and shell sheddable gene carriers with the aim of

increasing serum stability, facilitating unpacking ability of pDNA or siRNA, decreasing cytotoxicity and improving transfection efficiency.

- To synthesize and evaluate the potential applications of the shell detachable and biocleavable polyrotaxane based on PDMAEMA for redox-responsive gene delivery and further investigate their self-assembly behavior, which may lead to core-shell nanostructures for gene/drug co delivery.

This research should provide a series of new carriers for delivery systems and the results of the present study may extend the applications of these dual supramolecular self-assembled nanostructures to the field of drug and gene delivery. Furthermore, this research should be helpful to create a new approach to design a reduction-sensitive delivery system by introducing disulfide linkage into polyrotaxanes, which could achieve rapid intracellular release, low cytotoxicity, high transfection efficiency and effective unpacking ability.

This thesis mainly focuses on the study of star polyrotaxanes self-assembled nanostructures based on star PEG, α-CD, biodegradable end groups and cationic polymers, such as OEI and pDMAEMA. Other supramolecular structures such as rotaxanes, catenanes and polycatenanes and their applications are not considered. Furthermore, the possibility of using these supramolecular nanoaggregates as carriers in drug delivery and gene therapy was evaluated through *in vitro* experiments. The *in vivo* animal tests of the synthesized materials are very complicated and involve many biological issues, but these are not central of this study and hence are beyond the scope of this study.

1.3 ORGANIZATION OF THE THESIS

Based on the objectives outlined previously, the key is the preparation of novel functional materials for drug and gene delivery. In the following chapters, the detailed research on preparation processes for supramolecular self-assembled nanostructures and their drug and gene delivery capabilities will be reported. Project design and hypothesis are shown in Scheme 1.1. Encompassing the objectives outlined previously, this thesis is divided into the following chapters:
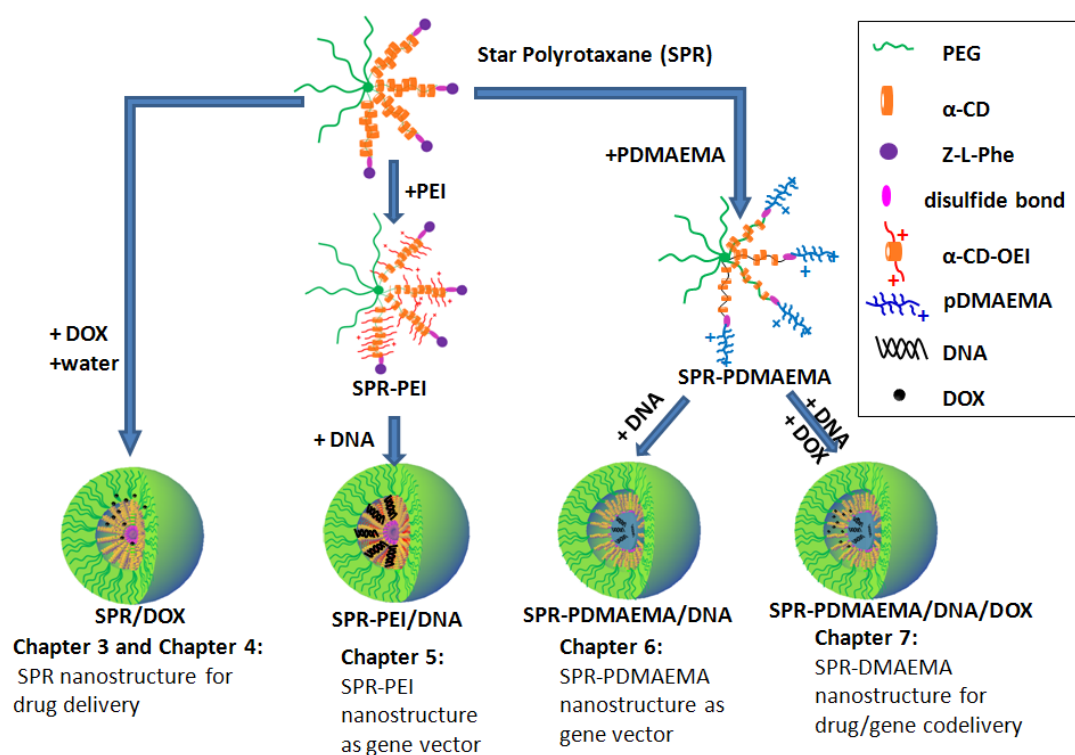
Scheme 1.1 Project design and hypothesis of the thesis

Chapter 2: Literature review on the topic of drug and gene delivery systems, their development and challenges. Brief summary of recent promising materials and structures for drug and gene delivery, such as core-shell nanostructures (e.g. polymeric micelles), CD-based supramolecular structures and environmentally sensitive and biodegradable vectors, was also presented.

Chapter 3: Report on the synthesis of triggered enzymatic biodegradable star polyrotaxanes based on star PEG and α-CD, their dual self-assembly behavior and their applications as drug delivery systems.

Chapter 4: Highlight on the utilization of disulfide bond on the polyrotaxane self-assembled nanostructures for stimuli-responsible drug delivery, which should be helpful to meet the conflicting requirements of an ideal drug delivery system, i.e. high stability in circulation while rapid degradation inside targeted cells;

Chapter 5: Research on the reduction sensitive and shell sheddable gene delivery based on core-shell nanostructures formed by polyrotaxanes with star PEG, oligoethylenimine (OEI) conjugated α-CD and disulfide linkage. This nanostructure was explored as an efficient gene carrier with increasing serum stability, facilitating DNA release ability, low cytotoxicity and high transfection efficiency.

Chapter 6: Demonstration of the application of disulfide linkage and low MW PDMAEMA on polyrotaxanes to form a shell detachable and biocleavable core-shell nanostructures for their promising applications in redox-responsive gene delivery.

Chapter 7: Further exploration on the dual self-assembly behavior of the star reductive polyrotaxanes based on PDMAEMA, which could be very useful as vectors for drug delivery and gene/drug codelivery.

Chapter 8: Conclusion on the work done with possible future endeavours.

1.4 REFERENCES

1. Fundueanu G, Constantin M, Ascenzi P. Preparation and characterization of pH- and temperature-sensitive pullulan microspheres for controlled release of drugs. Biomaterials 2008 Jun;29(18):2767-2775.
2. Huynh DP, Nguyen MK, Pi BS, Kim MS, Chae SY, Kang CL, et al. Functionalized injectable hydrogels for controlled insulin delivery. Biomaterials 2008 Jun;29(16):2527-2534.
3. Wang YC, Liu XQ, Sun TM, Xiong MH, Wang J. Functionalized micelles from block copolymer of polyphosphoester and poly(epsilon-caprolactone) for receptor-mediated drug delivery. Journal of Controlled Release 2008 May;128(1):32-40.
4. Mok H, Park JW, Park TG. Enhanced intracellular delivery of quantum dot and adenovirus nanoparticles triggered by acidic pH via surface charge reversal. Bioconjugate Chemistry 2008 Apr;19(4):797-801.
5. He CL, Kim SW, Lee DS. In situ gelling stimuli-sensitive block copolymer hydrogels for drug delivery. Journal of Controlled Release 2008 May;127(3):189-207.
6. Hou DD, Tong XM, Yu HQ, Zhang AY, Feng ZG. A kind of novel biodegradable hydrogel made from copolymerization of gelatin with polypseudorotaxanes based on alpha-CDs. Biomedical Materials 2007 Sep;2(3):S147-S152.
7. Cerritelli S, Velluto D, Hubbell JA. PEG-SS-PPS: Reduction-sensitive disulfide block copolymer vesicles for intracellular drug delivery. Biomacromolecules 2007 Jun;8(6):1966-1972.
8. Napoli A, Boerakker MJ, Tirelli N, Nolte RJM, Sommerdijk N, Hubbell JA. GluCOSe-oxidase based self-destructing polymeric vesicles. Langmuir 2004 Apr;20(9):3487-3491.
9. Quaglia F, Ostacolo L, Mazzaglia A, Villari V, Zaccaria D, Sciortino MT. The intracellular effects of non-ionic amphiphilic cyclodextrin nanoparticles in the delivery of anticancer drugs. Biomaterials 2009 Jan;30(3):374-382.
10. Xiao K, Luo JT, Fowler WL, Li YP, Lee JS, Xing L, et al. A self-assembling nanoparticle for paclitaxel delivery in ovarian cancer. Biomaterials 2009 Oct;30(30):6006-6016.
11. Beduneau A, Saulnier P, Benoit JP. Active targeting of brain tumors using nanocarriers. Biomaterials 2007 Nov;28(33):4947-4967.
12. Li YY, Zhang XZ, Cheng H, Zhu JL, Cheng SX, Zhuo RX. Self-assembled, thermosensitive PCL-g-P(NIPAAm-co-HEMA) micelles for drug delivery. Macromolecular Rapid Communications 2006 Nov;27(22):1913-1919.
13. Ni XP, Cheng A, Li J. Supramolecular hydrogels based on self-assembly between PEO-PPO-PEO triblock copolymers and alpha-cyclodextrin. Journal of Biomedical Materials Research Part A 2009 Mar;88A(4):1031-1036.
14. Tamilvanan S, Venkateshan N, Ludwig A. The potential of lipid- and polymer-based drug delivery carriers for eradicating biofilm consortia on device-related nosocomial infections. Journal of Controlled Release 2008 May;128(1):2-22.

15. Connal LA, Li Q, Quinn JF, Tjipto E, Caruso F, Qiao GG. PH-responsive poly(acrylic acid) core cross-linked star polymers: Morphology transitions in solution and multilayer thin films. Macromolecules 2008 Apr;41(7):2620-2626.

16. Kurkuri MD, Nussio MR, Deslandes A, Voelcker NH. Thermosensitive copolymer coatings with enhanced wettability switching. Langmuir 2008 Apr;24(8):4238-4244.

17. Sun XZ, Zeng MH, Wang B, Ye BH, Chen XM. Supramolecular architectures of metallomacrocyclic and coordination polymers with dicarboxylate and 4,4 '-bis(imidazol-1-ylmethyl)biphenyl ligands. Journal of Molecular Structure 2007 Feb;828(1-3):10-14.

18. Shah NM, Pool MD, Metters AT. Influence of network structure on the degradation of photo-cross-linked PLA-b-PEG-b-PLA hydrogels. Biomacromolecules 2006 Nov;7(11):3171-3177.

19. Nolkrantz K, Farre C, Brederlau A, Karlsson RID, Brennan C, Eriksson PS, et al. Electroporation of single cells and tissues with an electrolyte-filled capillary. Analytical Chemistry 2001 Sep;73(18):4469-4477.

20. Amiji MM. Polymeric gene delivery : principles and applications. Boca Raton, Fla.: CRC Press, 2005.

21. Cavazzana-Calvo M, Hacein-Bey S, de Saint Basile G, Gross F, Yvon E, Nusbaum P, et al. Gene therapy of human severe combined immunodeficiency (SCID)-X1 disease. Science 2000 Apr 28;288(5466):669-672.

22. Kaplitt MG, Feigin A, Tang C, Fitzsimons HL, Mattis P, Lawlor PA, et al. Safety and tolerability of gene therapy with an adeno-associated virus (AAV) borne GAD gene for Parkinson's disease: an open label, phase I trial. Lancet 2007 Jun 23;369(9579):2097-2105.

23. Ledley FD. Pharmaceutical approach to somatic gene therapy. Pharm Res 1996 Nov;13(11):1595-1614.

24. Yang ZR, Wang HF, Zhao J, Peng YY, Wang J, Guinn BA, et al. Recent developments in the use of adenoviruses and immunotoxins in cancer gene therapy. Cancer Gene Ther 2007 Jul;14(7):599-615.

25. Luo D, Saltzman WM. Synthetic DNA delivery systems. Nat Biotechnol 2000 Jan;18(1):33-37.

26. Jenekhe SA, Chen XL. Self-assembled aggregates of rod-coil block copolymers and their solubilization and encapsulation of fullerenes. Science 1998 Mar;279(5358):1903-1907.

27. Xiao NY, Li AL, Liang H, Lu J. A well-defined novel aldehyde-functionalized glycopolymer: Synthesis, micelle formation, and its protein immobilization. Macromolecules 2008 Apr;41(7):2374-2380.

28. Wang YC, Tang LY, Sun TM, Li CH, Xiong MH, Wang J. Self-assembled micelles of biodegradable triblock copolymers based on poly(ethyl ethylene phosphate) and poly(epsilon-caprolactone) as drug carriers. Biomacromolecules 2008 Jan;9(1):388-395.

29. Cheng C, Wei H, Shi BX, Cheng H, Li C, Gu ZW, et al. Biotinylated thermoresponsive micelle self-assembled from double-hydrophilic block copolymer for drug delivery and tumor target. Biomaterials 2008 Feb;29(4):497-505.

30. Maeda H, Wu J, Sawa T, Matsumura Y, Hori K. Tumor vascular permeability and the EPR effect in macromolecular therapeutics: a review. Journal of Controlled Release 2000 Mar;65(1-2):271-284.

31. Matsumura Y, Maeda H. A new concept for macromolecular therapeutic in cancer-chemotherapy-mechanism of tumoritrpic accumulation of proteins and the antitumor agent amancs. Cancer Research 1986 Dec;46(12):6387-6392.

32. Lin JP, Zhu JQ, Chen T, Lin SL, Cai CH, Zhang LS, et al. Drug releasing behavior of hybrid micelles containing polypeptide triblock copolymer. Biomaterials 2009 Jan;30(1):108-117.

33. Lo CL, Lin KM, Huang CK, Hsiue GH. Self-assembly of a micelle structure from graft and diblock copolymers: An example of overcoming the limitations of polyions in drug delivery. Advanced Functional Materials 2006 Dec;16(18):2309-2316.

34. Ko J, Park K, Kim YS, Kim MS, Han JK, Kim K, et al. Tumoral acidic extracellular pH targeting of pH-responsive MPEG-poly (beta-amino ester) block copolymer micelles for cancer therapy. Journal of Controlled Release 2007 Nov;123(2):109-115.

35. Harada A, Kamachi M. Complex formation between poly(ethylene glycol) and alpha-cyclodextrin. Macromolecules 1990 May;23(10):2821-2823.

36. Harada A, Li J, Kamachi M. The molecular necklace-a rotaxane containing many threaded alpha-cyclodextrins. Nature 1992 Mar;356(6367):325-327.

37. Wenz G, Keller B. Threading cyclodextrin rings on polymer-chains. Angew Chem-Int Edit Engl 1992 Feb;31(2):197-199.

38. Wenz G. Cyclodextrins as building blocks for supramolecular structures and functional units. Angew Chem-Int Edit Engl 1994 May;33(8):803-822.

39. Nepogodiev SA, Stoddart JF. Cyclodextrin-Based Catenanes and Rotaxanes. Chem Rev 1998 Jul 30;98(5):1959-1976.

40. Li J, Loh XJ. Cyclodextrin-based supramolecular architectures: Syntheses, structures, and applications for drug and gene delivery. Advanced Drug Delivery Reviews 2008 Jun;60(9):1000-1017.

41. Raymo FM, Stoddart JF. Interlocked Macromolecules. Chem Rev 1999 Jul 14;99(7):1643-1664.

42. Born M, Ritter H. Topologically unique side-chain polyrotaxanes based on triacetyl-beta-cyclodextrin and a poly(ether sulfone) main chain. Macromolecular Rapid Communications 1996 Apr;17(4):197-202.

43. Ooya T, Ito A, Yui N. Preparation of alpha-cyclodextrin-terminated polyrotaxane consisting of beta-cyclodextrins and pluronic as a building block of a biodegradable network. Macromol Biosci 2005 May;5(5):379-383.

44. Li J, Li X, Zhou ZH, Ni XP, Leong KW. Formation of supramolecular hydrogels induced by inclusion complexation between pluronics and alpha-cyclodextrin. Macromolecules 2001 Oct;34(21):7236-7237.

45. Peet J, Rusa CC, Hunt MA, Tonelli AE, Balik CM. Solid-state complexation of poly(ethylene glycol) with alpha-cyclodextrin. Macromolecules 2005 Jan;38(2):537-541.

46. Singla S, Zhao T, Beckham HW. Purification of cyclic polymers prepared from linear precursors by inclusion complexation of linear byproducts with cyclodextrins. Macromolecules 2003 Sep;36(18):6945-6948.

47. Ooya T, Yui N. Polyrotaxanes: Synthesis, structure, and potential in drug delivery. Critical Reviews in Therapeutic Drug Carrier Systems 1999;16(3):289-330.

48. Huang FH, Gibson HW. Polypseudorotaxanes and polyrotaxanes. Progress in Polymer Science 2005 Oct;30(10):982-1018.

49. Araki J, Ito K. Recent advances in the preparation of cyclodextrin-based polyrotaxanes and their applications to soft materials. Soft Matter 2007;3(12):1456-1473.

50. Li J. Cyclodextrin Inclusion Polymers Forming Hydrogels. Inclusion Polymers, 2009. p. 79-112.

51. Li J, Ni XP, Leong KW. Injectable drug-delivery systems based on supramolecular hydrogels formed by poly(ethylene oxide) and alpha-cyclodextrin. Journal of Biomedical Materials Research Part A 2003;65A(2):196-202.

52. Li J, Li X, Ni XP, Wang X, Li HZ, Leong KW. Self-assembled supramolecular hydrogels formed by biodegradable PEO-PHB-PEO triblock copolymers and alpha-cyclodextrin for controlled drug delivery. Biomaterials 2006;27(22):4132-4140.

53. Ooya T, Yui N. Synthesis of theophylline-polyrotaxane conjugates and their drug release via supramolecular dissociation. Journal of Controlled Release 1999 Apr;58(3):251-269.

54. Moon C, Kwon YM, Lee WK, Park YJ, Yang VC. In vitro assessment of a novel polyrotaxane-based drug delivery system integrated with a cell-penetrating peptide. Journal of Controlled Release 2007 Dec;124(1-2):43-50.

55. Yui N, Katoono R, Yamashita A. Functional Cyclodextrin Polyrotaxanes for Drug Delivery. Inclusion Polymers, 2009. p. 55-77.

56. Yang CA, Li HZ, Goh SH, Li J. Cationic star polymers consisting of alpha-cyclodextrin core and oligoethylenimine arms as nonviral gene delivery vectors. Biomaterials 2007 Jul;28(21):3245-3254.

57. Diaz-MosCOSo A, Le Gourrierec L, Gomez-Garcia M, Benito JM, Balbuena P, Ortega-Caballero F, et al. Polycationic Amphiphilic Cyclodextrins for Gene Delivery: Synthesis and Effect of Structural Modifications on Plasmid DNA Complex Stability, Cytotoxicity, and Gene Expression. Chemistry-a European Journal 2009;15(46):12871-12888.

58. Li J, Yang C, Li HZ, Wang X, Goh SH, Ding JL, et al. Cationic supramolecules composed of multiple oligoethylenimine-grafted beta-cyclodextrins threaded on a polymer chain for efficient gene delivery. Advanced Materials 2006 Nov;18(22):2969-+.

59. Yang CA, Li HZ, Wang X, Li J. Cationic supramolecules consisting of oligoethylenimine-grafted alpha-cyclodextrins threaded on poly(ethylene oxide) for gene delivery. Journal of Biomedical Materials Research Part A 2009 Apr;89A(1):13-23.

60. Yang C, Wang X, Li HZ, Goh SH, Li J. Synthesis and characterization of polyrotaxanes consisting of cationic alpha-cyclodextrins threaded on poly[(ethylene oxide)-ran-(propylene oxide)] as gene carriers. Biomacromolecules 2007 Nov;8(11):3365-3374.

61. Shuai XT, Merdan T, Unger F, Kissel T. Supramolecular gene delivery vectors showing enhanced transgene expression and good biocompatibility. Bioconjugate Chemistry 2005;16(2):322-329.

62.   Ruiz J, Ceroni M, Quinzani OV, Riera V, Piro OE. Reversible S-S bond breaking and bond formation in disulfide-containing dinuclear complexes of Mn. Angewandte Chemie-International Edition 2001;40(1):220-222.

63.   Go YM, Jones DP. Redox compartmentalization in eukaryotic cells. Biochim Biophys Acta-Gen Subj 2008 Nov;1780(11):1271-1290.

64.   Meng F, Hennink WE, Zhong Z. Reduction-sensitive polymers and bioconjugates for biomedical applications. Biomaterials 2009 Apr;30(12):2180-2198.

65.   Wu GY, Fang YZ, Yang S, Lupton JR, Turner ND. Glutathione metabolism and its implications for health. Journal of Nutrition 2004 Mar;134(3):489-492.

66.   Sun HL, Guo BN, Cheng R, Meng FH, Liu HY, Zhong ZY. Biodegradable micelles with sheddable poly(ethylene glycol) shells for triggered intracellular release of doxorubicin. Biomaterials 2009 Nov;30(31):6358-6366.

67.   Cheng R, Feng F, Meng F, Deng C, Feijen J, Zhong Z. Glutathione-responsive nano-vehicles as a promising platform for targeted intracellular drug and gene delivery. J Control Release 2011 May 30;152(1):2-12.

68.   Grigsby CL, Leong KW. Balancing protection and release of DNA: tools to address a bottleneck of non-viral gene delivery. J R Soc Interface 2010 Feb 6;7 Suppl 1:S67-82.

CHAPTER 2   LITERATURE REVIEW

2.1 DRUG DELIVERY SYSTEMS AND GENE THERAPY

2.1.1 Overview of drug delivery systems

Over the past few decades, drug delivery systems (DDSs) have been developed and studied in great depth to improve the curative effect of drugs [1-3]. In this method, the administered drug is encapsulated within a material that releases the therapeutic in a controlled manner that optimizes the dosage for a specified period of time. DDS can ameliorate the problems of conventional administration by enhancing drug solubility, prolonging duration time, reducing side effect, retaining drug bioactivity, and so on [4, 5]. For localized treatments, the delivery vehicle is acutely retained at the site of delivery, ensuring the local administration of the therapeutic. For therapeutics that is delivered through the vasculature, the delivery vehicle increases the circulation half-life, and in some cases, targets the therapeutic to a desired tissue. A variety of systems have been used as DDSs, such as vesicles [6-8] , nanoparticles [9, 10], micelles [11, 12], polymer gels [13], alipids [14], etc. At present, stimuli sensitive DDSs are an attractive theme for controlled release. The release

behaviors of drugs can be easily controlled by surrounding properties, such as pH [15] , temperature [16, 17], ionic strength [18] and electric field [19].

Nano-sized vehicles, which enable the encapsulation of various materials, have been extensively studied. For bioengineering applications, these capsules with the ability of encapsulation and delivery of drugs into cells open the door to the intracellular therapies such as gene therapy [20]. Future success of gene therapy will greatly depend on the understanding the genetic origins of disease and on the methods of delivering large numbers of specific drugs into a cell without disturbing the normal cellular process. The nano-scale multifunctional polymeric capsules which enable the encapsulation of various materials have great potentials in drug encapsulation, drug delivery and controlled release, and thus can be employed to solve the problems in the current intracellular medicinal therapies.

2.1.2 Gene therapy and gene delivery systems

Gene therapy refers to the delivery of a therapeutic gene of interest into the targeted cells or tissues with consequent temporary or "permanent" expression of the transgene [21]. Over the past two decades, it has gained much attention as a potential for treating disease caused by mutation or genetic defects, genetic disorders such as cystic fibrosis, combined immunodeficiency [22] and Parkinson's disease [23]. Gene therapy has also been considered as a suitable strategy for conventional protein therapy [24] and chemotherapy [25].

In clinical application, although over 400 clinical cases were carried out during the last 20 years [26], the issue of gene delivery has yet to be satisfied, the lack of a safe and efficient delivery vector is a fundamental obstacle to successful gene

18

therapy. To date, viral and non-viral gene carriers are two different strategies under investigation for introducing DNA into cells or tissues. Virus vectors, including retroviruses and adenoviruses, are regarded as the most effective vehicles for gene delivery[27]. The majority of gene therapy clinical trials have relied on viral vectors. However, they are challenged on many fundamental drawbacks, such as toxicity, immunogenicity, and limitations with respect to scale-up procedures[28]. Most importantly, recombinant viral vectors exists the possibility to revert to a wild-type or replication-competent virus[29], although they are regarded as non-replicative and non-pathogenic.

Non-viral vectors, compared with the viral counterparts, are relative safer, have greater flexibility and facile to large-scale production [30]. They consist of three categories: (i) naked DNA delivery, (ii) cationic liposomes and (iii) cationic polymers [31]. So far, cationic polymers and cationic liposomes are the most studied and used chemical vectors. However, in comparison with viral vectors, non-viral gene carriers are significantly less efficient due to the problems of low cell surface selectivity and internalization, low targeting to specific intracellular compartments and numerous of cellular barriers and immune defense mechanisms. To succeed, the ideal synthetic DNA delivery system should possess the following properties: ease of assembly (e.g., it should use modular components that can be "packaged" in vitro); efficient delivery leading to total transfection (i.e., DNA should be physically delivered to the majority of intended cells); stabilization of DNA before and after uptake (e.g., using nontoxic biocompatible materials); capability of bypassing or escaping from endocytotic pathways (e.g., by incorporating viral components); efficient decomplexation or

"unpackaging" (e.g. intracellular controlled release); efficient nuclear targeting; and high, persistent, and adjustable expression of therapeutic levels of proteins[32].

Cationic polymers are the major type of the nonviral gene vectors investigated in the past decade. They are generally possessed positive charged groups such as primary, secondary, tertiary and quaternary amines. This high density of positive charges allows the cationic polymers to form stable complexes with non-viral DNA. The formed polyplexes (polymer/DNA complexes) are positive charges, which could bind cells followed by endocytosis mediated by anionic proteglycans on the cell surface. These polymers vary widely in their structures, which range from linear to highly branched molecules that influence their complexation with nucleic acids and their transfection efficiency. Due to the easy modification, the cationic polymers are promising to meet the multiple functions required for safe and efficient gene delivery [33]. The polycations frequently used in gene delivery and transfection include, polyetheyleneimine [34], poly (L-lysine) [35], dendrimers [36], polybrene [37], gelatin [38], CD-containing polymers [39], and poly(2-dimethylaminoethyl methacrylate) (pDMAEMA) [40]. Although these gene vectors have been developed for over two decades, they are still limited in clinical application due to the poor efficiency, high toxicity and low in vivo stability.

2.2 POLYMERIC MICELLES FOR DRUG AND GENE DELIVERY

During the past decade, core-shell nanostructures have demonstrated their utility in delivery drugs and are currently recognized as promising formulations for enhancing the efficacy of drugs [41, 42]. Among these vectors, polymeric micelles are the most studied structures. A polymeric micelle is a supramolecular assembly of

block copolymers, having a characteristic core-shell structure; the drug-loaded core is surrounded by hydrophilic outer shells [43]. These polymeric micelles show distinct stability in solution. The core-shell structure of the micelle can improve solubility of hydrophobic drugs, and protect the incorporated drug from premature degradation [11, 44, 45]. As a nanosize carrier, micelle can easily permeate into the tumor and induce its passive accumulation due to the vascular leakiness and impaired lymphatic drainage in solid tumors, which have been known as the enhanced permeability and retention (EPR) [46, 47]. So the micelles offer the advantages of decreased side effects and improved drug availability.

Therefore, polymeric micelles with smaller sizes (20-100nm), which are self-assembled from amphiphilic block copolymers have shown great promise as nanocarriers for efficient drug delivery [48, 49]. Indeed, several micellar formulations encapsulating antitumor drugs are now undergoing clinical trials [50]. Furthermore, when environmentally sensitive (pH, temperature, enzyme, etc) functional groups are introduced into these amphiphilic copolymers, "smart" micelles are formed, and they can be used as environmentally controlled drug release system. Recently, there has been a strong incentive to develop polymeric micelles with smart functions such as target ability to specific tissues and chemical or physical stimuli-sensitivity. Such smart polymeric micelles are assumed to enhance the efficacy of the loaded drugs as well as to minimize side effects beyond current drug delivery formulations [51-53].

2.2.1 Polymeric micelles for drug delivery

Amphiphilic block copolymers are commonly used to construct micellar assemblies. In aqueous solution, the hydrophobic parts of these block copolymers aligned together to the centre and hydrophilic parts aligned towards the outside

environment to form the polymeric nanocapsules structures. After that, covalent bonds will be formed in the outside shell of this capsule to stabilize the whole system to make it more suitable for further applications. And the hydrophobic interior property of this capsule gives this system the ability to contain hydrophobic drug inside its cavity, which refers to drug delivery (Fig. 2.1) [54]. The majority of block copolymers have hydrophilic blocks of polyethylene glycol (PEG) [55]. This well studied, FDA-approved polymer is biocompatible. PEG demonstrates notable antifouling properties, and micelles having an outer shell of this polymer are able to resist protein adsorption and cellular adhesion. The nonfouling nature of PEG increases the residence time of circulation in blood and minimizes the detection by the immune system [56, 57].
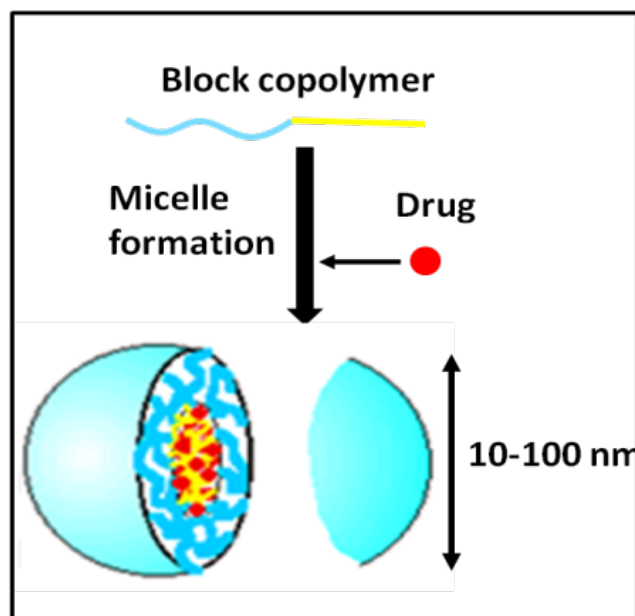
Fig. 2.1 Polymeric micelles as drug carriers

As a typical example, polycaprolactone (PCL) and polylactic acid (PLA) are commonly used as the hydrophobic portion to form micelle structure with PEG. They have been utilized for amphotericin B, pioglitazone, 9-nitro-20(S)-camptothecin (9-NC), and methotrexate (MTX) [58-60]. The self-assembly of block copolymers is

often spontaneous and can be performed in the presence of small molecules, leading to micelles encapsulated with drugs that have diameters up to hundreds of nanometers. Since the therapeutic is present during the self-assembly process, drugs are loaded easily. For example, PEG–PCL micelles have been used to encapsulate rapamycin, a small antibiotic, to form micelles that are less than 100 nm in diameter. Rapamycin can be encapsulated at concentrations of >1 mg ml^{-1}, which is exceptionally higher than the solubility of the free drug in water [58]. MTX, an anticancer and anti-rheumatoid arthritis agent, can be sequestered in micelles of PEG–PLA block copolymers in a similar manner. These micellar structures have diameters that range from 50 to 200 nm, with loading capacities of 12% by weight and encapsulation efficiencies as high as 50% [59].

The pH-sensitive micelles are very useful to therapeutic function by responding to low pH conditions in the endosomal or lysosomal compartment of the cells. Kataoka et al. at have recently developed micelle-forming PEG-b-P (Asp-Hyd-DOX) copolymer, which are prepared by chemically conjugating doxorubicin (DOX) to the side chain of PEG-b-poly (aspartic acid) copolymers via an acid-labile hydrazone bond [61, 62]. Such pH-sensitive polymeric micelles significantly released active DXR under low pH conditions corresponding to late endosomes and lysosomes. Consequently, the micelles effectively suppressed tumor growth in mice over a broad range of injection doses while the toxicity remained extremely low, which is in marked contrast to free DOX with a narrow therapeutic window [62]. Similarly, PEG-b-poly (L-histidine) copolymers possessing pKa values around a physiological pH, which act as amphiphilic copolymers to form polymeric micelles under a physiological pH condition while showing a hydrophilicity, biodegradability and

fusogenic activity at the lower pH conditions [63]. This micelle showed an accelerated release of DOX with lower pH.

2.2.2 Polymeric micelles for gene delivery

The efficient gene vectors should be a key technology in the forefront of modern medicine owing to their potential use for the treatment of intractable disease and tissue engineering. In addition to the delivery of hydrophobic drugs, micelle carriers can be utilized for the delivery of DNA. Inverted micelles have been designed to bind to and package DNA for delivery. Inverted micelles are composed of a hydrophilic outer shell (e.g PEG) and a polycationic inner core that can favorably interact with negatively charged DNA [64, 65]. Polylysine, polyethylenenimine (PEI) and polyphosphoramidate (PPA) have been used for the inner core. The diblocks alone in solution do not self-assemble, but when the polyanionic DNA is added, it binds the polycation blocks, decreasing the overall net charge, followed by micelle formation. The micelles protect the DNA from the enzymatic and hydrolytic degradation during delivery. When encountered by cells, the loaded micelles are endocytosed, the DNA is released, and the cells become efficiently transfected [64]. For example, Kataoka et al. reported the *in vivo* demonstration of this approach, and the gene for luciferase was encapsulated into PEG-polylysine inverted micelles, which exhibited sustained gene expression in the mice liver over 3 days [66].

DNA delivery is not limited only to inverted micelles. Micelles composed of hydrophobic cores and polycationic exteriors can also be used. For instance, micelles were formed, which consist of polypeptides with polyalanine as a hydrophobic block and polylysine/polyhistidinie as hydrophilic block that condense DNA on their outer corona. Even though DNA is bound to the outer shell of the micelle, it is still

protected from enzymatic degradation. Furthermore, these micelles were found to be noncytotoxic and capable of delivering genes to HEK293, HepG2, and 4T1 cancer cell lines [67]. Generally, the delivery of DNA-carrying micelles can be enhanced by decorating peptide, a protein that target the vehicle to a specific binding site [68, 69].

Recently, micelles capable of dual delivery of DNA and other therapeutics have also have been designed [70-72]. Specially, poly N-methyldietheneamine sebacate and (cholesteryl oxocarbonylamido ethyl) methyl bisethylene ammonium bromide sebacate (PMDS-co CES) form micelles with an inner hydrophobic core composed of cholesterol surrounded by polycationic polymer. The co-delivery of the micelle containing paclitaxel and the plasmid DNA suppressed tumor growth in a 4T1 mouse breast cancer model more effectively than the delivery of micelles with either therapeutic alone [70].

2.3 CYCLODEXTRIN BASED POLYROTAXANE FOR DRUG AND GENE DELIVERY

Since the first synthesis of polyrotaxanes with multiple α-CD rings threaded on a polymer [73-75], tremendous interest has been attracted on the studies of these series inclusion complexes and their applications on biomaterials [74-78]. Cyclodextrins (CDs), also known as cycloamyloses, and cyclomaltoses, are a series of natural cyclic oligosaccharides composed of 6, 7, and 8 D (+)-gluCOSe units linked by α-1,4-linkages, and named with α-, β-, and γ-CD, respectively. Their topological structures give a hydrophobic inner cavity with a depth of ca. 7.0 Å, and an internal diameter ca. 4.5, 7.0, and 8.5 Å for α-, β-, and γ-CD, respectively. Polyrotaxane is composed of three elements: the macrocycle wheels, the appropriate axle, and the

bulky end-caps on the terminal of the axle. According to the fascinating capability of macrocyclic CD rings as host molecules, various guest molecules have been investigated to form inclusion complexes with enhanced physical and biological properties for drug delivery (Fig. 2.2), and to thread into their cavities to create polypseudorotaxanes and polyrotaxanes with controllable size and structure for various functional nanomaterials [75-77, 79-84]
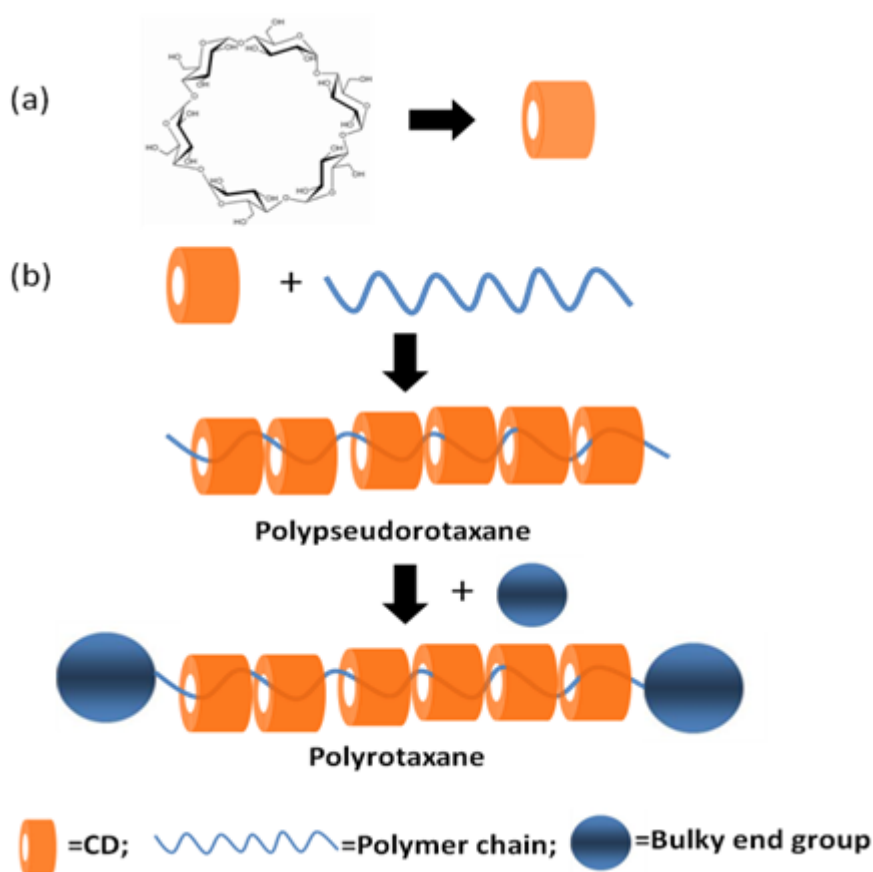
Fig. 2.2 Demonstration of CD and polyrotaxane: (a) structure of α-CD, (b) general synthesis procedure of polyrotaxane [74]

2.3.1 CD based polyrotaxanes and polypseudorotaxanes for drug delivery

There have been several recent attempts made to use cyclodextrin based polyrotaxanes and polypseudorotaxanes for drug delivery. Because both PEO and CDs are known to be biocompatible and CDs have been approved by the FDA as food

and drug formulations, it is easily to construct supramolecular inclusion complexes between CDs and PEO or its copolymers as a new class of bioabsorbable systems for controlled drug delivery. Based on different method for introducing drugs or proteins, there have been polypseudorotaxane hydrogels for sustained drug release and drug-conjugated biodegradable polyrotaxanes for controlled and targeting drug delivery.

2.3.1.1 Supramolecular hydrogels formed by α-CD and PEO and the copolymers

Supramolecular hydrogels based on polypseudorotaxanes of CDs and polymers is one of the most attractive physical cross-linking hydrogels. Generally, they are thixotropic and thermo-reversible, which is a unique property as injectable hydrogel drug delivery systems [85-87]. As a typical example, PEG of high molecular weights was found to form complexes with α-CD in aqueous solution to give gels in a wide range of concentrations [87, 88]. According to the rheological studies, the hydrogels displayed decreasing visCOSity when agitated and restored within hours after the agitation. This property renders the hydrogel formulations injectable even through a fine needle [85]. These unique hydrogel can be applied to injectable and bioabsorbable drug delivery systems due to their thixtropic and reversible properties [78]. The gels were entrapped by fluorescein isothiocyanate-labeled dextran (dextran-FITC) and characterized in terms of *in vitro* release [85]. It was found that the release rate decreases sharply with an increase in the molecular weight of PEO up to 35K Da and the release rate of gel formed with PEO 35K and 100K is quite sustained.

In spite of the promising properties of α-CD-PEO hydrogels, it is challenging to apply this hydrogel for *in vivo* drug delivery. Firstly, this hydrogel is not suitable for long-term drug release because the physical interaction is weak in aqueous environment due to the hydrophilic property of PEO; In addition, the high molecular

weight PEO is not biodegradable and it is difficult for filtration through human kidney membrane. Therefore, with regarding to the first problem of α-CD-PEO hydrogels, a new supramolecular hydrogels self-assembled between α-CD and triblock copolymer PEO-PPO-PEO were studied for long-term and controlled release of drugs [13, 82]. The gelation was induced by the complex formation between the PEO segments of the PEO-PPO-PEO triblock copolymer and partially threaded α-CDs. In addition to the injectable and reversible properties, the polypseudorotaxane hydrogel is thermo-sensitive. Furthermore, unlike the thermo-responsible hydrogels formed only with PEO-PPO-PEO triblock copolymers [89, 90], the addition of α-CD largely reduced the concentration of the copolymer needed for gel formation [13]. The *in vitro* controlled release properties showed that the hydrogel can achieve the sustained release for more than one week with a linear release kinetics [78]. Pluronics have also been threaded on hydroxypropyl-β-CD. They showed enhanced solubility of the drug and a temperature-dependent sustained release [91].

Considering that the high molecular weight PEO is not suitable for filtration through human kidney membrane, a biodegradable polymer will be advantageous because of the degradation of material into low molecular weight compounds, which can be eliminated from the body through natural pathway. PHB is one of the biodegradable polymers that can be used for drug delivery. PEO-PHB-PEO triblock copolymer was found to form block selective polypseudorotaxanes with α-CD (Fig.2. 3a) [92, 93]. For hydrogel formation, it was found that the cooperation effect of complexation of α-CD with PEO block together with the hydrophobic interaction between the middle PHB blocks results in the formation of the supramolecular hydrogel with a strong macromolecular network (Fig. 2.3b) [86].
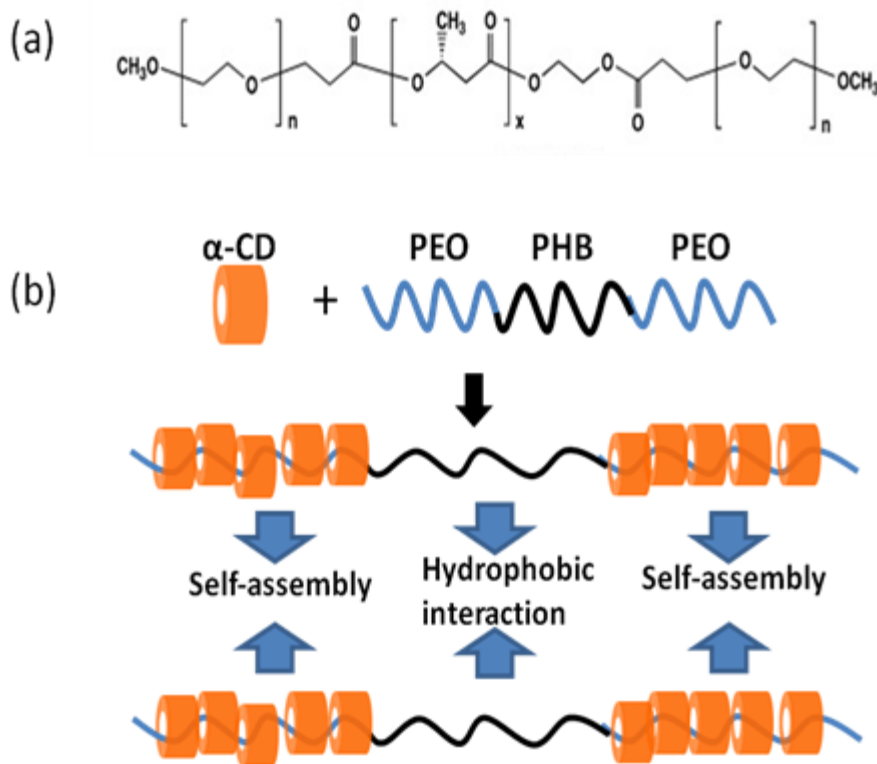
Fig. 2.3 (a) The stucture of PEO-PHB-PEO triblock copolymer, and (b) the schematic illustratios of the proposed structures of α-CD-PEO-PHB-PEO inclusion complex

In contrast to most physical hydrogels formed simply by copolymers, the *in vitro* release kinetics studies of dextran-FITC model drug form this α-CD-PEO-PHB-PEO hydrogel showed that it was suitable for relatively long-term sustained controlled release of macromolecular drugs. Specifically, it was found that the α-CD-PEO-PHB-PEO hydrogels with reasonably high α-CD concentration showed excellent controlled release property, sustaining the release of dextran-FITC for more than 1 month. This is a large improvement by comparasion with α-CD-PEO homopolymer hydrogel [85]. Furthermore, the hydrogels with lower α-CD concentrations resulted in a much faster release rate, indicating the complexation between α-CD and PEO blocks is important to form a stable supramolecular gel. As the same with α-CD-PEO hydrogel, this hydrogel was also found to be thixotropic and reversible. Therefore, this new supramolecular hydrogel is promising for

relatively long-term sustained controlled delivery of macromolecular drugs as an injectable formulation. More importantly, the biodegradable PEO-PHB-PEO copolymers will have the advantage that the hydrogel will be bioabsorbable and dissociation after drug release, which is a good benefit for the human body [86]. Similarly with copolymer PEO-PHB-PEO, another amphiphilic biodegradable copolymer PEO-PCL was also studied to form polypseudorotaxane hydrogels with α-CD. The new supramolecular hydrogels are promising for minimally invasive therapeutic delivery application with fine-tuned properties [94, 95].

Based on similar mechanism whereby α-CD could thread on part of PEO segments in a block or homo polymer to form supramolecular physical cross-linked structure, an increasing number of polypseudorotaxane-based physical hydrogels are appearing in the literature. For example, by mixing α-CD, PEG and PAA in an aqueous solution, the competition between host-guest and hydrogen-bonding interactions occurs [96]. Moreover, there are a few reports on hydrogel formation between α-CD and PEO or PPO-grafted polymers. Supramolecular physical gelation can be introduced by a specific host-guest interaction between α-CD and PEO-grafted dextrans [97]. Similar thermo- or pH-sensitive polypseudorotaxane hydrogels can be formed between α-CD and PEO-grafted chitosan [98], α-CD and PEO-grafted hyaluronic acid [99], β-CD and PPO-grafted dextran copolymer [100], and between α-CD and highly densely PEO grafted polymer brushes (PBIEM-g-P(PEOMA)) [101]. Recently, a water soluble polyrotaxane composed of multiple methylated α-CD rings threaded on a high molecular weight PEO chain and end-capped by bulky adamantly groups was developed [102, 103]. This Me-PR exhibited thermo-reversible sol-gel

transition in water depending on the degree of methylation and a gelation took place at high temperature.

Apart from the physical hydrogel, chemical gel cross-linked by biodegradable polyrotaxanes having ester linkages at the terminal of PEG are also reported as good example for drug delivery. These supramolecular networks are also called "sliding gels" [104-106]. Typically, Yui's lab prepared biodegradable and temperature-controlled hydrogels by crosslinking N-isopropylacrylamide (NIPAAm) and methacrylate(MA)-introduced polyrotaxane in which α-CDs are threaded onto a PEG chain capped with bulky end-groups via ester linkages [107]. These supramolecular hydrogels could be useful for biomedical applications because of their biocompatibility and thermo-controllable property.

2.3.1.2 Supramolecular micelles based on cyclodextrin for drug delivery

Although supramolecular hydrogels or self-aggregates constructed from CDs involving inclusion complexes have been intensively investigated not only for their theoretical merits but also for their potential drug delivery applications, the self-assembly micelles formed by amphiphilic copolymer threaded with CDs has not been used as a carrier for the controlled drug release. Being different from supramolecular hydrogels matrix for drug delivery, the polyrotaxane micelles could self-assemble the drug into a nanometer scale particle, which is always an attractive factor for effective drug delivery carriers. As a typical example, a kind of novel amphiphilic triblock copolymers containing polyrotaxane as a central block was synthesized via the ATRP (Fig. 2.4) [108]. Rather than the physically crosslinked hydrogels or the traditional PRs yielded as crystalline precipitates from aqueous solution, these triblock copolymer with polyrotaxane central block flanked by two hydrophilic brushlike

PEGMA oligomers would self-assemble into nano-sized particles with the unique core–shell structure in aqueous medium. In this system, PEGMA oligomers create a dense non-adhesive hydrophilic coating around the PR central block capable of suppressing protein and cell adhesion and extending residence time of the particles as carrier for the controlled drug release.
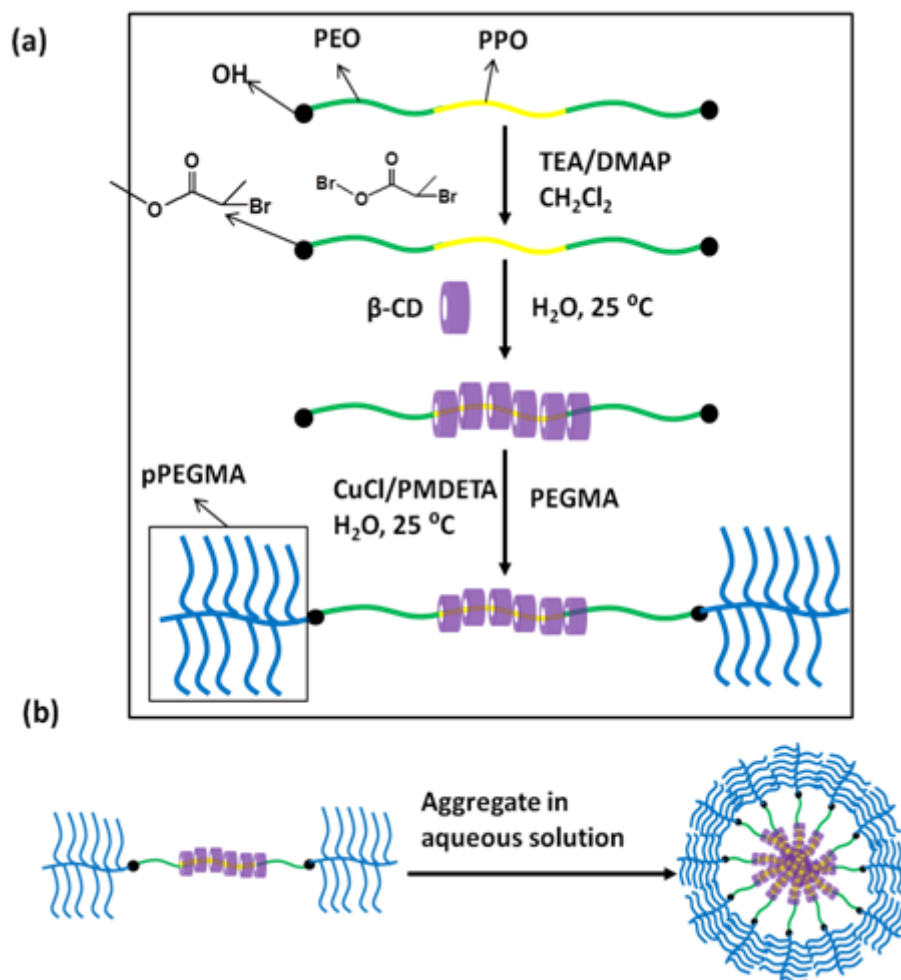
Fig. 2.4 (a) Synthetic pathway of PR-based triblock copolymer via ATRP of PEGMA in aqueous medium; (b) Schematic diagram of self-assembly micelles formed by the PR-based triblock copolymer in aqueous medium

Amphotericin B (AmB) was selected as a model drug to evaluate the drug release property of the polyrotaxane micelle system. Surprisingly, the nano-sized micelles were found to effectively solubilize AmB with high drug-loading content and drug-loading efficiency as well as long sustainable release profile. By comparison

with micelles form by Pluronic PPO-PEO-PPO without CDs, the polyrotaxane containing amphiphilic micelles released much slower, which indicated that encapsulated AmB may have some interaction with threaded β-CDs, giving longer and sustained release time. Moreover, the entrapment into self-aggregates of amphiphilic PR-derived triblock copolymers can protect AmB molecules from hydrolysis, aggregation and precipitation by minimizing contact with the bulk aqueous phase.

Another micellar structure was constructed by using the process of highly threaded pseudopolyrotaxane stacking to drive self assembly. Poly (ethylene oxide)-blcok poly ((dimethylamino ethylmethacrylate) (PEG-PDMA) polymer is an example. α-CD was able to thread over the PEG segment, but not the PDMA segment of this polymer axle. The threaded part of the polypseudorotaxanes aggregated, leaving the hydrophilic PDMA polymers exposed to solution, thus forming a micellar structure [109].

2.3.1.3 Drug-conjugated biodegradable polyrotaxane for drug delivery

In addition to hydrogel matrix for drug, CD-based polyrotaxanes could be widely applied as drug delivery systems with another strategy, which is by conjugating drug or functional proteins in on the CD rings. Polyrotaxane is fascinating and very promising for this kind of drug delivery due to several unique structural characteristics. Firstly, CDs bear many hydroxyl groups that could be easily modified by chemical reactions, allowing the conjugation of bioactive agent on the CD rings; Secondly, self-assembled polyrotaxanes display highly mobility of CDs as a result of the CD rotating around the polymer chain. This flexibility is expected to enhance multivalent ligand-receptor interaction, and is promising for applications

such as targeting drugs, drug-mediated drug delivery and tissue engineering [110].
Thirdly, CDs can dethread through the polymer chain when the end is capped through
biodegradable linkage, which insures the release of drug into the cell [111].

In the field of drug delivery, one of the most crucial issues is how to bind the
bioactive agents or ligands on receptor sites of proteins on the plasma cell membranes
effectively and specifically. Over the last decades, the approach of multivalent
interaction by using multiple ligands with receptor protein was considered as a
possible solution [112]. However, multivalent ligand-immobilized polymer resulted in
unsatisfying mainly because of a spatial mismatch between the ligand-polymer and
receptor [113] (Fig. 2.5a). Thus, as mentioned above, cyclodextrin-based
polyrotaxanes are advantageous in freely spinning through the polymer chain, which
opens the opportunity for multivalent interaction with biological systems (Fig. 2.5b).
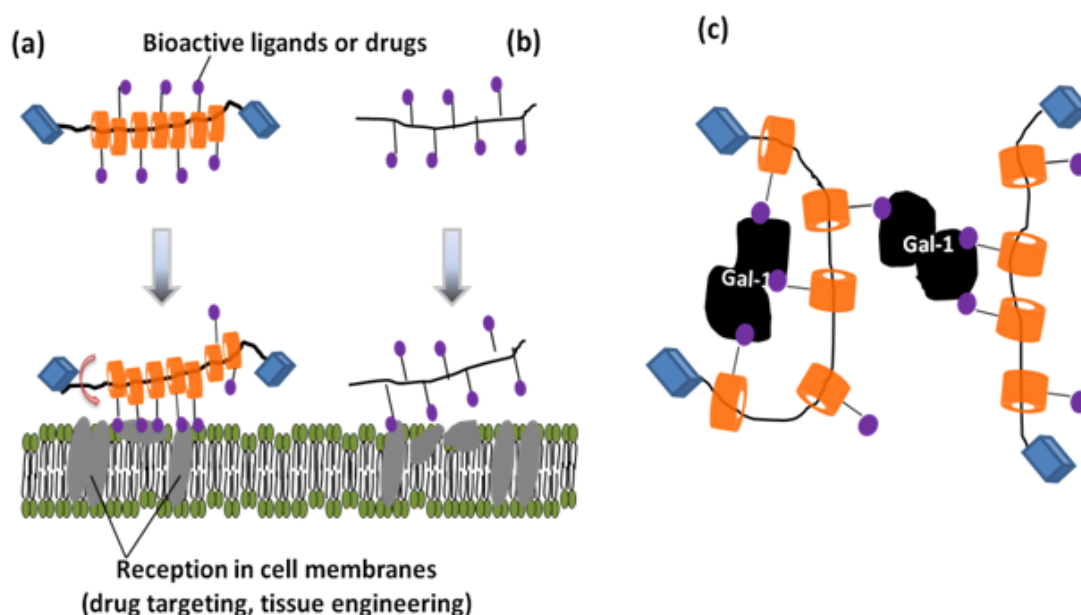
**Fig. 2.5 The effects of mobile CDs in polyrotaxanes on binding receptor proteins in a
multivalent manner (a) Image of ligand-polyrotaxane conjugate, (b) image of ligand-
immobilized polymer, and (c) possible binding models for Gal-1 and polyrotaxanes.**

34

Based on this hypothesis, a polyrotaxane consisting of lactoside-CD-polyviologen conjugated polyrotaxane was investigated for its ability to inhibit galectin-1-mediated T-cell aggulutination. Due to the rotating properties, the polyrotaxane showed an enhancement for the agglutination [114]. Similarly, biotin was conjugated to α-CD or β-CD which was treaded in PEO or PPO chains and end caps with biodegradable L-phenylalanine (Z-Phe). In contrast to biotin-CD conjugate, this biotin-polyrotaxane conjugate model significantly switches monovalent binding to multivalent binding, and results in a much greater inhibitory potency [115, 116]. Furthermore, by conjugating maltose with α-CD-PEO polyrotaxane, Yui's lab found that it exhibits a much stronger inhibitory effect than maltose and the mobility of α-CD along the PEG chain plays a crucial role in rapid binding of concanavalin A [117-119].

Biodegradability is one of the indispensable properties for drug delivery systems. As compared to biodegradable hydrogel matrices for drug release, drug-conjugated biodegradable polyrotaxane can be advantageous in both controlling the drug release by degradation rate of terminal group and the number of CDs threaded onto the biodegradable polymer, and the dethreading of CDs modified with appropriate drugs may enhance drug permeation across biological barriers (Fig. 2.6). The first example of biodegradable polyrotaxanes was reported in 1995 [120]. The supramolecular assemblies were formed between α-CD and PEO chain, capped with L-Phe via biodegradable peptide linkages. When the peptide linkages were enzymatically degraded by protease such as papain, the polyrotaxanes would degrade to PEO, α-CD and L-Phe. In order to investigate the degradation and CD release kinetics of this new drug release system, hydroxyl-propylated (HP) modified

polyrotaxanes were synthesized [121]. The *in vitro* release study shows that HP-α-CD

can be released when either of two terminal peptides was cleaved, and the rate of

degradation can be controlled by changing the degree of hydrophobicity of the α-CDs

in the polyrotaxanes. Furthermore, the oxypropyl groups next to L-Phe moiety can

enhance the interaction with papain to increase the HP-α-CD release [122]. Thus the

designed polyrotaxanes are feasible as novel drug carriers in which the degradation of

terminal moiety can induce the release of drugs.
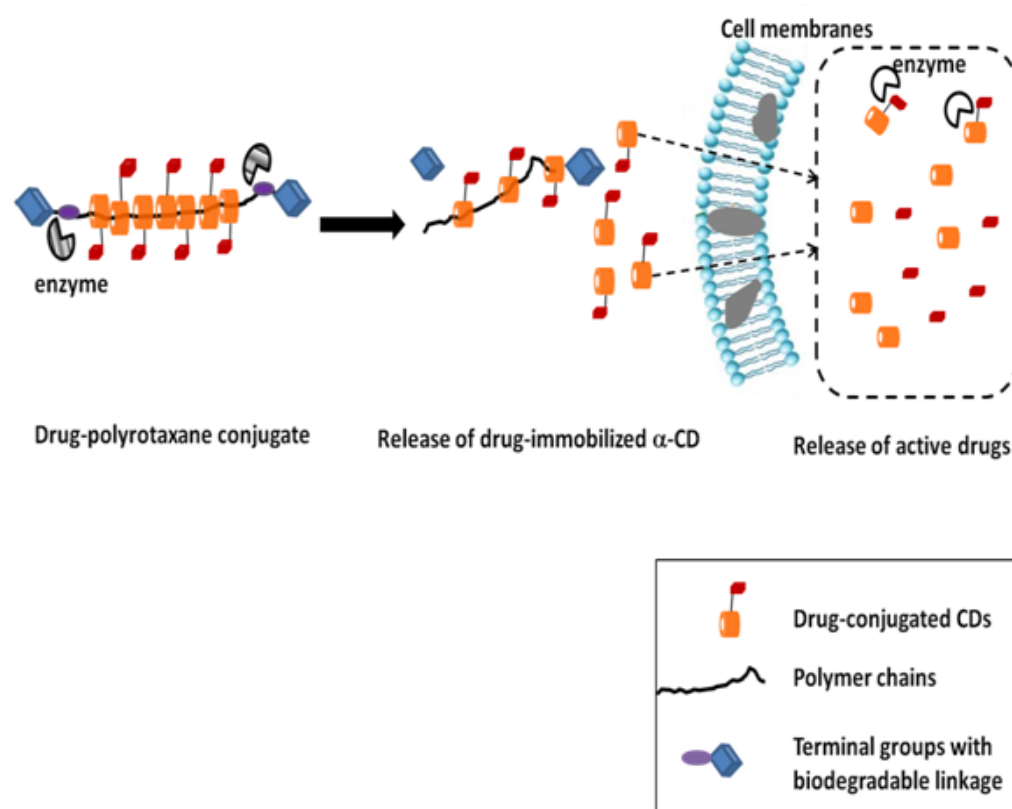
Fig. 2.6 The schematic illustration of drug-conjugated polyrotaxane and the concept of triggered drug release via enzymatic degradations

The incorporation of drugs to HP-α-CD in the polyrotaxane was accomplished

in 1999. Theophylline-polyrotaxane conjugates were synthesized by coupling

theophylline with α-CD that threaded onto PEG chain capped with L-Phe [111]. Upon

enzymatic degradation of the terminal groups, theophylline-CD conjugates were

completely released via dissociation of the supramolecular structure without steric hindrance. The bonds between drug and α-CDs can also hydrolysis to release the active drugs in cells (Fig. 2.6). In addition, by utilizing different enzymes (papain and α-chymotrypsin), sustained release of drug was observed, ranging from 50 h to 250 h. Based on the similar technology, another drug, the anti-cancer drug doxorubincin (DOX), was also conjugated to polyrotaxane polymer via hydrolyzable linkages, and a cell-penetrating low molecular weight protamine (LMWP) peptide was further attached to the chain end in order to facilitate the intracellular uptake of tumor cells [123]. It was demonstrated that the LMWP-PR-DOX conjugates yielded a sustained release of DOX over a period of greater than 4 days and this LMWP-PR-DOX conjugate offers a great potential for intracellular drug delivery into tumor cells in achieving highly effective and safe drug therapy.

2.3.2 CD based polyrotaxanes and polypseudorotaxanes for gene delivery

2.3.2.1 Cyclodextrin-containing cationic polymers for gene delivery

Gene delivery using polycations is believed as one of the greatest challenges for inventing nonviral gene carrier systems instead of toxic virus-based vector systems [124]. Because the hydroxyl groups in CD rings offers opportunity for multiple modification, CDs were explored for oligonucleotide delivery, which enhanced the absorption and resistance to nucleases [125]. The first CD-containing cationic polymer for gene delivery was reported in 1999 [126, 127]. Generally, the CD-containing cationic polymers showed lower cytotoxicity and efficient gene transfection [128, 129]. More importantly, the CD-containing polycations can be further modified by inclusion complex formation [130]. Take the pegylation for example; PEO-adamantane was used to form complex formations with β-CD

modified polyethylenimine (PEI) by the supramolecular interaction between adamantane and β-CD. It was found to stabilize the polyplex nanoparticles and result in enhanced gene transfection [131, 132]. So far, a number of cationic polymers have been modified by grafting CDs on the polymers to study the gene delivery, such as linear and branched PEI [133], and polyamidoamine(PAMAM) dentrimer [134, 135].

Most recently, a new series of cationic star polymers consisting of α-CD core and oligoethylenimine(OEI) arms were synthesized as nonviral gene delivery vectors [136]. The α-CD-PEI star polymers could inhibit the migration of pDNA on agarose gel as a result of nanoparticles with sizes ranging from 100 to 200 nm. The star cationic polymer was found to display lower *in vitro* cytotoxicity than branched PEI (Mw=25K), and the transfection efficiency is excellent, being comparable to or even higher than that of branched PEI (25K). With a similar star structure, a kind of polycationic amphiphilic cyclodextrins was reported [137]. The structure contains both cationic elements and lipophilic tails, which is similar to the lipid structure. The nanoparticle stability and transfection efficiency can be rationally modulated by judicious tailoring of the molecular topology.

2.3.2.2 Cyclodextrin-containing cationic polyrotaxane for gene delivery

Another new class of CD-containing gene carriers was developed based on cationic polyrotaxanes where multiple cationic CDs are threaded onto a polymer chain and capped by bulky ends. By taking advantage of the CD's ability to slide and rotate along the polymer axle, this system appears to be able to generate well-matched DNA complexes, and thus accomplish the gene transfection with a minimum amount of cationic polyrotaxanes. It is similar to the concept of multivalent interaction discussed earlier. Therefore, CD-containing cationic polyrotaxanes are a promising

system for non-viral gene delivery. The first example of this system would be the cationic supramolecules composed of multiple OEI-grafted β-CD threaded on a Pluronic PEO-PPO-PEO triblock copolymer chain and end capped with 2,4,6-trinitrobenzene sulfonate (TNBS) (Fig. 2.7) [138]. This system may have the following advantages. Firstly, β-CD is known to selectively thread around the PPO segments [139], providing low spatial hindrance using spare PEO segments and permitting efficient OEI grafting degree. Secondly, due to the free mobility of OEI-grafted β-CD along both PPO and PEO segments, it is flexible to condense DNA efficiently. Thirdly, because shorter length of PEI was used the system showed much less toxicity than PEI (25K) in cell cultures. Finally, there are a lot of "flapping" OEI chains with many primary and secondary amines, which is beneficial for interaction with DNA and cell membranes. As a result, the cationic supramolecular gene delivery vectors showed good DNA binding ability, low cytotoxicity, and high gene transfection efficacy that is similar to PEI (25K). It even exhibits higher transfection efficiency than dimethylaminoethyl(DMAEC)-α-CD polyrotaxane systems [140]. In further development, the β-CD-OEI/PEO-PPO-PEO system was reported to display high and sustained gene delivery capability in cancer cells in the presence or absence of serum [141].
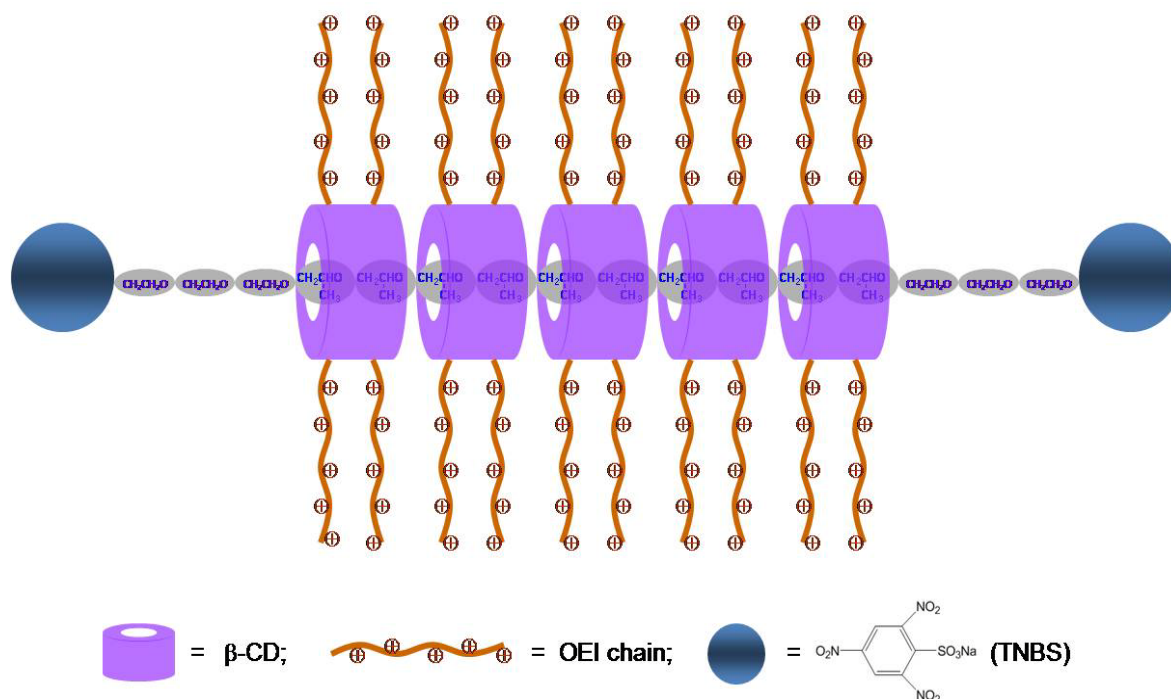
Fig. 2.7 structures of cationic polyrotaxanes with multiple OEI-grafted β-CD rings[138].

By utilizing the similar system, a few of cationic polyrotaxanes based on other CDs and chains were synthesized, including cationic supramolecules consisting of OEI-grafted α-CD threaded on PEO [142] and polyrotaxane consisting of cationic OEI-grafted α-CD threaded on PEO-PPO random copolymer [143]. Generally, these cationic polyrotaxanes showed strong DNA binding ability, low cytotoxicity, high gene delivery capability and they have a high potential as novel non-viral gene carriers in clinical gene therapy. In another study, soluble polyrotaxanes were formed for gene delivery by threading α-CD molecules over PEO and PCL chains of the ternary block copolymer PEO-PCL-PEI. The gene transfection efficiency was of the same order of magnitude as PEI (25K) but with much lower toxicity [144]. In addition to amino-grafted CD polyrotaxane, LPEI/γCD-based polypseudorotaxanes have also been examined for gene delivery [145]. The γ-CD-based polypseudorotaxane had improved cellular uptake and lower toxicity. The transfection efficiency of this

polypseudorotaxane was comparable to or greater than that of the LPEI, especially at higher N/P ratios.

2.4 ENVIRONMENTALLY SENSITIVE AND BIODEGRADABLE VECTORS

The most evident problem associated with non-degradable polymeric vectors is that they are not easily removed by the physiological clearance systems and, therefore, can possibly accumulate within cells or tissues to elicit further cytotoxicity. The biodegradable polymers, which exhibit a suitable and controllable degradation profile in the body after certain periods of time, have been extensively investigated over the past two decades [146]. Recent studies of biodegradable vectors focus on various stimuli-triggered responses such as enzymes, pH, redox and temperature. The linkages can be divided into protease-catalyzed peptide bond, simple hydrolysis based ester bond, pH-triggered hydrazone bond and disulfide bond for reduction with reductive agents or enzymes.

The stimuli-responsive DDS must be degraded only via disease-derived stimuli to achieve degradation-controlled release at a desired release rate. In particular, biodegradable hydrogels have been proposed as excellent candidates for such controlled drug delivery systems because they have several advantages such as excellent biocompatibility, high responsiveness to specific degradation, and acceptable mechanical strength for implantation [86]. In this system, degradation-controlled drug release cannot be guaranteed in these hydrogels because of high diffusivity of drugs through these polymer matrices. Chemical immobilization of drug on biodegradable hydrogel matrix or water-soluble polymer backbone has been a general strategy when the drug is introduced into these polymer systems [111]. Such a

drug-immobilized polymer system or polymer-drug conjugate is to provide prolonged release action of the drug by the hydrolysis or biological scission of the covalent bonds.

In the field of gene delivery, one of the most important difficulties arisen in the strategy of using polycations as gene carriers is how to make sure the endosomal/lysosomal escape of polyplex and how to release DNA into the cytoplasm, finally reaching the nucleus through the nucleus membrane. With regard to this issue, the introduction of biodegradable moieties into polycations to dissociate the polyplex has been studied recently [147]. Generally the biodegradable vectors demonstrate a reduced cytotoxicity and higher or comparable transfection efficiency to an unmodified polycation like PLL or PEI, thus the biodegradable polymers shows great potential to be used as a gene vector. There are a large variety of biodegradable polymeric vectors including Polyesters, Polyurethanes, PLL-based, PEI-based, Phosphorus containing polymers, Polysaccharide based, biodegradable nanoparticles and Poly(2-(dimethylamino)ethyl methacrylate) (pDMAEMA)[148].

2.4.1 Enzymatic triggered biodegradable systems for drug and gene delivery

Among various stimuli-triggered responses, enzyme is one of the widely used triggers. Usually, the enzymatic triggered biodegradable systems contain a ester bond, which could be simplify hydrolyzed to protease-catalyzed peptide bond under enzymes.

For example, supramolecular assemblies were formed between α-CD and PEO chain, capping with L-Phe via biodegradable peptide linkages. When the peptide linkages were enzymatically degraded by protease such as papain, the polyrotaxanes

will degrade to PEO, α-CD and L-Phe. When the peptide linkages were enzymatically degraded by protease such as papain, the polyrotaxanes will degrade to PEO, α-CD and L-Phe. In order to investigate the degradation and CD release kinetics of this new drug release system, hydroxyl-propylated (HP) modified polyrotaxanes were synthesized [121] (Fig. 2.8). After that, drug, theophylline, was conjugated to this polyrotaxane for delivery. Upon enzymatic degradation of the terminal groups, theophylline-CD conjugates were completely released via dissociation of the supramolecular structure without steric hindrance. The bonds between drug and α-CDs can also undergo hydrolysis to release the active drugs in cells [111]. Similarly, polyrotaxane composed of PLLA and α-CD end with z-l-Phe exhibited papain-triggered hydrolysis [149]. Moreover, in order to examine the enzymatic degradation controlling, two different peptide end capped polyrotaxanes, L-phenylalanylglycyl-glycine terminated and L-tyrosineglycylglycine-glycine terminated polyrotaxane, were also synthesized [150, 151].
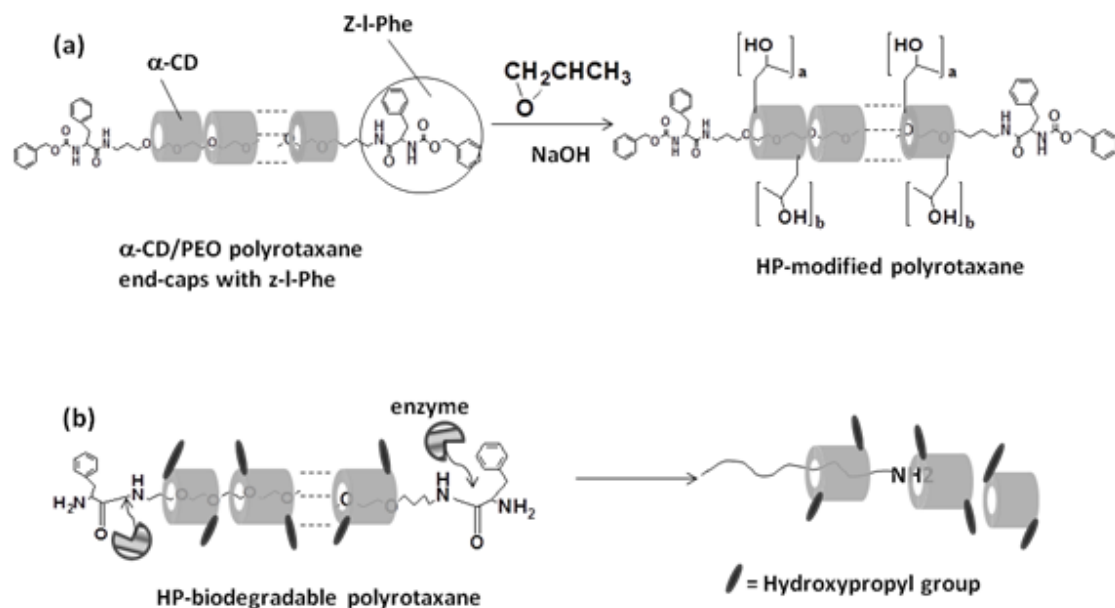
Fig. 2.8 Structure (a) and the degradation mechanism (b) of CD/PEO polyrotaxanes with Z-L-Phe

In gene delivery, due to the flexibility and multivalent interaction, the cationic polyrotaxane with biodegradable terminal linkage has received much attraction. If the end caps can be cleaved intracellularly, the cationic CDs would dethread and disrupt the endosomal membrane because of cholesterol and/or phospholipid inclusion. At the same time, the CD release can convert the multivalent interactions into monovalent interaction thereby releasing the DNA for transfection (Fig. 2.9) [152, 153]. The assumption was first evaluated in Yui's lab [153]. Aminoethylcarbamoyl (AEC) groups were introduced to α-CD which was threaded onto a PEG chain capped with Z-l-Phe linking via labile linkage. In contrast to PEI, the gene delivery system showed enhanced and tight complex formation even at lower N/P ratio.
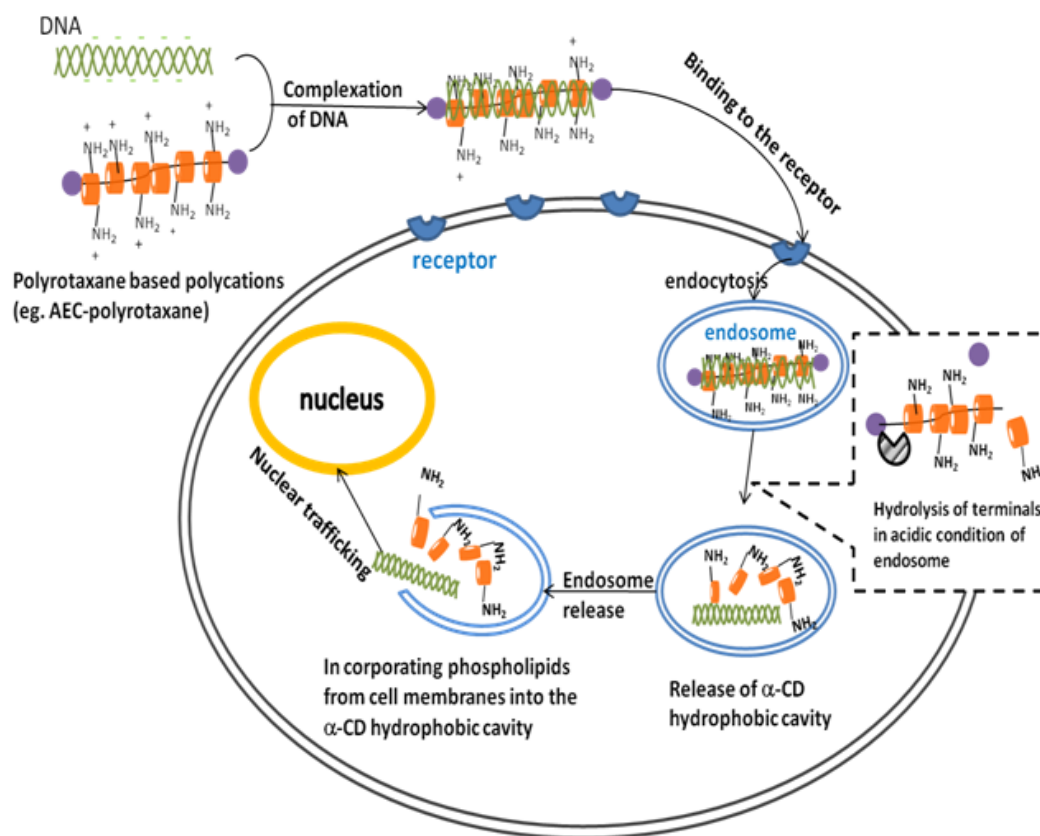
Fig.2.9 Strategies of gene delivery using aminoethylcarbamoyl (AEC)-polyrotaxane

2.4.2 pH-sensitive biodegradable systems for drug and gene delivery

Recently, the pH-triggered dethreading of polyrotaxane was also demonstrated. α-CD terminated polyrotaxane consisting of β-CD and pluronic was biodegradable under acidic conditions due to cleavage of hydrazone bonds in low pH [81]. Similarly, it was reported that α-CD-PEG polyrotaxanes also exhibited dethreading in low pH environment [154]. Such stimuli-responsive polyrotaxane systems can open up a new paradigm of biodegradable materials for biomedical applications.

Similarly, supramolecular aggregates that possessed pH-induced reversible micelle-gel transition were synthesized. The polypseudorotaxane consisted of hydrophilic copolymer PEG-b-PLL-HBr copolymer and α-CD [155]. Micellization of this hydrophilic copolymer due to the block-specific threading of α-CD molecules onto the PEG block yielded supramolecular-structured nanoparticles, which undergoes pH-inducible gelation in aqueous media. Firstly, in pH=4.5, the PLL block was nonthreaded while the PEG block of PEG-b-PLL was included inside the cavity of α-CD, inducing the micelle-like aggregation of the hydrophilic block copolymer to nanoparticles around 30 nm. The water soluble supramolecular nanoparticles possess an insoluble core consisting of inclusion formation α-CD and PEG and a soluble shell of free PLL. When increasing the pH value of the aqueous solution, the solubility of the PLL shell of the nanoparticles was changed and above pH 10, PLL became less soluble and aggregated in aqueous solution, leading to the gel formation. Subsequently it will become micelle solution again when changing to acid condition. The driving force for the formation of the supramolecular hydrogel is believed to be the synergetic effect of selective complexation between PEG block and α-CD, and the pH-inducible hydrophobic interaction between PLL block at pH 10. Such pH

switchable and reversible supramolecular hydrogels may find application in biomedical fields, such as controlled drug or protein release

2.4.3 Disulfide-linkage based biodegradable polymers for drug and gene delivery

In the past decades, reduction-sensitive biodegradable polymers have emerged as an attractive class of biomedical materials as the delivery systems for both biotherapeutics (pDNA, siRNA, peptides and pharmaceutical proteins) as well as low molecular weight drugs. Usually, bioreducible disulfide linkage was introduced to these materials in the main chain, side chain, or in the cross-linker.

The disulfide bonds are subject to rapid degradation under a reductive environment via thiol-disulfide exchange reactions [156]. In eukaryotic cells, Glutathione tripeptide (GSH) is the major redox [157]. Under different intracellular environment, GSH maintain distinct and non-equilibrium level [158]. For example, in cell surface or blood fluids, the concentration of GSH is low (approximately 2-20 μM). So the disulfide linkage is sufficiently stable under the conditions in the circulation as well as in extracellular matrices. However, in the cytosol, disulfide bond may be prone to rapid degradation in minutes to hours due to the high concentration of GSH (0.5-10mM) [159]. Therefore, reduction-sensitive gene carriers in principle could meet the conflicting requirements of an ideal delivery system, i.e. high stability in circulation while rapid degradation inside targeted cells [160].

For cancer therapy, it is often more desirable to accomplish rapid drug release after carriers arrive at the pathological site, which may enhance the therapeutic efficacy as well as reduce the probability of drug resistance in cells. Due to the stimuli-responsive properties of disulfide linkage, reduction-sensitive polymers have

received a tremendous amount of interest for intracellular drug delivery. As a typical example, biodegradable micelles with sheddable PEG shells were synthesized based on poly (ethylene glycol)-SS-poly (ε-caprolactone) (PEG-SS-PCL) diblock copolymer and applied for rapid intracellular release of DOX (Fig. 2.10) [161]. Owning to the reductive cleavage disulfide bonds, it was found that the PEG-SS-PCL micelles were subject to fast aggregation in the presence of 10 mM dithiothreitol (DTT), which is analogous to the intracellular environment such as cytosol. Furthermore, in contrast to the reduction insensitive control, the shell-sheddable micelles with disulfide linkage showed much faster DOX release under a reductive environment. However, no difference in release rate was observed under the non-reductive conditions. The micelles also showed faster higher anticancer efficacy in comparison to the insensitive control. Therefore, the biodegradable micelles with disulfide-linkage are very promising for efficient intracellular drug delivery and to achieve improved anti-cancer therapy. Based on this theory, disulfide bonds were introduced to some other polymer micelles for stimuli-responsive drug delivery [162-165].
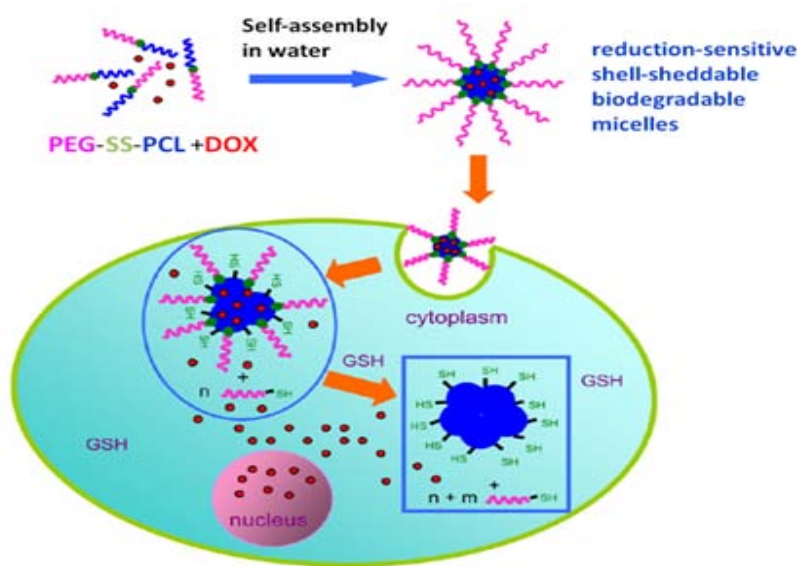
Fig. 2.10 Illustration of reduction-sensitive shell-sheddable biodegradable micelles for efficient intracellular release of anticancer drugs [161]

In gene therapy, the rapid degradation due to the disulfide linkage on the one hand could lead to polyplex dissociation and efficient intracellular release of DNA or siRNA, on the other hand, they may result in low toxicity by avoiding accumulation of high molecular weight polycations inside cells, and finally increasing the transfection efficiency [166]. For example, disulfide bonds were used as cross-linker for the formation of low molecular weight PEI to 25K molecular weight PEI. Gosselin et. al found that the properties of 25KPEI was improved by introducing SS linkage, such as sufficient DNA release, decreased cytotoxicity and high transfection activity [167]. More importantly, disulfide linkage could bring a better balance between DNA release and DNA protection. A group of bioreducible poly (amido amine)s was synthesized with multiple disulfide bonds in the main chain and side chain. The results indicates that the bioreducible polycations could allow sufficient DNA protection in extracellular environment, rapid DNA intracellular release, markedly lower cytotoxicity and enhanced transfection [168].

Due to the dethreading nature of polyrotaxane, disulfide linkage could also be introduced in polyrotaxane. Yui's group designed a cytocleavable polyrotaxane that has supramolecular structure of DMAEC-α-CDs threading onto a PEG chain capped with benzyloxycarbonyl tyrosine (Z-Tyr) via disulfide (SS) linkage (Fig. 2.11a) [140, 169]. The *in vitro* dissociation experiment showed that the DMAEC-SS-PRX systems exhibit sufficient cleavage of SS linkages, as a result of the rapid endosomal escape and pDNA release (Fig. 2.11b). Furthermore, by comparison with a variety of DMAEC-SS-PRXs with different number of DMAEC groups, it was found that the polyplex with lowest number of DMAEC exhibited a much faster pDNA release in cytoplasm. Thus the transfection activity was related to an appropriate timing for

DNA release and high transfection and stability can be achieve by optimizing numbers of DMAEC [170].
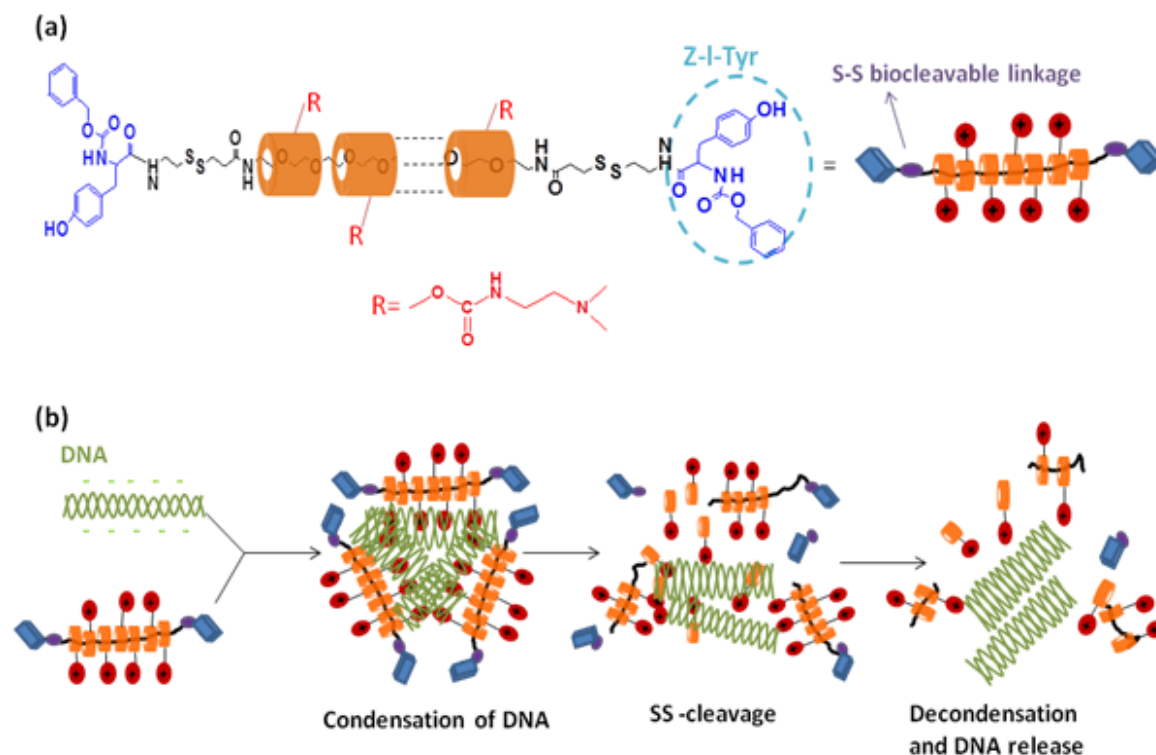
Fig. 2.11 (a) Chemical structure of biocleavable polyrotaxane, and (b) image of the polyplex formation and terminal cleavage-triggered decondesation of the polyplex

2.4.4 Polymer with sheddable shell for drug and gene delivery

Before entering to the target cell, the drug/gene delivery carriers are faced with a set of extracellular barriers, including protein adsorption and cellular adhesion. Specifically, in gene delivery, the stability of polyplex largely depends on the structure and charge. The complexes will aggregate when the charge of the system become neutral. In the case of *in vivo* gene delivery, the polyplex particles could be prone to rapid aggregation due to the negatively charged plasma proteins in the serum or blood, which affect the stability of the positively charged polyplexes. The aggregation could result in nucleic payload release or rapid clearance of the

polyplexes by reticuloendothelial system [171]. Therefore, many polyplexes, including PEI25K, PDMAEMA systems, cannot maintain their stability and high transfection efficiency upon intravenous injection [172].

Introducing a sheddable shell by attaching hydrophilic polymer is one of the most attractive methods to maintain the stability of delivery vehicles against serum. Hydrophilic polymers, such as polyethylene glycol (PEG), N-(2-hydroxypropyl) methacrylamide (HPMA), could be modified to the polymer vectors and formed a "brush" like shell on the surface of the particles [173, 174]. Owing to the steric and surface charge shielding effects of the hydrophilic shell, decreased particle to particle and particle-protein interaction could be achieved, followed by enhanced stability of polyplex against salt-, protein-, and biological non-specific interaction. Basically, the effects depend on grafting density, length of the hydrophilic polymer and the method of conjugation.

Because PEG shows many well-known properties, such as high solubility, biocompatibility and reduced immunogenicity, it is widely modified to polyplex for polymeric or liposomal gene delivery [175-177]. Specifically, PEG shell layer could stabilize the aggregation in the interior of micelles and at the same time provide a "stealth" layer on the surface which could resist protein adsorption and cellular adhesion [178, 179]. For example, supramolecular PEGylated polyplexes were formed based on the self-assembly between admantyl modified PEG and chitosan-grafted-(polyethylenimine-β-CD) [180]. It was found that in contrast to polyplex without PEG the PEGylated polyplexes significantly improved their stability under physiological conditions. A similar method for introducing PEG was also developed by Davis and co-workers [181].

Although PEG modifications are widely applied, they may challenged to some drawbacks, such as lower transfection efficiency and reduced internalization of untargeted polyplexes [182], degradation of DNA by nucleases [183], and lower DNA binding ability [184]. Recently, polymer poly(methacryloxyloxyethyl phosphorylcholine) (pMPC), which has a similar structure to the polar phospholipid group of cell membrane, was developed for the stabilization of polyplex. Similar to PEG, the pMPC-based modifications could avoid the aggregation and unfavourable interactions in the biological fluids [185, 186]. Licciardi et. al reports that the copolymer micelles with hydrophilic MPC shell are biocompatible and could suppress the unwanted interactions between drug and plasma protein [185].

2.5 POLETHYLENEIMINE (PEI) AS GENE DELIVERY VECTORS

PEI has been one of the most popularly employed cationic gene carriers due to its superior transfection efficiency and consistency of transfection in many different types of cells. They are often considered as the gold standard of gene transfection. The first successful polyethyleneimine-mediated DNA and oligonucleotides transfer was conducted in 1995 by Jean-Paul Behr [34]. Since then, numerous publications have appeared on studies of PEI as gene delivery vectors. PEI has been derivatized to improve the physicochemical and biological properties of polyplexes [187]. There are two principal structures for PEI, branched and linear. Branched PEI could be synthesized by polymerization under acidic conditions based on aziridine monomers while linear PEI can be obtained by polymerization or hydrolyzation of poly (2-propyl-2-oxazoline) under highly acidic conditions [188, 189].

The development of well-known "proton sponge" effect has explained, in some part, the high transfection efficiency of PEI. PEI has high cationic charge density resulting from every third carbon [190]. In according to theoretical calculations, the ratio of primary/secondary/tertiary amines of branched PEI is 1:2:1 [191]. Due to the high density of amines, the nitrogens of PEI could be protonated and the protonation degree is proportional to the pH of the environment. Basically, by comparison with physiological pH, less amines remain unprotonated at pH of 5 [192]. The unprotonated amines with different pKa values confer a buffering capacity over a wide range of pH. The buffering property gives PEI an opportunity to escape from the endosome [190], protecting the DNA from degradation in the endosomal compartment during the maturation of the endosome to lysosome, facilitating intracellular trafficking of DNA [193]. Some studies confirmed, at least partially, confirmed this theory. The buffering effect of PEI was supported by the study of Sonawane, which found higher chloride concentration and decreased acidification of PEI polyplexes in contrast to those of polylysine [194]. It was also found that, the transfection efficiency of PEI could be reduced after the removal of protonable amines in PEI or by introducing bafilomycin A, an inhibitor of the intracellular proton pump, into the system. The results verified the "proton sponge" effect [195, 196].

The molecular weight is often considered as one of the most important factors that could influence the transfection activity of PEI. Godbey et al. found that when increasing the molecular-weight of bPEI for transfection, both transfection efficiency and cytotoxicity increased [197-199]. It is probably because the high cation density of PEI contributes to the formation of highly condensed particles by interacting with DNA but this may confer significant cytotoxicity [200]. The toxicity could be due to

the necrosis, which is caused by aggregation and adherence on the cell surface [201].Typically, the optimal molecular weight of PEI is between 5~25 kDa [187]. Apart from molecular weight, the branched type and size of PEI polyplex could also affect the transfection efficiency *in vitro*. Aggregated polyplexes could increase cellular association and improve nuclear access due to membrane rupture [202]. For example, linear PEI shows lower complexation capability and larger polyplex aggregates than branched PEI [203], but studies with linear PEIs found that LPEI at 22kDa exhibited even higher transfection efficiency and lower cytotoxicity compared to branched PEI [204-206].

Due to the amine nitrogens, PEI is flexible to be conjugated with functional groups to improve their properties. For example, PEI-PEG grafted copolymers demonstrated a reduced cytotoxicity while maintaining transfection efficiency [207]. Conjugation of a targeting moiety like folate or antibody shows varied transfection efficiency in different cells, indicating that transfection efficiency is not based solely on the properties of the polymer but also cell type as different internalization might be involved [208, 209].

2.6 POLY(2-(DIMETHYLAMINO)ETHYL METHACRYLATE) (PDMAEMA) AS GENE VECTORS

Due to the biocompatibility of methacrylate polymers, they are also applied to the microencapsulation of cells without tissue rejection in cell transplantation [210]. The combination properties of methacrylates, such as biocompatibility, relatively easy synthesis and functionalization, make them as promising candidates for gene delivery

and led to the idea of synthesis of poly (2-[dimethylamino]ethyl methacrylate) (pDMAEMA)-based polymers for gene therapy.

pDMAEMA is a synthetic polymer with tertiary amino groups on the side chain (Fig. 2.12). It is water soluble and owning to its positive charged surface, it could compact DNA into small particles by electrostatic interaction [211]. Basically, the degree of cellular uptake of the polyplex strongly depends on the size and charge of pDMAEMA, which is relative to the ratio of the polymer to DNA [212]. At low pDMAEMA: pDNA ratios (w/w), the polyplex have a negative charge and relative large particle size. When the polymer: plasmid ratios are above 3:1, small and positive zeta potential can be observed, which are favorable factors for transfection [213]. It was found that the polyplexes with a size around 200 nm and positive zeta potential (25mV-30mV) possess the highest transfection activity [214]. In addition to the polymer/DNA ratio, the molecular weight of pDMAEMA also adds effect on the DNA condensation. It has been reported that the average molecular weight of pDMAEMA should be above 100Kg/mol in order to give sufficient condensation of pDNA [215]. The PDMAEMA/pDNA complexes show higher transfection efficiency than that of DEAE-dextran/DNA and poly(L-lysine) (PLL)/DNA complexes. And their cytotoxicity is higher than DEAE-dextran, but lower than PLL [215]. Interestingly, in contrast to DEAE-dextran and PLL, the transfection activity of the polymer complexes is not affected by serum protein. A recent study showed that higher molecular weight PDMAEMA had a greater binding affinity to pDNA than lower molecular weight. Furthermore the molecular weight of PDMAEMA was found to have an influence on transfection efficiency, and the gene expression increased with the increasing molecular weight. However, cellular uptake of polyplexes was

determined to be insensitive to PDMAEMA molecular weight [216]. In another study, three kinds of PDMAEMA (linear, highly-branched, and star-shaped) were synthesized to investigate the gene delivery ability. It was found that the DNA compaction and cellular uptake are similar for all three polycations, but the star-shaped PDMAEMA showed the highest transfection efficiency, which is of similar orders as branched PEI [217].
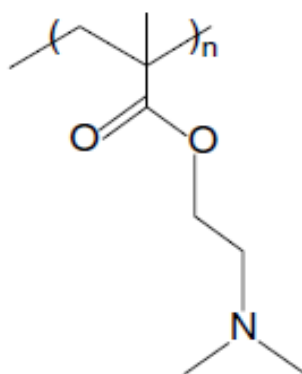
Fig. 2.12 Chemical structure of pDMAEMA

There have been several attempts made to explain the high transfection efficiency of pDMAEMA. Assuming the polyplexes enter cells through endocytosis, earlier workers proposed that PDMAEMA acts with a "proton sponge" effect to enhance endosome/lysosome escape. At physiological pH, pDMAEMA, which like PEI, is partially protonated due to its average pKa value of 7.5. It might result in the disruption of endosmes, facilitating the release of DNA into the cytosol [218]. The proton sponge effect could also cause the release of cytotoxic lysosomal enzymers into the cytosol, and resulting in high cytotoxicity [218]. However, Dubruel's and Jones's groups found some different results from the above hypothesis [219-221]. For example, in Dubruel's study, the polymethacrylates which containing acid functions show buffering properties in analogy with "PEI proton sponge". But they have a

lower transfection efficiency, probably owning to a limited cell uptake. The result indicates that the buffering capability of the synthetic polymers is not necessarily the crucial factor in the transfection process [219, 220].

Cytotoxicity, lack of cell specificity and serum-induced aggregation are the major obstacles to application of pDMAEMA-based polyplexes to gene delivery. Similar with PEI, the molecular weight of the polymer plays an important role to the cytotoxicity [201]. Generally, the cytotoxicity of polymer appears to increase with the increasing of molecular weight. Membrane disruption, apoptosis and cytotoxicity of PDMAEMA increased with their chain length [222]. Therefore, it was suggested that one of the most rational ways to decrease cytotoxicity and enhance gene transfection efficiency could be achieved by combining low molecular weight transfection segments with degradable linkages and forming a combined large molecular weight transfection polymer. In addition, because it was reported that higher zeta potential of polyplexes could lead to significant cytotoxicity [223], PEGlyation is a well verified method to decrease cytotoxicity due to its shielding effect on the surface charge of particles [224-226]. Furthermore, PEG shell layer could also stabilize the aggregation in the interior of micelles and at the same time provide a "stealth" layer on the surface which could resist protein adsorption and cellular adhesion [178, 179].

Recently, a group of reduction-responsive polymer and conjugates was synthesized based on PDMAEMA for gene delivery [227-229]. Generally, they contain disulfide-linkage, which is prone to rapid degradation in reductive intracellular environment and cell nucleus. They showed distinct features different from their normally hydrolytically degradable counterparts: on the one hand they could lead to polyplex dissociation and efficient intracellular release of DNA or

siRNA, on the other hand, they may result in low toxicity by avoiding accumulation of high molecular weight polycations inside cells, and finally increasing the transfection efficiency [158]. For example, based on the structure of PDMAEMA-PCL-PDMAEMA triblock copolymers for high efficient siRNA delivery [230], Zhu, et. al designed reduction-responsive cationic biodegradable micelles by introducing SS bonds into the systems. PDMAEMA-SS-PCL-SS-PDMAEMA triblock copolymers were prepared through RAFT polymerization. They found that the micelles could effectively condense DNA into stable polyplexes under physiological salt conditions. However, they are subject rapidly degradation and releasing DNA in and intracellular mimicking reductive environment. More importantly, the reduction-sensitive micelles revealed much lower cytotoxicity than the reduction-insensitive control, indicating that the reduction-responsive biodegradable micelles are a promising candidate for safe and efficient gene delivery [227].

In addition to gene delivery, biodegradable PDMAEMA-PCL-PDMAEMA triblock copolymer was also prepared for siRNA and paclitaxel codelivery. Significant enhanced gene silencing efficiency of the polycations micelles was observed as compared to 20K PDMAEMA or 25K PEI. Moreover, due to the improved cellular uptake, micelle loaded with paclitaxel displayed higher drug efficacy than free drug. These results suggested that cationic biodegradable micelles are highly promising for the combinatorial delivery of siRNA and lipophilic anticancer drugs [230].

2.7 REFERENCES

1. Fundueanu G, Constantin M, Ascenzi P. Preparation and characterization of pH- and temperature-sensitive pullulan microspheres for controlled release of drugs. Biomaterials 2008 Jun;29(18):2767-2775.
2. Huynh DP, Nguyen MK, Pi BS, Kim MS, Chae SY, Kang CL, et al. Functionalized injectable hydrogels for controlled insulin delivery. Biomaterials 2008 Jun;29(16):2527-2534.
3. Wang YC, Liu XQ, Sun TM, Xiong MH, Wang J. Functionalized micelles from block copolymer of polyphosphoester and poly(epsilon-caprolactone) for receptor-mediated drug delivery. Journal of Controlled Release 2008 May;128(1):32-40.
4. Mok H, Park JW, Park TG. Enhanced intracellular delivery of quantum dot and adenovirus nanoparticles triggered by acidic pH via surface charge reversal. Bioconjugate Chemistry 2008 Apr;19(4):797-801.
5. He CL, Kim SW, Lee DS. In situ gelling stimuli-sensitive block copolymer hydrogels for drug delivery. Journal of Controlled Release 2008 May;127(3):189-207.
6. Hou DD, Tong XM, Yu HQ, Zhang AY, Feng ZG. A kind of novel biodegradable hydrogel made from copolymerization of gelatin with polypseudorotaxanes based on alpha-CDs. Biomedical Materials 2007 Sep;2(3):S147-S152.
7. Cerritelli S, Velluto D, Hubbell JA. PEG-SS-PPS: Reduction-sensitive disulfide block copolymer vesicles for intracellular drug delivery. Biomacromolecules 2007 Jun;8(6):1966-1972.
8. Napoli A, Boerakker MJ, Tirelli N, Nolte RJM, Sommerdijk N, Hubbell JA. GluCOSe-oxidase based self-destructing polymeric vesicles. Langmuir 2004 Apr;20(9):3487-3491.
9. Quaglia F, Ostacolo L, Mazzaglia A, Villari V, Zaccaria D, Sciortino MT. The intracellular effects of non-ionic amphiphilic cyclodextrin nanoparticles in the delivery of anticancer drugs. Biomaterials 2009 Jan;30(3):374-382.
10. Xiao K, Luo JT, Fowler WL, Li YP, Lee JS, Xing L, et al. A self-assembling nanoparticle for paclitaxel delivery in ovarian cancer. Biomaterials 2009 Oct;30(30):6006-6016.
11. Beduneau A, Saulnier P, Benoit JP. Active targeting of brain tumors using nanocarriers. Biomaterials 2007 Nov;28(33):4947-4967.
12. Li YY, Zhang XZ, Cheng H, Zhu JL, Cheng SX, Zhuo RX. Self-assembled, thermosensitive PCL-g-P(NIPAAm-co-HEMA) micelles for drug delivery. Macromolecular Rapid Communications 2006 Nov;27(22):1913-1919.
13. Ni XP, Cheng A, Li J. Supramolecular hydrogels based on self-assembly between PEO-PPO-PEO triblock copolymers and alpha-cyclodextrin. Journal of Biomedical Materials Research Part A 2009 Mar;88A(4):1031-1036.
14. Tamilvanan S, Venkateshan N, Ludwig A. The potential of lipid- and polymer-based drug delivery carriers for eradicating biofilm consortia on device-related nosocomial infections. Journal of Controlled Release 2008 May;128(1):2-22.

15. Connal LA, Li Q, Quinn JF, Tjipto E, Caruso F, Qiao GG. PH-responsive poly(acrylic acid) core cross-linked star polymers: Morphology transitions in solution and multilayer thin films. Macromolecules 2008 Apr;41(7):2620-2626.

16. Kurkuri MD, Nussio MR, Deslandes A, Voelcker NH. Thermosensitive copolymer coatings with enhanced wettability switching. Langmuir 2008 Apr;24(8):4238-4244.

17. Sun XZ, Zeng MH, Wang B, Ye BH, Chen XM. Supramolecular architectures of metallomacrocyclic and coordination polymers with dicarboxylate and 4,4 '-bis(imidazol-1-ylmethyl)biphenyl ligands. Journal of Molecular Structure 2007 Feb;828(1-3):10-14.

18. Shah NM, Pool MD, Metters AT. Influence of network structure on the degradation of photo-cross-linked PLA-b-PEG-b-PLA hydrogels. Biomacromolecules 2006 Nov;7(11):3171-3177.

19. Nolkrantz K, Farre C, Brederlau A, Karlsson RID, Brennan C, Eriksson PS, et al. Electroporation of single cells and tissues with an electrolyte-filled capillary. Analytical Chemistry 2001 Sep;73(18):4469-4477.

20. Bateman AR, Harrington KJ, Melcher AA, Vile RG. Cancer gene therapy: developments to 2000. Expert Opinion on Investigational Drugs 2000 Dec;9(12):2799-2813.

21. Rideout WM, 3rd, Hochedlinger K, Kyba M, Daley GQ, Jaenisch R. Correction of a genetic defect by nuclear transplantation and combined cell and gene therapy. Cell 2002 Apr 5;109(1):17-27.

22. Cavazzana-Calvo M, Hacein-Bey S, de Saint Basile G, Gross F, Yvon E, Nusbaum P, et al. Gene therapy of human severe combined immunodeficiency (SCID)-X1 disease. Science 2000 Apr 28;288(5466):669-672.

23. Kaplitt MG, Feigin A, Tang C, Fitzsimons HL, Mattis P, Lawlor PA, et al. Safety and tolerability of gene therapy with an adeno-associated virus (AAV) borne GAD gene for Parkinson's disease: an open label, phase I trial. Lancet 2007 Jun 23;369(9579):2097-2105.

24. Ford KG, Souberbielle BE, Darling D, Farzaneh F. Protein transduction: an alternative to genetic intervention? Gene Ther 2001 Jan;8(1):1-4.

25. Yang ZR, Wang HF, Zhao J, Peng YY, Wang J, Guinn BA, et al. Recent developments in the use of adenoviruses and immunotoxins in cancer gene therapy. Cancer Gene Ther 2007 Jul;14(7):599-615.

26. Breyer B, Jiang W, Cheng H, Zhou L, Paul R, Feng T, et al. Adenoviral vector-mediated gene transfer for human gene therapy. Curr Gene Ther 2001 Jul;1(2):149-162.

27. Anderson WF. Human gene therapy. Nature 1998 Apr 30;392(6679 Suppl):25-30.

28. Verma IM, Somia N. Gene therapy -- promises, problems and prospects. Nature 1997 Sep 18;389(6648):239-242.

29. Tripathy SK, Black HB, Goldwasser E, Leiden JM. Immune responses to transgene-encoded proteins limit the stability of gene expression after injection of replication-defective adenovirus vectors. Nat Med 1996 May;2(5):545-550.

30. Barthel F, Remy JS, Loeffler JP, Behr JP. Gene transfer optimization with lipospermine-coated DNA. DNA Cell Biol 1993 Jul-Aug;12(6):553-560.

31. Park TG, Jeong JH, Kim SW. Current status of polymeric gene delivery systems. Adv Drug Deliv Rev 2006 Jul 7;58(4):467-486.

32. Ferber D. Gene therapy. Safer and virus-free? Science 2001 Nov 23;294(5547):1638-1642.

33. Mairhofer J, Grabherr R. Rational vector design for efficient non-viral gene delivery: challenges facing the use of plasmid DNA. Mol Biotechnol 2008 Jun;39(2):97-104.

34. Boussif O, Lezoualc'h F, Zanta MA, Mergny MD, Scherman D, Demeneix B, et al. A versatile vector for gene and oligonucleotide transfer into cells in culture and in vivo: polyethylenimine. Proc Natl Acad Sci U S A 1995 Aug 1;92(16):7297-7301.

35. Wagner E, Ogris M, Zauner W. Polylysine-based transfection systems utilizing receptor-mediated delivery. Adv Drug Deliv Rev 1998 Mar 2;30(1-3):97-113.

36. Bielinska AU, Yen A, Wu HL, Zahos KM, Sun R, Weiner ND, et al. Application of membrane-based dendrimer/DNA complexes for solid phase transfection in vitro and in vivo. Biomaterials 2000 May;21(9):877-887.

37. Mumper RJ, Duguid JG, Anwer K, Barron MK, Nitta H, Rolland AP. Polyvinyl derivatives as novel interactive polymers for controlled gene delivery to muscle. Pharm Res 1996 May;13(5):701-709.

38. Leong KW, Mao HQ, Truong-Le VL, Roy K, Walsh SM, August JT. DNA-polycation nanospheres as non-viral gene delivery vehicles. J Control Release 1998 Apr 30;53(1-3):183-193.

39. Yang C, Li H, Goh SH, Li J. Cationic star polymers consisting of alpha-cyclodextrin core and oligoethylenimine arms as nonviral gene delivery vectors. Biomaterials 2007 Jul;28(21):3245-3254.

40. You YZ, Manickam DS, Zhou QH, Oupicky D. Reducible poly(2-dimethylaminoethyl methacrylate): synthesis, cytotoxicity, and gene delivery activity. J Control Release 2007 Oct 8;122(3):217-225.

41. Kataoka K. Smart polymeric micelles as nanocarriers for gene and drug delivery, 2004.

42. Nishiyama N, Okazaki S, Cabral H, Miyamoto M, Kato Y, Sugiyama Y, et al. Novel cisplatin-incorporated polymeric micelles can eradicate solid tumors in mice. Cancer Research 2003;63(24):8977-8983.

43. Kataoka K, Harada A, Nagasaki Y. Block copolymer micelles for drug delivery: design, characterization and biological significance. Advanced Drug Delivery Reviews 2001 Mar;47(1):113-131.

44. Wang YC, Tang LY, Sun TM, Li CH, Xiong MH, Wang J. Self-assembled micelles of biodegradable triblock copolymers based on poly(ethyl ethylene phosphate) and poly(epsilon-caprolactone) as drug carriers. Biomacromolecules 2008 Jan;9(1):388-395.

45. Cheng C, Wei H, Shi BX, Cheng H, Li C, Gu ZW, et al. Biotinylated thermoresponsive micelle self-assembled from double-hydrophilic block copolymer for drug delivery and tumor target. Biomaterials 2008 Feb;29(4):497-505.

46. Maeda H, Wu J, Sawa T, Matsumura Y, Hori K. Tumor vascular permeability and the EPR effect in macromolecular therapeutics: a review. Journal of Controlled Release 2000 Mar;65(1-2):271-284.

47. Matsumura Y, Maeda H. A new concept for macromolecular therapeutics in cancer-chemotherapy mechanism of tumoritropic accumulation of proteins and the antitumor agent smancs. Cancer Research 1986 Dec;46(12):6387-6392.

48. Jenekhe SA, Chen XL. Self-assembled aggregates of rod-coil block copolymers and their solubilization and encapsulation of fullerenes. Science 1998 Mar;279(5358):1903-1907.

49. Xiao NY, Li AL, Liang H, Lu J. A well-defined novel aldehyde-functionalized glycopolymer: Synthesis, micelle formation, and its protein immobilization. Macromolecules 2008 Apr;41(7):2374-2380.

50. Matsumura Y, Hamaguchi T, Ura T, Muro K, Yamada Y, Shimada Y, et al. Phase I clinical trial and pharmacokinetic evaluation of NK911, a micelle-encapsulated doxorubicin. British Journal of Cancer 2004 Nov;91(10):1775-1781.

51. Lin JP, Zhu JQ, Chen T, Lin SL, Cai CH, Zhang LS, et al. Drug releasing behavior of hybrid micelles containing polypeptide triblock copolymer. Biomaterials 2009 Jan;30(1):108-117.

52. Lo CL, Lin KM, Huang CK, Hsiue GH. Self-assembly of a micelle structure from graft and diblock copolymers: An example of overcoming the limitations of polyions in drug delivery. Advanced Functional Materials 2006 Dec;16(18):2309-2316.

53. Ko J, Park K, Kim YS, Kim MS, Han JK, Kim K, et al. Tumoral acidic extracellular pH targeting of pH-responsive MPEG-poly (beta-amino ester) block copolymer micelles for cancer therapy. Journal of Controlled Release 2007 Nov;123(2):109-115.

54. Discher BM, Won YY, Ege DS, Lee JCM, Bates FS, Discher DE, et al. Polymersomes: Tough vesicles made from diblock copolymers. Science 1999 May;284(5417):1143-1146.

55. Qiu LY, Zheng C, Jin Y, Zhu KJE. Polymeric micelles as nanocarriers for drug delivery. Expert Opinion on Therapeutic Patents 2007 Jul;17(7):819-830.

56. Nishiyama N, Kataoka K. Current state, achievements, and future prospects of polymeric micelles as nanocarriers for drug and gene delivery. Pharmacology & Therapeutics 2006 Dec;112(3):630-648.

57. Croy SR, Kwon GS. Polymeric micelles for drug delivery. Current Pharmaceutical Design 2006;12(36):4669-4684.

58. Forrest ML, Won CY, Malick AW, Kwon GS. In vitro release of the mTOR inhibitor rapamycin from poly(ethylene glycol)-b-poly(epsilon-caprolactone) micelles. Journal of Controlled Release 2006 Jan;110(2):370-377.

59. Zhang Y, Jin T, Zhuo RX. Methotrexate-loaded biodegradable polymeric micelles: Preparation, physicochemical properties and in vitro drug release. Colloids and Surfaces B-Biointerfaces 2005 Aug;44(2-3):104-109.

60. Yang ZL, Li XR, Yang KW, Liu Y. Amphotericin B-loaded poly(ethylene glycol)-poly(lactide) micelles: Preparation, freeze-drying, and in vitro release. Journal of Biomedical Materials Research Part A 2008 May;85A(2):539-546.

61. Bae Y, Fukushima S, Harada A, Kataoka K. Design of environment-sensitive supramolecular assemblies for intracellular drug delivery: Polymeric micelles that are responsive to intracellular pH change. Angewandte Chemie-International Edition 2003;42(38):4640-4643.

62. Bae Y, Nishiyama N, Fukushima S, Koyama H, Yasuhiro M, Kataoka K. Preparation and biological characterization of polymeric micelle drug carriers

with intracellular pH-triggered drug release property: Tumor permeability, controlled subcellular drug distribution, and enhanced in vivo antitumor efficacy. Bioconjugate Chemistry 2005 Jan-Feb;16(1):122-130.

63. Lee ES, Na K, Bae YH. Polymeric micelle for tumor pH and folate-mediated targeting. Journal of Controlled Release 2003 Aug;91(1-2):103-113.

64. Putnam D. Polymers for gene delivery across length scales. Nature Materials 2006 Jun;5(6):439-451.

65. Jiang X, Dai H, Ke CY, Mo X, Torbenson MS, Li ZP, et al. PEG-b-PPA/DNA micelles improve transgene expression in rat liver through intrabiliary infusion. Journal of Controlled Release 2007 Oct;122(3):297-304.

66. Harada-Shiba M, Yamauchi K, Harada A, Takamisawa I, Shimokado K, Kataoka K. Polyion complex micelles as vectors in gene therapy - pharmacokinetics and in vivo gene transfer. Gene Therapy 2002 Mar;9(6):407-414.

67. Wiradharma N, Khan M, Tong YW, Wang S, Yang YY. Self-assembled cationic peptide nanoparticles capable of inducing efficient gene expression in vitro. Advanced Functional Materials 2008 Mar;18(6):943-951.

68. Nah JW, Yu L, Han SO, Ahn CH, Kim SW. Artery wall binding peptide-poly (ethylene glycol)-grafted-poly(L-lysine)-based gene delivery to artery wall cells. Journal of Controlled Release 2002 Jan;78(1-3):273-284.

69. Vinogradov S, Batrakova E, Li S, Kabanov A. Polyion complex micelles with protein-modified corona for receptor-mediated delivery of oligonucleotides into cells. Bioconjugate Chemistry 1999 Sep-Oct;10(5):851-860.

70. Wang Y, Gao SJ, Ye WH, Yoon HS, Yang YY. Co-delivery of drugs and DNA from cationic core-shell nanoparticles self-assembled from a biodegradable copolymer. Nature Materials 2006 Oct;5(10):791-796.

71. Wang Y, Ke CY, Beh CW, Liu SQ, Goh SH, Yang YY. The self-assembly of biodegradable cationic polymer micelles as vectors for gene transfection. Biomaterials 2007 Dec;28(35):5358-5368.

72. Wang Y, Wang LS, Goh SH, Yang YY. Synthesis and characterization of cationic micelles self-assembled from a biodegradable copolymer for gene delivery. Biomacromolecules 2007 Mar;8(3):1028-1037.

73. Harada A, Kamachi M. Complex formation between poly(ethylene glycol) and alpha-cyclodextrin. Macromolecules 1990 May;23(10):2821-2823.

74. Harada A, Li J, Kamachi M. The molecular necklace-a rotaxane containing many threaded alpha-cyclodextrins. Nature 1992 Mar;356(6367):325-327.

75. Wenz G, Keller B. Threading cyclodextrin rings on polymer chains. Angew Chem-Int Edit Engl 1992 Feb;31(2):197-199.

76. Wenz G. Cyclodextrin as building blocks for supramolecular structures and functional units. Angew Chem-Int Edit Engl 1994 May;33(8):803-822.

77. Nepogodiev SA, Stoddart JF. Cyclodextrin-Based Catenanes and Rotaxanes. Chem Rev 1998 Jul 30;98(5):1959-1976.

78. Li J, Loh XJ. Cyclodextrin-based supramolecular architectures: Syntheses, structures, and applications for drug and gene delivery. Adv Drug Deliv Rev 2008 Jun;60(9):1000-1017.

79. Raymo FM, Stoddart JF. Interlocked Macromolecules. Chem Rev 1999 Jul 14;99(7):1643-1664.

80. Born M, Ritter H. Topologically unique side-chain polyrotaxanes based on triacetyl-beta-cyclodextrin and a poly(ether sulfone) main chain. Macromolecular Rapid Communications 1996 Apr;17(4):197-202.

81. Ooya T, Ito A, Yui N. Preparation of alpha-cyclodextrin-terminated polyrotaxane consisting of beta-cyclodextrins and pluronic as a building block of a biodegradable network. Macromol Biosci 2005 May;5(5):379-383.

82. Li J, Li X, Zhou ZH, Ni XP, Leong KW. Formation of supramolecular hydrogels induced by inclusion complexation between pluronics and alpha-cyclodextrin. Macromolecules 2001 Oct;34(21):7236-7237.

83. Peet J, Rusa CC, Hunt MA, Tonelli AE, Balik CM. Solid-state complexation of poly(ethylene glycol) with alpha-cyclodextrin. Macromolecules 2005 Jan;38(2):537-541.

84. Singla S, Zhao T, Beckham HW. Purification of cyclic polymers prepared from linear precursors by inclusion complexation of linear byproducts with cyclodextrins. Macromolecules 2003 Sep;36(18):6945-6948.

85. Li J, Ni XP, Leong KW. Injectable drug-delivery systems based on supramolecular hydrogels formed by poly(ethylene oxide) and alpha-cyclodextrin. Journal of Biomedical Materials Research Part A 2003;65A(2):196-202.

86. Li J, Li X, Ni XP, Wang X, Li HZ, Leong KW. Self-assembled supramolecular hydrogels formed by biodegradable PEO-PHB-PEO triblock copolymers and alpha-cyclodextrin for controlled drug delivery. Biomaterials 2006;27(22):4132-4140.

87. Wang J, Li L, Zhu YY, Liu P, Guo XH. Hydrogels assembled by inclusion complexation of poly(ethylene glycol) with alpha-cyclodextrin. Asia-Pacific Journal of Chemical Engineering 2009 Sep-Oct;4(5):544-550.

88. Li J, Harada A, Kamachi M. Sol-gel transition durintg inclusion complex-formation between alpha-cyclodextrin and high-molecular-weight poly(ethylene glycol)s in aqueous-solution. Polymer Journal 1994;26(9):1019-1026.

89. Bromberg LE, Ron ES. Temperature-responsive gels and thermogelling polymer matrices for protein and peptide delivery. Advanced Drug Delivery Reviews 1998 May;31(3):197-221.

90. Loh XJ, Goh SH, Li J. New biodegradable thermogelling copolymers having very low gelation concentrations. Biomacromolecules 2007 Feb;8(2):585-593.

91. Rodriguez-Perez AI, Rodriguez-Tenreiro C, Alvarez-Lorenzo C, Concheiro A, Torres-Labandeira JJ. Drug solubilization and delivery from cyclodextrin-pluronic aggregates. Journal of Nanoscience and Nanotechnology 2006 Sep-Oct;6(9-10):3179-3186.

92. Li X, Li J, Leong KW. Preparation and characterization of inclusion complexes of biodegradable amphiphilic poly(ethylene oxide)-poly[(R)-3-hydroxybutyrate]-poly(ethylene oxide) triblock copolymers with cyclodextrins. Macromolecules 2003 Feb;36(4):1209-1214.

93. Li X, Li J, Leong KW. Role of intermolecular interaction between hydrophobic blocks in block-selected inclusion complexation of amphiphilic poly(ethylene oxide)-poly[(R)-3-hydroxybutyrate]-poly(ethylene oxide) triblock copolymers with cyclodextrins. Polymer 2004 Sep;45(20):6845-6851.

94. Liu KL, Goh SH, Li J. Controlled synthesis and characterizations of amphiphilic poly[(R,S)-3-hydroxybutyrate]-poly(ethylene glycol)-poly [(R,S)-3-hydroxybutyrate] triblock copolymers. Polymer 2008 Feb;49(3):732-741.

95. Liu KL, Zhu JL, Li J. Elucidating rheological property enhancements in supramolecular hydrogels of short poly[(R,S)-3-hydroxybutyrate]-based amphiphilic triblock copolymer and alpha-cyclodextrin for injectable hydrogel applications. Soft Matter 2010;6(10):2300-2311.

96. Wang YP, Zhou L, Sun GM, Xue J, Jia ZF, Zhu XY, et al. Construction of different supramolecular polymer systems by combining the host-guest and hydrogen-bonding interactions. Journal of Polymer Science Part B-Polymer Physics 2008 Jun;46(12):1114-1120.

97. Huh KM, Ooya T, Lee WK, Sasaki S, Kwon IC, Jeong SY, et al. Supramolecular-structured hydrogels showing a reversible phase transition by inclusion complexation between poly(ethylene glycol) grafted dextran and alpha-cyclodextrin. Macromolecules 2001 Dec;34(25):8657-8662.

98. Huh KM, Cho YW, Chung H, Kwon IC, Jeong SY, Ooya T, et al. Supramolecular hydrogel formation based on inclusion complexation between poly(ethylene glycol)-modified chitosan and alpha-cyclodextrin. Macromolecular Bioscience 2004 Feb;4(2):92-99.

99. Nakama T, Ooya T, Yui N. Temperature- and pH-controlled hydrogelation of poly(ethylene glycol)-grafted hyaluronic acid by inclusion complexation with alpha-cyclodextrin. Polymer Journal 2004;36(4):338-344.

100. Choi HS, Kontani K, Huh KM, Sasaki S, Ooya T, Lee WK, et al. Rapid induction of thermoreversible hydrogel formation based on poly(propylene glycol)-grafted dextran inclusion complexes. Macromolecular Bioscience 2002 Aug;2(6):298-303.

101. He LH, Huang J, Chen YM, Xu XJ, Liu LP. Inclusion interaction of highly densely PEO grafted polymer brush and alpha-cyclodextrin. Macromolecules 2005 May;38(9):3845-3851.

102. Karino T, Okumura Y, Zhao CM, Kidowaki M, Kataoka T, Ito K, et al. Sol-gel transition of hydrophobically modified polyrotaxane. Macromolecules 2006 Dec;39(26):9435-9440.

103. Kidowaki M, Zhao CM, Kataoka T, Ito K. Thermoreversible sol-gel transition of an aqueous solution of polyrotaxane composed of highly methylated alpha-cyclodextrin and polyethylene glycol. Chemical Communications 2006(39):4102-4103.

104. Fleury G, Schlatter G, Brochon C, Travelet C, Lapp A, Lindner P, et al. Topological polymer networks with sliding cross-link points: The "sliding gels". Relationship between their molecular structure and the viscoelastic as well as the swelling properties. Macromolecules 2007 Feb;40(3):535-543.

105. Zhao CM, Domon Y, Okumura Y, Okabe S, Shibayama M, Ito K. Sliding mode of cyclodextrin in polyrotaxane and slide-ring gel. Journal of Physics-Condensed Matter 2005 Aug;17(31):S2841-S2846.

106. Murayama H, Bin Imran A, Nagano S, Seki T, Kidowaki M, Ito K, et al. Chromic slide-ring gel based on reflection from photonic bandgap. Macromolecules 2008 Mar;41(5):1808-1814.

107. Ooya T, Akutsu M, Kumashiro Y, Yui N. Temperature-controlled erosion of poly(N-isopropylacrylamide)-based hydrogels crosslinked by methacrylate-

introduced hydrolyzable polyrotaxane. Science and Technology of Advanced Materials 2005 Jul;6(5):447-451.

108. Zhang XW, Zhu XQ, Ke FY, Ye L, Chen EQ, Zhang AY, et al. Preparation and self-assembly of amphiphilic triblock copolymers with polyrotaxane as a middle block and their application as carrier for the controlled release of Amphotericin B. Polymer 2009 Aug;50(18):4343-4351.

109. Huang J, Ren LX, Zhu H, Chen YM. Hydrophilic block copolymer aggregation in solution induced by selective threading of cyclodextrins. Macromolecular Chemistry and Physics 2006 Oct;207(19):1764-1772.

110. Yui N, Katoono R, Yamashita A. Functional Cyclodextrin Polyrotaxanes for Drug Delivery. Inclusion Polymers, 2009. p. 55-77.

111. Ooya T, Yui N. Synthesis of theophylline-polyrotaxane conjugates and their drug release via supramolecular dissociation. Journal of Controlled Release 1999 Apr;58(3):251-269.

112. Mammen M, Choi SK, Whitesides GM. Polyvalent interactions in biological systems: Implications for design and use of multivalent ligands and inhibitors. Angewandte Chemie-International Edition 1998;37(20):2755-2794.

113. Cairo CW, Gestwicki JE, Kanai M, Kiessling LL. Control of multivalent interactions by binding epitope density. Journal of the American Chemical Society 2002 Feb;124(8):1615-1619.

114. Nelson A, Belitsky JM, Vidal S, Joiner CS, Baum LG, Stoddart JF. A self-assembled multivalent pseudopolyrotaxane for binding galectin-1. Journal of the American Chemical Society 2004 Sep;126(38):11914-11922.

115. Ooya T, Yui N. Multivalent interactions between biotin-polyrotaxane conjugates and streptavidin as a model of new targeting for transporters. Journal of Controlled Release 2002 Apr;80(1-3):219-228.

116. Ito A, Ooya T, Yui N. Preparation of polypseudorotaxane consisting of fluorescent molecule-modified beta-cyclodextrins and biotin-terminated poly(propylene glycol) with high yield. Journal of Inclusion Phenomena and Macrocyclic Chemistry 2007 Apr;57(1-4):233-236.

117. Ooya T, Eguchi M, Yui N. Supramolecular design for multivalent interaction: Maltose mobility along polyrotaxane enhanced binding with concanavalin A. Journal of the American Chemical Society 2003 Oct;125(43):13016-13017.

118. Ooya T, Utsunomiya H, Eguchi M, Yui N. Rapid binding of concanavalin A and maltose-polyrotaxane conjugates due to mobile motion of alpha-cyclodextrins threaded onto a poly(ethylene glycol). Bioconjugate Chemistry 2005 Jan-Feb;16(1):62-69.

119. Yui N, Ooya T, Kawashima T, Saito Y, Tamai I, Sai Y, et al. Inhibitory effect of supramolecular polyrotaxane-dipeptide conjugates on digested peptide uptake via intestinal human peptide transporter. Bioconjugate Chemistry 2002 May-Jun;13(3):582-587.

120. Ooya T, Mori H, Terano M, Yui N. Synthesis of a biodegradable polymeric supramolecular assembly for drug-delivery. Macromolecular Rapid Communications 1995 Apr;16(4):259-263.

121. Ooya T, Yui N. Synthesis and characterization of biodegradable polyrotaxane as a novel supramolecular-structured drug carrier. Journal of Biomaterials Science-Polymer Edition 1997;8(6):437-455.

122. Watanabe J, Ooya T, Yui N. Effect of acetylation of biodegradable polyrotaxanes on its supramolecular dissociation via terminal ester hydrolysis. Journal of Biomaterials Science-Polymer Edition 1999;10(12):1275-1288.

123. Moon C, Kwon YM, Lee WK, Park YJ, Yang VC. In vitro assessment of a novel polyrotaxane-based drug delivery system integrated with a cell-penetrating peptide. Journal of Controlled Release 2007 Dec;124(1-2):43-50.

124. Nishiyama N, Iriyama A, Jang WD, Miyata K, Itaka K, Inoue Y, et al. Light-induced gene transfer from packaged DNA enveloped in a dendrimeric photosensitizer. Nature Materials 2005 Dec;4(12):934-941.

125. Smith DK. A supramolecular approach to medicinal chemistry: Medicine beyond the molecule. Journal of Chemical Education 2005 Mar;82(3):393-400.

126. Gonzalez H, Hwang SJ, Davis ME. New class of polymers for the delivery of macromolecular therapeutics. Bioconjugate Chemistry 1999 Nov-Dec;10(6):1068-1074.

127. Davis ME, Brewster ME. Cyclodextrin-based pharmaceutics: Past, present and future. Nature Reviews Drug Discovery 2004 Dec;3(12):1023-1035.

128. Reineke TM, Davis ME. Structural effects of carbohydrate-containing polycations on gene delivery. 1. Carbohydrate size and its distance from charge centers. Bioconjugate Chemistry 2003 Jan-Feb;14(1):247-254.

129. Reineke TM, Davis ME. Structural effects of carbohydrate-containing polycations on gene delivery. 2. Charge center type. Bioconjugate Chemistry 2003 Jan-Feb;14(1):255-261.

130. Pack DW, Hoffman AS, Pun S, Stayton PS. Design and development of polymers for gene delivery. Nature Reviews Drug Discovery 2005 Jul;4(7):581-593.

131. Pun SH, Davis ME. Development of a nonviral gene delivery vehicle for systemic application. Bioconjugate Chemistry 2002 May-Jun;13(3):630-639.

132. Pun SH, Bellocq NC, Liu AJ, Jensen G, Machemer T, Quijano E, et al. Cyclodextrin-modified polyethylenimine polymers for gene delivery. Bioconjugate Chemistry 2004 Jul-Aug;15(4):831-840.

133. Tang GP, Guo HY, Alexis F, Wang X, Zeng S, Lim TM, et al. Low molecular weight polyethylenimines linked by beta-cyclodextrin for gene transfer into the nervous system. Journal of Gene Medicine 2006 Jun;8(6):736-744.

134. Kihara F, Arima H, Tsutsumi T, Hirayama F, Uekama K. Effects of structure of polyamidoamine dendrimer on gene transfer efficiency of the dendrimer conjugate with alpha-cyclodextrin. Bioconjugate Chemistry 2002 Nov-Dec;13(6):1211-1219.

135. Wada K, Arima H, Tsutsumi T, Chihara Y, Hattori K, Hirayama F, et al. Improvement of gene delivery mediated by mannosylated dendrimer/alpha-cyclodextrin conjugates. Journal of Controlled Release 2005 May;104(2):397-413.

136. Yang CA, Li HZ, Goh SH, Li J. Cationic star polymers consisting of alpha-cyclodextrin core and oligoethylenimine arms as nonviral gene delivery vectors. Biomaterials 2007 Jul;28(21):3245-3254.

137. Diaz-MosCOSo A, Le Gourrierec L, Gomez-Garcia M, Benito JM, Balbuena P, Ortega-Caballero F, et al. Polycationic Amphiphilic Cyclodextrins for Gene Delivery: Synthesis and Effect of Structural Modifications on Plasmid DNA Complex Stability, Cytotoxicity, and Gene Expression. Chemistry-a European Journal 2009;15(46):12871-12888.

138. Li J, Yang C, Li HZ, Wang X, Goh SH, Ding JL, et al. Cationic supramolecules composed of multiple oligoethylenimine-grafted beta-cyclodextrins threaded on a polymer chain for efficient gene delivery. Advanced Materials 2006 Nov;18(22):2969-+.

139. Harada A, Okada M, Li J, Kamachi M. Preparation and characterization of inclusion complexes of poly(propylene glycol) with cyclodextrins. Macromolecules 1995 Nov;28(24):8406-8411.

140. Ooya T, Choi HS, Yamashita A, Yui N, Sugaya Y, Kano A, et al. Biocleavable polyrotaxane - Plasmid DNA polyplex for enhanced gene delivery. Journal of the American Chemical Society 2006;128(12):3852-3853.

141. Yang C, Wang X, Li HZ, Tan E, Lim CT, Li J. Cationic Polyrotaxanes as Gene Carriers: Physicochemical Properties and Real-Time Observation of DNA Complexation, and Gene Transfection in Cancer Cells. Journal of Physical Chemistry B 2009 Jun;113(22):7903-7911.

142. Yang CA, Li HZ, Wang X, Li J. Cationic supramolecules consisting of oligoethylenimine-grafted alpha-cyclodextrins threaded on poly(ethylene oxide) for gene delivery. Journal of Biomedical Materials Research Part A 2009 Apr;89A(1):13-23.

143. Yang C, Wang X, Li HZ, Goh SH, Li J. Synthesis and characterization of polyrotaxanes consisting of cationic alpha-cyclodextrins threaded on poly[(ethylene oxide)-ran-(propylene oxide)] as gene carriers. Biomacromolecules 2007 Nov;8(11):3365-3374.

144. Shuai XT, Merdan T, Unger F, Kissel T. Supramolecular gene delivery vectors showing enhanced transgene expression and good biocompatibility. Bioconjugate Chemistry 2005;16(2):322-329.

145. Yamashita A, Choi HS, Ooya T, Yui N, Akita H, Kogure K, et al. Improved cell viability of linear polyethylenimine through gamma-cyclodextrin inclusion for effective gene delivery. Chembiochem 2006;7(2):297-302.

146. Antonov EN, Bagratashvili VN, Whitaker MJ, Barry JJA, Shakesheff KM, Konovalov AN, et al. Three-dimensional bioactive and biodegradable scaffolds fabricated by surface-selective laser sintering. Advanced Materials 2005 Feb;17(3):327-+.

147. Saito G, Swanson JA, Lee KD. Drug delivery strategy utilizing conjugation via reversible disulfide linkages: role and site of cellular reducing activities. Advanced Drug Delivery Reviews 2003;55(2):199-215.

148. Luten J, van Nostrum CF, De Smedt SC, Hennink WE. Biodegradable polymers as non-viral carriers for plasmid DNA delivery. Journal of Controlled Release 2008 Mar;126(2):97-110.

149. Ohya Y, Takamido S, Nagahama K, Ouchi T, Katoono R, Yui N. Polyrotaxane Composed of Poly-L-lactide and alpha-Cyclodextrin Exhibiting Protease-Triggered Hydrolysis. Biomacromolecules 2009 Aug;10(8):2261-2267.

150. Ooya T, Arizono K, Yui N. Synthesis and characterization of an oligopeptide-terminated polyrotaxane as a drug carrier. Polymers for Advanced Technologies 2000 Aug-Dec;11(8-12):642-651.

151. Ooya T, Eguchi M, Yui N. Enhanced accessibility of peptide substrate toward membrane-bound metalloexopeptidase by supramolecular structure of polyrotaxane. Biomacromolecules 2001 Spr;2(1):200-203.

152. Loethen S, Kim JM, Thompson DH. Biomedical applications of cyclodextrin based polyrotaxanes. Polymer Reviews 2007;47(3):383-418.

153. Ooya T, Yamashita A, Kurisawa M, Sugaya Y, Maruyama A, Yui N. Effects of polyrotaxane structure on polyion complexation with DNA. Science and Technology of Advanced Materials 2004 May;5(3):363-369.

154. Loethen S, Ooya T, Choi HS, Yui N, Thompson DH. Synthesis, characterization, and pH-triggered dethreading of alpha-cyclodextrin-poly(ethylene glycol) polyrotaxanes bearing cleavable endcaps. Biomacromolecules 2006 Sep;7(9):2501-2506.

155. Yuan RX, Shuai XT. Supramolecular micellization and pH-inducible gelation of a hydrophilic block copolymer by block-specific threading of alpha-cyclodextrin. Journal of Polymer Science Part B-Polymer Physics 2008 Apr;46(8):782-790.

156. Ruiz J, Ceroni M, Quinzani OV, Riera V, Piro OE. Reversible S-S bond breaking and bond formation in disulfide-containing dinuclear complexes of Mn. Angewandte Chemie-International Edition 2001;40(1):220-222.

157. Go YM, Jones DP. Redox compartmentalization in eukaryotic cells. Biochim Biophys Acta-Gen Subj 2008 Nov;1780(11):1271-1290.

158. Meng F, Hennink WE, Zhong Z. Reduction-sensitive polymers and bioconjugates for biomedical applications. Biomaterials 2009 Apr;30(12):2180-2198.

159. Wu GY, Fang YZ, Yang S, Lupton JR, Turner ND. Glutathione metabolism and its implications for health. Journal of Nutrition 2004 Mar;134(3):489-492.

160. Sun HL, Guo BN, Cheng R, Meng FH, Liu HY, Zhong ZY. Biodegradable micelles with sheddable poly(ethylene glycol) shells for triggered intracellular release of doxorubicin. Biomaterials 2009 Nov;30(31):6358-6366.

161. Sun H, Guo B, Cheng R, Meng F, Liu H, Zhong Z. Biodegradable micelles with sheddable poly(ethylene glycol) shells for triggered intracellular release of doxorubicin. Biomaterials 2009 Oct;30(31):6358-6366.

162. Sun HL, Guo BN, Li XQ, Cheng R, Meng FH, Liu HY, et al. Shell-Sheddable Micelles Based on Dextran-SS-Poly(epsilon-caprolactone) Diblock Copolymer for Efficient Intracellular Release of Doxorubicin. Biomacromolecules 2010;11(4):848-854.

163. Sun PJ, Zhou DH, Gan ZH. Novel reduction-sensitive micelles for triggered intracellular drug release. Journal of Controlled Release 2011 Oct;155(1):96-103.

164. Liu J, Pang Y, Huang W, Huang X, Meng L, Zhu X, et al. Bioreducible micelles self-assembled from amphiphilic hyperbranched multiarm copolymer for glutathione-mediated intracellular drug delivery. Biomacromolecules 2011 May 9;12(5):1567-1577.

165. Li YL, Zhu L, Liu Z, Cheng R, Meng F, Cui JH, et al. Reversibly stabilized multifunctional dextran nanoparticles efficiently deliver doxorubicin into the nuclei of cancer cells. Angew Chem Int Ed Engl 2009;48(52):9914-9918.

166. Cheng R, Feng F, Meng F, Deng C, Feijen J, Zhong Z. Glutathione-responsive nano-vehicles as a promising platform for targeted intracellular drug and gene delivery. J Control Release 2011 May 30;152(1):2-12.

167. Gosselin MA, Guo WJ, Lee RJ. Efficient gene transfer using reversibly cross-linked low molecular weight polyethylenimine. Bioconjugate Chemistry 2001 Nov-Dec;12(6):989-994.

168. Lin C, Blaauboer CJ, Timoneda MM, Lok MC, van Steenbergen M, Hennink WE, et al. Bioreducible poly(amido amine)s with oligoamine side chains: synthesis, characterization, and structural effects on gene delivery. J Control Release 2008 Mar 3;126(2):166-174.

169. Yamashita A, Yui N, Ooya T, Kano A, Maruyama A, Akita H, et al. Synthesis of a biocleavable polyrotaxane-plasmid DNA (pDNA) polyplex and its use for the rapid nonviral delivery of pDNA to cell nuclei. Nature Protocols 2006;1(6):2861-2869.

170. Yamashita A, Kanda D, Katoono R, Yui N, Ooya T, Maruyama A, et al. Supramolecular control of polyplex dissociation and cell transfection: Efficacy of amino groups and threading cyclodextrins in biocleavable polyrotaxanes. Journal of Controlled Release 2008 Oct;131(2):137-144.

171. Roth JA, Cristiano RJ. Gene therapy for cancer: what have we done and where are we going? J Natl Cancer Inst 1997 Jan 1;89(1):21-39.

172. Wang Y, Ke CY, Weijie Beh C, Liu SQ, Goh SH, Yang YY. The self-assembly of biodegradable cationic polymer micelles as vectors for gene transfection. Biomaterials 2007 Dec;28(35):5358-5368.

173. Kim JK, Choi SH, Kim CO, Park JS, Ahn WS, Kim CK. Enhancement of polyethylene glycol (PEG)-modified cationic liposome-mediated gene deliveries: effects on serum stability and transfection efficiency. Journal of Pharmacy and Pharmacology 2003 Apr;55(4):453-460.

174. Rejmanova P, Kopecek J, Duncan R, Lloyd JB. Stability in rat plasma and serm of lysosomally degradable oligopeptide sequences in n-(2-hydroxypropyl) methacrylamide copolymers. Biomaterials 1985;6(1):45-48.

175. Choi JH, Choi JS, Suh H, Park JS. Effect of poly(ethylene glycol) grafting on polyethylenimine as a gene transfer vector in vitro. Bulletin of the Korean Chemical Society 2001 Jan;22(1):46-52.

176. Luo D, Haverstick K, Belcheva N, Han E, Saltzman WM. Poly(ethylene glycol)-conjugated PAMAM dendrimer for biocompatible, high-efficiency DNA delivery. Macromolecules 2002 Apr;35(9):3456-3462.

177. Cullis PR. Stabilized plasmid-lipid particles for systemic gene therapy. Cellular & Molecular Biology Letters 2002;7(2):226-226.

178. Roux E, Passirani C, Scheffold S, Benoit JP, Leroux JC. Serum-stable and long-circulating, PEGylated, pH-sensitive liposomes. Journal of Controlled Release 2004 Feb;94(2-3):447-451.

179. Gref R, Minamitake Y, Peracchia MT, Trubetskoy V, Torchilin V, Langer R. Biodegradable long-circulating polymeric nanospheres. Science 1994 Mar;263(5153):1600-1603.

180. Ping Y, Liu CD, Zhang ZX, Liu KL, Chen JH, Li J. Chitosan-graft-(PEI-beta-cyclodextrin) copolymers and their supramolecular PEGylation for DNA and siRNA delivery. Biomaterials 2011 Nov;32(32):8328-8341.

181. Hwang SJ, Davis ME. Cationic polymers for gene delivery: designs for overcoming barriers to systemic administration. Curr Opin Mol Ther 2001 Apr;3(2):183-191.

182. Lomas H, Massignani M, Abdullah KA, Canton I, Lo Presti C, MacNeil S, et al. Non-cytotoxic polymer vesicles for rapid and efficient intracellular delivery. Faraday Discuss 2008;139:143-159; discussion 213-128, 419-120.

183. Pathak A, Patnaik S, Gupta KC. Recent trends in non-viral vector-mediated gene delivery. Biotechnol J 2009 Nov;4(11):1559-1572.

184. Fernandez CA, Rice KG. Engineered nanoscaled polyplex gene delivery systems. Mol Pharm 2009 Sep-Oct;6(5):1277-1289.

185. Licciardi M, Giammona G, Du JZ, Armes SP, Tang YQ, Lewis AL. New folate-functionalized biocompatible block copolymer micelles as potential anti-cancer drug delivery systems. Polymer 2006 Apr;47(9):2946-2955.

186. Lam JKW, Ma Y, Armes SP, Lewis AL, Baldwin T, Stolnik S. Phosphorylcholine-polycation diblock copolymers as synthetic vectors for gene delivery. Journal of Controlled Release 2004 Nov;100(2):293-312.

187. Neu M, Fischer D, Kissel T. Recent advances in rational gene transfer vector design based on poly(ethylene imine) and its derivatives. J Gene Med 2005 Aug;7(8):992-1009.

188. Godbey WT, Wu KK, Mikos AG. Poly(ethylenimine) and its role in gene delivery. J Control Release 1999 Aug 5;60(2-3):149-160.

189. Brissault B, Kichler A, Guis C, Leborgne C, Danos O, Cheradame H. Synthesis of linear polyethylenimine derivatives for DNA transfection. Bioconjug Chem 2003 May-Jun;14(3):581-587.

190. Boussif O, Lezoualc'h F, Zanta M, Mergny M, Scherman D, Demeneix B, et al. A versatile vector for gene and oligonucleotide transfer into cells in culture and in vivo: polyethylenimine. Proc Natl Acad Sci U S A 1995 Aug;92(16):7297-7301.

191. Klotz IM, Sloniewsky AR. Macromolecule-small molecule interactions: a synthetic polymer with greater affinity than serum albumin for small molecules. Biochem Biophys Res Commun 1968 May 10;31(3):421-426.

192. Suh J, Paik, H.J., and Hwang, P.K. Ionization of polyethylenimine and polyellylamine at various pHs. *Bioorganic Chemistry* 1994;22(3):318-327.

193. Godbey WT, Barry MA, Saggau P, Wu KK, Mikos AG. Poly(ethylenimine)-mediated transfection: a new paradigm for gene delivery. J Biomed Mater Res 2000 Sep 5;51(3):321-328.

194. Sonawane ND, Szoka FC, Jr., Verkman AS. Chloride accumulation and swelling in endosomes enhances DNA transfer by polyamine-DNA polyplexes. J Biol Chem 2003 Nov 7;278(45):44826-44831.

195. Akinc A, Thomas M, Klibanov AM, Langer R. Exploring polyethylenimine-mediated DNA transfection and the proton sponge hypothesis. J Gene Med 2005 May;7(5):657-663.

196. Kichler A, Leborgne C, Coeytaux E, Danos O. Polyethylenimine-mediated gene delivery: a mechanistic study. J Gene Med 2001 Mar-Apr;3(2):135-144.

197. Fischer D, Li Y, Ahlemeyer B, Krieglstein J, Kissel T. In vitro cytotoxicity testing of polycations: influence of polymer structure on cell viability and hemolysis. Biomaterials 2003 Mar;24(7):1121-1131.

198. Godbey WT, Wu KK, Mikos AG. Size matters: molecular weight affects the efficiency of poly(ethylenimine) as a gene delivery vehicle. J Biomed Mater Res 1999 Jun 5;45(3):268-275.

199. Godbey WT, Wu KK, Mikos AG. Poly(ethylenimine)-mediated gene delivery affects endothelial cell function and viability. Biomaterials 2001 Mar;22(5):471-480.

200. Fischer D, Bieber T, Li Y, Elsässer H, Kissel T. A novel non-viral vector for DNA delivery based on low molecular weight, branched polyethylenimine: effect of molecular weight on transfection efficiency and cytotoxicity. Pharm Res 1999 Aug;16(8):1273-1279.

201. Fischer D, Bieber T, Li Y, Elsasser HP, Kissel T. A novel non-viral vector for DNA delivery based on low molecular weight, branched polyethylenimine: effect of molecular weight on transfection efficiency and cytotoxicity. Pharm Res 1999 Aug;16(8):1273-1279.

202. Ogris M, Steinlein P, Kursa M, Mechtler K, Kircheis R, Wagner E. The size of DNA/transferrin-PEI complexes is an important factor for gene expression in cultured cells. Gene Ther 1998 Oct;5(10):1425-1433.

203. Reschel T, Konak C, Oupicky D, Seymour LW, Ulbrich K. Physical properties and in vitro transfection efficiency of gene delivery vectors based on complexes of DNA with synthetic polycations. J Control Release 2002 May 17;81(1-2):201-217.

204. Ferrari S, Moro E, Pettenazzo A, Behr J, Zacchello F, Scarpa M. ExGen 500 is an efficient vector for gene delivery to lung epithelial cells in vitro and in vivo. Gene Ther 1997 Oct;4(10):1100-1106.

205. Coll J, Chollet P, Brambilla E, Desplanques D, Behr J, Favrot M. In vivo delivery to tumors of DNA complexed with linear polyethylenimine. Hum Gene Ther 1999 Jul;10(10):1659-1666.

206. Wightman L, Kircheis R, Rössler V, Carotta S, Ruzicka R, Kursa M, et al. Different behavior of branched and linear polyethylenimine for gene delivery in vitro and in vivo. J Gene Med;3(4):362-372.

207. Petersen H, Fechner P, Martin A, Kunath K, Stolnik S, Roberts C, et al. Polyethylenimine-graft-poly(ethylene glycol) copolymers: influence of copolymer block structure on DNA complexation and biological activities as gene delivery system. Bioconjug Chem;13(4):845-854.

208. Chiu S, Ueno N, Lee R. Tumor-targeted gene delivery via anti-HER2 antibody (trastuzumab, Herceptin) conjugated polyethylenimine. J Control Release 2004 Jun;97(2):357-369.

209. Benns J, Maheshwari A, Furgeson D, Mahato R, Kim S. Folate-PEG-folate-graft-polyethylenimine-based gene delivery. J Drug Target 2001 Apr;9(2):123-139.

210. Mallabone CL, Crooks CA, Sefton MV. Microencapsulation of human diploid fibroblasts in cationic polyacrylates. Biomaterials 1989 Aug;10(6):380-386.

211. van de Wetering P, Cherng JY, Talsma H, Crommelin DJ, Hennink WE. 2-(Dimethylamino)ethyl methacrylate based (co)polymers as gene transfer agents. J Control Release 1998 Apr 30;53(1-3):145-153.

212. Zabner J, Fasbender AJ, Moninger T, Poellinger KA, Welsh MJ. Cellular and molecular barriers to gene transfer by a cationic lipid. J Biol Chem 1995 Aug 11;270(32):18997-19007.

213. Curiel DT, Wagner E, Cotten M, Birnstiel ML, Agarwal S, Li CM, et al. High-efficiency gene transfer mediated by adenovirus coupled to DNA-polylysine complexes. Hum Gene Ther 1992 Apr;3(2):147-154.

214. Cherng JY, van de Wetering P, Talsma H, Crommelin DJ, Hennink WE. Effect of size and serum proteins on transfection efficiency of poly ((2-dimethylamino)ethyl methacrylate)-plasmid nanoparticles. Pharm Res 1996 Jul;13(7):1038-1042.

215. Van de Wetering PC, J. Y.; Talsma, H.; Hennink, W. E. . Relation between transfection efficiency and cytotoxicity of poly(2-dimethylamino)ethyl methacrylate)/plasmid complexes. Journal of controlled release 1997;49:59-69.

216. Layman JM, Ramirez SM, Green MD, Long TE. Influence of polycation molecular weight on poly(2-dimethylaminoethyl methacrylate)-mediated DNA delivery in vitro. Biomacromolecules 2009 May 11;10(5):1244-1252.

217. Schallon A, Jerome V, Walther A, Synatschke CV, Muller AHE, Freitag R. Performance of three PDMAEMA-based polycation architectures as gene delivery agents in comparison to linear and branched PEI. Reactive & Functional Polymers 2010 Jan;70(1):1-10.

218. van de Wetering P, Moret EE, Schuurmans-Nieuwenbroek NM, van Steenbergen MJ, Hennink WE. Structure-activity relationships of water-soluble cationic methacrylate/methacrylamide polymers for nonviral gene delivery. Bioconjug Chem 1999 Jul-Aug;10(4):589-597.

219. Dubruel P, Christiaens B, Vanloo B, Bracke K, Rosseneu M, Vandekerckhove J, et al. Physicochemical and biological evaluation of cationic polymethacrylates as vectors for gene delivery. Eur J Pharm Sci 2003 Mar;18(3-4):211-220.

220. Dubruel P, Christiaens B, Rosseneu M, Vandekerckhove J, Grooten J, Goossens V, et al. Buffering properties of cationic polymethacrylates are not the only key to successful gene delivery. Biomacromolecules 2004 Mar-Apr;5(2):379-388.

221. Jones RA, Poniris MH, Wilson MR. pDMAEMA is internalised by endocytosis but does not physically disrupt endosomes. J Control Release 2004 May 18;96(3):379-391.

222. Cai JG, Yue YA, Rui D, Zhang YF, Liu SY, Wu C. Effect of Chain Length on Cytotoxicity and Endocytosis of Cationic Polymers. Macromolecules 2011 Apr;44(7):2050-2057.

223. Jevprasesphant R, Penny J, Jalal R, Attwood D, McKeown NB, D'Emanuele A. The influence of surface modification on the cytotoxicity of PAMAM dendrimers. Int J Pharm 2003 Feb 18;252(1-2):263-266.

224. Wen Y, Pan S, Luo X, Zhang W, Shen Y, Feng M. PEG- and PDMAEG-graft-modified branched PEI as novel gene vector: synthesis, characterization and gene transfection. J Biomater Sci Polym Ed 2010;21(8-9):1103-1126.

225. Wen Y, Pan S, Luo X, Zhang X, Zhang W, Feng M. A biodegradable low molecular weight polyethylenimine derivative as low toxicity and efficient gene vector. Bioconjug Chem 2009 Feb;20(2):322-332.

226. Lin S, Du FS, Wang Y, Ji SP, Liang DH, Yu L, et al. An acid-labile block copolymer of PDMAEMA and PEG as potential carrier for intelligent gene delivery systems. Biomacromolecules 2008 Jan;9(1):109-115.

227. Zhu CH, Jung S, Meng FH, Zhu XL, Park TG, Zhong ZY. Reduction-responsive cationic biodegradable micelles based on PDMAEMA-SS-PCL-SS-PDMAEMA triblock copolymers for gene delivery. Journal of Controlled Release 2011 Nov;152:E188-E190.

228. Dai FY, Sun P, Liu YJ, Liu WG. Redox-cleavable star cationic PDMAEMA by arm-first approach of ATRP as a nonviral vector for gene delivery. Biomaterials 2010 Jan;31(3):559-569.

229. Jiang X, Lok MC, Hennink WE. Degradable-brushed pHEMA-pDMAEMA synthesized via ATRP and click chemistry for gene delivery. Bioconjugate Chemistry 2007 Nov-Dec;18(6):2077-2084.

230. Zhu C, Jung S, Luo S, Meng F, Zhu X, Park TG, et al. Co-delivery of siRNA and paclitaxel into cancer cells by biodegradable cationic micelles based on

PDMAEMA-PCL-PDMAEMA triblock copolymers. Biomaterials 2010 Mar;31(8):2408-2416.

CHAPTER 3   SYNTHESIS OF ENZYMATIC BIODEGRADABLE STAR POLYROTAXANES AND THEIR SELF-ASSEMBLY BEHAVIOR FOR DRUG DELIVERY

3.1 INTRODUCTION

Over the past few decades, core-shell nanostructures (e.g. micelles) have shown great promise as carriers for efficient drug delivery [1]. They offer the advantages of improved drug solubility, drug availability and decreased side effects due to the enhanced permeability and retention (EPR) effect [2, 3]. In these core-shell structures, PEG is widely modified as the hydrophilic shell due to the properties of biocompatibility and reduced immunogenicity, which could stabilize the particle aggregation and resist protein adsorption [4]. Usually, the inner core of the nanostructures is hydrophobic polymer or inorganic metals (e.g gold) [5, 6], Since the first synthesis of polyrotaxane with multiple α-cyclodextrin (CD) rings threaded around a polymer chain [7], CD-based polyrotaxanes have been receiving increasing attention in drug delivery [8-10]. Due to the threading and dethreading nature of polyrotaxanes, recent studies in biodegradable polyrotaxanes focus on various stimuli-triggered responses such as enzymes and pH [11-13].

Recently, biodegradable core-shell structures have attracted much interest due to that they exhibited a suitable and controllable degradation profile in the body after certain periods of time [14]. The biodegradable synthetic polymers such as poly (lactic acid-co-glycolic acid) (PLGA), poly (lactic acid) (PLA) and poly (ε-caprolactone) (PCL) are among the most frequently studied and they displayed gradual degradation kinetics inside body with degradation times ranging from days to months [15, 16]. However, as efficient drug delivery carriers for cancer therapy, the polymers must achieve faster degradation and drug release only after arriving at the pathological site. Therefore the development of structures with stimuli-responsive or triggered decomposition properties is an important challenge for drug delivery systems.

In spite of many studies on the formation of star polymers reported so far,[17, 18] little is known about the star polyrotaxane derived from controlled threading of α-CD onto star PEG (sPEG), not to mention any examples on the dual self-assembly behaviour of the star polyrotaxanes, which may lead to core-shell nanostructures. Uniquely, the inner core of the structure is formed by polyrotaxanes, which is different from traditional core-shell nanostructures [2, 3, 5]. These may potentially lead to some specific interactions (e.g. hydrogen bond) between the drug and core.[19, 20] Furthermore, little research has been done on the further applications of the core-shell polyrotaxane nanostructures in sustain drug delivery. By comparison with covalently conjugating drugs into the polyrotaxane, these new core-shell nanostructures could easily load drug with high efficiency via non-covalent interactions and it could be achieved simultaneously in aqueous environment without impairing the chemical integrity of the drug.

In this research, star polyrotaxane (SPR) is successful synthesized. The SPR could further self-assembled into nanostructures in water with polyrotaxane core and PEG shell (Scheme 3.1). Their self-assembly behavior and biodegradability were confirmed. After encapsulating DOX, the polyrotaxanes showed high drug loading efficiency and enzymatic-triggered *in vitro* drug release. And in a further development of intracellular study, the DOX loaded SPR was found to accomplish much faster internalization, rapid uptake inside cells and significantly higher anticancer efficacy as compared to the free DOX control.
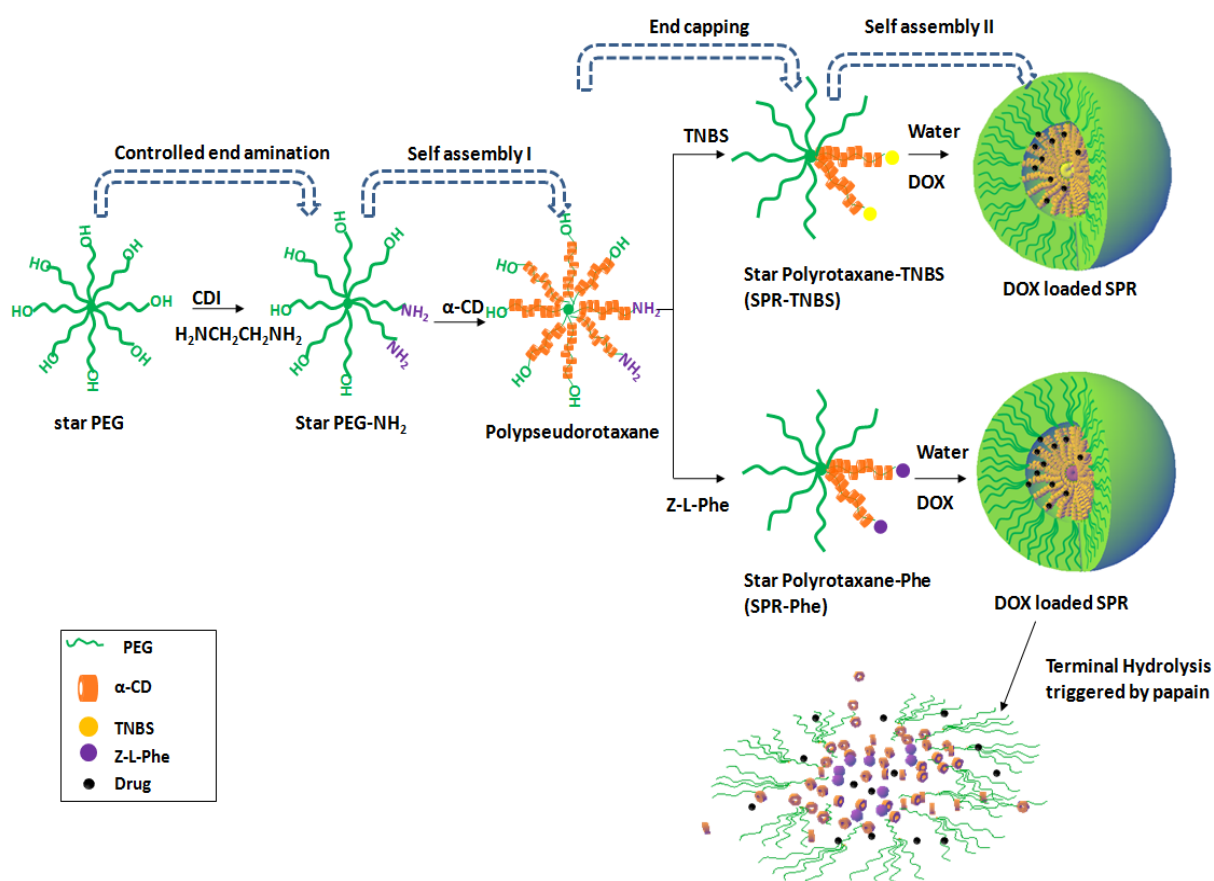
Scheme 3.1 Illustration of the preparation of core-shell nanostrucutures dual self-assemebled form star polymers

3.2 MATERIALS AND METHODS

3.2.1 Materials

1,3-Dicyclohexyl-Carbodiimide (DCC), hydroxysuccinimide (NHS), ethylenediamine, 1,1'-Carbonyldiimidazole (CDI), N-carbobenzyloxy-L-phenylalanine (Z-L-Phe-OH), doxorubicin (DOX), papain (activity: 14 units/mg), ethylenediaminetetraacetic acid (EDTA), 2-mercaptoethanol and sodium hydroxide (NaOH) were received from Sigma-Aldrich and used as received. 8-arm polyethylene glycol (8-arm PEG: Mn=9468) and trinitrobenzene sulfonic salt (TNBS) were purchased from Fluka. α-Cyclodextrin (α-CD) was purchased from TCI. Diethyl ether, methanol, dimethylformamide (DMF), 1,4-dioxane and dimethyl sulfoxide (DMSO) were purchased from Merck. 3-(4,5-dimethylthiazol-2-yl)-2,5-diphenyl tetrazolium bromide (MTT), penicillin, and streptomycin were obtained from Sigma.

3.2.2 Synthesis methods
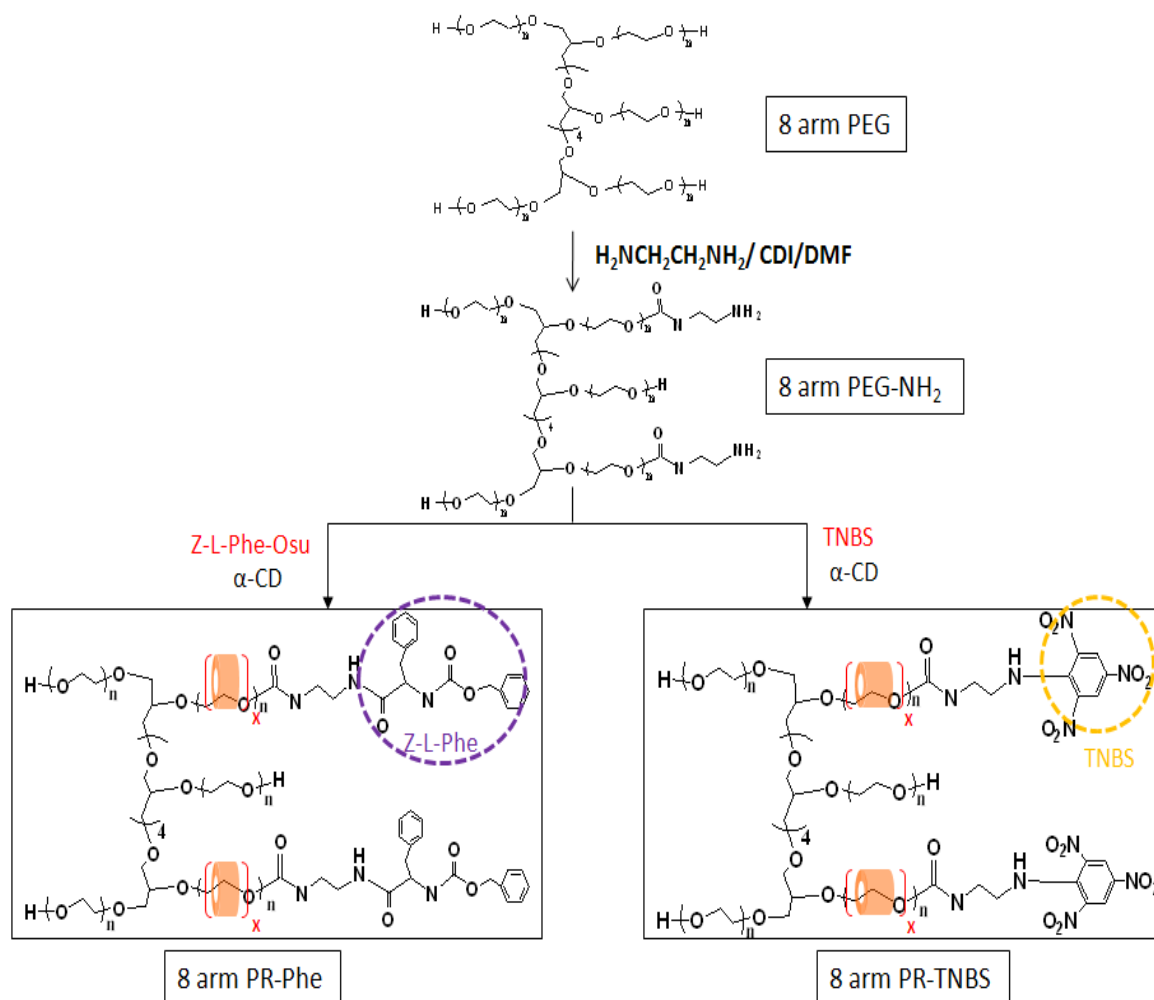
Scheme 3.2 Synthesis routes and structures of the biodegradable polyrotaxanes (SPR)

3.2.2.1 Synthesis of 8-arm PEG-bis-(Amine) (PEG-NH$_2$)

8-arm PEG (1g, 0.1056 mmol) was heated in a flask at 80 °C in vacuum overnight to remove water. When the flask cooled, 10 mL of anhydrous DMF was injected under nitrogen and the solution was added dropwise over a period of 6 h under nitrogen to 15 mL of anhydrous DMF solution in which 1,1'-carbonyldiimidazol (CDI) (0.07g, 0.4224 mmol) was dissolved, followed by stirring overnight under nitrogen at room temperature. The resulting solution was slowly added dropwise over a period of 3 h into 2.4 g (40 mmol) of ethylenediamine, which

78

was dissolved in 10 mL of anhydrous DMF with stirring at room temperature. The

mixture was further stirred overnight. Excess ethylenediamine and DMF was removed

by vacuum evaporation in 60 °C. The resulting viscous liquid was dissolved in 2 mL

methanol and purified by column chromatography on a Sephadex LH-20 column with

methanol as eluent to give as a viscous yellowish liquid (Yield, 0.72g (72%)) [21].

3.2.2.2 Synthesis of Polyrotaxanes (PPR-NH$_2$)

8-arm-PEG-bis (Amine) (0.1g, 0.01056 mmol) was added to 13.8 mL of α-CD

saturated aqueous solution (0.145 g/mL) in centrifuge tubes, followed by alternately

immersing the tubes in an ultrasonic water bath for 20 min. The reaction mixture was

further stirred overnight at room temperature. The precipitated inclusion complex was

isolated by centrifugation, and freeze-dried in vacuum (Yield, 1g) [7].

3.2.2.3 Synthesis of polyrotaxanes (PR-TNBS/PR-Phe)

Partial polyrotaxane with TNBS end group (PR-TNBS) was prepared in

aqueous solution, as reported previously [22]. Pseudopolyrotaxane (1g, 0.01506 mmol)

was dissolved in 15 mL DI water to obtain a turbid solution. 1.0g NaHCO$_3$ was added

to the solution to adjust the pH (~9) and in order to block the ends of IC, 0.4g (3.7

mol) of sodium salt of 2,4,6-trinitrobenzene sulfonic acid (TNBS) was added. The

mixture was further stirred overnight at the room temperature. The resulting solution

was centrifuged and the precipitate was washed with water for 3 times, followed by

dissolving in DMSO and dialyses against DI water for 4 days (MWCO of dialysis

tube is 2000). Then the product was further purified by gel chromatography on a

Sephadex G-75 column with DMSO as eluent. The obtain solution was put in dialysis

tube (MWCO=2000) and dialysis against DI water for 4 days to remove excess

DMSO. Finally, the resulting solution was freeze-dried to obtained yellowish polyrotaxane (Yield, 0.6 g (60%)).

Partial polyrotaxane with Z-L-phenylalanine end groups (PR-Phe) was synthesized in two steps, as reported previously [11, 21, 23]. Firstly, N-Hydroxysuccinimide ester of Z-L-phenylalanine (Z-L-Phe-OSu) was prepared by condensation reaction of N-carbobenzy-loxy-L-phenylalanine (Z-L-Phe-OH) with N-hydroxysuccinimide (NHS), and 1,3-dicyclohexylcarbodiimide (DCC) was used as condensing agent, as reported previously [24]. Briefly, 2g DCC (10.02 mmol) was dissolved in 10 mL anhydrous 1,4-dioxane and the solution was added by dropwise into 20 mL anhydrous 1,4-dioxane, in which Z-L-Phe-OH (1g, 3.34 mmol) and NHS (0.768g, 6.68 mmol) were dissolved, followed by stirring the solution overnight under nitrogen at room temperature. The mixture was filtered to remove byproduct and the filtrate was vapor evaporation to concentrate dioxane. The obtained viscous yellowish liquid was washed with excess ether. After centrifuge, the white precipitation was recrystallized in the mix solution of dichloromethane and ether. Finally, the crystal product was centrifuged and freeze-dried. Yield, 1.3g (73.5%)

Secondly, the resulting Z-L-Phe-Osu (0.33g, 0.84 mmol) was dissolved in 5 mL of anhydrous DMSO, followed by the addition of Pseudopolyrotaxane (1g, 0.01056 mmol). The suspension was stirred at room temperature for 48 h and the obtained solution was precipitated in ether as a crude complex. The complex was dissolved in DMSO and purified by dialysis and G-75 column the same as the purification of PR-TNBS (Yield, 0.12g (60%)).

3.2.2.4 Self-assembly and DOX encapsulation

The solubility of partial polyrotaxane was different based on the threaded number of α-CD. Generally, the solubility was decreased with the increase of threaded number and threaded arms. For the soluble polyrotaxanes, the core-shell nanostructure could be prepared by directly dissolving the polymer in water and allowing it to stay overnight to ensure complete dissolution [25]. For TEM and particle size measurements, the solution was filtered through a 0.45 μm Whatman PVDF filter into a dust-free vial. In the case of the insoluble polyrotaxanes, the nanoaggregates could be prepared by dialysis [26, 27]. Specifically, polyrotaxane (PR-α 28-TNBS) was dissolved in DMSO with concentration of 2 mg/mL, followed by dialysis against DI water for 2 days to remove DMSO (MWCO=2000).

The soluble polyrotaxane was loaded with Doxorubicin (DOX) followed by the method reported before [19]. 5 mg soluble polyrotaxane (PR-α 8-Phe, PR-α 12-TNBS) was added to 0.5 mg Doxorubicin hydrochloride (DOX·HCl) and dissolved together with 1 mL DI water, and the solution was stirred overnight at room temperature. Solution of sodium hydroxide (NaOH) was added to the solution to adjust the pH to 8~9 and stirred for 3 h. Because DOX is insoluble in basic condition, the unloaded DOX molecular were precipitated and removed by ultracentrifugation. The obtained solution with loaded DOX was lyophilized (Yield, 6 mg).

The insoluble polyrotaxane could be loaded with DOX followed by the dialysis method reported before [28-30]. Before loading doxorubicin to the micelle-like nanoaggregates, DOX·HCl was stirred with twice the number of mole of TEA in DMSO overnight to obtain the DOX base. 10mg polyrotaxane (PR-α 20-TNBS and PR-α 28-TNBS) was dissolved in 5 mL DMSO with DOX base solution (1 mg DOX base) and stirred for 5 h at room temperature. The solution was transferred to a

dialysis membrane (MWCO=2000) and dialyzed against NaOH solution (pH=9) for 24 h (exchange per 4 hrs). The obtained solution was adjust back to pH=5 with HCl and then freeze-dried (Yield, 10 mg).

3.2.3 Measurements and Characterization

3.2.3.1 Proton Nuclear Magnetic Resonance (^{1}H-NMR) spectra

^{1}H-NMR spectra were recorded on a Bruker AV-400 NMR spectrometer at 400 MHz at room temperature. The ^{1}H NMR measurements were carried out with an acquisition time of 3.2 s, a pulse repetition time of 2.0 s, a 30° pulse width, 5208 Hz spectral width, and 32 K data points. Chemical shifts were referenced to the solvent peak (δ=2.49 ppm for d_6-DMSO). In this research, the ^{1}H-NMR spectra were used to determine the relative amount and the existence of the 8-arm PEG-bis-(Amine), α-cyclodextrin, TNBS and Z-L-Phe.

3.2.3.2 Thermal Gravimetric Analysis (TGA) and Differntial scanning calorimetry (DSC)

Thermogravimetric analyses (TGA) were made using a TA Instruments SDT 2960. 2~4 mg samples were heated at 20 °C/min from room temperature to 800 °C in a dynamic nitrogen atmosphere (flow rate = 70 mL/min). TGA was used mainly for the determination of the thermal stability of polymers and the percentages of chemical components in the proposed structure based on the decomposition temperature of specific chemicals.

Differential scanning calorimetry (DSC) measurements were performed using a TA Instruments 2920 differential scanning calorimeter equipped with an auto-cool

accessory and calibrated using indium. The following protocol was used for each sample: heating from room temperature to 200 °C at 20 °C min^{-1}, holding at 200 °C for 2 min, cooling from 200 °C to -30 °C at 5 °C min^{-1}, and finally reheating from -30 °C to 200 °C at 5 °C min^{-1}. Data were collected during the second heating run. Transition temperatures were taken as peak maxima [31].

3.2.3.3 Critical Aggregation concentration (CAC) determination

The CAC values were determined by the dye solubilization method [32]. The hydrophobic dye 1,6-diphenyl-1,3,4-hexatriene (DPH) was dissolved in methanol with a stock concentration of 0.6mM. Partial polyrotaxane (PR-Phe) was dissolved in water with variable concentration in the range of 0.0001 to 10 mg/mL, while keeping the concentration of DPH constant. 1 mL of polyrotaxane aqueous solution was mixed with 10 μL DPH stock solution and equilibrated at room temperature overnight. A UV-vis spectra in the range of 330-430 nm were recorded at room temperature. And the CAC values were determined by the plot of the difference in absorbance at 378 nm and at 400 nm (A_{378}-A_{400}) versus logarithmic concentration.

3.2.3.4 Transmission Electron Microscopy (TEM)

The morphologies of the core-shell structure were imaged on a JEOL JEM-2010F FasTEM field emission transmission electron microscope, operated at 100 kv. The sample for TEM was prepared by directly depositing one drop of sample solution onto copper grids, which were coated in advance with supportive Formvar films and carbon. The polymer samples were dyed with phosphotungstic salt to increase the contrast under the TEM experiment. Then the samples were kept in a vacuum oven for 48 h for drying at room temperature before TEM imaging.

3.2.3.5 Dynamic light scattering (DLS) measurements

Size and distribution of the core-shell structure were measured on a DLS instrument (Zetasizer Nano ZS, Malvern Instruments Ltd, USA), with a laser light wave length of 633 nm at a 173° scattering angle. The results were expressed in volume-averaged scales as unimode. The measurement was performed at 25 °C.

3.2.3.6 Biodegradation behavior evaluation

The biodegradability of PR-Phe in the presence or absence of papain was investigated by TEM and particle size. 1 mg PR-Phe was dissolved in 1 ml PBS containing papain (3 mg, 50 unit), ethylenediaminetetraacetic acid (EDTA, 2 μmol/mL), and 2-mercaptoethanol (10 μmol/mL) [11, 23]. The solution was shaken under 100 rpm at 37 °C for 20 days, and a new dose of papain (20 units/mL) was added every 5 days. The degradation behavior and morphology difference of the polymer was characterized and observed by TEM and particle size after 1, 4 and 15 days. In order to make a comparison, the control sample with 1 mg PR-Phe was dissolved in 1 mL PBS without papain, and it was characterized with the same procedure as above.

3.2.3.7 Characterization of the drug delivery systems

The amount of DOX encapsulated in the polyrotaxane nanoparticles was analyzed by fluorescence measurement (excitation at 480 nm) [26]. For determination of drug loading content, 1 mL DMSO was added into 1mg DOX-loaded SPR, the nanostructures were broken up and the DOX was dissolved in the solution. The characteristic emission absorbance of DOX at 588 nm was recorded and compared with a standard curve generated DOX/DMSO solutions with different DOX

concentrations varying from 0 to 60 μg/mL. Drug loading content (DLC) and drug loading efficiency (DLE) were calculated according to the following formula:

DLC (wt%) = (weight of loaded drug/weight of polymer) $\times$ 100%

DLE (wt%) = (weight of loaded drug /weight of drug in feed) $\times$ 100%

The morphologies of DOX-loaded polyrotaxane nanoaggregates were examined using transmission electron microscope (TEM, JEOL JEM-2010F) and particle size, the same procedures as before.

3.2.3.8 *In vitro* drug release study

Release of drugs from the drug-loaded SPR was studied using the dialysis method [19, 33, 34]. 3 mg PR-TNBS/DOX and PR-Phe/DOX were put in dialysis membrane tube (MWCO=2000 Da) together with papain (50 unit/mL), followed by dialyzing against 15 mL medium of PBS (pH=7.4) containing ethylenediaminetetraacetic acid (EDTA, 2 μmol/mL), and 2-mercaptoethanol (10 μmol/mL) [11, 23]. The release system was shaken under 100 rpm at 37 °C for 60 days. At designed time intervals, 1 mL release medium was removed and replaced with fresh medium. The medium removed was analyzed for its drug content by using fluorescence measurement (excitation at 480 nm). The recorded intensity was compared with a standard curve containing DOX/PBS solution with concentration varied from 0 to 5 μg/mL. In order to make a comparison, free DOX without polymer, PR-TNBS/DOX and PR-Phe/DOX were put into dialysis tube without papain, followed by dialyzing against blank PBS and they were measured with the same procedure above

3.2.3.9 Cell viability assay

In vitro cytotoxicity tests on the polymer were performed by 3-(4,5-dimethylthiazol-2-yl)-2,5-diphenyl tetrazolium bromide (MTT) assay in a 96-well cell culture plate [35]. In brief, L929 mouse fibroblasts (MB231 human breast cancer cell and Hela cervical cancer cell) were cultivated in DMEM containing 10% fetal bovine serum (FBS) and 1% penicillin/streptomycin at 37 °C, 5% CO_2 and 95% relative humidity. For cell viability assay, cells were seeded into 96-well plates (NUNC, Wiesbaden, Germany) at a density of 1×10^5 cells/mL. After 24 h, the culture media was replaced with serum-supplemented culture media containing serial dilutions of the polymers, and the cells were incubated for 24 h, at 37 °C in a humidified 5% CO_2 atmosphere. Control cells were treated with an equivalent volume of DMEM. 10 μL of sterile, filtered MTT stock solution in PBS (5 mg/mL) was added to each well, reaching a final concentration of 0.5 mg/mL. After 4 h of incubation at 37 °C, the MTT solution was removed and the insoluble formazan crystals that formed were dissolved in 100 μL of dimethylsulfoxide (DMSO). The absorbance of the formazan product was measured at 570 nm using a fluorometer (FLUOstar Optima Microplate Fluorometer).

3.2.3.10 Intracellular cell uptake and distribution

The cellular uptake and intracellular distribution behaviors of DOX-loaded SPR-TNBS and SPR-Phe were followed with fluorescence microscopy using MDA-MB-231cell line in a 96-well cell culture plate [26, 33]. MB231 cells were cultured in DMEM containing 10% fetal bovine serum (FBS) and 1% penicillin/streptomycin for 1 day. Then they were seeded in a 96-well plate at a density of 1×10^5 cells/mL with

100 µL medium and cultured at 37 °C, 5% CO_2 and 95% relative humidity. After 24 h incubation, the medium in 96-well plate was changed with the DOX-loaded polymer solution with different DOX concentration. The cells were incubated with DOX-loaded polyrotaxanes at 37 °C in a humidified 5% CO_2-containing atmosphere. After 10 min, 1 h, 2 h, 24 h and 48 h, the culture media were removed and the cells were rinsed three times with DMEM prior to the fluorescence observation.

3.3 RESULTS AND DISCUSSION

3.3.1 Synthesis of 8-arm PEG-bis (Amine)

8-arm PEG-bis (Amine) was synthesized by the CDI reaction. Specifically, the hydroxyl groups at the end of 8-arm PEG were activated with CDI, followed by reaction with large excess of ethylenediamine to give terminal amino groups. The reaction was completed in anhydrous DMF under nitrogen because the polarity of the reaction solvent has a strong influence on the conversion. To minimize intermolecular crosslinking, the PEG was added to the CDI solution and the molar ratio of ethylenediamine to PEG was more than 50 times in the conjugate reaction. In this reaction, different amino grafted degree could be accomplished by controlling the amount of CDI and four kinds of mole ratio of CDI to PEG in feed were used in this experiment (4:1, 12:1, 16:1 and 40:1, respectively). It was found that the degree of reaction increased with increasing of CDI concentration and the reaction time.
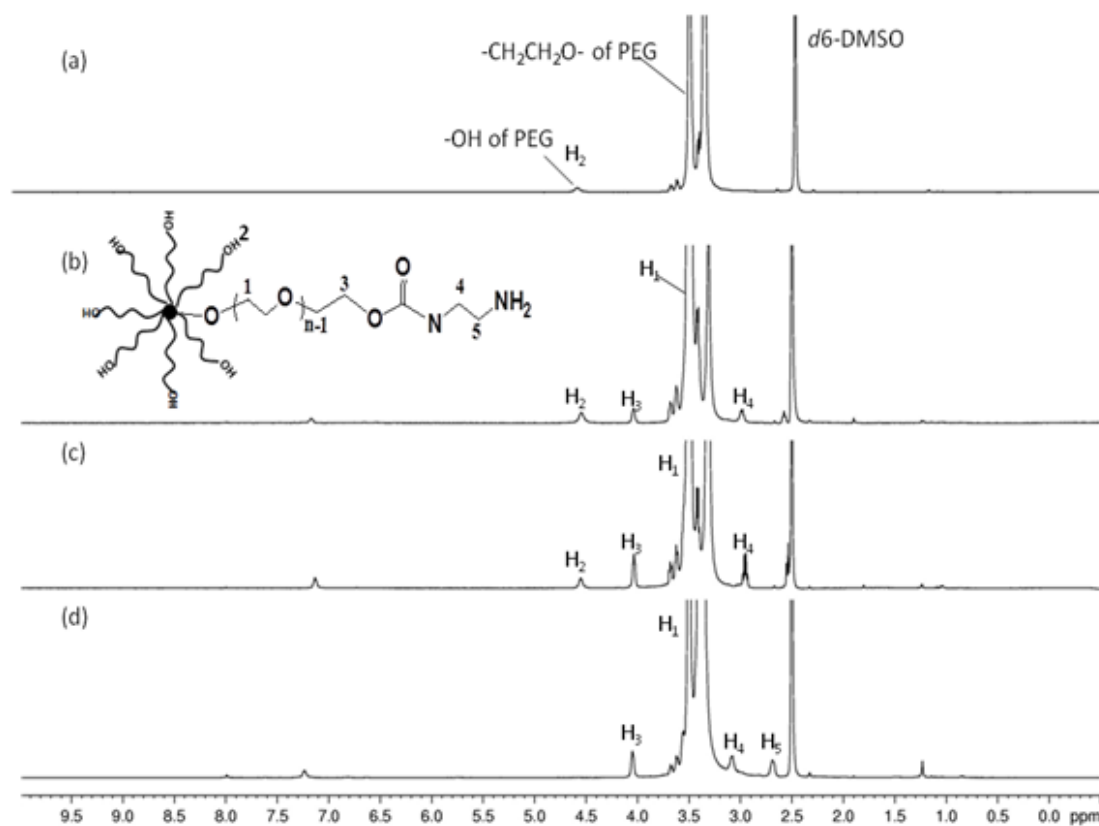
Fig. 3.1 ^{1}**H-NMR spectrum of (a) 8-arm PEG (Mw=9468, n=25), (b) PEG-11.3%-NH$_2$ (feeding ratio of CDI/PEG=4:1), (c) PEG-52%-NH$_2$ (feeding ratio=16:1), (d) PEG-96%-NH$_2$ (feeding ratio=40:1) in** d_6**-DMSO.**

Fig. 3.1 shows the ^{1}H NMR result of 8-arm PEG-bis-(Amine) (molar ratio: 4:1, 16:1 and 40:1) in comparison with pure 8-arm PEG. In the spectrum, 8-arm PEG (10k) is showed as a control (400 MHz, d_6-DMSO, 22°C). In the spectrum of 8-arm PEG-bis-(Amine), the chemical shift of H$_3$ in PEG was change from 3.5 ppm (in pure PEG) to 4.05 ppm (in the product), which is attributed to end grafting of ethylenediamine. And due to the different end grafting degree, the peak of H$_2$ (-OH of PEG) was decreased or disappeared after the reaction. Furthermore, the integration ratios of each component are with the similar ratio of the original PEG and ethylenediamine. This result confirms the successful conjugation of 8-arm PEG with ethylenediamine.

By comparing Fig. 3.1 (b), 3.1 (c) and 3.1 (d), it was found that when the feeding ratio of CDI to PEG increases, the peak of H$_3$ (which represents the grafted

arms in PEG) increases and the peak of H_2 (which represents the un-grafted arm) decrease. This is because the more CDI used, the more grafted degree will be obtained. Therefore, the grafted degree can be indirectly calculated on the basis of integration value of H_3 and H_2. The results are summarized in table 3.1, together with the elemental analysis (EA) results. Based on the above result, it was found that although large excess CDI were used, fully grafted 8-arm PEG cannot be obtained, probably because the CDI reaction is not very effective and the influence of water in CDI.

Table 3.1 Composition and EA results of 8-arm PEG-bis (Amine)

sample	CD/PEG in feed	NH$_2$ grafted degree [a]	Anal.calcd [b]			Found [c]		
			C%	H%	N%	C%	H%	N%
PEG-11.3%-NH$_2$	4	11.3% (1 arm)	52.84	8.83	0.26	52.69	9.01	0.16
PEG-28%-NH$_2$	12	28% (2 arm)	52.91	9	0.66	54.68	9.24	0.64
PEG-52%-NH$_2$	16	52% (4 arm)	53.7	8.97	1.21	54.53	9.23	1.12
PEG-96%-NH$_2$	40	96% (7.7 arm)	52.63	8.79	2.22	51.98	8.87	2.11

[a] Data was all calculated on the basis of ^{1}H NMR in DMSO-D$_6$
[b] Theoretical elemental analysis calculated for the corresponding compound.
[c] Elemental analysis found.

3.3.2 Synthesis of partial polyrotaxane

After grafting ethylenediamine, 8-arm PEG-bis-amine with different grafted ratio was allowed to react with saturated solution of α-CD to obtain polypseudorotaxane, following similar procedures described in previous report [36], in which it was found that α-CD will form an inclusion complex with ratio of EO to CD is 2, approximately. Then the end of PEG was blocked to form polyrotaxane with two kinds of end groups: TNBS and Z-L-Phe. Following ^{1}H-NMR spectra showed the chemical components of the product structures (Fig. 3.2).
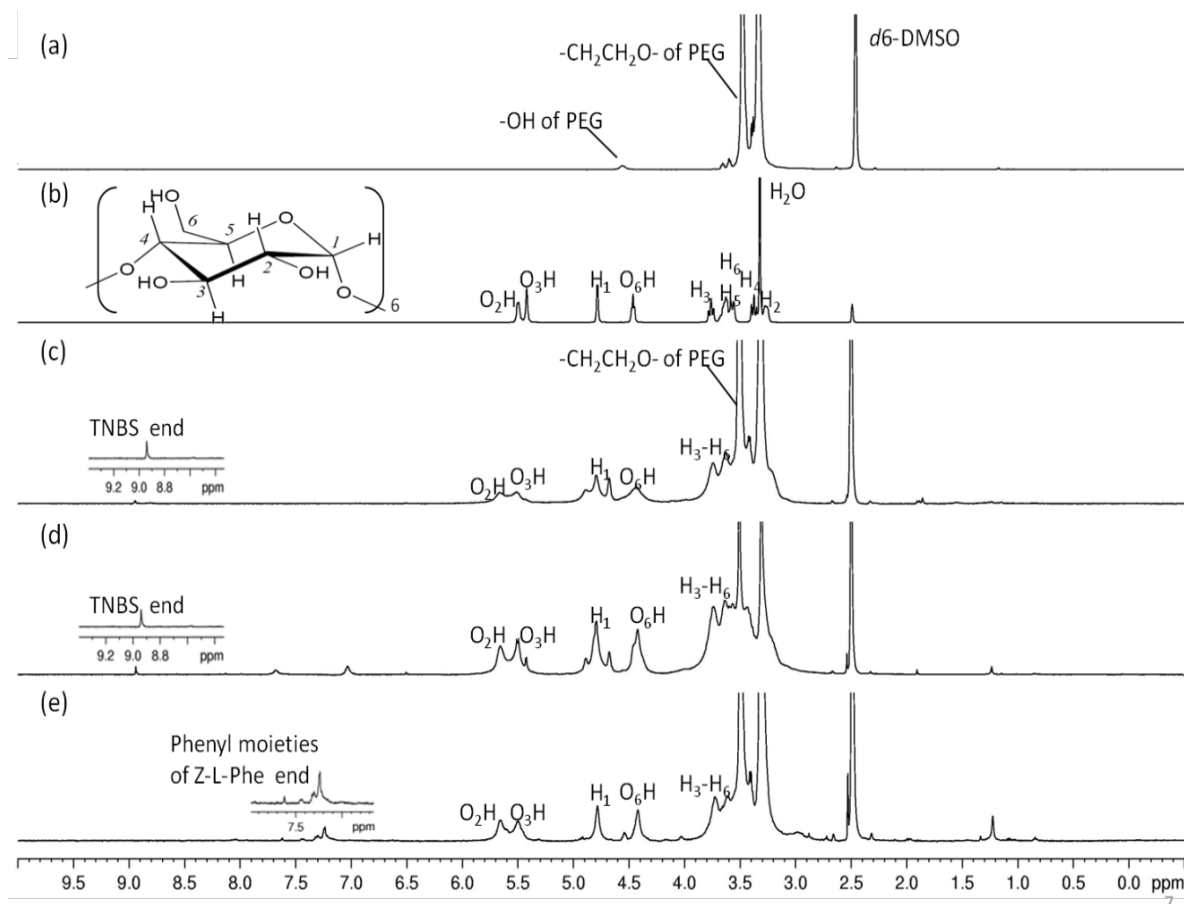
Fig. 3.2 [1]**H-NMR of (a) 8-arm PEG (Mn=9468), (b) α-CD, (c) PR-α 12-TNBS, (d) PR-α 65-TNBS and (e) PR-α 8-Phe in d$_6$-DMSO.**

In Fig. 3.2 (c)-(d), the signals for α-CD, the threading 8-arm PEG (δ=3.5) and the end capping groups (TNBS, δ=8.95) were all observed. In Fig. 3.2 (e), instead of TNBS, the end capping group of Z-L-Phe was observed at δ 7.2-7.4. Furthermore, it was observed that the peaks of α-CDs in Fig. 3.2 (b) were clearly sharp, but those of polyrotaxanes were broadened (Fig. 3.2 (c)-(e)). These results suggest that the mobility of α-CDs in polyrotaxane is restricted by the PEG chain after forming the supramolecular structure. These results showed good agreements with our supposed structure, which confirming the forming of the polyrotaxane with TNBS and Z-L-Phe end groups [21, 37].

In Fig. 3.2 (c), the PEG-11.3%-NH$_2$ was used for the inclusion complexation, and higher grafted degree PEG-96%-NH$_2$ was used in Fig. 3.2 (d). By comparison, it

was found that more threaded α-CDs will be obtained in higher grafted degree probably because higher end capping in higher grafted degree, resulting less dethreaded α-CDs in DMSO. The average numbers of threaded α-CD in the final products could be calculated by comparing the resonance peak of H_1 of α-CD (δ=4.79) with that of PEG (δ=3.50). And the number of threaded arms can be estimated by comparing the peak area of TNBS/Z-L-Phe end and PEG. By calculation, the following polyrotaxane was confirmed (Table. 3.2):

Table 3.2 Composition of polyrotaxane and compared with TGA results

Sample name	Grafted ratio of Precursor PEG	CD threaded arm per polymer [a]	CD threaded number per polymer [a]	CD threaded number per polymer (TGA)[b]
PR-α 12-TNBS	PEG-11.3%-NH$_2$	1	10	12
PR-α 20-TNBS	PEG-28%-NH$_2$	2	20	20
PR-α 28-TNBS	PEG-52%-NH$_2$	2	26	28
PR-α 65-TNBS	PEG-96%-NH$_2$	6.7	62	65
PR-α 8-Phe	PEG-28%-NH$_2$	1	8	9

[a] Data was all calculated on the basis of ^{1}H NMR in DMSO-D$_6$
[b] Data was calculated based on TGA.

By comparison with TNBS end polyrotaxane, the polyrotaxane with Phe end threaded less α-CD with the same grafted degree of PEG. This is because in the synthesis of polyrotaxane-Z-L-Phe, the reaction was finished in DMSO, which results some CD dethreading before the end capping.

3.3.3 TGA and DSC assessment
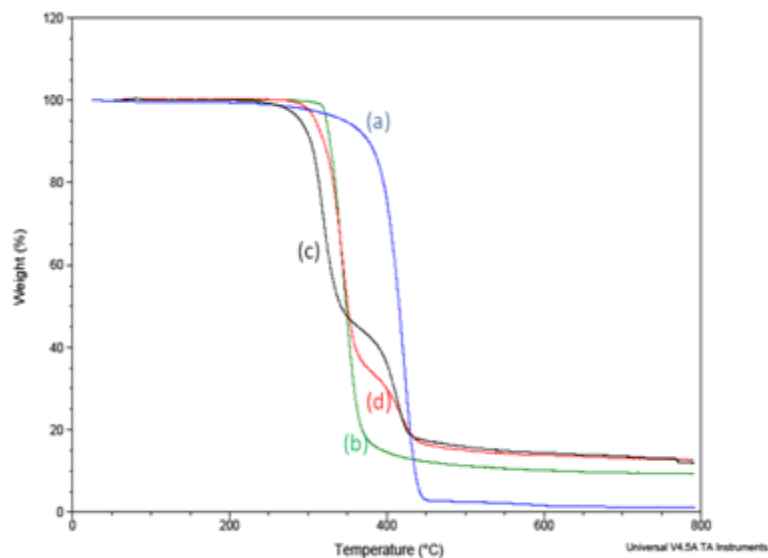
Fig. 3.3 TGA of (a) 8-arm PEG, (b) α-CD, (c) PR-α 20-TNBS and (d) PR-α 65-TNBS

The thermal stability of the polyrotaxane was evaluated using thermogravimetric analysis (TGA) and compared with free α-CD and the starting polymers. Fig. 3.3 shows the weight loss curves for polyrotaxanes by comparing with 8-arm PEG and α-CD. As shown in Fig. 3.3, PR-α 20-TNBS shows an initial weight loss of 55.04% and second weight loss of 28.91% on heating with onset of thermal decomposition at 229 °C and 365 °C, respectively. This two-step thermal degradation could be attributed to the first decomposition of α-CD and the second one to naked PEG component mainly. The similar thermal decomposition could also be found in PR-α 65-TNBS (Fig. 3.3(d)). However, the onsets of the decomposition of α-CD and PEG in the polyrotaxane are observed at 269 °C and 373 °C, respectively, which are higher than those of the CD and PEG blocks in PR-α 20-TNBS. Therefore, by comparison with pure PEG and α-CD, it could be concluded that the PEG and CD blocks was stabilized by the formation of polyrotaxane. Furthermore, the more α-CD threaded, more stable ICs could be obtained. The higher decomposition temperatures

of polyrotaxane are due to the contribution of complex formation to thermal stability

of both α-CD and PEG [31, 38]. Although the TGA method may not be as accurate as

the ^{1}H NMR due to the partially overlapping of the two weight loss steps, the two-step

weight loss behavior can also be used to estimate the ratio between α-CD and PEG in

the polyrotaxanes (Table 3.2). The results further confirmed the ^{1}H NMR result and

the proposed polyrotaxane compositions.
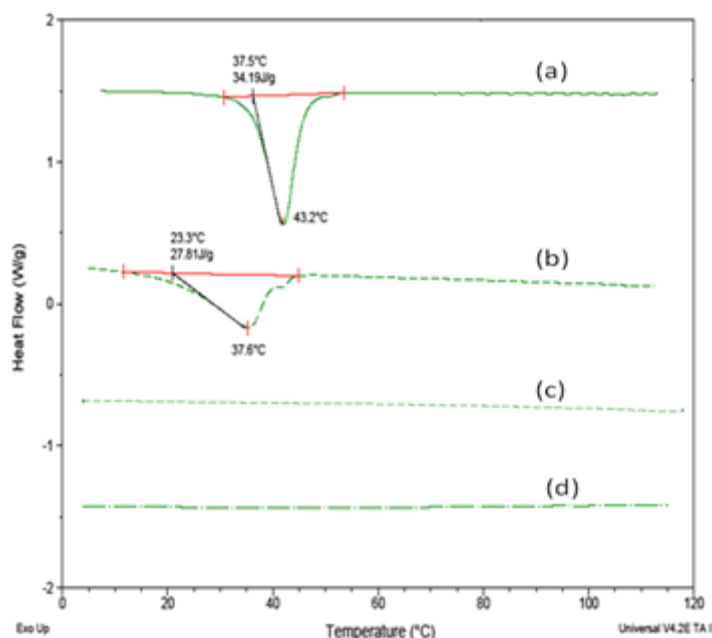
Fig. 3.4 DSC curves (second heating run at 20 °C /min) for (a) 8-arm PEG, (b) 10K-PR-α 12-TNBS, (c) 10K-PR-α 20-TNBS and (d) 10K-PR-α 65-TNBS.

The thermal properties of the obtained polyrotaxanes, corresponding 8-arm

PEG in the solid state were investigated by DSC. Fig. 3.4 shows the DSC curves for

three kinds of partial polyrotaxane and pure 8-arm PEG. In 8-arm PEG curve (Fig.

3.4a), heating process display one melting peak (endothermic peak) at 43.2^{o}C and one

exothermic peak at 21°C on the cooling trace. It attributes to the melting and

recrystallization of PEG crystals. However, no obvious melting peak was observed in

PR-α 20-TNBS and PR-α 65-TNBS because the polymer chain is closely included in

the channels formed by CDs in the polyrotaxane. Interestingly, in PR-α 12-TNBS,

there is a clear endothermic peak which is due to the melting of PEG crystallites. The results indicated that PEG is partially covered by α-CD and most likely many PEG arms were uncomplexed by α-CD. In the polyrotaxanes, there is a trend that both fusion temperature and enthalpy change increase with and decrease number of threaded α-CDs. This is in accordance with the fact that the polyrotaxanes with less threaded CDs have more uncomplexed portion of PEG chains [31].

3.3.4 CAC determination

It was found that the solubility of the polyrotaxanes decreased with the increasing number of threaded α-CDs. Among the synthesized 5 kinds of polyrotaxanes, PR-α 8-Phe, PR-α 12-TNBS, PR-α 20-TNBS is soluble in water and the solubility is PR-α 8-Phe > PR-α 12-TNBS > PR-α 20-TNBS. While PR-α 28-TNBS and PR-α 65-TNBS is insoluble. Considering the influence of TNBS in UV spectra and fluorescence, PR-α 8-Phe was selected to determine the CAC of the partial polyrotaxane.
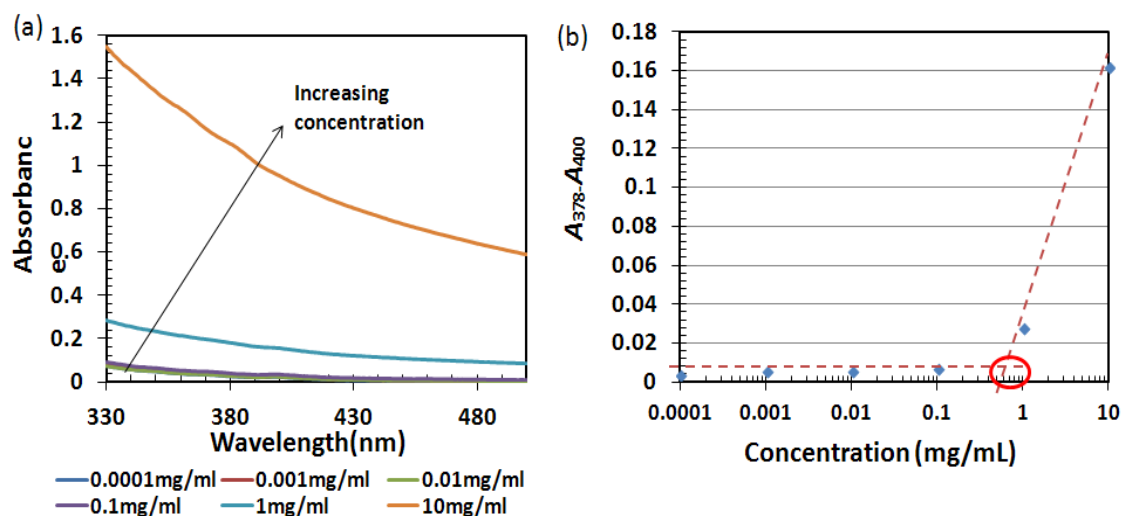
Fig. 3.5 (a) UV-vis spectra changes of DPH with increasing PR-α 8-Phe concentration in water at 25 °C. (b) CAC determination by extrapolation of the difference in absorbance at 378 nm and 400 nm

This experiment was conducted by varying the aqueous polymer concentration in the range of 0.0001 mg/mL to 10 mg/mL, while keeping the concentration of DPH constant. DPH shows a higher absorption coefficient in a hydrophobic environment than in water. Thus, with increasing polymer concentration, the absorbance at 344, 358 and 378 nm increased (Fig. 3.5a). The point where the absorbance suddenly increases corresponds to the concentration at which core-shell nanostructures are formed. When the micelle-like nanoaggregates is formed, DPH partitions preferentially into the hydrophobic core formed in the aqueous solution [39, 40]. The CAC was determined by extrapolating the absorbance at 378 nm minus the absorbance at 400 nm (A_{378}-A_{400}) versus logarithmic concentration (Fig. 3.5b). It was found that the CAC values for polyrotaxane PR-α 8-Phe are 0.8 mg/mL.

3.3.5 Particle Size and TEM observation of self-assemblies
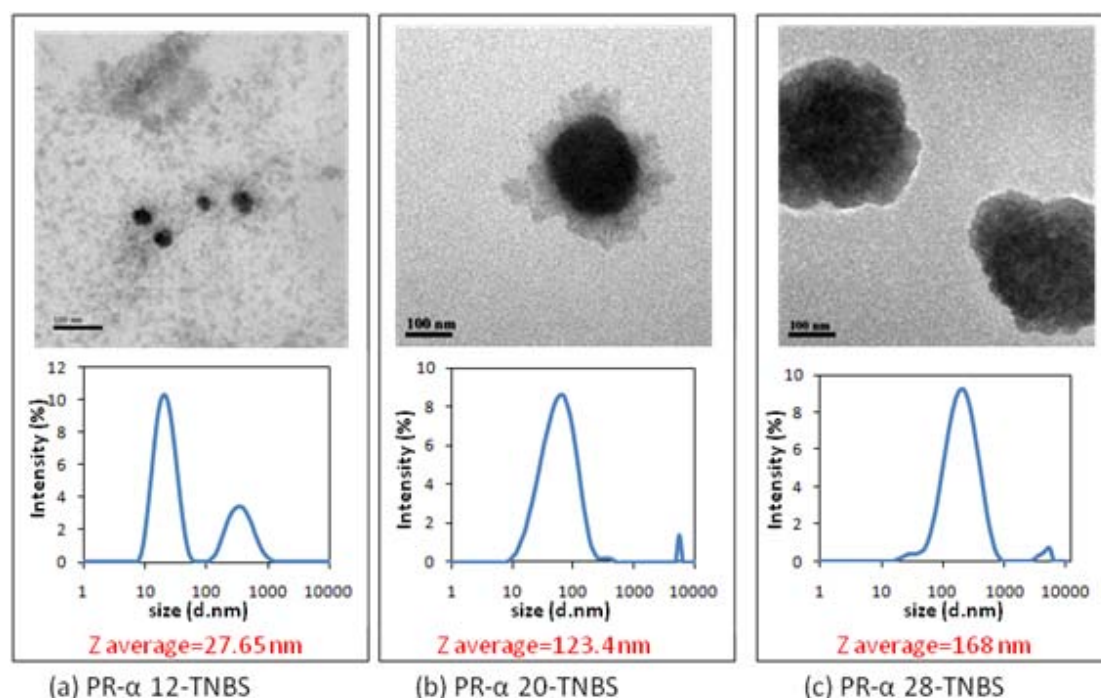
(a) PR-α 12-TNBS   (b) PR-α 20-TNBS   (c) PR-α 28-TNBS

Fig. 3.6 Particle size distribution (intensity distribution) and TEM images of the self-assembly of PR-α 12-TNBS (a), PR-α 20-TNBS (b) and PR-α 28-TNBS (c).

To convince the self-assembly behavior and characterize the size and morphology of the polyrotaxane particles, TEM and DLS experiment was conducted. Fig. 3.6 shows the size and morphologies of the nanoaggregates formed by partial polyrotaxanes with different numbers of threaded α-CDs. Among the four kinds of polyrotaxanes synthesized, PR-α 12-TNBS and PR-α 20-TNBS form nanoparticles by directly dissolved in water (conc.=1 mg/mL). PR-α 28-TNBS nanoaggregates were formed by dialysis method. While insoluble PR-α 65-TNBS cannot form nanoaggregates by dialysis, probably because more than half of the PEG arms were covered by CD and the hydrophobic environment dominated in the systems attributing to the precipitate which cannot be stable in water as form of nanoparticles.

These nanoaggregates were imaged with staining of the polymer shell with sodium salt of phosphotungstic acid. As shown in the TEM images of Fig. 3.6, spherical core-shell nanostructures are observed in the three kinds of polyrotaxanes. Their average size is around 20~150 nm, which have been confirmed by particle size and size distribution determined by DLS measurement. The smaller size observed by TEM as compared to that determined by DLS is most likely due to shrinkage of the PEG shell [25]. The small sizes of particles may enable them to prolong circulation in blood and slower elimination by the reticuloendothelium system (RES) [29]. In Fig. 3.6a, a bimodal size distribution was evidenced in PR-α 12-TNBS. It suggested that there coexist polymer aggregates and unassociated single polyrotaxane in the aqueous solution. It may be because only little CDs exist in PR-α 12-TNBS, and the dominated hydrophilic segment content prevents the self-assembly, resulting in some uncomplexed single polyrotaxane molecules. With increased number of CDs, the size distribution became monomodal due to the increase of hydrophobic segments.

Furthermore, by comparison Fig. 3.6(a)-(c), it could be found that with increase in the number of threaded α-CDs, the formed micelle-like aggregates tend to be larger (from 27 nm to 168 nm), showing that the presence of more CDs as the polyrotaxane core increases the particle volume. Therefore, the particle size and size distribution of the formed structure could be changed by controlling the threaded number of CDs in the partial polyrotaxanes.

3.3.6 Biodegradation behavior characterization

In our experiment, in addition to synthesize partial polyrotaxane with TNBS end, another terminal group (Z-L-Phe) was introduced in the systems with enzymatic biodegradable linkage. The most attractive character of such polyrotaxane will involve the control of drug release utilizing the enzymatic-triggered dissociation of supramolecular structure. Thus regulating the degradability of the polyrotaxane would be important before loading drug in the systems. In our approach, TEM and DLS were used to characterize the biodegradation behavior of the systems.

	Day 0	Day 4	Day 15
(a) Papain	Z-average=53.55	Z-average=35.16	Z-average= 28.05 nm
(b) No Papain	Z-average=53.55 nm	Z-average=53.77 nm	Z-average= 50.90 nm
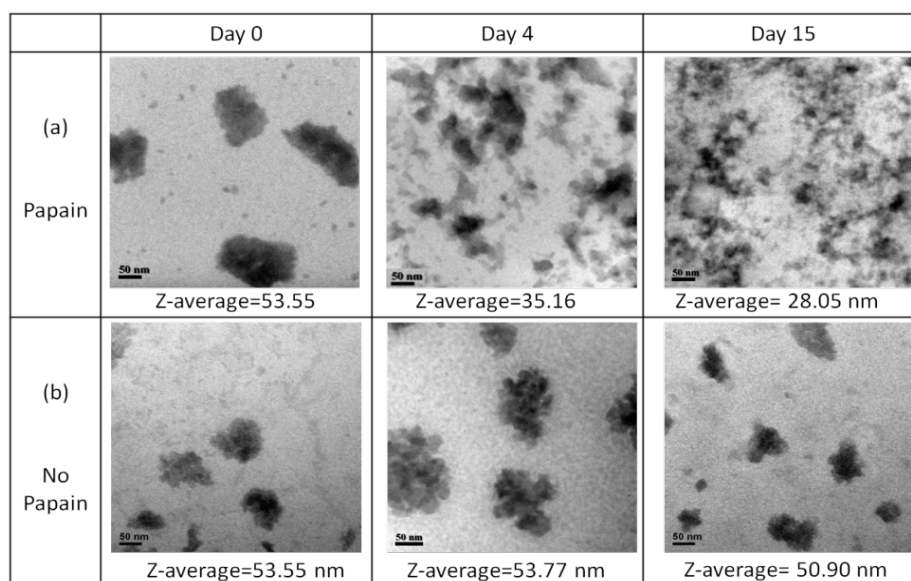
Fig. 3.7 TEM images of PR-α 8-Phe nanoparticles in PBS solution with (a) and without papain (b) after 0, 4 and 15 days (concentration 1 mg/mL)
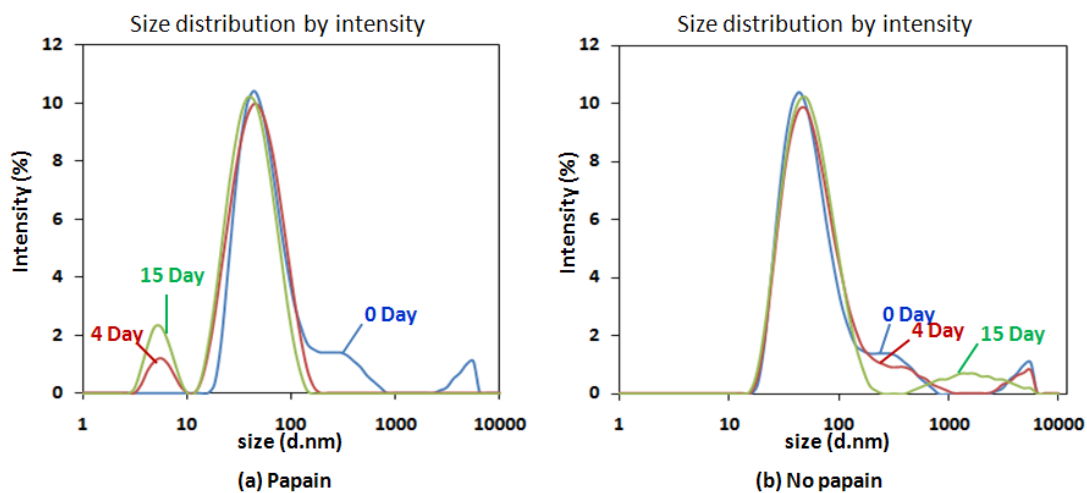
Fig. 3.8 The size change of PR-α 8-Phe nanoparticle in PBS with (a) and without papain (b) determined by DLS measurement

The size and morphology change of the PR-α 8-Phe nanoparticle in response to papain, which can cleave the Phe-Gly peptide linkages, in PBS was followed by TEM and DLS measurement (Fig. 3.7 and Fig. 3.8). Notably, as shown in Fig. 3.7a, the SPR self-assembled nanostructures degraded into small pieces with irregular morphologies after 4 days in the presence of papain and the average size of nanoparticle decreased from 53 nm to 35 nm. The size of nanoaggregates became smaller with more small pieces after 15 days in the presence of papain. In contrast, no change in particle morphology was discerned after 15 days in the absence of papain under otherwise the same conditions (Fig. 3.7b). The result confirmed the effects of dissociation of the supramolecular structure by enzymatic cleavage of the peptide linkages on the particle degradation behavior of PR-α 8-Phe in the presence of protease papain [11]. This was further verified by the DLS measurement regarding to the change of size distribution. In Fig. 3.8a, in the presence of papain, with increasing the time, large aggregates decreased and smaller aggregates increased, indicating the polyrotaxane was degraded into small pieces. However, no such changes were observed in the absence of papain (Fig. 3.8b).

3.3.7 Drug loading content determination and morphologies observation

DOX is one of the most potent anticancer drugs and used widely in the treatment of different types of solid malignant tumors [41, 42]. DOX is known to interact with DNA by intercalation and inhibition of macromolecular biosynthesis. It is crucial, therefore, to delivery and release DOX in the cytoplasm and/or right into the cell nucleus. In this chapter, we use DOX as the model molecule to evaluate the potential application of the core-shell nanostructures as drug carrier.

Table 3.3 Drug loading content and drug loading efficiency by dialysis method [28]

sample	Final drug concentration (μg/1 mg polymer)	Loading content [a] (wt.%)	Theory loading content (wt.%)	Loading efficiency [b] (%)
PR-α 12-TNBS	14.551μg	1.455%	10%	14.55%
PR-α 20-TNBS	18.462μg	1.846%	10%	14.77%
PR-α 28-TNBS	12.25μg	1.225%	10%	15.31%

Table 3.4 Drug loading content and drug loading efficiency by dissolve method [19]

sample	Final drug concentration (μg/1 mg polymer)	Loading content [a] (wt.%)	Theory loading content (wt.%)	Loading efficiency [b] (%)
PR-α 12-TNBS	48.99 μg	4.899%	10%	78.38%
PR-α 8-Phe	91.67 μg	9.16%	16.7%	73.3%
Pure DOX (control)	47.14 μg	-	-	4.71%

[a] Loading content (wt%) = (weight of loaded drug/weight of polymer) ✕ 100%

[b] Loading efficiency (wt%) = (weight of loaded drug /weight of drug in feed) ✕ 100%

Because of the different solubility in water, two methods were used to load drug in our experiment. Dialysis method was used for the insoluble polyrotaxanes and dissolve method was used for soluble polyrotaxanes. Table 3.3 and 3.4 show the drug loading efficiency of star polyrotaxanes with different numbers of threaded CDs. The results showed that the drug loading efficiencies for three polyrotaxanes were approximately 14%~15%. The loading content increases with increasing of threading

CDs. This can be explained that the more hydrophobic part in the polymer chain makes it possible to have more interaction points in the formed structure, giving rise to a higher loading content [27, 43]. In table 3.4, the drug content loaded by dissolve method is much more than the dialysis method, maybe because the dialysis process will cause drug losing (drug release rate>drug loading rate). Pure DOX was used as control to verify the dissolve method. With the same procedure in the absence of polyrotaxanes, only 4.71 wt% free DOX were found in the final product. In contrast, in the presence of polyrotaxane, approximately 78 wt% DOX was observed. The result confirmed the high drug load efficiency and capacity of the polyrotaxane. In addition to the hydrophobic interaction, the high drug load efficiency may be attributed to the hydrogen-bond interaction between hydroxyl group of CDs and amide group of DOX under neutral and basic conditions [19].
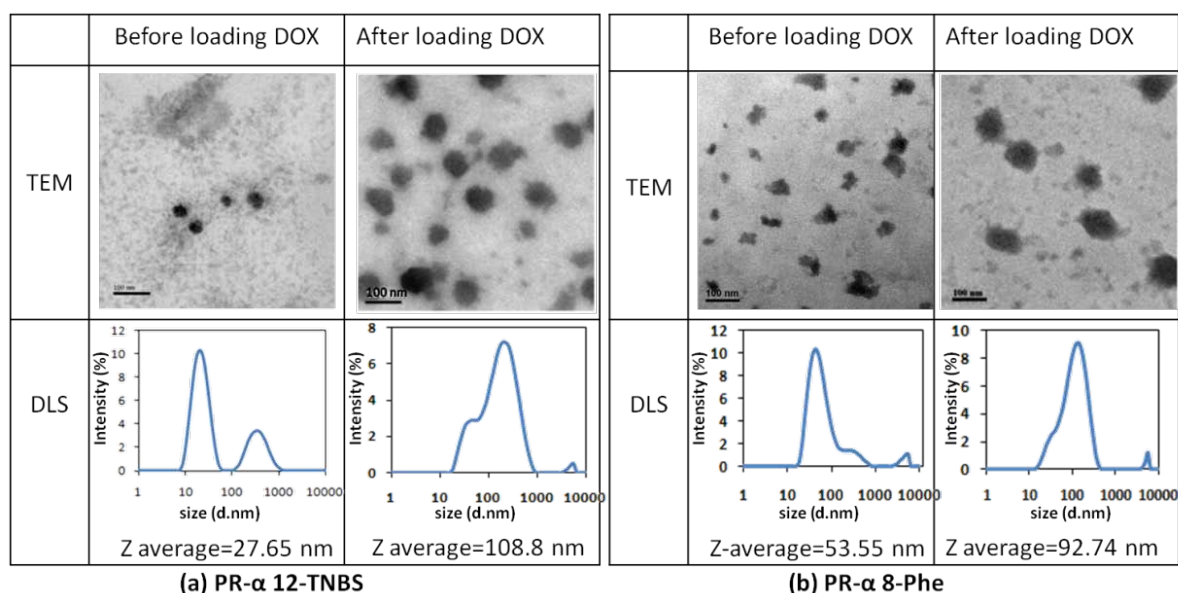
Fig. 3.9 Morphology and size distribution of DOX loaded PR-α 12-TNBS (a) and PR-α 8-Phe (b)

TEM photographs and size distribution of the PR nanoaggregates after loading drugs are shown in Fig. 3.9. In Fig. 3.9a, the drug loaded PR-α 12-TNBS have an average size of 105±5 nm, and comparing with the aggregates without drug (27±4

nm), the particle sizes become larger when the drug is incorporated, showing that the presence of DOX in the polyrotaxane core of the nanoparticle increased volume [27, 29]. Furthermore, after loading drugs, the size distribution of PR-α 12-TNBS changed from bimodal to monomodal, and the morphologies became more regular. Therefore, the entrapping of drugs into the PR core contributes not only to the increase in the size of the nanoparticles but also to the unimodal size distribution. The drugs also enhanced the hydrophobic interaction and helped the self-assembly. Similar phenomenon has also been observed in DOX loaded PR-α 8-Phe in Fig. 3.9b.

3.3.8 *In vitro* drug release behaviors

The controlled-drug release behavior of DOX from polyrotaxane nanoaggregates (PR-α 12-TNBS and PR-α 8-Phe) were investigated using a dialysis tube (MWCO=2000) in pH7.4 PBS at 37 °C in the presence or absence of papain, with the similar initial drug loading efficiency and the same drug loading content.

(a) DOX loaded PR-α 8-Phe   (b) DOX loaded PR-α 12-TNBS
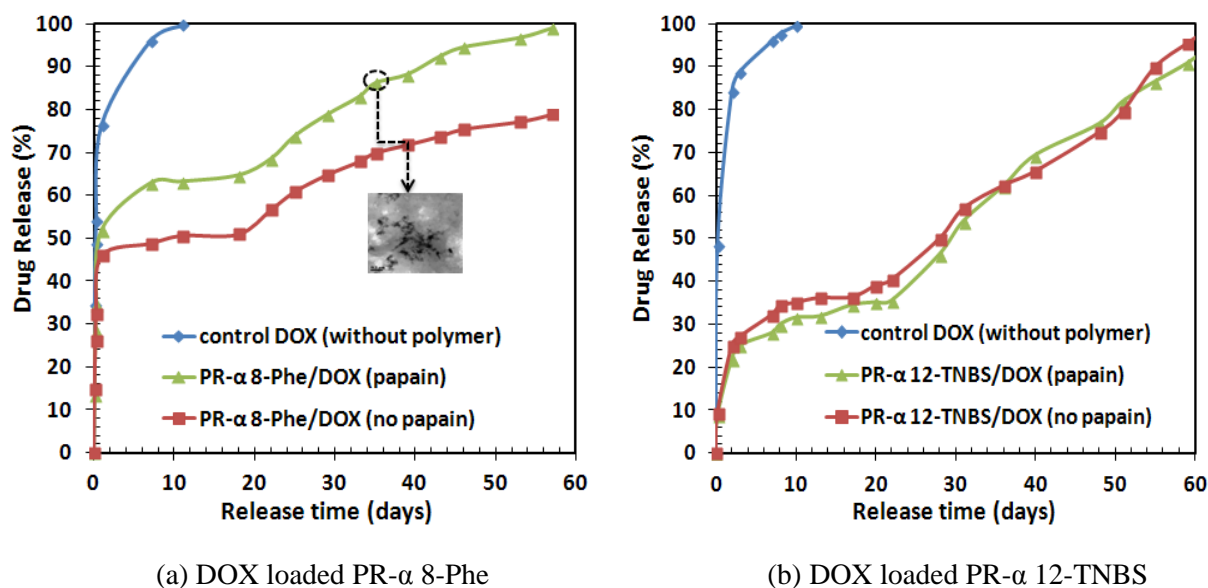
Fig. 3.10 In vitro release profile of DOX from polyrotaxane aggregates in PBS at pH 7.4 and 37 °C, in presence or absence of papain. (a) DOX loaded PR-α 8-Phe; (b) DOX loaded PR-α 12-TNBS; Photograph shows the TEM images of 35 days release of PR-α 8-Phe with papain.

Fig. 3.10 shows the release profiles at 37 °C of different DOX loaded polyrotaxanes. In Fig. 3.10b, PR-α 12-TNBS exhibited sustained and slow DOX release into surrounding PBS, with rapid release of 20% of the drug in the first 24 h, and cumulative release of 30% of the drug by 18 days, after which there was a slow linear release of 75% of the drug by 57 days. DOX loaded PR-α 8-Phe in the presence or absence of papain also exhibit the similar release profile (Fig. 3.10a). On the basis of the results, a release mechanism based on progressive surface erosion of PR nanostructures can be hypothesized. We hypothesize that the DOX release from the nanoparticle could be divided to 3 phases. In the first stage of 24 h release, the DOX in the exterior of particle, which was not loaded tightly in PEG shell, was released because of passive diffusion. Form 1 days to 18 days, the DOX was tightly loaded in the center of particles because of hydrophobic and hydrogen-bond interaction. There existed a balance between the drug load interaction and drug diffusion to the bulk solution, which resulted in very slowly release rate in this time period. In the final stage, the nanoaggregates collapsed eventually because of the higher osmotic pressure and the drug in the center of particle was released slowly with linear release. The similar release profile has also been observed from other micelle/nanoparticle based drug delivery systems [34, 44]. By comparing Fig. 3.10a and 3.10b, it was found that PR-α 8-Phe exhibited a higher bust release rate than PR-α 12-TNBS, maybe because less threaded CDs resulted in weaker hydrogen-bond interactions and loser drug loading.

In comparison with free DOX without polymers, the polyrotaxane based drug delivery systems exhibited a sustained and long term DOX release lasting about 60 days. The sustained release could be attributed not only to the hydrophobic interaction

between drug and the partial polyrotaxane, more importantly, it could also be due to the hydrogen-bond interaction between hydroxyl group of CDs and amide group of DOX under neutral and basic conditions [19]. It is worthy of note that a sustained release rate is importance for intravenous delivery when a targeting in specific area of the body is attained. In fact, when the nanocarrier reaches its pharmacological target by accumulating in solid tumors through EPR effect [45, 46], its eventual ability to slowly release its drug content in extracellular compartment can be considered highly beneficial to prolong therapeutic effect [44]. The long induction time ensures sufficient time for the particles to accumulate in the small vasculature before the drug is released [47]. Importantly, due to the stability and the ability to retain the entrapped drug molecule of our system, sustained release could decrease the concentration of free drug in circulations, resulting in a decreased accumulation of the drug in the heart tissues and reduced cardiotoxicity, which is a serious drawback for DOX as anti-cancer therapy [48, 49].

Remarkably, by comparing the release profiles in Fig. 3.10a, it was found that PR-α 8-Phe released DOX rapidly in the presence of papain in contrast to that without papain. This is in line with the previous observation that PR-α 8-Phe were degraded into small pieces in response to papain. In contrast, no drug release difference was observed within 60 days for the reduction insensitive PR-α 12-TNBS nanoaggregates under the same conditions (Fig. 3.10b). Therefore, it is evident that fast drug release from PR-α 8-Phe is triggered by reduction of Z-L-Phe linkage. Interestingly, unlike other triggered-biodegradable drug release profile [50], the release rate of the PR nanostructures was sustained even in the presence of papain (Fig 3.10a). It probably because even the particles were degraded into small pieces by papain, it still could

compact and load drugs to prevent it from releasing suddenly. The phenomenon could be observed by TEM images in Fig. 3.10a. This unique property could be highly beneficial to prolong the therapeutic effect and decrease the cardiotoxicity.

3.3.9 In vitro cytotoxicity

Blank PR-α 8-Phe and PR-α 12-TNBS were evaluated for their cytotoxicity against L929 cells with an MTT assay. As shown in Fig. 3.11(a), both drug carrier with different end groups did not exhibit detectable cytotoxicity at all concentrations up to 1 mg/mL. Therefore, the polymer was expected to be safe for biomedical applications. After loading DOX, the L929 cells exhibited a dose-responsive viability due to the cytotoxicity of DOX (Fig. 3.11b). It indicated that our polyrotaxane nanoparticles could successfully delivery DOX into cells.

(a) Blank Polyrotaxane
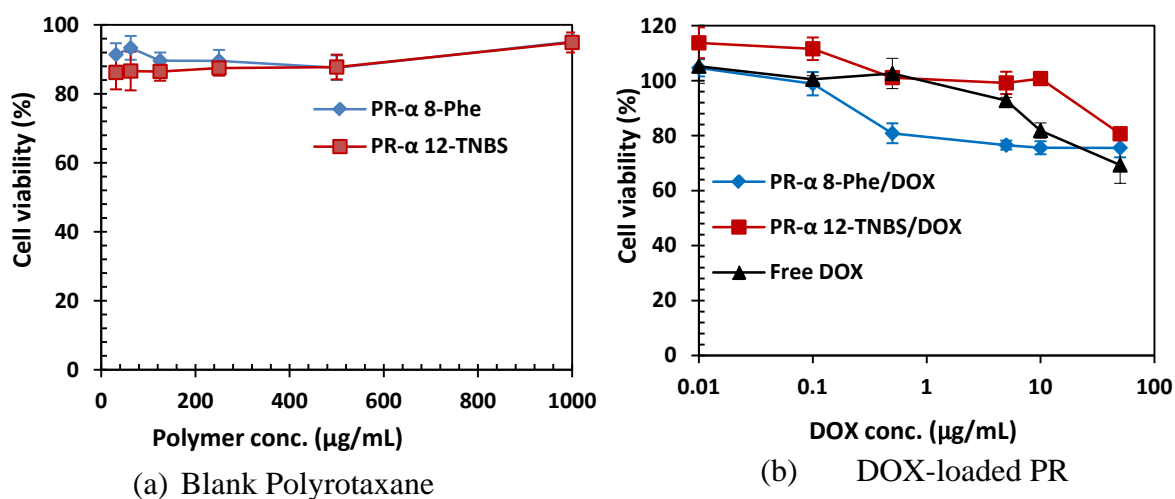
(b) DOX-loaded PR

Fig. 3.11 The cytotoxicity of (a) blank polyrotaxane and (b) DOX-loaded PR against normal L929 fibroblast cells after 24h incubation. Data represent mean ± standard deviation (n=3).

(a) DOX loaded PR in MB231 cells

(b) DOX loaded PR in Hela cells

(c) Blank polymer in MB231 cells
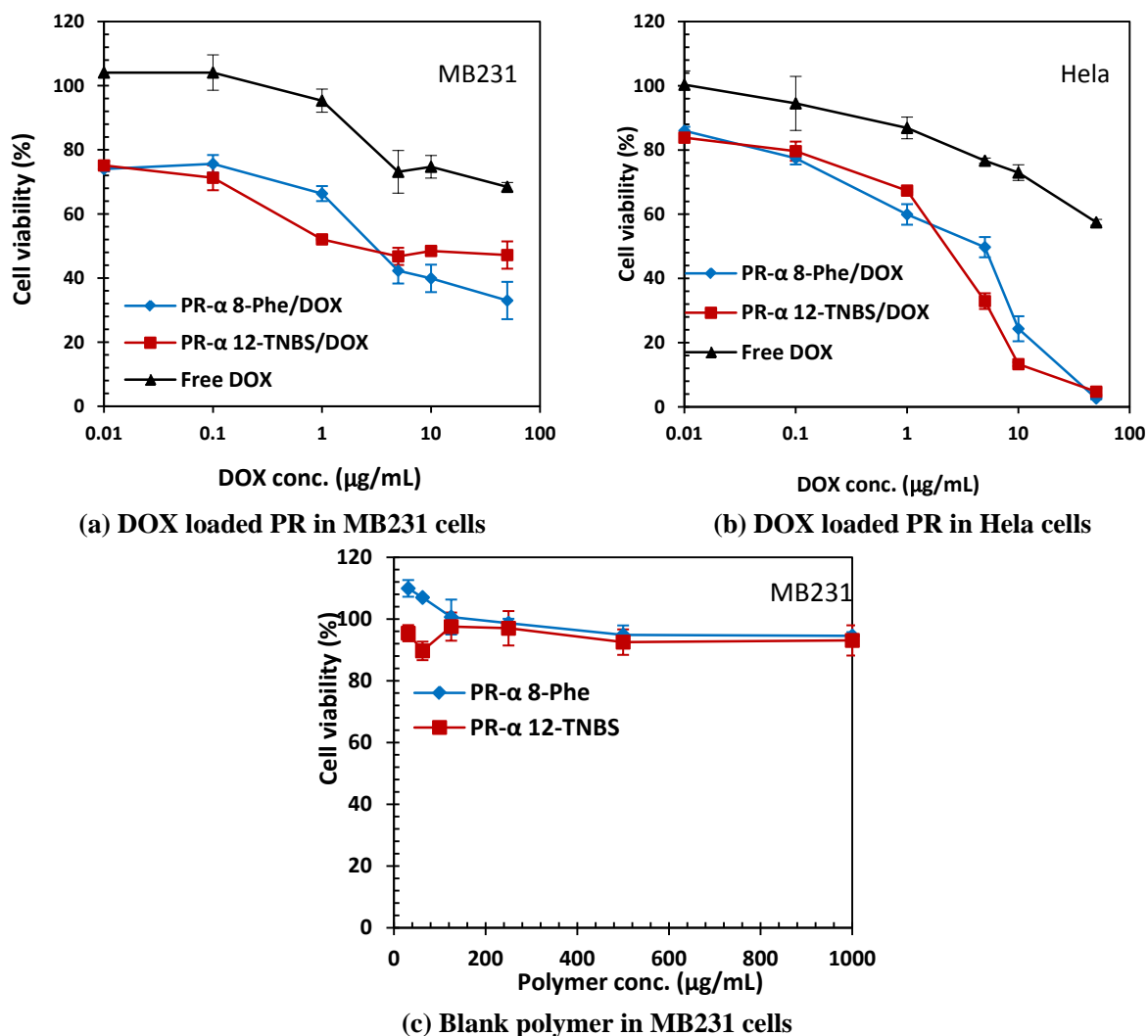
Fig. 3.12 The cytotoxicity of star PR with or without DOX loading against cancer cells after 24h incubation. (a) MB231 cells with DOX loading; (b) Hela cells with DOX loading; (c) MB231 cells without DOX loading. Data represent mean ± standard deviation (n=3).

The *in vitro* anticancer activity of the DOX loaded polyrotaxane was performed on MB231 and HeLa cancer cells. Cytotoxicity of DOX delivered by the polyrotaxane (PR-α 8-Phe and PR-α 12-TNBS) was compared against free DOX in these two cell lines using MTT method. As shown in Fig. 3.12 (a)-(b), similar dose-response viability was observed in both MB231 and Hela cells for all three DOX formulas, suggesting our polyrotaxanes could successfully delivery DOX into the cancer cell. Remarkably, both DOX loaded PRs exhibited significantly higher potent in killing cancer cells than free DOX, especially in low drug concentration. The high

cytotoxicity could be attributed to higher cell uptake when delivered by the core-shell nanostructures (detail showed in Fig. 3.13). It could also due to the ability of our carriers to release the drug slowly to cells which could permit their prolonged arrest in mitosis. Furthermore, for drugs acting at a specific phase of cell cycle (eg. when DOX blocks cell cycle progress at the metaphase/anaphase transition), the capability of the delivery system with sustained drug release can allow DOX to act on a higher number of cells in a specific phase of cell cycle as compared to a bolus administration [44]. Additionally, there was no cellular toxicity caused by the blank polyrotaxane (Fig. 3.12c) at the studied concentration range, eliminating the possibility that polymers themselves were responsible for the cytotoxicity.

3.3.10 Intracellular uptake and distribution
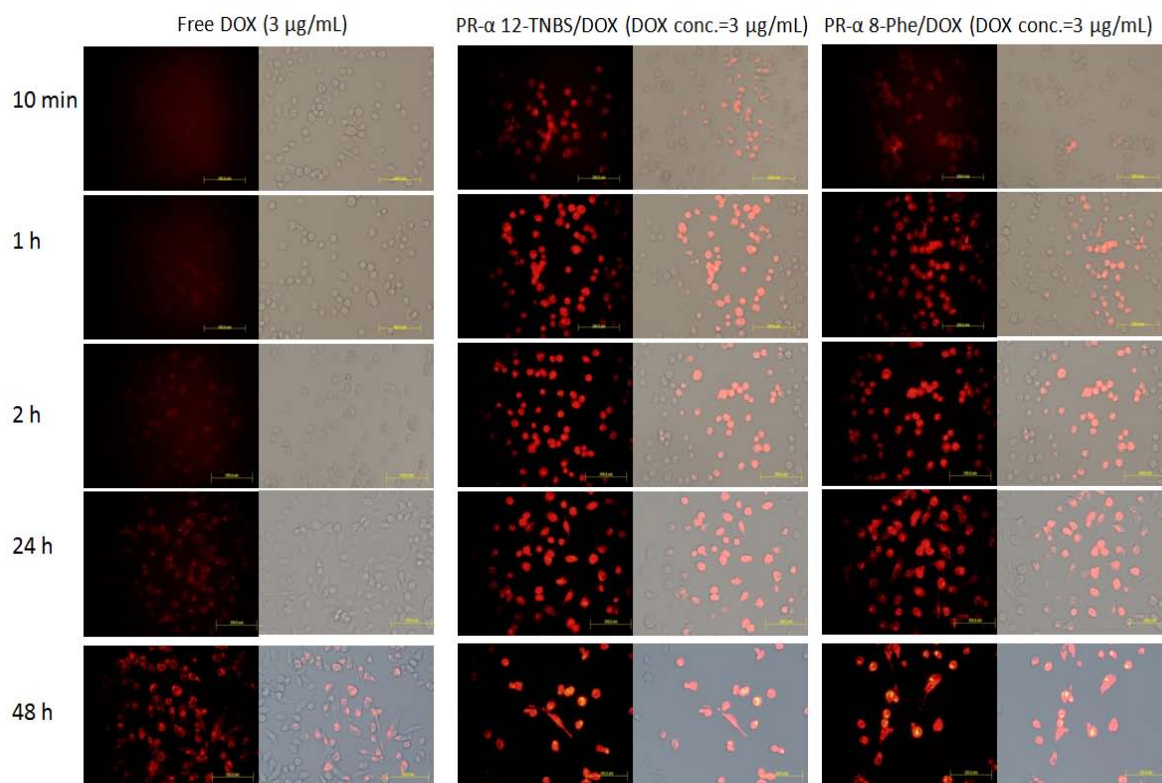
Fig. 3.13 Cellular uptake and internalization of (a) Free DOX, (b) DOX-loaded PR-α 12-TNBS and (c) DOX-loaded PR-α 8-Phe in MB231 cells at 10 min, 1 h, 2 h, 24 h and 48 h followed by fluorescence microscopy. (*DOX Concentration=3μg/mL, left: fluorescence light; right: overlay of fluorescence light and bright light*). Scale length=100μm.

DOX exhibited its own fluorescence with an excitation and emission wavelengths of 480 and 580 nm, respectively. The cellular uptake and internalization behavior of DOX loaded PR-α 8-Phe and PR-α 12-TNBS were followed with fluorescence microscopy using MB231 cell line, by comparing with free DOX. As shown in Fig. 3.13 (b) and (c), PR/DOX could be rapidly uptaken by the cells and the uptake increases with time. Notably, in contrast to free DOX without transport carriers (Fig 3.13a), the PR/DOX complexes exhibited much a faster and higher cell uptake, as reflected by the higher intensity of fluorescence within the exposed cells. Furthermore, the nanoparticles were able to internalize into the cells, as the red fluorescence were seen to be overlaid inside the cells, which implicated that the drugs were successfully internalized and delivered into the cells. The high internalization of our carriers may due to the small size and core-shell nanostructures with water soluble PEG shell, which increased the cell-impermeability and stability of DOX [29]. The sustained drug release also prolonged the therapeutic effect of the drugs and increased the residence time within MB231 cells. In addition, in contrast with free DOX, much less viable cells were found for DOX loaded polymer after 48 h incubation. And the MTT studies reveal that smaller number of viable cells was found for PR/DOX, indicating a greater drug efficacy for our shell-sheddable drug carriers (Fig. 3.12).

Furthermore, this CD-based core-shell nanostructure with hydrophilic shell could be very useful *in vivo* situation. Geze et al. studied the biodistribution of β-CD nanoparticles in mice after intravenous administration [51]. It was found that as the other uncoated particulate nanocarriers, they were rapidly cleared from the blood compartment in the reticulo-endothelial system, particularly in liver and spleen macrophages. Therefore, DOX-loaded polyrotaxane which present a hydrophilic

coating would be great interest in this sense due to the long-circulating properties as compared to other structures [44].

3.4 CONCLUSIONS

A novel star polyrotaxane is successful synthesized by controlled threading of α-CD on star PEG, and blocking the end of the polymer with both enzymatic biodegradable linkage. The SPR could further self-assembled into nanostructures in water with polyrotaxane core and hydrophilic PEG shell with particle size around 20-150 nm. The enzymatic biodegradability of the nanoparticles was confirmed by TEM and particle size. The nano-sized particles provide high capacity for DOX loading with sustained *in vitro* release for more than 2 months. Furthermore, PR-phe/DOX exhibited a faster release, suggesting their stimuli-responsible properties, which would be benefic to the controlled drug delivery.

Remarkably, the PR/DOX was capable of fast cell internalization and cell uptake to yield significantly enhanced drug efficacy as compared to free DOX. And the DOX-loaded polyrotaxane which present a hydrophilic coating would be great interest *in vivo* due to the long-circulating properties as compared to other structures. Taken together, our star polyrotaxanes boast many favorable properties of drug carries, which include excellent biocompatibility and triggered-biodegradability, adequate drug loading capacity, sustained and controlled drug release, higher cell uptake and highly anti-cancer efficacy.

3.5 REFERENCES

1.   Jenekhe SA, Chen XL. Self-assembled aggregates of rod-coil block copolymers and their solubilization and encapsulation of fullerenes. Science 1998 Mar;279(5358):1903-1907.

2.   Cheng C, Wei H, Shi BX, Cheng H, Li C, Gu ZW, et al. Biotinylated thermoresponsive micelle self-assembled from double-hydrophilic block copolymer for drug delivery and tumor target. Biomaterials 2008 Feb;29(4):497-505.

3.   Chen YC, Liao LC, Lu PL, Lo CL, Tsai HC, Huang CY, et al. The accumulation of dual pH and temperature responsive micelles in tumors. Biomaterials 2012 Jun;33(18):4576-4588.

4.   Gref R, Minamitake Y, Peracchia MT, Trubetskoy V, Torchilin V, Langer R. Biodegradable long-circulating polymeric nanospheres. Science 1994 Mar;263(5153):1600-1603.

5.   Jang SG, Kramer EJ, Hawker CJ. Controlled Supramolecular Assembly of Micelle-Like Gold Nanoparticles in PS-b-P2VP Diblock Copolymers via Hydrogen Bonding. Journal of the American Chemical Society 2011 Oct;133(42):16986-16996.

6.   Wu YL, Li J. Synthesis of supramolecular nanocapsules based on threading of multiple cyclodextrins over polymers on gold nanoparticles. Angew Chem Int Ed Engl 2009;48(21):3842-3845.

7.   Harada A, Li J, Kamachi M. The molecular necklace-a rotaxane containing many threaded ahpha-cyclodextrins. Nature 1992 Mar;356(6367):325-327.

8.   Li J, Loh XJ. Cyclodextrin-based supramolecular architectures: Syntheses, structures, and applications for drug and gene delivery. Advanced Drug Delivery Reviews 2008 Jun;60(9):1000-1017.

9.   Araki J, Ito K. Recent advances in the preparation of cyclodextrin-based polyrotaxanes and their applications to soft materials. Soft Matter 2007;3(12):1456-1473.

10.   Li JJ, Zhao F, Li J. Polyrotaxanes for applications in life science and biotechnology. Appl Microbiol Biotechnol 2011 Apr;90(2):427-443.

11.   Ohya Y, Takamido S, Nagahama K, Ouchi T, Katoono R, Yui N. Polyrotaxane Composed of Poly-L-lactide and alpha-Cyclodextrin Exhibiting Protease-Triggered Hydrolysis. Biomacromolecules 2009 Aug;10(8):2261-2267.

12.   Ooya T, Yui N. Synthesis of theophylline-polyrotaxane conjugates and their drug release via supramolecular dissociation. Journal of Controlled Release 1999 Apr;58(3):251-269.

13.   Loethen S, Ooya T, Choi HS, Yui N, Thompson DH. Synthesis, characterization, and pH-triggered dethreading of alpha-cyclodextrin-poly(ethylene glycol) polyrotaxanes bearing cleavable endcaps. Biomacromolecules 2006 Sep;7(9):2501-2506.

14.   Antonov EN, Bagratashvili VN, Whitaker MJ, Barry JJA, Shakesheff KM, Konovalov AN, et al. Three-dimensional bioactive and biodegradable scaffolds fabricated by surface-selective laser sintering. Advanced Materials 2005 Feb;17(3):327-+.

15. Fung LK, Saltzman WM. Polymeric implants for cancer chemotherapy. Advanced Drug Delivery Reviews 1997;26(2-3):209-230.

16. Ikada Y, Tsuji H. Biodegradable polyesters for medical and ecological applications. Macromolecular Rapid Communications 2000;21(3):117-132.

17. Zhou Y, Huang W, Liu J, Zhu X, Yan D. Self-Assembly of Hyperbranched Polymers and Its Biomedical Applications. Advanced Materials 2010 Nov 2;22(41):4567-4590.

18. Lee VY, Havenstrite K, Tjio M, McNeil M, Blau HM, Miller RD, et al. Nanogel Star Polymer Architectures: A Nanoparticle Platform for Modular Programmable Macromolecular Self-Assembly, Intercellular Transport, and Dual-Mode Cargo Delivery. Advanced Materials 2011 Oct 18;23(39):4509-+.

19. Yang XY, Chen LT, Huang B, Bai F, Yang XL. Synthesis of pH-sensitive hollow polymer microspheres and their application as drug carriers. Polymer 2009 Jul;50(15):3556-3563.

20. Yang C, Attia AB, Tan JP, Ke X, Gao S, Hedrick JL, et al. The role of non-covalent interactions in anticancer drug loading and kinetic stability of polymeric micelles. Biomaterials 2012 Apr;33(10):2971-2979.

21. Yang C, Li J. Thermoresponsive Behavior of Cationic Polyrotaxane Composed of Multiple Pentaethylenehexamine-grafted alpha-Cyclodextrins Threaded on Poly(propylene oxide)-Poly(ethylene oxide)-Poly(propylene oxide) Triblock Copolymer. Journal of Physical Chemistry B 2009 Jan;113(3):682-690.

22. Harada A, Li J, Nakamitsu T, Kamachi M. Preparation and characterization of polyrotaxanes containing many threaded alpha-cyclodextrins. Journal of Organic Chemistry 1993 Dec;58(26):7524-7528.

23. Ooya T, Yui N. Synthesis and characterization of biodegradable polyrotaxane as a novel supramolecular-structured drug carrier. Journal of Biomaterials Science-Polymer Edition 1997;8(6):437-455.

24. Anderson GW, Callahan FM, Zimmerman JE. Use of esters of n-hydroxysuccinimide in peptide synthesis. Journal of the American Chemical Society 1964;86(9):1839-&.

25. Zhang XW, Zhu XQ, Ke FY, Ye L, Chen EQ, Zhang AY, et al. Preparation and self-assembly of amphiphilic triblock copolymers with polyrotaxane as a middle block and their application as carrier for the controlled release of Amphotericin B. Polymer 2009 Aug;50(18):4343-4351.

26. Sun HL, Guo BN, Cheng R, Meng FH, Liu HY, Zhong ZY. Biodegradable micelles with sheddable poly(ethylene glycol) shells for triggered intracellular release of doxorubicin. Biomaterials 2009 Nov;30(31):6358-6366.

27. Lin JP, Zhang SN, Chen T, Lin SL, Jin HT. Micelle formation and drug release behavior of polypeptide graft copolymer and its mixture with polypeptide block copolymer. International Journal of Pharmaceutics 2007 May;336(1):49-57.

28. Lee ES, Na K, Bae YH. Doxorubicin loaded pH-sensitive polymeric micelles for reversal of resistant MCF-7 tumor. Journal of Controlled Release 2005 Mar;103(2):405-418.

29. Lee ALZ, Wang Y, Cheng HY, Pervaiz S, Yang YY. The co-delivery of paclitaxel and Herceptin using cationic micellar nanoparticles. Biomaterials 2009 Feb;30(5):919-927.

30.   Wei L, Cai CH, Lin JP, Chen T. Dual-drug delivery system based on hydrogel/micelle composites. Biomaterials 2009 May;30(13):2606-2613.

31.   Li X, Li J, Leong KW. Preparation and characterization of inclusion complexes of biodegradable amphiphilic poly(ethylene oxide)-poly[(R)-3-hydroxybutyrate]-poly(ethylene oxide) triblock copolymers with cyclodextrins. Macromolecules 2003 Feb;36(4):1209-1214.

32.   Loh XJ, Goh SH, Li J. New biodegradable thermogelling copolymers having very low gelation concentrations. Biomacromolecules 2007 Feb;8(2):585-593.

33.   Moon C, Kwon YM, Lee WK, Park YJ, Yang VC. In vitro assessment of a novel polyrotaxane-based drug delivery system integrated with a cell-penetrating peptide. Journal of Controlled Release 2007 Dec;124(1-2):43-50.

34.   Xiao K, Luo JT, Fowler WL, Li YP, Lee JS, Xing L, et al. A self-assembling nanoparticle for paclitaxel delivery in ovarian cancer. Biomaterials 2009 Oct;30(30):6006-6016.

35.   Loh XJ, Colin Sng KB, Li J. Synthesis and water-swelling of thermo-responsive poly(ester urethane)s containing poly(epsilon-caprolactone), poly(ethylene glycol) and poly(propylene glycol). Biomaterials 2008 Aug;29(22):3185-3194.

36.   Harada A, Kamachi M. Complex-formation between poly (ethylene glycol) and alpha-cyclodextrin. Macromolecules 1990 May;23(10):2821-2823.

37.   Li J, Yang C, Li HZ, Wang X, Goh SH, Ding JL, et al. Cationic supramolecules composed of multiple oligoethylenimine-grafted beta-cyclodextrins threaded on a polymer chain for efficient gene delivery. Advanced Materials 2006 Nov;18(22):2969-+.

38.   Ni XP, Cheng A, Li J. Supramolecular hydrogels based on self-assembly between PEO-PPO-PEO triblock copolymers and alpha-cyclodextrin. Journal of Biomedical Materials Research Part A 2009 Mar;88A(4):1031-1036.

39.   Bae SJ, Suh JM, Sohn YS, Bae YH, Kim SW, Jeong B. Thermogelling poly(caprolactone-b-ethylene glycol-b-caprolactone) aqueous solutions. Macromolecules 2005 Jun;38(12):5260-5265.

40.   Hwang MJ, Suh JM, Bae YH, Kim SW, Jeong B. Caprolactonic poloxamer analog: PEG-PCL-PEG. Biomacromolecules 2005 Mar-Apr;6(2):885-890.

41.   Akinc A, Anderson DG, Lynn DM, Langer R. Synthesis of poly(beta-amino ester)s optimized for highly effective gene delivery. Bioconjugate Chemistry 2003 Sep-Oct;14(5):979-988.

42.   Adams ML, Lavasanifar A, Kwon GS. Amphiphilic block copolymers for drug delivery. Journal of Pharmaceutical Sciences 2003 Jul;92(7):1343-1355.

43.   Oh I, Lee K, Kwon HY, Lee YB, Shin SC, Cho CS, et al. Release of adriamycin from poly(gamma-benzyl-L-glutamate)/poly(ethylene oxide) nanoparticles. International Journal of Pharmaceutics 1999 Apr;181(1):107-115.

44.   Quaglia F, Ostacolo L, Mazzaglia A, Villari V, Zaccaria D, Sciortino MT. The intracellular effects of non-ionic amphiphilic cyclodextrin nanoparticles in the delivery of anticancer drugs. Biomaterials 2009 Jan;30(3):374-382.

45.   Duncan R. The dawning era of polymer therapeutics. Nature Reviews Drug Discovery 2003 May;2(5):347-360.

46.   Matsumura Y, Maeda H. A new concept for macromolecular therapeutics in cancer-chemotherapy mechanism of tumoritropic accumulation of proteins and the antitumor agent smancs. Cancer Research 1986 Dec;46(12):6387-6392.

47. Branco MC, Schneider JP. Self-assembling materials for therapeutic delivery. Acta Biomaterialia 2009 Mar;5(3):817-831.

48. Brown MD, Schatzlein A, Brownlie A, Jack V, Wang W, Tetley L, et al. Preliminary characterization of novel amino acid based polymeric vesicles as gene and drug delivery agents. Bioconjugate Chemistry 2000 Nov-Dec;11(6):880-891.

49. Son YJ, Jang JS, Cho YW, Chung H, Park RW, Kwon IC, et al. Biodistribution and anti-tumor efficacy of doxorubicin loaded glycol-chitosan nanoaggregates by EPR effect. Journal of Controlled Release 2003 Aug;91(1-2):135-145.

50. Sun H, Guo B, Cheng R, Meng F, Liu H, Zhong Z. Biodegradable micelles with sheddable poly(ethylene glycol) shells for triggered intracellular release of doxorubicin. Biomaterials 2009 Oct;30(31):6358-6366.

51. Geze A, Chau LT, Choisnard L, Mathieu JP, Marti-Batlle D, Riou L, et al. Biodistribution of intravenously administered amphiphilic beta-cyclodextrin nanospheres. Int J Pharm 2007 Nov 1;344(1-2):135-142.

CHAPTER 4 DUAL SUPRAMOLECULAR SELF-ASSEMBLED NANOSTRUCTURES BASED ON STAR POLYMERS FOR STIMULI-RESPONSIVE DRUG RELEASE

4.1 INTRODUCTION

For cancer therapy, reduction-sensitive biodegradable polymers with disulfide linkage have emerged as a fascinating class of biomedical materials for drug delivery. The disulfide linkages are sufficiently stable under physiological conditions; In the cytosol, however, due to the high levels of glutathione they may be subject to rapid degradation. Therefore, reduction-sensitive drug carriers in principle could meet the conflicting requirements of an ideal drug delivery system, i.e. high stability in circulation while rapid degradation inside targeted cells.[1, 2]

Since the first synthesis of polyrotaxane with multiple α-CD rings threaded around a polymer chain [3, 4], CD-based polypseudorotaxanes and polyrotaxanes have been receiving increasing attention due to their intriguing supramolecular architecture of sliding/dethreading and promising bio-applications [5-8]. Due to the threading and dethreading nature of polyrotaxanes, recent studies in biodegradable

polyrotaxanes focus on various stimuli-triggered responses such as enzymes[9-11], pH, redox[12], and temperature.

In our previous studies, star enzymatic biodegradable polyrotaxanes were successfully synthesized by controlled threading of α-CD onto star PEG (sPEG) and their dual self-assembled behaviours to core-shell nanostructures were further confirmed. This unique core-shell structure with PR core may potentially lead to some specific interactions (e.g. hydrogen bond) between the drug and core, which is different from traditional core-shell nanostructures.[13-15] And the core-shell polyrotaxane nanostructures were found to be advantages in sustain drug delivery with triggered drug release, higher cell uptake and enhanced drug efficacy.

In this chapter, with the aim of meeting the conflicting requirements of an ideal drug delivery system, i.e. high stability in circulation while rapid degradation inside targeted cells, we further developed a reduction-sensitive biodegradable system for rapid intracellular drug release based on the similar polyrotaxane self-assembled nanostructures. Disulfide linkage was introduced to the core-shell nanostructures self-assembled from SPR (Scheme 4.1). This new SPR nanostructure shows great potential to be used as drug carriers with the advantages of reduction-sensitive biodegradability, improved solubility, low side effects, high drug load efficiency with sustained drug release, improved cell uptake and high anti-cancer efficiency. Furthermore, due to the stability and the ability to retain the entrapped drug molecule of our system, sustained release could also decrease the concentration of free drug in circulations, resulted in a decreased accumulation of the drug in the heart tissues and reduced cardiotoxicity, which is a serious drawback for DOX as anti-cancer therapy.[16, 17]
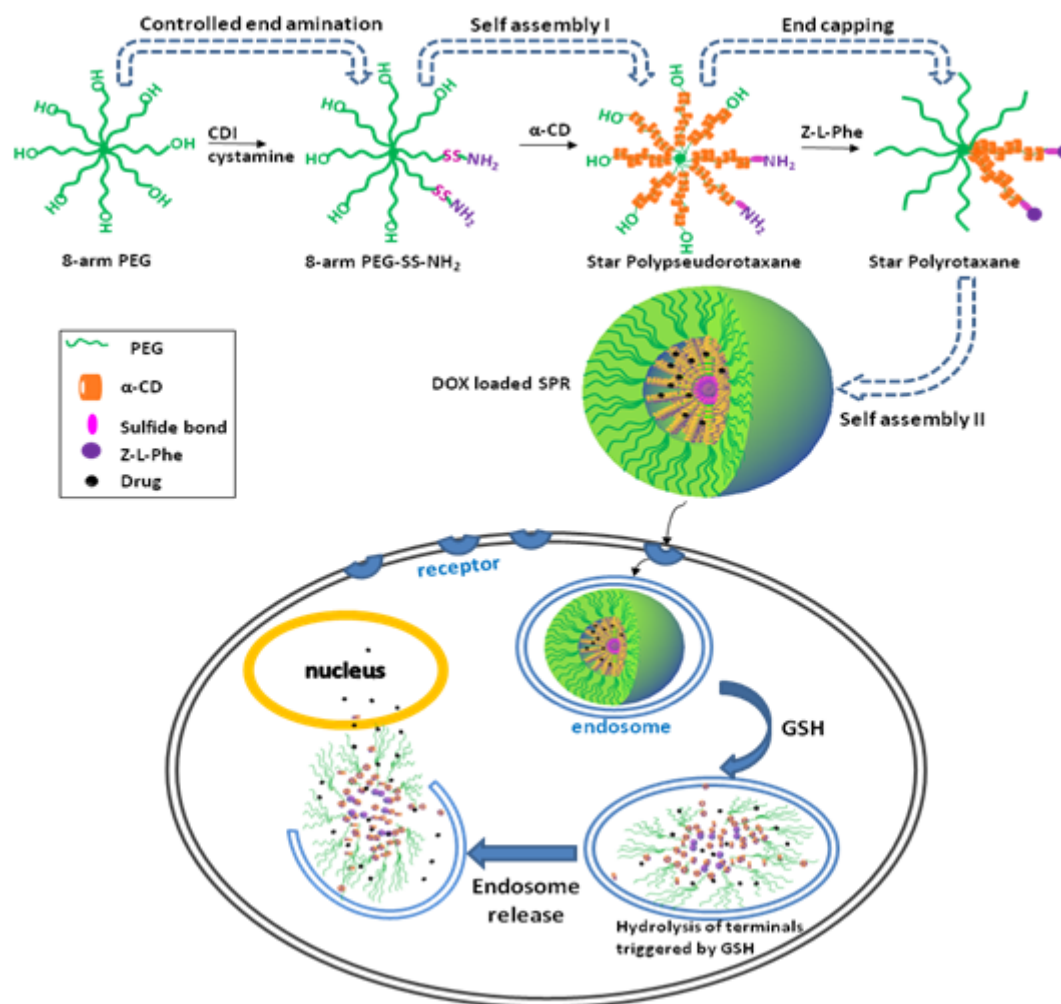
Scheme 4.1 Illustration of bio-reductive SPR and the intracellular drug release

4.2 MATERIALS AND METHODS

4.2.1 Materials

DCC, NHS, ethylenediamine, cystamine dihychloride, TEA, CDI, Z-L-Phe-OH, DOX, dithiothreitol (DTT) and NaOH were received from Sigma-Aldrich and used as received. 8 arm star PEG (Mn=9468) were purchased from Fluka. α-CD was purchased from TCI. Diethyl ether, methanol, DMF, 1,4-dioxane and DMSO were purchased from Merck. Penicillin, streptomycin and MTT were obtained from Sigma.

4.2.2 Synthesis Methods
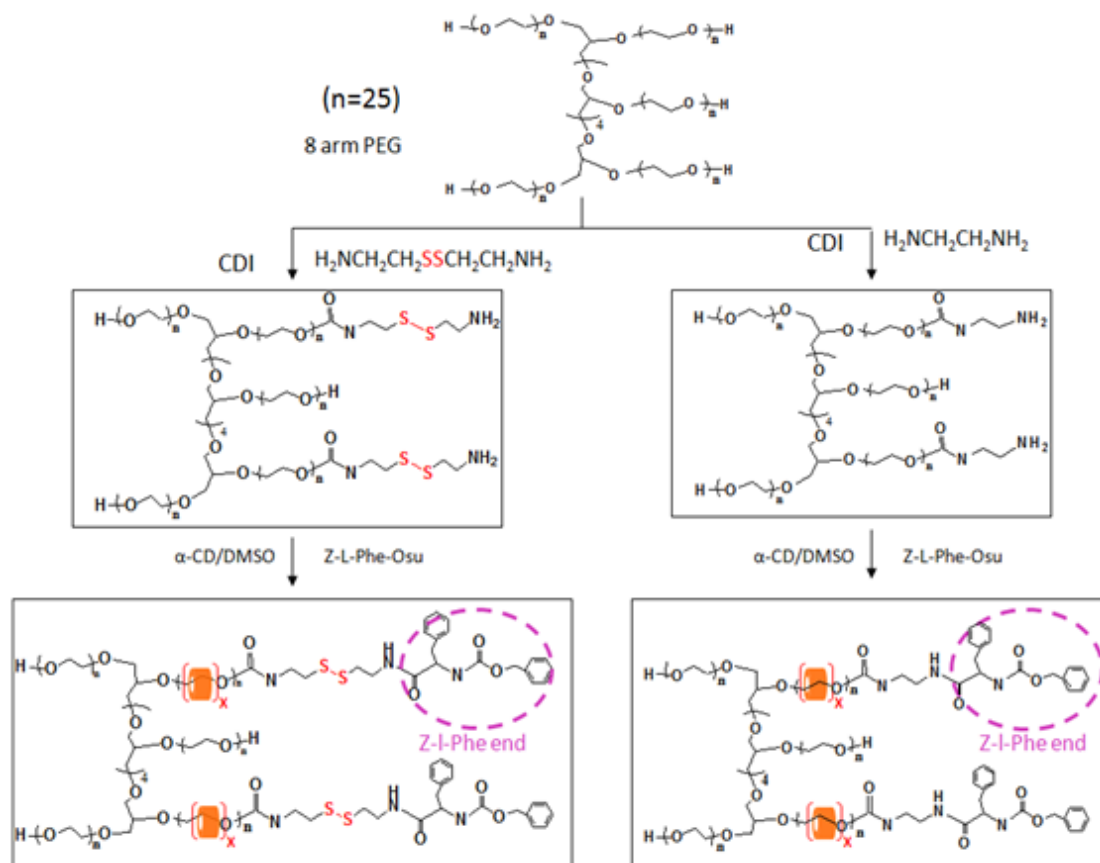
Scheme 4.2 Synthesis method and structures of bio-reductive SPR

4.2.2.1 Synthesis of PEG-SS-NH$_2$ and PEG-NH$_2$

8-arm PEG (1g, 0.1056 mmol) was heated at 80 °C overnight, followed by adding of 10 mL of anhydrous DMSO. Then the solution was added dropwise under nitrogen to 15 mL of anhydrous DMSO solution in which CDI (0.07g, 0.8448 mmol) was dissolved. Then the mixture was stirred overnight under nitrogen at R.T. The resulting solution was added dropwise into 3.8 g (16.896 mmol) of cystamine dihychloride, which was dissolved in 10 mL DMSO together with TEA (4.71 ml, 33.792 mmol), followed by stirring overnight. DMSO was removed by vacuum evaporation in 65 °C and the resulting viscous liquid was dissolved in mix solvent of

DI water and dichloride methane. The organic layer was collected and it was further purified by column chromatography on a Sephadex LH-20 column with methanol as eluent to give as a viscous yellowish liquid (Yield, 0.72g (72%)) [18-20]. The synthesis of PEG-NH$_2$ are the same with the previous protocols (3.2.2.1) [21].

4.2.2.2 Synthesis of Polyrotaxanes (PPR-SS-NH$_2$ and PPR-NH$_2$)

The synthesis procedure is the same with the protocols presented in 3.2.2.2.

4.2.2.3 Synthesis of polyrotaxanes (PR-SS-Phe/PR-Phe)

Partial polyrotaxane with Z-L-phenylalanine end groups (PR-SS-Phe) was synthesized in two steps, as reported previously [21-23]. The synthesis procedure is the same with the protocols presented in 3.2.2.3.

4.2.2.4 Self-assembly and DOX encapsulation

The solubility of polyrotaxane was decreased with the increase of CD threaded numbers. The polyrotaxane PR-α 8-SS-Phe and PR-α 8-Phe are soluble in water, and the micelle-like nanoaggregates could be prepared by directly dissolving the polymer in water and allowing it to stay overnight to ensure complete dissolution [24]. In the case of the insoluble polyrotaxane (PR-α 20-SS-Phe), the core-shell nanostructures could be prepared by dialysis [1, 25]. The procedures are the same with protocols in 3.2.2.4

DOX was loaded into the polyrotaxane nanoaggregates followed by the method reported before [26]. 10 mg soluble polyrotaxane (PR-α 8-SS-Phe and PR-α 8-Phe) was added to 1 mg DOX·HCl and dissolved together with 1 mL DI water, and the solution was stirred overnight at room temperature. Solution of sodium hydroxide

(NaOH) was added to the solution to adjust the pH to 8~9 and stirred for 3 h. Because DOX is insoluble in basic condition, the unloaded DOX molecular were precipitated and removed by ultracentrifugation. The obtained solution was then lyophilized.

The drug loading of insoluble polyrotaxane (PR-α 20-SS-Phe) was achieved in two steps. Firstly, 10 mg polyrotaxane was dissolved in DMSO and dialyzed against DI water for 2 days to form micelle-like aggregates. Secondly 1 mg DOX·HCl was added into the resulted nanoparticle solution and stirred overnight at R.T. After adjusting the pH to 8~9, unloaded DOX molecular were centrifuged and removed. Then the solution with loaded DOX was freeze-dried (Yield, 10 mg).

4.2.3 Measurements and Characterization

4.2.3.1 Proton Nuclear Magnetic Resonance (^{1}H-NMR) spectra

The procedures are the same with protocols in 3.2.3.1

4.2.3.2 Critical micellization concentration (CAC) determination

The CAC values were determined by the dye solublization method [27]. Partial polyrotaxane (PR-α 8-SS-Phe and PR-α 8-Phe) was characterized. The procedures are the same with presented protocols in 3.2.3.3.

4.2.3.3 Transmission Electron Microscopy (TEM) and Dynamic light scattering (DLS)

The procedures are the same with presented protocols in 3.2.3.4 and 3.2.3.5.

4.2.3.4 Biodegradation behavior evaluation-size exclusion chromatogram (SEC)

30 mg polyrotaxane (PR-α 20-SS-Phe) was added in 6 mL PBS containing DTT (10 mM), followed by shaking under 100 rpm at 37 °C for 6 days. Then the

result solutions were freeze-dried and size exclusion chromatography (SEC) was carried out with a Sephadex G-75 column using DMSO as eluent. Fractions were collected per 1.5 mL and their optical rotation were recorded at wavelength 589 nm with cell length 10 cm and response 2s [1, 28, 29]. (Control: Polyrotaxane was added in 6 ml PBS without DTT and it was characterized with the same procedure above).

4.2.3.5 Biodegradation behavior evaluation-TEM and DLS

2 mg PR-α 20-SS-Phe was dissolved in 1 ml DMSO and dialysis against DI water for 2 days (MW=2000). Then DTT (10 mM) was added to the resulted nanoaggregates solution, followed by shaking under 100 rpm at 37 °C for 6 days. The degradation behavior and morphology difference of the polymer was characterized and observed by TEM and Particle size after 0, 1 and 6 days. In order to make a comparison, the control sample of PR-α 20-SS-Phe nanoparticles was formed and treated without DTT, and it was characterized with the same procedure above. [1, 30]

4.2.3.6 Characterization of the drug delivery systems

The amount of DOX encapsulated in the polyrotaxane nanostructures was analyzed by fluorescence measurement (excitation at 480 nm) [1]. The procedures are the same with presented protocols in 3.2.3.7.

4.2.3.7 *In vitro* drug release study

Release of drugs from the drug-loaded polyrotaxanes was studied using the dialysis method [11, 26, 31]. 3 mg DOX loaded polyrotaxane nanoaggregates were put in dialysis membrane tube (MW=2000 Da), followed by dialyzing against 15 mL medium of PBS (pH=7.4) containing DTT (10 mM) [28, 30]. The release system was

shaken under 100 rpm at 37 °C for 60 days. At designed time intervals, 1 mL release medium was removed and replaced with fresh medium. The removed medium was analyzed for its drug content with fluorescence measurement (excitation at 480 nm). The recorded intensity was compared with a standard curve containing DOX/PBS (containing DTT) solution with concentration varied from 0 to 5 μg/mL. In order to make a comparison, polyrotaxanes were put into dialysis tube without DTT, followed by dialyzing against blank PBS and they are measured with the same procedure above.

4.2.3.8 Cell viability assay

The procedures are the same with presented protocols in 3.2.3.9.

4.2.3.9 Intracellular cell uptake and distribution

The procedures are the same with presented protocols in 3.2.3.10.

4.3 RESULTS AND DISCUSSION

4.3.1 Synthesis of polyrotaxane (PR-SS-Phe and PR-Phe)

Scheme 4.1 shows the synthesis procedures of partial polyrotaxane. Firstly, 8-arm PEG-SS-NH$_2$/PEG-NH$_2$ was synthesized by the CDI reaction. Specifically, the hydroxyl groups at the end of 8-arm PEG were activated with CDI, followed by reaction with large excess of cystamine/ethylenediamine to give terminal amino groups. Next, PEG-SS-NH$_2$/PEG-NH$_2$ was allowed to react with saturated solution of α-CD to obtain polypseudorotaxane, following similar procedures described in previous report [32], in which it was found that α-CD will form an inclusion complex

with ratio EO/CD of 2, approximately. Then the end of PEG was blocked to form

polyrotaxane with Z-L-Phe.
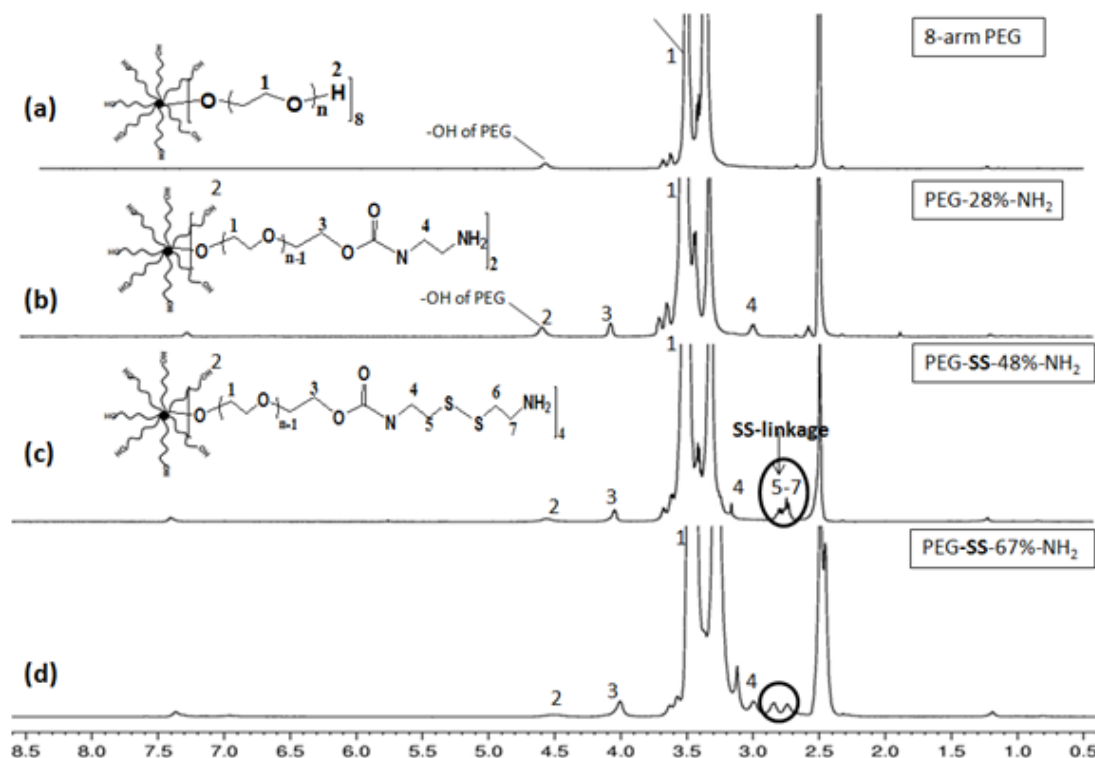
Fig. 4.1 ^{1}H-NMR spectrum of (a) 8-arm PEG (Mw=9468, n=25), (b) PEG-11.3%-NH$_2$ (feeding ratio of CDI/PEG=4:1), (c) PEG-48%-SS-NH$_2$ (feeding ratio=8:1), (d) PEG-67%-SS-NH$_2$ (feeding ratio=24:1) in d$_6$-DMSO.

Fig. 4.1 shows the ^{1}H NMR result of 8-arm PEG-SS-NH$_2$/PEG-NH$_2$ in

comparison with pure 8-arm PEG. In contrast to Fig. 4.1(b), Fig. 4.1(c)-(d) exhibited

unique peak of δ=2.7~2.8, which was attributed to the SS-linkage. Furthermore, due

to the end grafting of cystamine/ethylenediamine, the chemical shift of H$_3$ in PEG was

change from 3.5 ppm (in pure PEG) to 4.05 ppm (in the product). And by comparing

Fig. 4.1 (b)-(d), it was found that with the increase of feed ratio, the integration ratio

of H$_2$ (-OH of PEG) was decreased after the reaction. The results confirm the

successful conjugation of 8-arm PEG with cystamine/ethylenediamine. Quantitative

comparisons between the integral intensities of peaks H$_3$ and peak H$_2$ were used to

derive the grafted ratio of the polymer and the results are summarized in Table 4.1.
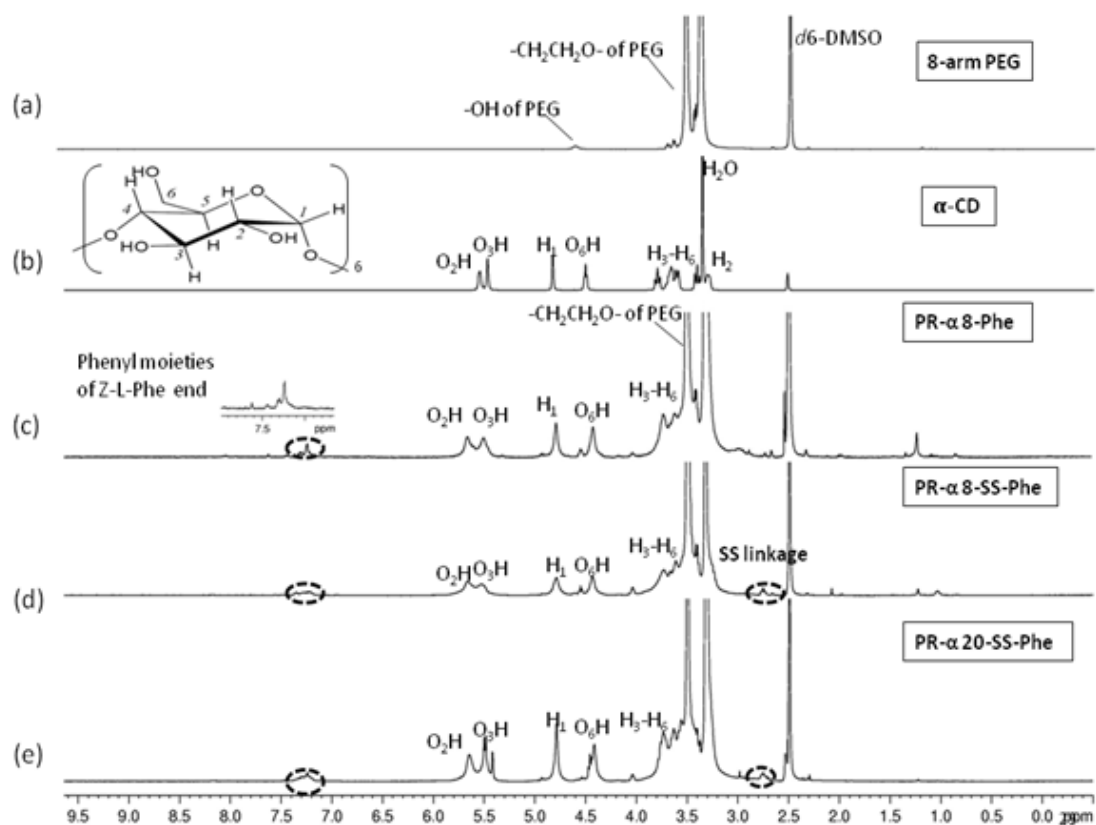
Fig. 4.2 ^{1}H-NMR of (a) 8-arm PEG (Mn=9468), (b) α-CD, (c) PR-α 8-Phe, (d) PR-α 8-SS-Phe and (e) PR-α 20-SS-Phe in d$_6$-DMSO.

Fig 4.2 shows the ^{1}H NMR of polyrotaxane in comparison with pristine α-CD and 8-arm PEG. In Fig. 4.1(c)-(e), the signals for α-CD, 8-arm PEG and the end capping groups (Z-L-Phe, δ=7.2-7.4) were all observed. Furthermore, it was found that the peaks of α-CDs in polyrotaxanes were broadened; suggesting the mobility of α-CDs in polyrotaxane is restricted by the PEG chain after forming the supramolecular structure. These results provide us clear evidence for the physically interlocked supramolecular structure of 8 arm PEG covered by α-CDs with Z-L-Phe end groups [20, 21]. The polyrotaxane compositions could be derived by quantitative comparison between the resonance peak due to H$_1$ of α-CD (δ=4.79), the peak due to the PEG (δ=3.50) and the peak area of Z-L-Phe end. By calculation, 3 kinds of polyrotaxanes are confirmed (Table 4.1). TGA was also further used to estimate the

ratio between α-CD and PEG in the polyrotaxanes. And the results were in good agreement with the ^{1}H NMR.

Table 4.1 The polyrotaxane compositions with different threaded number of CDs

Polyrtoaxanes	Grafted ratio of Precursor PEG	α-CD threaded arm per polymer (^{1}H NMR)[a]	CD threaded number per polymer (^{1}H NMR)[a]	CD threaded number per polymer (TGA)[b]
PR-α 8-Phe	PEG-28%-NH$_2$	1 arm	8	10
PR-α 8-SS-Phe	PEG-48%-SS-NH$_2$	1 arm	8	9
PR-α 20-SS-Phe	PEG-67%-SS-NH$_2$	3 arms	20	21

[a] Data was calculated on the basis of ^{1}H NMR

[b] Data was calculated according to the result of TGA.

4.3.2 Self-assembly and CAC determination
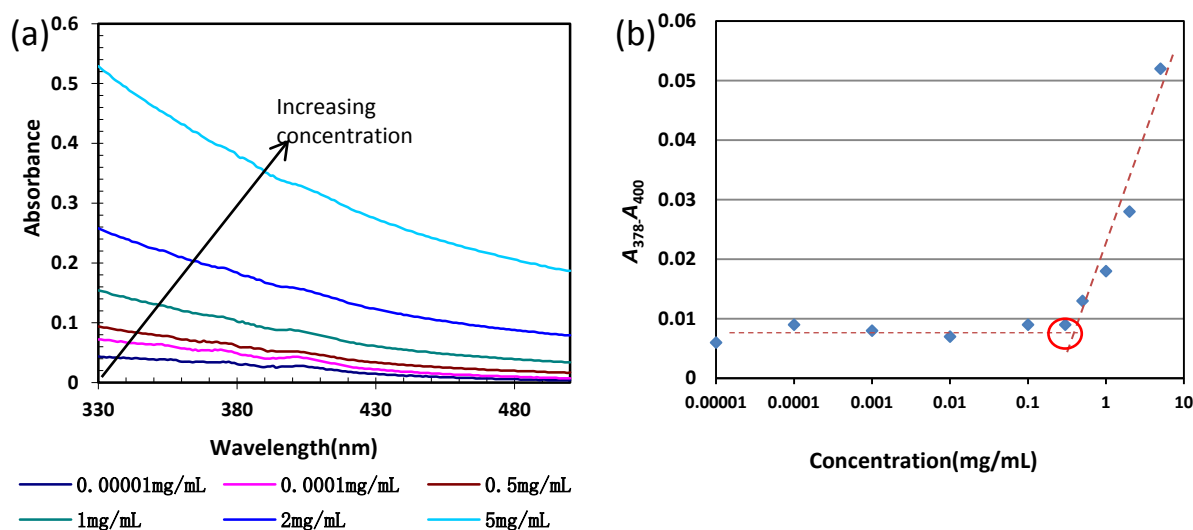
Fig. 4.3 (a) UV-vis spectra changes of DPH with increasing PR-α 8-SS-Phe concentration in water at 25 °C. (b) CAC determination by extrapolation of the difference in absorbance at 378 nm and 400 nm

Both PR-α 8-Phe and PR-α 8-SS-Phe were soluble and the core-shell nanostructures were formed by directly dissolving in water. Their CAC were determined by DPH method [33, 34]. DPH shows a higher absorption coefficient in a hydrophobic environment than in water. Thus, with increasing polymer concentration, the absorbance at 344, 358 and 378 nm increased (Fig. 4.3a). The CAC was

determined by extrapolating the absorbance at 378 nm minus the absorbance at 400 nm (A_{378}-A_{400}) versus logarithmic concentration (Fig. 4.3b). It was found that the CAC values for water-soluble polyrotaxane PR-α 8-SS-Phe are 0.3 mg/mL. Similarly, PR-α 8-Phe showed a CAC of 0.8 mg/mL, which is higher than PR-α 8-SS-Phe (Data shown in Fig. 3.5 of chapter 3)

4.3.3 TEM and Particle Size of the self-assembly
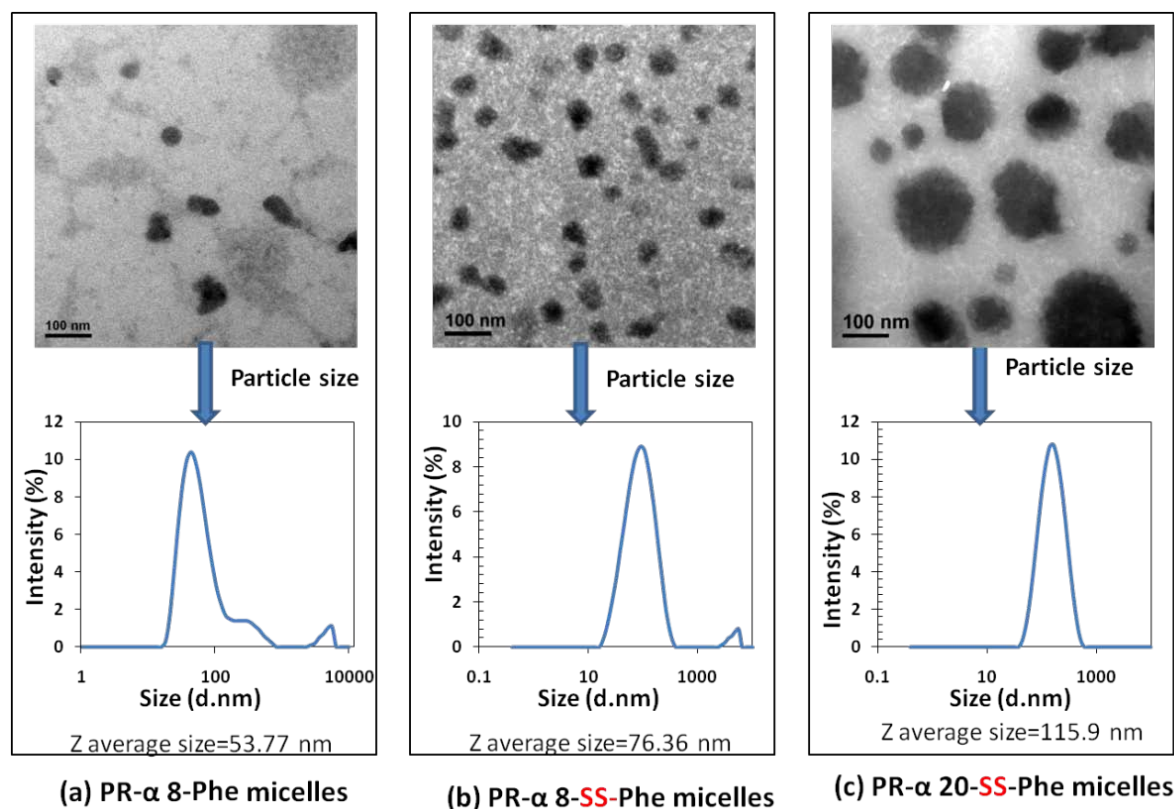
Fig. 4.4 Particle size distribution and TEM images of the self-assembly of PR-α 8-Phe (a), PR-α 8-SS-Phe (b) and PR-α 20-SS-Phe (c). (conc.=1 mg/mL).

To convince the self-assembly and characterize the size and morphology, TEM and DLS experiments were conducted. As shown in Fig. 4.4, spherical particles were observed in the three kinds of polyrotaxanes. It was found that all three SPR nanoparticles exhibited very small size (<120 nm), and the small sizes of nanoparticles may enable them to prolong circulation in blood and slower elimination

by the reticuloendothelium system (RES) [35]. PR-α 8-SS-Phe was found to form nanoaggregates with size of 76 nm and the nanoparticles based on PR-α 20-SS-Phe showed higher average sizes of 116 nm. It is probably because the presence of more CDs in the polyrotaxane core increased particle volume. Therefore, given the CAC, TEM and DLS analytical data as mentioned above, the self-assembly behavior of the synthesized partial polyrotaxanes can be confirmed.

4.3.4 Biodegradation behavior characterization-SEC studies

In our experiment, terminal group was introduced with disulfide-linkage. The most attractive character of such polyrotaxane will involve the control of intracellular drug release utilizing the dissociation of supramolecular structure. In our approach, size exclusion chromatography (SEC) was used to verify the degradation of the polyrotaxane in response to DTT, a reductive environment analogous to that of the intracellular compartments such as cytosol and the cell nucleus.
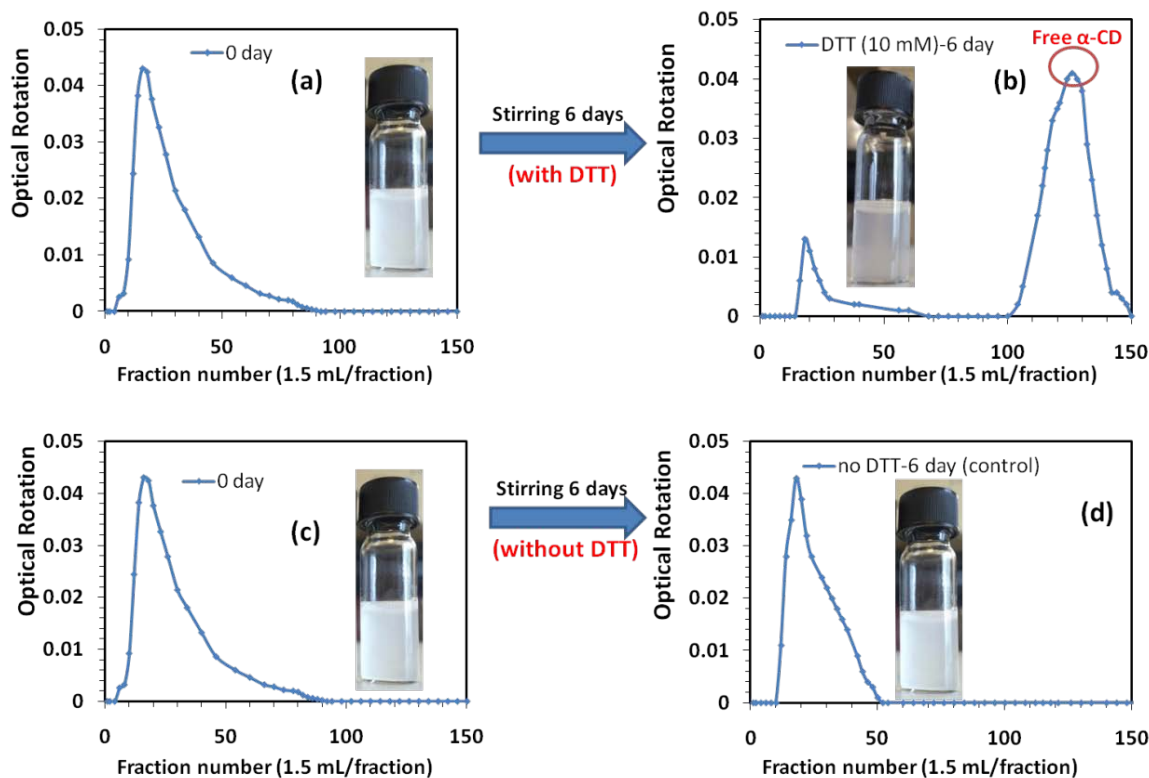
Fig. 4.5 Size exclusion chromatograms of polyrotaxane PR-α 20-SS-Phe before treating with DTT (a, c), after treating with PBS/DTT (10 mM) or PBS for 6 days (b,d). Pictures showed the images of PR-α 20-SS-Phe/H$_2$O mixture (5 mg/mL) before or after treating with DTT.

SEC study was conducted to evaluate the degradation behavior of PR-α 20-SS-Phe in response to DTT, by using G-75 column with DMSO as eluent. Briefly, 30 mg PR-α 20-SS-Phe was added in 6 mL PBS water containing DTT (10 mM), followed by shaking under 100 rpm at 37 °C for 6 days. Then the result solutions were freeze-dried and purified by SEC on a Sephadex G-75 column using DMSO as eluent. Fig. 4.5 (a)-(b) show the size exclusion chromatograms of the polyrotaxane before and after treating with DTT (10 mM). Before adding DTT (Fig.4.5a), PR-α 20-SS-Phe was eluted out at higher MW region of the column with a unimodal peak. It indicates that the polyrotaxane is pure and the CDs are threaded into the polymer. After being stirred for 6 days in the presence of DTT (10 mM) (Fig. 4.5b), the unimodal peak was divided into two peaks. The first peak was eluted out at higher

MW region. It showed the same position but lower optical rotation in comparison with Fig. 4.5(a), suggesting the fraction is the polyrotaxane but with less CD threaded. The second peak was eluted out much later in the lower MW region of the column, indicating that the fraction is free α-CD. In order to make a comparison, 30 mg PR-α 20-SS-Phe was added in 6 mL blank PBS (no DTT) and characterized with the same procedure. It was found that no change in optical rotation was discerned after 6 days in the absence of DTT under otherwise the same conditions (Fig. 4.5c-d). Therefore, the results confirm the dethreading behavior of α-CDs after treating with DTT.

In order to give a visualized picture, the photo images of PR-α 20-SS-Phe/H2O mixture before or after treating with DTT was presented. Specifically, before adding DTT, PR-α 20-SS-Phe was added into water (5 mg/mL) and a turbid solution was observed due to the insoluble properties of PR-α 20-SS-Phe (Fig. 4.5a). After treating with DTT for 6 days, the solution became clear (Fig. 4.5b), suggesting the increase of solubility due to the dethreading of α-CD. In contrast, no change in the solubility was observed after 6 days in the absence of DTT under otherwise the same conditions (Fig 4.5c-d).

4.3.5 Biodegradation behavior characterization-TEM and DLS studies
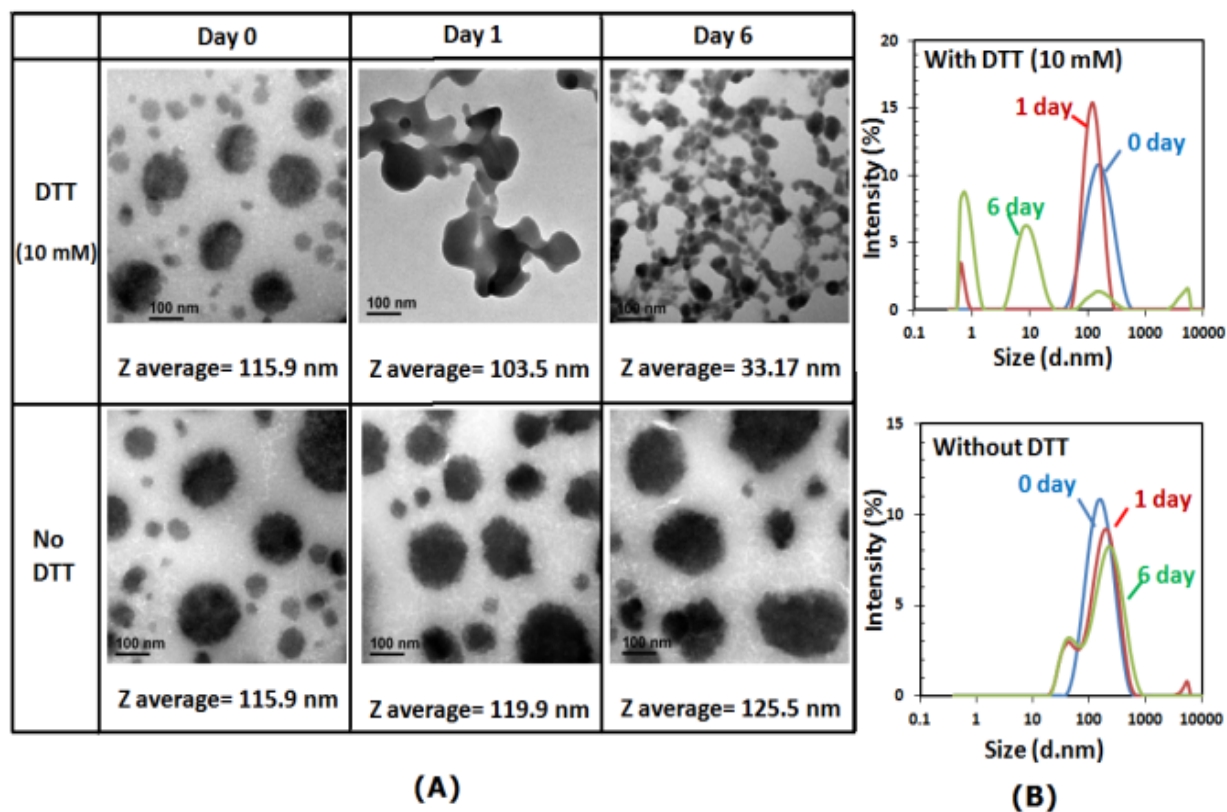
Fig.4.6 TEM images (a) and size change (b) of polyrotaxane nanoparticels in PBS solution with and without DTT (10 mM) after 0, 1 and 6 days (concentration 1 mg/mL).

The size and morphology changes of PR-α 20-SS-Phe nanostructure in response to DTT (10 mM) in PBS were followed by TEM and DLS measurement (Fig. 4.6). Notably, as shown in Fig. 4.6(a), the SPR nanoaggregates degraded into small pieces with irregular morphologies after 6 days in the presence of DTT and the average size decreased from 116 nm to 33 nm. In contrast, no change in particle morphology was discerned after 6 days in the absence of DTT under otherwise the same conditions. The result confirms the effects of dissociation of the supramolecular structure by cleavage of the disulfide linkages on the hydrolysis behaviour of PR-α 20-SS-Phe in the presence of DTT [1]. This was further verified by the DLS measurement. In Fig. 4.6(b), with increasing the incubating time, large aggregates decreased and smaller aggregates increased, indicating the polyrotaxane

nanoaggregates are degraded into small pieces in the presence of DTT. However, no such changes were observed in the absence of DTT under the same condition. Similarly, PR-α 8-SS-Phe also showed the same degradation behaviour in response to DTT.

4.3.6 Drug loading efficiency and morphologies observation

In this chapter, DOX was used as the model molecule to verify the drug delivery ability. The SPR nanostructure showed adequate drug loading efficiencies around 43%~46% (Table 4.2), which is similar or even higher than the traditional micelle structures based on amphiphilic block copolymers.[25, 36] Moreover, because of the presence of DOX in the polyrotaxane core, the SPR nanoaggregates showed a larger size after loading drugs, which is confirmed by TEM and DLS (Fig. 4.7).[35]

Table 4.2 Drug loading content and loading efficiency for DOX loaded polyrotaxanes

sample	Final drug concentration (µg/1 mg polymer)	Loading content [a] (wt.%)	Theory loading content (wt.%)	Loading efficiency [b] (%)
PR-α 8-Phe	43.65 µg	4.36 %	10%	43.65%
PR-α 8-SS-Phe	36.50 µg	3.65%	10%	43.80%
PR-α 20-SS-Phe	46.35 µg	4.64%	10%	46.35%
Pure DOX (control)	47.14 µg	-	-	4.71%

[a] Loading content (wt%) = (weight of loaded drug/weight of polymer) ✕ 100%

[b] Loading efficiency (wt%) = (weight of loaded drug /weight of drug in feed) ✕ 100%

(a) PR-α 8-Phe

(b) PR-α 8-SS-Phe

(c) PR-α 20-SS-Phe
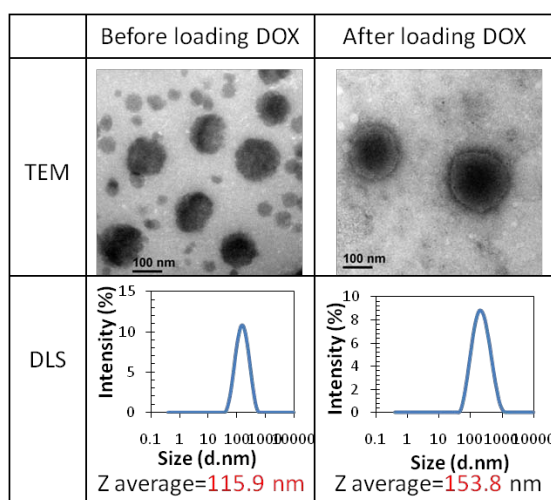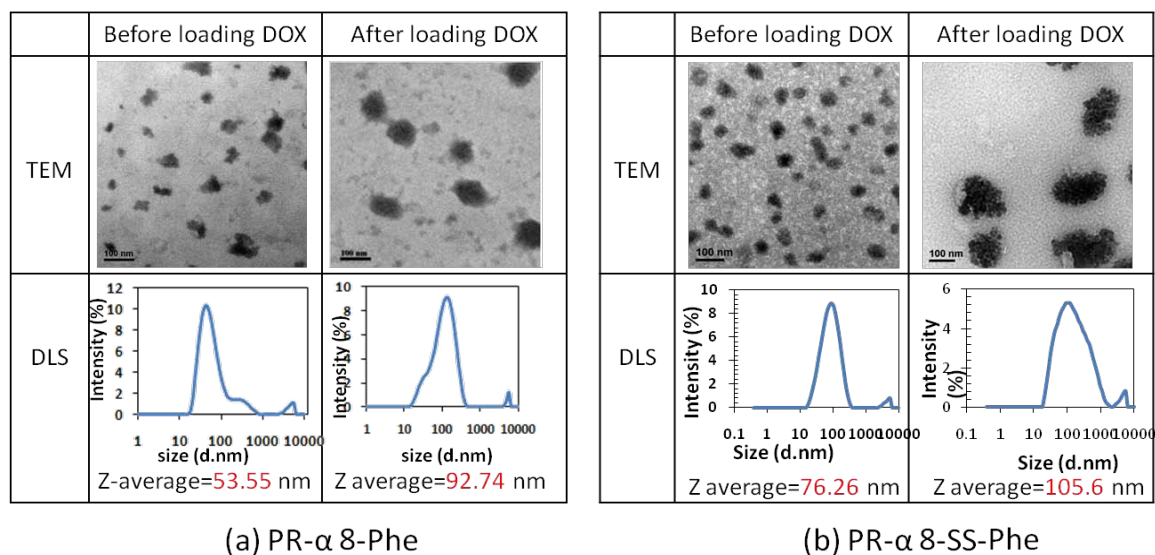
Fig. 4.7 Morphology and size distribution of PR-α 8-Phe (a), PR-α 8-SS-Phe(b) and PR-α 20-SS-Phe (c) before and after loading drugs.

4.3.7 In vitro drug release behaviors
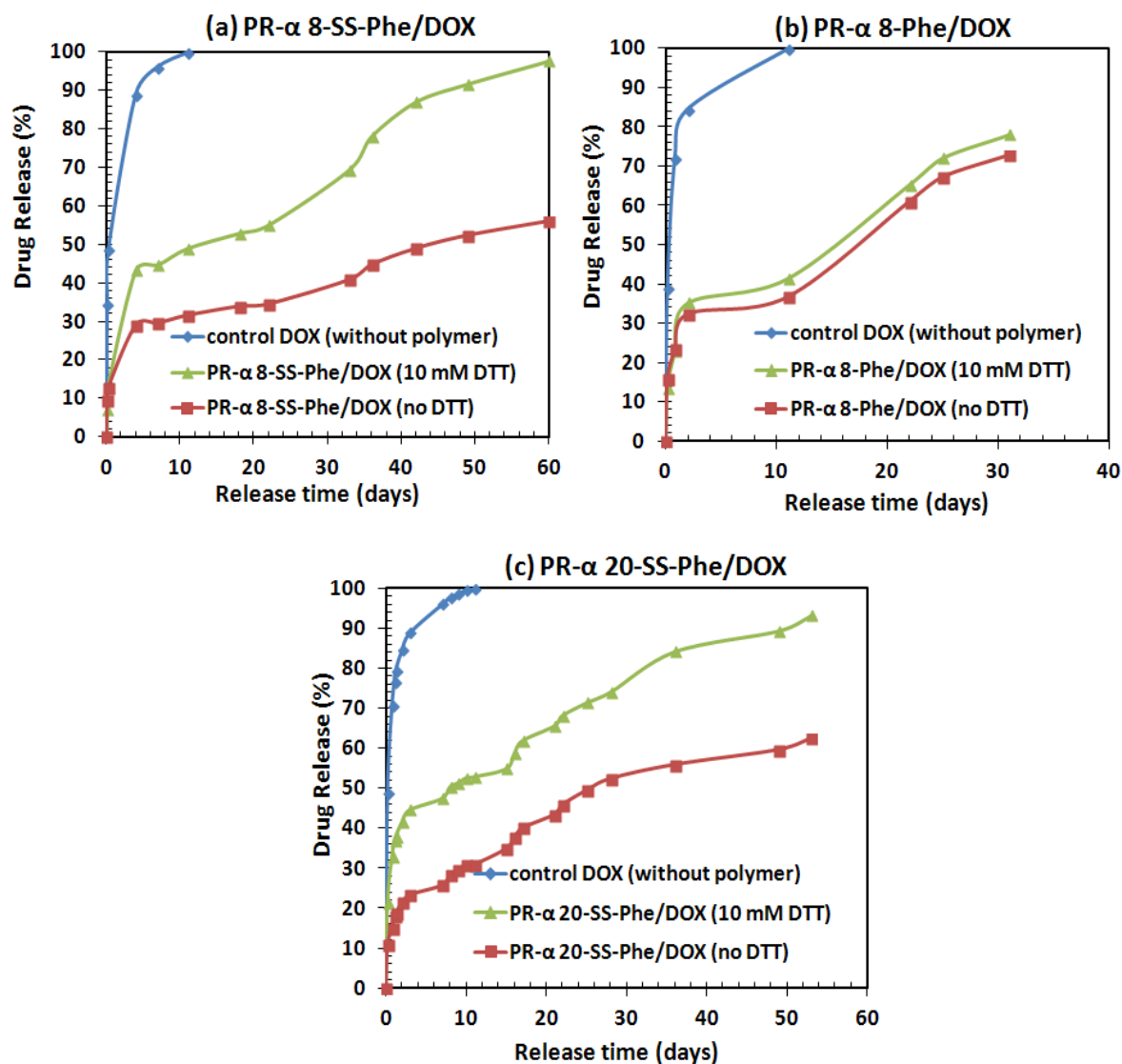
Fig. 4.8 *In vitro* **release profile of DOX from polyrotaxanes in PBS at pH 7.4 and 37 °C, in presence or absence of DTT: (a) DOX loaded PR-α 8-SS-Phe; (b) DOX loaded PR-α 8-Phe; (c) DOX loaded PR-α 20-SS-Phe.**

The release of DOX from polyrotaxanes was investigated using a dialysis tube in pH7.4 PBS at 37 °C. As shown in Fig. 4.8, the polyrotaxane nanostructures exhibited a sustained DOX release lasting about 60 days, in comparison with free DOX without polymers. The sustained DOX release from core-shell nanostructures was similarly observed in some other cyclodextrin based nanoparticles [31, 37]. Based on related researches [26, 38], the long-term release could be attributed not

131

only to the hydrophobic interaction between drug and the polyrotaxane core; more importantly, it could also be due to the hydrogen-bond interaction between hydroxyl group of CDs and amide group of DOX under neutral and basic conditions, owning to the unique structures of star PR. It is worthy of note that a sustained release rate is crucial important to prolong therapeutic effect for intravenous delivery when a targeting in specific area is attained. [37, 39]

Remarkably, the results also showed that both PR-α 8-SS-Phe and PR-α 20-SS-Phe (Fig. 4.8a and c) released DOX faster in the presence of 10 mM DTT in contrast to that without DTT (Fig. 4.8b). This is in line with the previous observation that the nanoaggregates are degraded into small pieces in response to DTT, a reductive environment analogous to that of the intracellular compartments such as cytosol and the cell nucleus. In contrast, no drug release difference was observed within 30 days for the reduction insensitive PR-α 8-Phe under the same conditions (Fig. 4.8b). Therefore, it is evident that faster drug release from star PR was triggered by reduction of the disulfide bond. There are some reductive-biodegradable micelles triggered by disulfide-linkage for DOX delivery.[30, 36, 40] Interestingly, in our systems, rather than rapidly releasing DOX, the nanoaggregates showed sustained release profile within 30 days even in the presence of DTT. This unique property could be highly beneficial to prolong the therapeutic effect. More importantly, the highly stability and sustained drug release of our systems could decrease the concentration of free drug in circulations, resulting in a decreased accumulation of the drug in the heart tissues and reduced cardiotoxicity, which is a serious drawback for DOX as anti-cancer therapy.[16, 17]

4.3.8 In vitro cytotoxicity
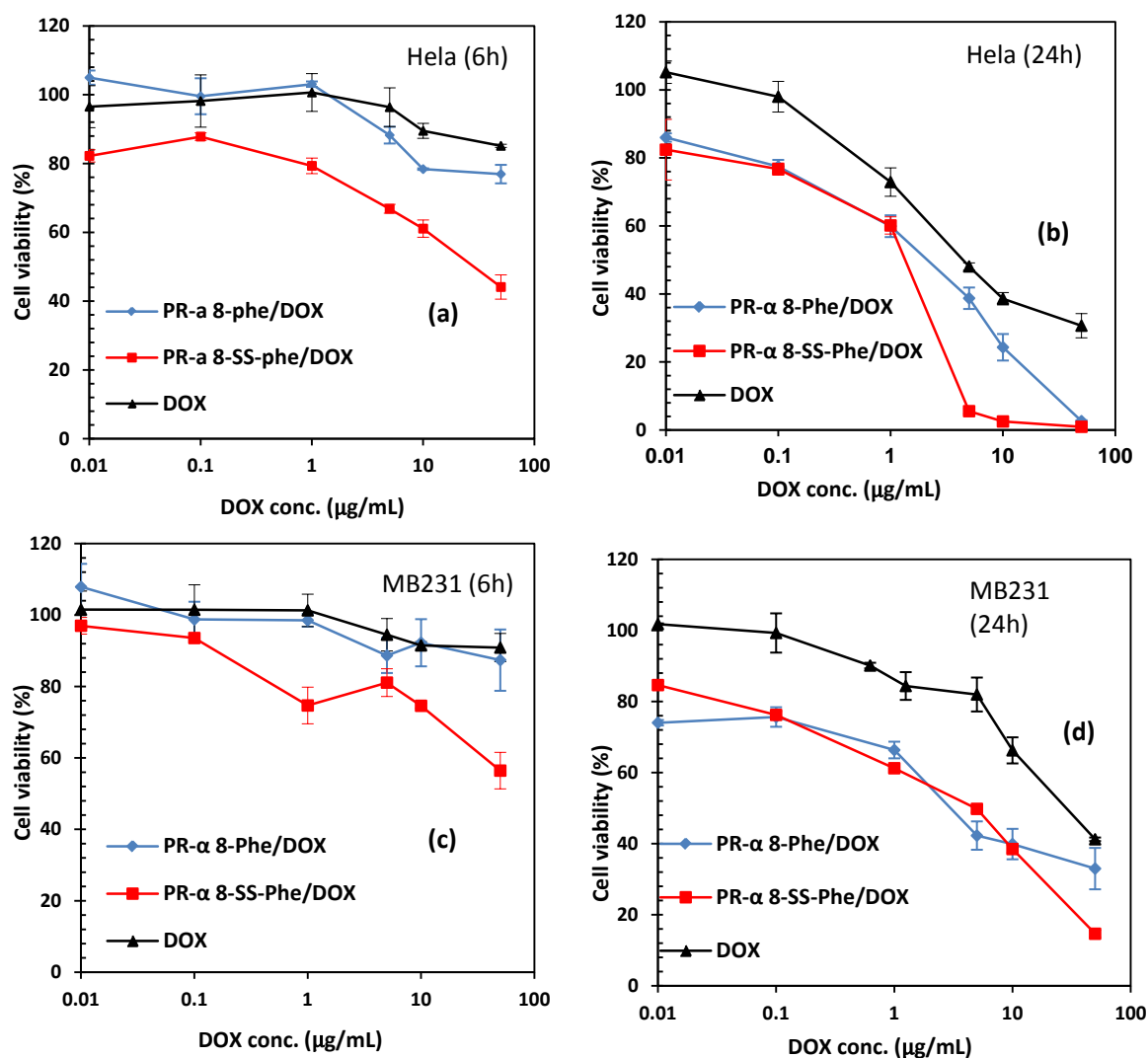
Fig. 4.9 The cytotoxicity of DOX loaded PR-α 8-SS-Phe/PR-α 8-Phe against cancer cells after 6 or 24h incubation: Hela cells after 6 h (a) and 24 h (b) incubation; MB231 cells after 6 h (c) and 24 h (d) incubation. Free DOX was set as control (n=3)

Table 4.3 IC$_{50}$ values (µg/mL) for DOX loaded PR-α 8-SS-Phe/PR-α 8-Phe

	MB231 (6 h)	MB231 (24 h)	Hela (6 h)	Hela (24 h)
PR-α 8-SS-Phe/DOX	50	4.9	36.1	2.3
PR-α 8-Phe/DOX	>50	3.7	>50	3.8
DOX	>50	35.97	>50	6.6

The *in vitro* anticancer activity of the DOX loaded polyrotaxane was performed on MB231 and HeLa cancer cells (Fig. 4.9). As shown in Fig. 4.9, dose-response viability was observed in both cell lines, suggesting our polyrotaxane could successfully delivery DOX into the cancer cell. It fitted with other researches based

on the cytotoxicity of free DOX [14, 40]. Furthermore, both DOX loaded polyrotaxane exhibited similar even higher potent in killing cancer cells than free DOX (IC_{50} values were shown in Table 4.3). The high cytotoxicity could be attributed to higher cell uptake when delivered by the polyrotaxanes. It could also be due to the capability of the delivery system with sustained drug release, which can allow DOX to act on a higher number of cells in a specific phase of cell cycle [37]. More importantly, in comparison with PR-α 8-Phe, DOX loaded PR-α 8-SS-Phe exhibited higher potent in killing cancer cells than the similar structures without SS linkage, indicating that the higher anticancer efficacy is due to the triggered intracellular degradation of the nanostructures. Similar phenomenon could also be examined by comparing the cytotoxicity of PR-SS-α 20-Phe/DOX and PR-α 8-Phe/DOX on Hela cell lines (Fig. 4.10).
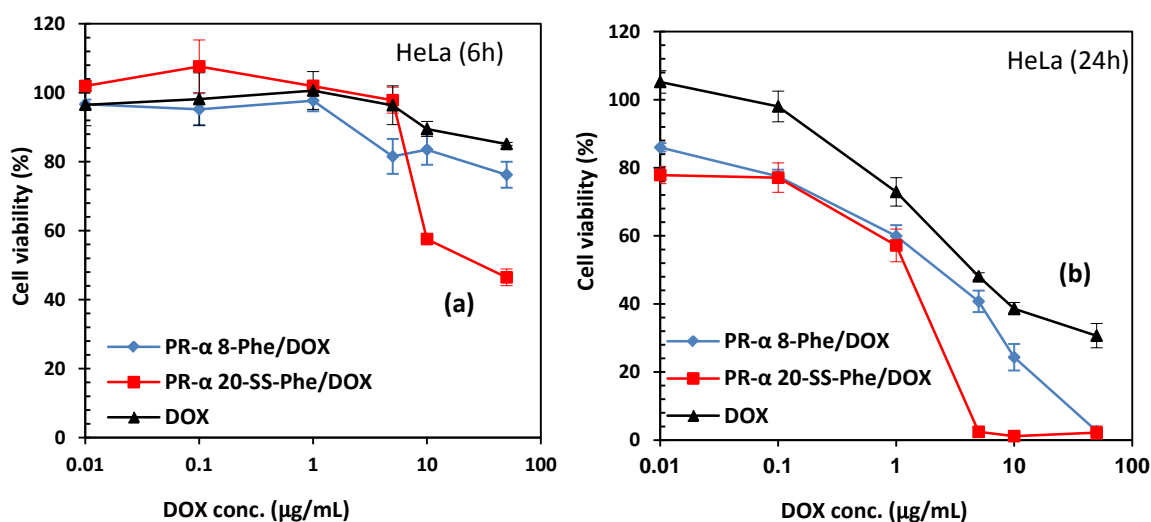
Fig. 4.10 The cytotoxicity of DOX loaded PR-α 20-SS-Phe/PR-α 8-Phe against HeLa cells after 6 h (a) or 24 h (b) incubation. (n=3).

4.3.9 Intracellular uptake and release of DOX
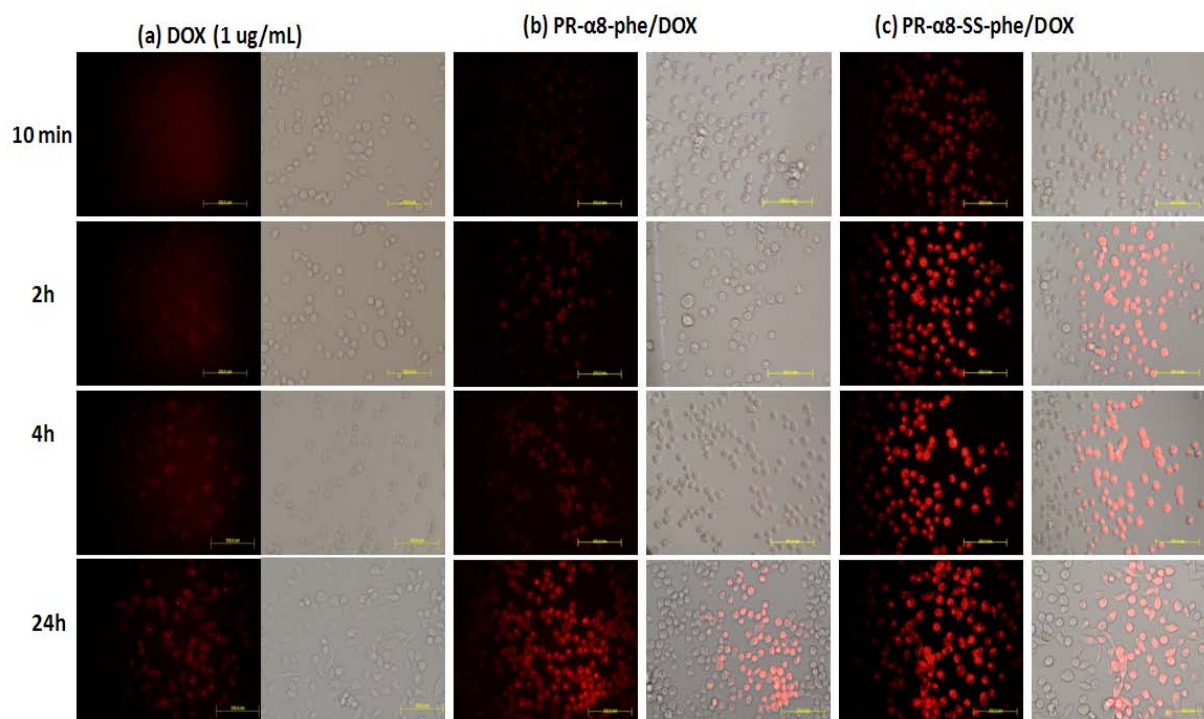
Fig. 4.11 Cellular uptake and internalization of (a) Free DOX, (b) DOX-loaded PR-α 8-Phe and (c) DOX-loaded PR-α 8-SS-Phe in MB-231 cells at 10 min, 2 h, 4 h, and 24 h followed by fluorescence microscopy. (DOX conc.=1 μg/mL). Scale length=100μm.

The cellular uptake and internalization behavior of DOX loaded PR were followed with fluorescence microscopy using MB231 cell line. As shown in Fig. 4.11, DOX loaded polyrotaxanes could be rapidly uptaken by the cells and the uptake increased with time. Notably, in contrast to free DOX without transport carriers (Fig. 4.11a), the PR/DOX complexes exhibited a much faster and higher cell uptake. The high internalization and cell uptake of our core-shell carriers may be due to the small size and water soluble PEG shell, which increased the cell-impermeability and stability of DOX [35]. The sustained drug release also could prolong the therapeutic effect of the drugs and increase the residence time within MB231 cells. Since it has been reported that fluorescence is observed only when DOX is released due to the self-quenching effect of DOX in nanoparticles [30, 41], it is clear from these fluorescence images that DOX has been efficiently released from PR-α 8-SS-

135

Phe/DOX. More importantly, by comparing Fig. 4.11b and 4.11c, PR-α 8-SS-Phe/DOX showed stronger fluorescence of DOX than that without SS linkage, indicating the faster internalization and faster intracellular drug release of the systems with disulfide linkage.

4.4 CONCLUSIONS

In summary, a novel star polyrotaxane was successfully developed by controlled threading of α-CD onto star PEG and end blocked with bioreducible linkage. This unique polyrotaxane could self-assemble into core-shell nanostructures, which would be applied as a reduction-sensitive drug delivery system. The biodegradability of polyrotaxane with disulfide bond in response to DTT was confirmed by TEM and particle size. After encapsulating DOX, the nano-sized particles showed high drug loading efficiency and sustained *in vitro* release for more than 2 months. Furthermore, the biodegradable SPR exhibited a triggered faster *in vitro* release under a reductive environment in contrast to the reduction-insensitive control. In a further development of intracellular study, the biodegradable core-shell structures were capable of faster internalization, rapid intracellular uptake and higher anticancer efficacy as compared to reduction insensitive control and free DOX. Taken together, our SPR nanostructures boast many favorable properties as a drug carries, which include excellent biocompatibility and reduction-sensitive biodegradability, adequate drug loading capacity, sustained drug release, higher cell uptake and highly drug efficacy.

4.5 REFERENCES

1. Sun HL, Guo BN, Cheng R, Meng FH, Liu HY, Zhong ZY. Biodegradable micelles with sheddable poly(ethylene glycol) shells for triggered intracellular release of doxorubicin. Biomaterials 2009 Nov;30(31):6358-6366.

2. Liu J, Pang Y, Huang W, Huang X, Meng L, Zhu X, et al. Bioreducible micelles self-assembled from amphiphilic hyperbranched multiarm copolymer for glutathione-mediated intracellular drug delivery. Biomacromolecules 2011 May 9;12(5):1567-1577.

3. Harada A, Li J, Kamachi M. The molecular necklace-a rotaxane containing many threaded alpha-cyclodextrins. Nature 1992 Mar;356(6367):325-327.

4. Harada A, Li J, Kamachi M. Synthesis of a tubular polymer from threaded cyclodextrins. Nature 1993 Aug;364(6437):516-518.

5. Ooya T, Yui N. Polyrotaxanes: Synthesis, structure, and potential in drug delivery. Critical Reviews in Therapeutic Drug Carrier Systems 1999;16(3):289-330.

6. Huang FH, Gibson HW. Polypseudorotaxanes and polyrotaxanes. Progress in Polymer Science 2005 Oct;30(10):982-1018.

7. Li J, Loh XJ. Cyclodextrin-based supramolecular architectures: Syntheses, structures, and applications for drug and gene delivery. Advanced Drug Delivery Reviews 2008 Jun;60(9):1000-1017.

8. Araki J, Ito K. Recent advances in the preparation of cyclodextrin-based polyrotaxanes and their applications to soft materials. Soft Matter 2007;3(12):1456-1473.

9. Ooya T, Mori H, Terano M, Yui N. Synthesis of a biodegradable polymeric supramolecular assembly for drug-delivery. Macromolecular Rapid Communications 1995 Apr;16(4):259-263.

10. Ooya T, Yui N. Synthesis of theophylline-polyrotaxane conjugates and their drug release via supramolecular dissociation. Journal of Controlled Release 1999 Apr;58(3):251-269.

11. Moon C, Kwon YM, Lee WK, Park YJ, Yang VC. In vitro assessment of a novel polyrotaxane-based drug delivery system integrated with a cell-penetrating peptide. Journal of Controlled Release 2007 Dec;124(1-2):43-50.

12. Ooya T, Choi HS, Yamashita A, Yui N, Sugaya Y, Kano A, et al. Biocleavable polyrotaxane - Plasmid DNA polyplex for enhanced gene delivery. Journal of the American Chemical Society 2006 Mar;128(12):3852-3853.

13. Cheng C, Wei H, Shi BX, Cheng H, Li C, Gu ZW, et al. Biotinylated thermoresponsive micelle self-assembled from double-hydrophilic block copolymer for drug delivery and tumor target. Biomaterials 2008 Feb;29(4):497-505.

14. Chen YC, Liao LC, Lu PL, Lo CL, Tsai HC, Huang CY, et al. The accumulation of dual pH and temperature responsive micelles in tumors. Biomaterials 2012 Jun;33(18):4576-4588.

15. Jang SG, Kramer EJ, Hawker CJ. Controlled Supramolecular Assembly of Micelle-Like Gold Nanoparticles in PS-b-P2VP Diblock Copolymers via

Hydrogen Bonding. Journal of the American Chemical Society 2011 Oct;133(42):16986-16996.

16. Brown MD, Schatzlein A, Brownlie A, Jack V, Wang W, Tetley L, et al. Preliminary characterization of novel amino acid based polymeric vesicles as gene and drug delivery agents. Bioconjugate Chemistry 2000 Nov-Dec;11(6):880-891.

17. Son YJ, Jang JS, Cho YW, Chung H, Park RW, Kwon IC, et al. Biodistribution and anti-tumor efficacy of doxorubicin loaded glycol-chitosan nanoaggregates by EPR effect. Journal of Controlled Release 2003 Aug;91(1-2):135-145.

18. Yang C, Li H, Wang X, Li J. Cationic supramolecules consisting of oligoethylenimine-grafted alpha-cyclodextrins threaded on poly(ethylene oxide) for gene delivery. J Biomed Mater Res A 2009 Apr;89(1):13-23.

19. Sun H, Guo B, Cheng R, Meng F, Liu H, Zhong Z. Biodegradable micelles with sheddable poly(ethylene glycol) shells for triggered intracellular release of doxorubicin. Biomaterials 2009 Oct;30(31):6358-6366.

20. Li J, Yang C, Li HZ, Wang X, Goh SH, Ding JL, et al. Cationic supramolecules composed of multiple oligoethylenimine-grafted beta-cyclodextrins threaded on a polymer chain for efficient gene delivery. Advanced Materials 2006 Nov;18(22):2969-+.

21. Yang C, Li J. Thermoresponsive Behavior of Cationic Polyrotaxane Composed of Multiple Pentaethylenehexamine-grafted alpha-Cyclodextrins Threaded on Poly(propylene oxide)-Poly(ethylene oxide)-Poly(propylene oxide) Triblock Copolymer. Journal of Physical Chemistry B 2009 Jan;113(3):682-690.

22. Ohya Y, Takamido S, Nagahama K, Ouchi T, Katoono R, Yui N. Polyrotaxane Composed of Poly-L-lactide and alpha-Cyclodextrin Exhibiting Protease-Triggered Hydrolysis. Biomacromolecules 2009 Aug;10(8):2261-2267.

23. Ooya T, Yui N. Synthesis and characterization of biodegradable polyrotaxane as a novel supramolecular-structured drug carrier. Journal of Biomaterials Science-Polymer Edition 1997;8(6):437-455.

24. Zhang XW, Zhu XQ, Ke FY, Ye L, Chen EQ, Zhang AY, et al. Preparation and self-assembly of amphiphilic triblock copolymers with polyrotaxane as a middle block and their application as carrier for the controlled release of Amphotericin B. Polymer 2009 Aug;50(18):4343-4351.

25. Lin JP, Zhang SN, Chen T, Lin SL, Jin HT. Micelle formation and drug release behavior of polypeptide graft copolymer and its mixture with polypeptide block copolymer. International Journal of Pharmaceutics 2007 May;336(1):49-57.

26. Yang XY, Chen LT, Huang B, Bai F, Yang XL. Synthesis of pH-sensitive hollow polymer microspheres and their application as drug carriers. Polymer 2009 Jul;50(15):3556-3563.

27. Loh XJ, Goh SH, Li J. New biodegradable thermogelling copolymers having very low gelation concentrations. Biomacromolecules 2007 Feb;8(2):585-593.

28. Tang LY, Wang YC, Li Y, Du JZ, Wang J. Shell-detachable micelles based on disulfide-linked block copolymer as potential carrier for intracellular drug delivery. Bioconjug Chem 2009 Jun;20(6):1095-1099.

29. Yang C, Li H, Goh SH, Li J. Cationic star polymers consisting of alpha-cyclodextrin core and oligoethylenimine arms as nonviral gene delivery vectors. Biomaterials 2007 Jul;28(21):3245-3254.

30. Sun HL, Guo BN, Li XQ, Cheng R, Meng FH, Liu HY, et al. Shell-Sheddable Micelles Based on Dextran-SS-Poly(epsilon-caprolactone) Diblock Copolymer for Efficient Intracellular Release of Doxorubicin. Biomacromolecules 2010;11(4):848-854.

31. Xiao K, Luo JT, Fowler WL, Li YP, Lee JS, Xing L, et al. A self-assembling nanoparticle for paclitaxel delivery in ovarian cancer. Biomaterials 2009 Oct;30(30):6006-6016.

32. Harada A, Kamachi M. Complex-formation between poly (ethylene glycol) and alpha-cyclodextrin. Macromolecules 1990 May;23(10):2821-2823.

33. Bae SJ, Suh JM, Sohn YS, Bae YH, Kim SW, Jeong B. Thermogelling poly(caprolactone-b-ethylene glycol-b-caprolactone) aqueous solutions. Macromolecules 2005 Jun;38(12):5260-5265.

34. Hwang MJ, Suh JM, Bae YH, Kim SW, Jeong B. Caprolactonic poloxamer analog: PEG-PCL-PEG. Biomacromolecules 2005 Mar-Apr;6(2):885-890.

35. Lee ALZ, Wang Y, Cheng HY, Pervaiz S, Yang YY. The co-delivery of paclitaxel and Herceptin using cationic micellar nanoparticles. Biomaterials 2009 Feb;30(5):919-927.

36. Sun PJ, Zhou DH, Gan ZH. Novel reduction-sensitive micelles for triggered intracellular drug release. Journal of Controlled Release 2011 Oct;155(1):96-103.

37. Quaglia F, Ostacolo L, Mazzaglia A, Villari V, Zaccaria D, Sciortino MT. The intracellular effects of non-ionic amphiphilic cyclodextrin nanoparticles in the delivery of anticancer drugs. Biomaterials 2009 Jan;30(3):374-382.

38. Yang C, Attia AB, Tan JP, Ke X, Gao S, Hedrick JL, et al. The role of non-covalent interactions in anticancer drug loading and kinetic stability of polymeric micelles. Biomaterials 2012 Apr;33(10):2971-2979.

39. Zhao YZ, Sun CZ, Lu CT, Dai DD, Lv HF, Wu Y, et al. Characterization and anti-tumor activity of chemical conjugation of doxorubicin in polymeric micelles (DOX-P) in vitro. Cancer Lett 2011 Dec 8;311(2):187-194.

40. Li YL, Zhu L, Liu Z, Cheng R, Meng F, Cui JH, et al. Reversibly stabilized multifunctional dextran nanoparticles efficiently deliver doxorubicin into the nuclei of cancer cells. Angew Chem Int Ed Engl 2009;48(52):9914-9918.

41. Bae Y, Fukushima S, Harada A, Kataoka K. Design of environment-sensitive supramolecular assemblies for intracellular drug delivery: polymeric micelles that are responsive to intracellular pH change. Angew Chem Int Ed Engl 2003 Oct 6;42(38):4640-4643.

CHAPTER 5   REDUCTION-SENSITIVE AND SHELL SHEDDABLE NANOSTRUCTURES BASED ON STAR POLYROTAXANES FOR GENE DELIVERY

5.1 INTRODUCTION

Over the past two decades, gene delivery has gained much attention as the potentials for treating disease caused by mutation or genetic defects, genetic disorders such as cystic fibrosis, combined immunodeficiency and Parkinson's disease [1-3]. Among various non-viral vectors, PEI has been one of the most popularly employed cationic gene carriers due to its superior transfection efficiency and consistency of transfection in many different types of cells. They are often considered as the gold standard of gene transfection. It was reported that the higher molecular weight PEI showed higher transgene expression but it could also lead to significant cytotoxicity [4-6], probably due to the necrosis, which caused by aggregation and adherence on the cell surface [7, 8]. In contrast, low molecular weight PEI was less toxic but showed poor transfection efficiency due to the lower ability to condense DNA [15]. Therefore, it was suggested that one of the most rational ways to decrease cytotoxicity and enhance gene transfection efficiency could be achieved by combining low molecular weight transfection segments with degradable linkages and forming a

combined large molecular weight transfection polymer. Recently, a new class of CD-containing gene carriers was developed based on cationic polyrotaxanes where multiple cationic CDs are threaded onto a polymer chain and capped by bulky ends [9-12]. By taking advantage of the CD's ability to slide and rotate along the polymer axle, this system seems possible to generate well-matched DNA complexes, and thus accomplish the gene transfection with a minimum amount of cationic polyrotaxanes.

Non-vial gene carriers are challenged with a set of obstacles before and after entering cells, including stability in biological fluids, stimuli DNA release inside targeting cells, low cytotoxicity and high gene transfection efficiency [13]. In order to increase DNA release, bioreducible polymers have emerged as an attractive delivery system [14, 15]. These materials usually contain disulfide linkage, which is subject to rapid degradation via thiol–disulfide exchange in cytosol [16, 17]. The rapid degradation on the one hand could lead to polyplex dissociation and efficient intracellular release of DNA or siRNA, on the other hand, they may result in low toxicity by avoiding accumulation of high molecular weight polycations inside cells, and finally increasing the transfection efficiency [18-20].

Serum stability is another barrier for gene delivery. In the case of *in vivo* gene delivery, the polyplex particles could prone rapid aggregation due to the negatively charged plasma proteins in the serum or blood, which affect the stability of the positively charged polyplexes. Introducing a sheddable shell by attaching hydrophilic polymer is one of the most attractive methods to maintain the stability of delivery vehicles against serum. For example, PEG shell layer could stabilize the aggregation in the interior of micelles and at the same time provide a "stealth" layer on the surface which could resist protein adsorption and cellular adhesion [21, 22]. Furthermore,

PEGlyation is a well verified method to decrease cytotoxicity due to its shielding effect on the surface charge of particles [23-25].

In this chapter, with the aim of increasing the serum stability and achieving an optimal balance between DNA protection and DNA release to maximize transfection, we present a novel reduction-sensitive cationic polyrotaxanes for effective gene delivery. Herein, star polyrotaxanes were synthesized based on partially threaded α-CD and star PEG with disulfide-linkage, followed by conjugating multiple oligoethylenimine (OEI) arms onto α-CD rings (Scheme 5.1). In contrast to previous OEI based cationic polyrotaxane for gene delivery [26, 27], disulfide linkages were introduced to polyrotaxane chain, which would allow the system sensitive to reduction environment, resulting in sufficiently DNA protection extracellularly, rapid degradation and DNA release intracellular, decreased cytotoxicity and enhanced transfection efficiency. More importantly, owning to the unique supramolecular structure of 8-arm PEG with controlled threaded CDs, the naked PEG arms would form a sheddable hydrophilic shell, which could stabilize the polyplex, enhance their serum tolerant ability and further decrease the cytotoxicity.
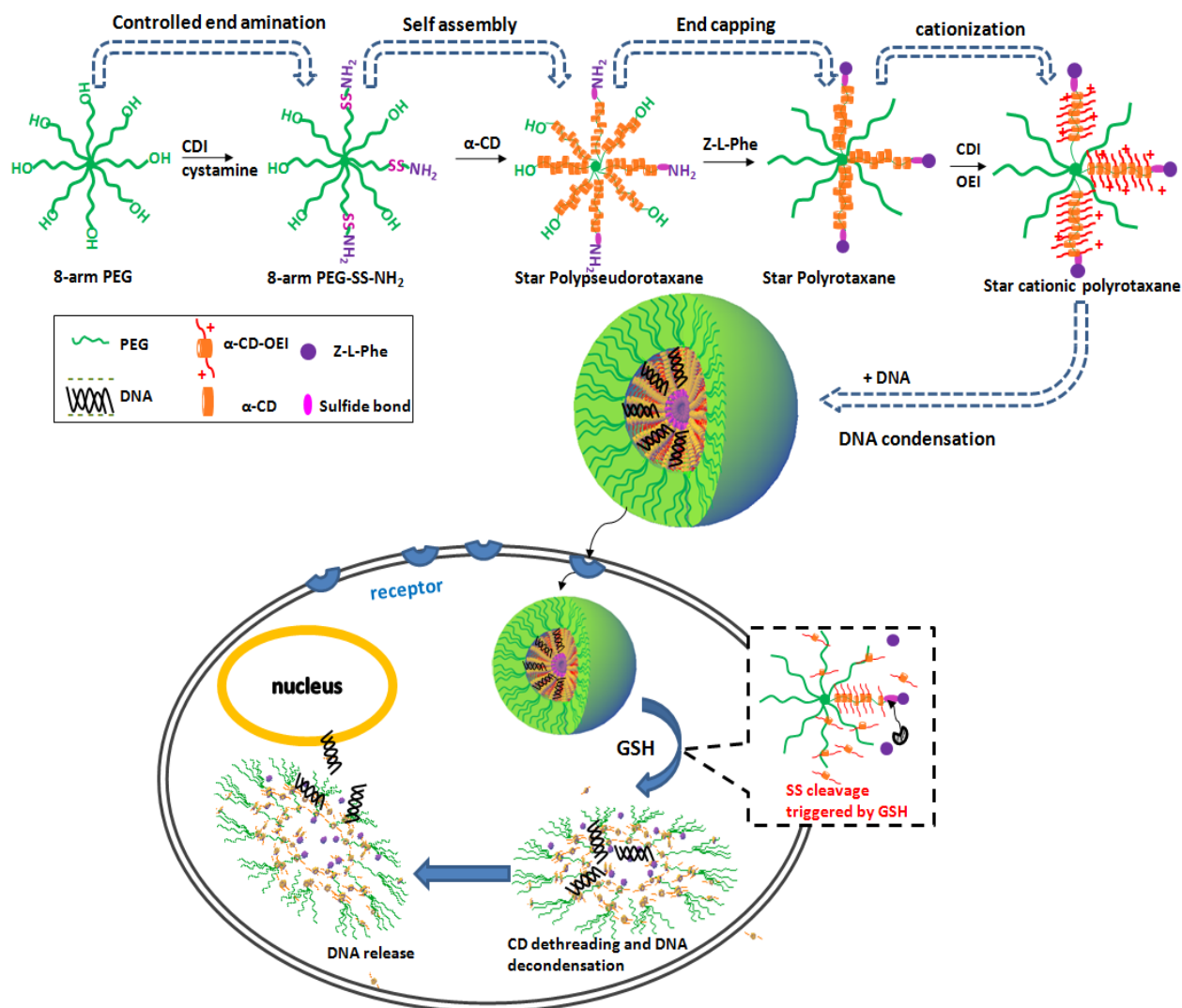
Scheme 5.1 Illustration of star polyrotaxanes and intracellular DNA release

5.2 MATERIALS AND METHODS

5.2.1 Materials

Star PEG (Mn=9468) was purchased from Fluka. α-CD was purchased from TCI. Linear PEI with a molecular weight of 423 Da, branched PEI with a molecular weight of 600 Da, and branched PEI (Mn= 25 kDa) were supplied by Aldrich. NHS, DCC, ethylenediamine, TEA, CDI, DTT, Z-L-Phe-OH were received from Sigma-

Aldrich and used as received. Diethyl ether, methanol, DMF, DMSO were purchased

from Merck. Penicillin, streptomycin and MTT were obtained from Sigma.

5.2.2 Synthesis Methods
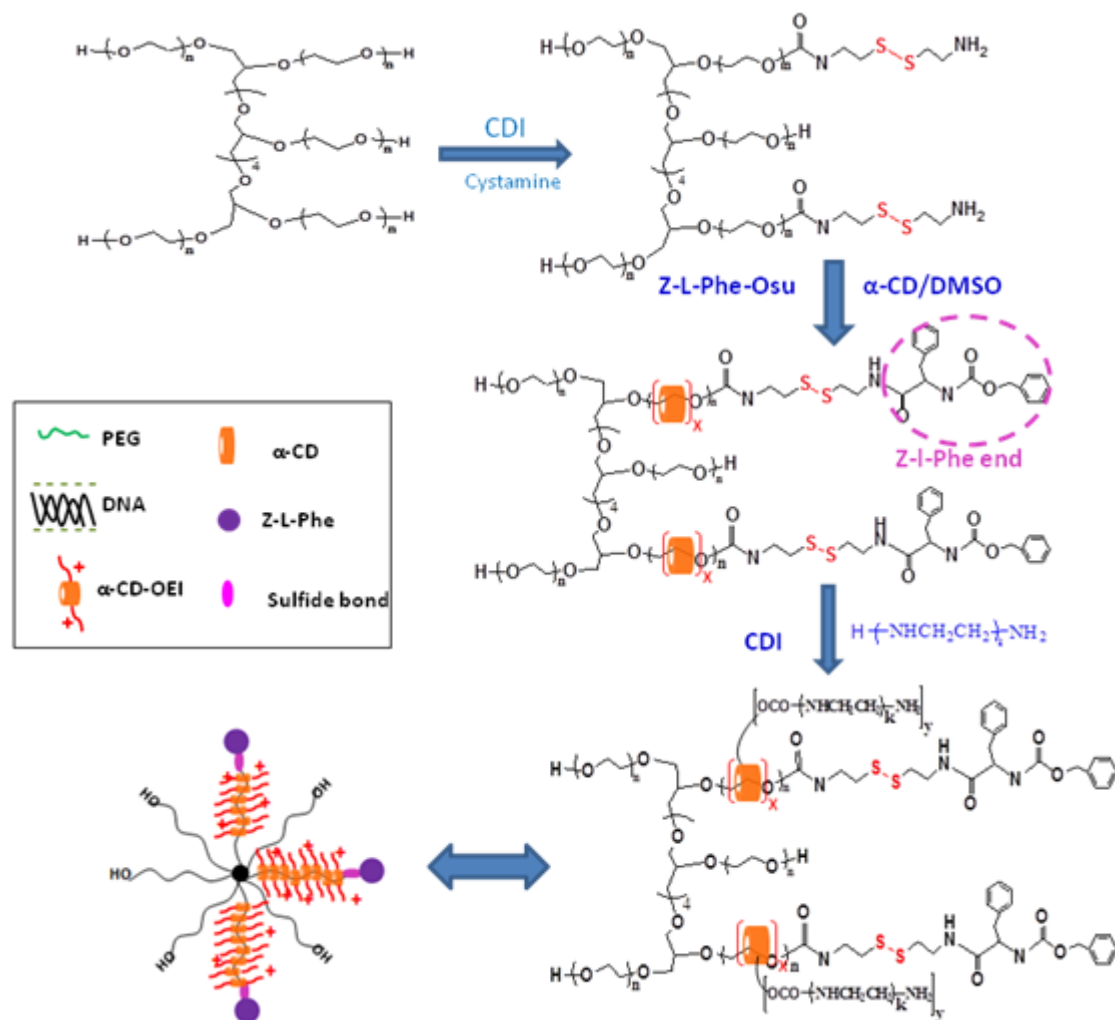
Scheme 5.2 Synthesis procedure for the cationic polyrotaxane

5.2.2.1 Synthesis of PEG-SS-NH$_2$ and PEG-NH$_2$

The synthesis procedures of PEG-SS-NH$_2$ and PEG-NH$_2$ are the same with the

methods we presented before. (4.2.2.1)

5.2.2.2 Synthesis of Polyrotaxanes (PPR-SS-NH$_2$ and PPR-NH$_2$)

The synthesis procedures of PPR-SS-NH$_2$ and PPR-NH$_2$ are the same with the methods we presented before. (3.2.2.2)

5.2.2.3 Synthesis of polyrotaxanes (PR-SS-Phe/PR-Phe)

The synthesis procedures of PR-SS-Phe and PR-Phe are the same with the methods we presented before. (4.2.2.3)

5.2.2.4 Synthesis of cationic polyrotaxanes (PR-SS-Phe-OEI/PR-Phe-OEI)

The synthesis of OEI-based cationic polyrotaxane is followed by method reported before [26]. The resulting polyrotaxane (PR-SS-Phe/PR-Phe) (0.2g, 4.6×10^{-6} mol) were dried at 40 °C under vacuum overnight. After the flask cooled, 20 mL of anhydrous DMSO was injected and the solution was added dropwise during a period of 4 h under nitrogen to 40 mL of anhydrous DMSO solution in which CDI (2.59 g, 16.55 mmol) was dissolved, and the mixture was stirred overnight under nitrogen at room temperature. The product was precipitated in a mixture solution of tetrahydrofuran (THF) (300 mL) and Et$_2$O (600 mL), which was further centrifuged and washed with THF three times. Then, the precipitate was dissolved in 40 mL of anhydrous DMSO, and the solution was added dropwise during a period of 3 h into 10.5g (24.8 mmol) of OEI423 or 14.9g (24.8 mmol) of OEI600, which was dissolved in 40 mL DMSO, followed by stirring the mixture overnight under N$_2$. THF (900 mL) was poured into the reaction mixture to precipitate the product. And the resulting crude product was purified by SEC on a Sephadex G-50 column using deionized water as the eluent. Finally, 0.16 g of yellow solid was obtained (yield, 42%).

5.2.3 Measurements and Characterization

5.2.3.1 Proton Nuclear Magnetic Resonance (^{1}H-NMR)

Same with the methods we presented before. (3.2.3.1)

5.2.3.2 Elemental analysis

Nitrogen content was recorded on a EA1112 Automatic Elemental Analyzer. Samples are further dried in a glass oven overnight before use. 1.92 mg sample is loaded into an aluminium sample cup and then placed onto the sampling cartridge. The furnace temperature are gradually increased to 950 °C with a constant carrier gas flow rate at 140 mL/min. Sulfanilamide is used as standard and analyzed before use.

5.2.3.3 Plasmid amplification

The plasmid used as report gene was pRL-CMV (Promega, USA), which encoding *Renilla* lucierase, originally cloned from the marine organism *Renilla reniformis*. The plasmid DNA was amplified by using Qiagen Endofree Plasmid Mega Kit (Qiagene, Hilden, Germany). The quantity and quality of the purified pDNA was assessed by optical density at 260 and 280 nm. The purified pDNA was resuspended in TE buffer (10 mM Tris-Cl, oH7.5, 1 mM EDTA).

5.2.3.4 Cells and media

All cell lines were purchased from ATCC (Rockville, MD). COS7 and MB231 cells were maintained in Dulbecco's Modified Eagle's Medium (DMEM) supplemented with 10% heat-inactivated fetal bovine serum, 100 units/mg penicillin,

100 μg/mL streptomycine at 37°C and 5% CO_2.DMEM medium was purchased from Gibco BRL (Gaithersburg, MD).

5.2.3.5 Gel retardation experiment

Gel retardation assay was employed to investigate the DNA binding ability of polymers. In general, polymer/DNA complexes were prepared at various N/P ratios ranging from 1 to 10 in PBS (pH = 7.4). After 30 min incubation, the complexes were mixing with 5μL of 5× gel-loading buffer (BlueJuice^TM, Invitrogen, USA), and then electrophoresced on a 0.9% (w/v) agarose gel (Bio-Rad) containing 0.5 ug/mL ethidium bromide. Gel electrophoresis was carried out in 1×TAE buffer (40 mM Tris-acetate, 1 mM EDTA) at 100 V for 30 min in a Sub-Cell system (Bio-Rad Laboratories, CA). The location of DNA bands was analyzed on UV illuminator and photographed by a GelDoc system (Synoptics Ltd., UK).

5.2.3.6 Particle size and zeta-potential measurements

The particle size and zeta potential of polymer/DNA complexes were measured by a Zetasizer Nano ZS (Malvern Instruments Ltd., MA, USA), with a laser beam at wavelength of 633 nm (scattering angle: 90°) at 25 °C. 100 μL of polyplexes solution containing 3 μg of pDNA were prepared at various N/P ratios from 1 to 50. After incubating for 30 min at room temperature, the complexes were diluted to 1 mL by 15 mM of KCl solution at the time of measurement. The measurements were performed using a capillary zeta potential cell in automatic mode.

5.2.3.7 Stability of polymer/DNA complexes

The salt stabilities of polymer/DNA complexes in PBS were determined by dynamic light scattering [28]. Briefly, 100 μL of polyplexes containing 5 μg or 10 μg of pDNA were prepared at N/P ratios of 50. After incubating for 30 min at room temperature, the complexes were diluted with 800 μL of deionized water and 100 μL of 10×PBS solution to generate 1×PBS buffer solution (150 mM PBS). The mixtures were incubated at 37 °C and their mean hydrodynamic diameter was measured at designed time intervals.

The protein stabilities of polymer/DNA complexes in 5% (wt) bovine serum albumin (BSA) solution were determined by the same method above [29]. The 500 μL of polyplex with 10 μg DNA were mixed with an equal volume of 10 wt% BSA dissolved in PBS. The mixture was incubated at 37 °C and determined at time interval, defined as t_i. The average diameter of particles in PBS before BSA treatment, t_o, was also measured. The ratio of particle sizes was calculated as t_i/t_o.

5.2.3.8 Biodegradation behavior of polymer/DNA complexes

Polymer/DNA complexes containing 3 μg of pDNA were prepared at various N/P ratios from 1 to 50. After 30 min, polymer/DNA polyplexes were treated with same volume of 20 mM DTT solution or water. The mixture was incubated at 37 °C and determined at time interval, defined as t_i. The average diameter of particles in water before DTT treatment, t_o, was also measured by dynamic light scattering. The change ratio of particle size was calculated as t_i/t_o.

5.2.3.9 DNA release ability

The pDNA release ability of polyplex in response to 10 mM DTT was evaluated by gel retardation method, followed by the previous report [20, 30-32].

Generally, polyrotaxane were mixed with 0.4 µg pDNA at N/P ratio of 50 and incubated for 30 min. Then, the polyplex solution was incubated with 10 mM DTT for 5 h at 37 °C. After incubation, the resulting solution was treated with 1µL of heparin sodium salt solution (0-600 µg/mL) to release DNA. After further incubation at room temperature for 20 min, the mixed solution was separated into its components by gel electrophoresis (35 min at 100 V) (same as the procedure in 5.2.3.4).

5.2.3.10 Cell viability assay

In vitro cytotoxicity tests on the polymer were performed by MTT assay in a 96-well cell culture plate [33]. In brief, MB231 and COS7 cells were seeded into 96-well plates at a density of 1×10^5 cells/mL. After 24 h, the culture medium was replaced with serum-supplemented culture medium containing serial dilutions of the polymers, and the cells were incubated for 24 h. Next, 10 µL of sterile, filtered MTT stock solution in PBS (5 mg/mL) was added to each well. After 4 h of incubation at 37 °C, the unreacted dye was removed by aspiration and the insoluble formazan crystals were dissolved in 100 µL of dimethylsulfoxide (DMSO). The absorbance of the formazan product was measured at 570 nm using a fluorometer (FLUOstar Optima Microplate Fluorometer).

5.2.3.11 In vitro transfection and luciferase assay

MB231 and COS7 cells were seeded onto 24-well plate at a density of 5×10^4 per well in 500 µL DMEM medium with 10% FBS 24h prior to transfection. After the confluence of the cells reaching to 70-80%, the culture medium was replaced with 300 µL fresh complete medium (with 10%, 20% and 30% FBS) or serum free medium. Polyplexes with different N/P ratios containing 1 µg pDNA were added to each well

and were further incubated with cells for 4h. Then the culture media were changed back to 500 μL medium containing 10% FBS and cells are incubated for further 20 hours. At the end of transfection, the cells were washed with PBS three times and 100 μL of luciferase lysis buffer (Promega, USA) was then added to each well to lysis the cells for 30 min. The relative luciferase activity (RLU) was determined by luciferase assay kit (Promega, USA) on a single-well luminometer (Berthold lumat LB9507, Germany). The units were normalized to protein content using Coomassie Plus^{TM} Protein Assay (Thermo Scientific, USA) and the absorption was measured on a microplate reader (Spectra Plus, TECAN) at 570 nm by comparing with standard BSA concentration. Results are expressed as relative light units per milligram of cell protein lysate (RLU/mg protein).

5.2.3.12 *In vitro* GFP expression

Plasmid pEGFP-N1 (Clontech Laboratories Inc., USA) encoding a red-shifted variant of wild type green fluorescence protein (GFP) and (FITC) was used to examine the GFP expression and FITC expression. Similar with the protocol of *in vitro* luciferase expression, COS7 cells were seeded on 24-well plate at a density of 5×10^4 per well in 500 μL DMEM medium with 10% FBS. After 24h, the medium was replaced with 300 μL of fresh medium with 10% FBS, in which 20 μL polyplexes containing 1μg of pEGFP-N1were added. After 4 h, the transfection medium was replaced with medium with 10% FBS and cultured for another 44 hours. At the end of transfection, the cells were washed with PBS twice and GFP transfected cells were imaged under fluorescent microscope. GFP fluorescence was excited at 488 and emission was collected using a 515 nm filter. ImageJ (NIH) was used for comparative analysis and quantifying the transfection efficiency. The cells with GFP Expression

above threshold levels were automatically counted from the threshold green channel image series using the Analyze Particles function in ImageJ [34]. The GFP expression was obtained by dividing the pixel area within the threshold set for the chromogen by the total pixel area of the region[35, 36].

5.2.3.13 GSH inhibition

D,L-Buthionine sulfoxamine (BSO), a known GSH inhibitor, was used as previously described by Christensen et al [37]. For investigation of cell viability and transfection efficiency changed after treating with BSO, cells were pre-treated with 300 μM BSO solution (diluted by 20 mM stock solution in PBS) for 24 h prior to adding complexes solution. The rest procedures were the same as cell viability and transfection protocols above.

5.2.3.14 statistical analysis

Except for cell viability assay, all cell experiments were performed in triplicate and the results are expressed as mean $\pm$ standard deviation. Student's t-test was used to assess statistical significance of difference between group means.

5.3 RESULTS AND DISCUSSION

5.3.1 Synthesis of cationic polyrotaxanes (PR-SS-Phe/OEI and PR-Phe/OEI)

Scheme 5.1 (b) shows the synthesis procedures of partial cationic polyrotaxane. Firstly, 8-arm PEG-SS-NH$_2$/PEG-NH$_2$ was synthesized by the CDI reaction. Specifically, the hydroxyl groups at the end of 8-arm PEG were activated with CDI, followed by reaction with large excess of cystamine/ethylenediamine to

give terminal amino groups. Next, PEG-SS-NH2/PEG-NH2 was allowed to react with saturated solution of α-CD to obtain polypseudorotaxane, following similar procedures described in previous report [38], in which it was found that α-CD will form an inclusion complex with ratio EO/CD of 2, approximately. Then the end of PEG was blocked to form polyrotaxane with Z-L-Phe. Finally, OEIs with different MW, linear OEI with MW of 423 and branched OEI600, were grafted to the α-CD molecules of polyrotaxanes to give cationic polyrotaxanes. To ensure that there was no intra- or intermolecular crosslinking, a large excess of OEI (100 times relative to α-CD) was used in the grafting reactions.

5.3.2 Characterization of cationic polyrotaxanes
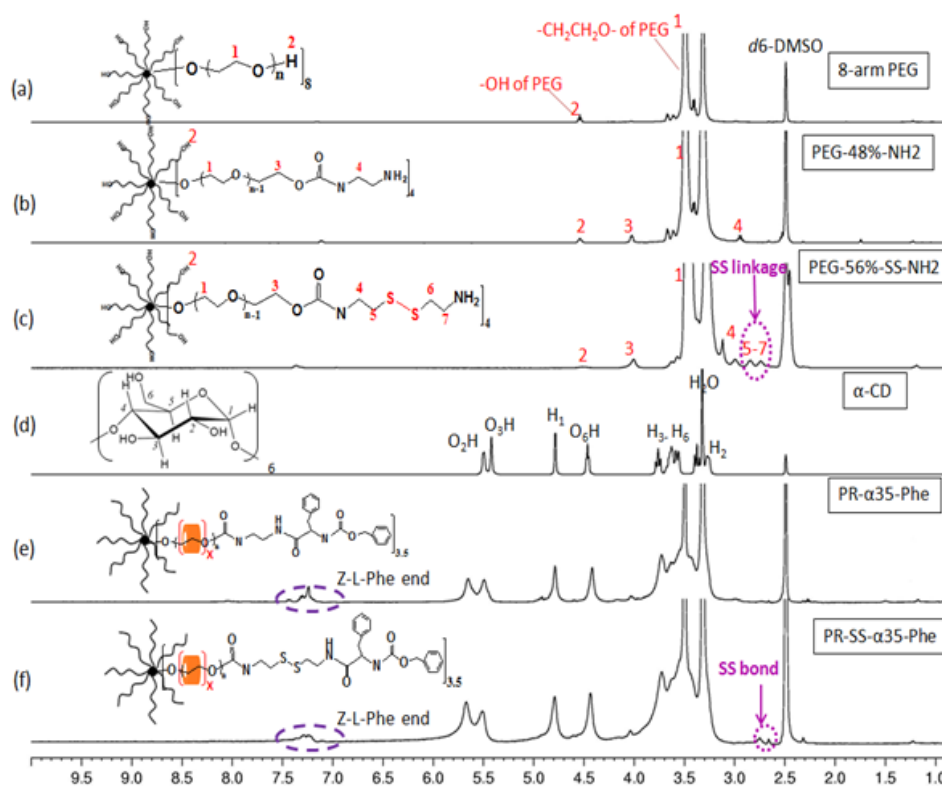
Fig. 5.1 [1]**H-NMR spectrum of (a) 8-arm PEG, (b) PEG-48%-NH2, (c) PEG-56%-SS-NH2, (d) α-CD, (e) PR-α35-Phe and (f) PR-SS-α35-Phe in d6-DMSO.** (In PEG-n%-(SS)-NH2, n means the grafted ratio of terminal amino group; In PR-α n-(SS)-Phe, n means the average number of α-CDs threaded on each molecular polymer, calculated by ^{1}H NMR)

Fig 5.1(a)-(c) show the ^{1}H NMR result of 8-arm PEG-SS-NH$_2$/PEG-NH$_2$ in comparison with pure 8-arm PEG. The unique peak of $\delta=2.7\sim2.8$ was attributed to the SS-linkage. Furthermore, the integration ratio of H$_2$ (-OH of PEG) was decreased after the CDI reaction. The results confirm the successful conjugation of 8-arm PEG with cystamine/ethylenediamine. By calculation, it was found that the grafted degree for PEG-SS-NH$_2$/PEG-NH$_2$ is 48% and 56%, suggesting that about 4 arm of 8-arm PEG is grafted with cystamine/ethylenediamine. Fig 5.1(b)-(f) show the ^{1}H NMR of polyrotaxane. In Fig. 5.1(e)-(f), the signals for α-CD, the threading 8-arm PEG and the end groups (Z-L-Phe, $\delta=7.2-7.4$) were all observed. The polyrotaxane compositions (shown in Table 5.1) could be derived by comparison between the resonance peak due to H$_1$ of α-CD, PEG ($\delta=3.50$) and Z-L-Phe end.
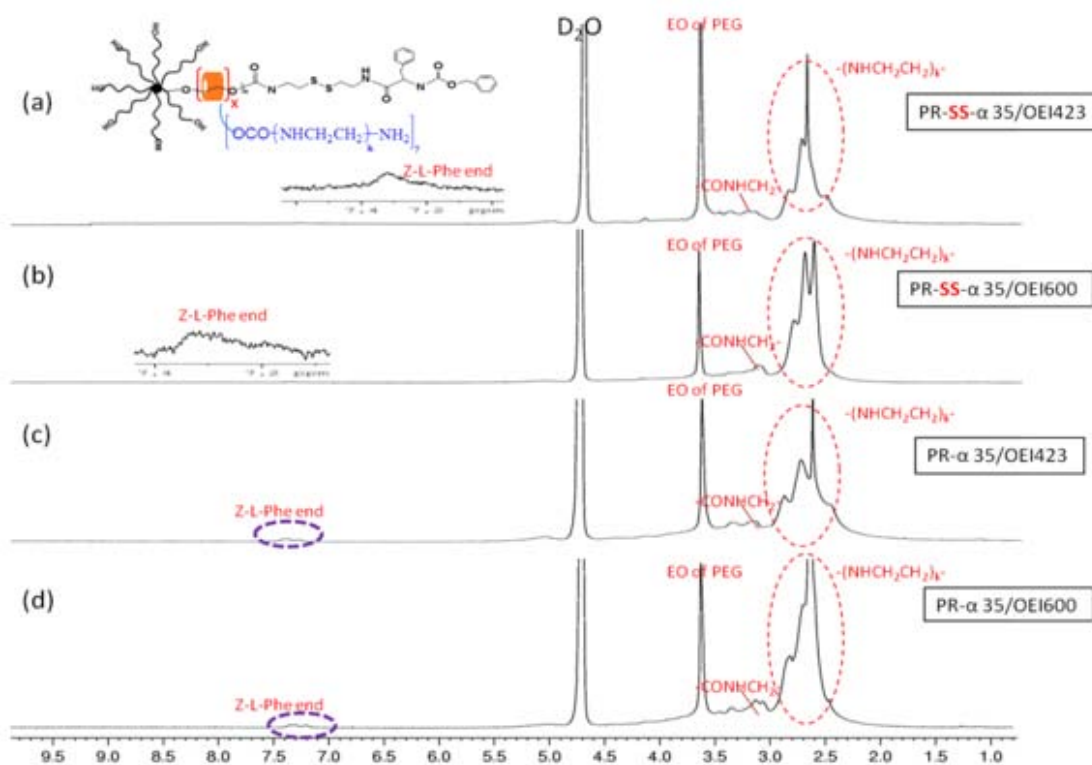
Fig. 5.2 ^{1}H-NMR of (a) α-CD, (b) PR-SS-α 35/OEI423, (c) PR-SS-α 35/OEI600, (d) PR-α 35/OEI423 and (e) PR-α 35/OEI600 in D$_2$O.

Fig. 5.2 shows the ^{1}H NMR spectra of the star polyrotaxanes in comparison with pristine α-CD. In the spectra of Fig.5.2b-e, the signals for α-CD, the grafting OEI chains, the threading 8-arm PEG, and the Z-L-Phe ends were observed, while the peaks were much broadened because of the restriction of the molecular motion by molecular interlocking and the grafting of the OEI units [39]. The grafted ratio of CD/OEI could be estimated by comparing the integration of the signals for OEI (δ=2.5~3.0), PEG (δ=3.5) and threaded ratio of CD/PEG in polyrotaxane (calculated based on Fig. 5.1). The elemental analysis of the synthesized cationic polyrotaxane was presented in Table 5.2. By calculation, the compositions of the cationic polyrotaxane, which determined based on ^{1}H NMR results (Table 5.1), are also in good agreement with the elemental analysis results. Therefore, from the results of ^{1}H NMR and elemental analysis, it could be conclude that the cationic 8-arm polyrotaxane threaded with OEI grafted α-CD and end blocked with disulfide-linkage were successful synthesized.

Table 5.1 The cationic polyrotaxane compositions with OEI grafted-CDs

sample name	Grafted ratio of Precursor PEG [a]	α-CD threaded arm per polymer (^{1}H NMR)[a]	CD threaded number per polymer (^{1}H NMR)[a]	Grafted ratio of OEI/CD [a]
PR-SS-α 35/OEI423	PEG-56%-SS-NH2	3.5 arms	35	2
PR-SS-α 35/OEI600	PEG-56%-SS-NH2	3.5 arms	35	2.25
PR-α 35/OEI423	PEG-48%-NH2	3.5 arms	35	2
PR-α 35/OEI600	PEG-48%-NH2	3.5 arms	35	2.15

[a] Data was all calculated on the basis of ^{1}H NMR.

Table 5.2 Elemental analysis of the cationic polyrotaxanes

sample	composition [a]	Anal.calcd [b]				Found [c]			
		N%	C%	H%	S%	N%	C%	H%	S%
PR-SS-α 35/OEI423	$PEG_1CD_{35}SS_4OEI_{70}$	13.81	44.89	8.18	1.88	14.37	45.02	7.84	1.94
PR-SS-α 35/OEI600	$PEG_1CD_{35}SS_4OEI_{78}$	16.87	45.76	9.12	1.45	16.35	46.12	8.96	1.56
PR-α 35/OEI423	$PEG_1CD_{35}OEI_{70}$	13.96	44.81	7.45	—	14.51	45.51	7.81	—
PR-α 35/OEI600	$PEG_1CD_{35}OEI_{76}$	16.05	46.88	8.89	—	16.42	46.64	8.69	—

[a] The compounds are denoted PEGxCDySSzOEIn where x are number of PEG, y are the number of threaded CD, z are number of SS linkage, and n are number of OEI repeat units, determined by ^{1}H NMR (Table 5.1).
[b] Theoretical elemental analysis calculated for the corresponding compound.
[c] Elemental analysis found.

5.3.3 Gel retardation experiment
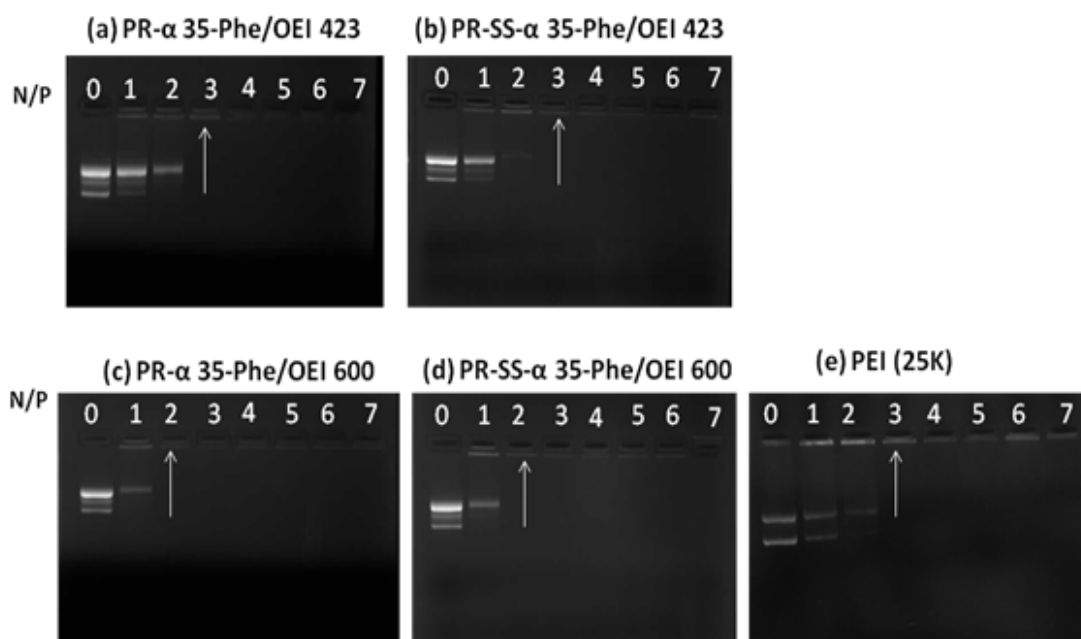
Fig. 5.3 Electrophoretic mobility of plasmid DNA in the polyplexes formed by (a) PR-α 35/OEI423, (b) PR-SS-α 35/OEI423, (c) PR-α 35/OEI600, (d) PR-SS-α 35/OEI600 and (e)25KPEI at different N/P ratio

The DNA condensation ability of polycation is a prerequisite for the successful gene delivery. In this chapter, gel retardation assay was performed to investigate the DNA binding ability of the OEI based cationic polyrotoaxanes. As shown in Fig. 5.3, all cationic polyrotaxane exhibited good DNA binding at N/P ratio

of 3, where total DNA retardation was detected, showing similar to PEI25k. The results show the higher DNA condensation ability of OEI600 based polyrotaxane than that of OEI423, which is probably due to their relatively higher charge density and high nitrogen content in comparison with OEI423. Furthermore, in comparison with PEI25k (Fig. 5.3e), PR-α 35/OEI600 and PR-SS-α 35/OEI600 (Fig. 5.3c-d) exhibited better DNA condensation capability even with lower nitrogen content and charge density. It is probably because of the OEI-grafted CD rings, which can freely move along PEG arms in solution, giving flexibility for efficient complexation with DNA. Similar results could also be found in our previous work [9].

5.3.4 Particle size and Zeta potential
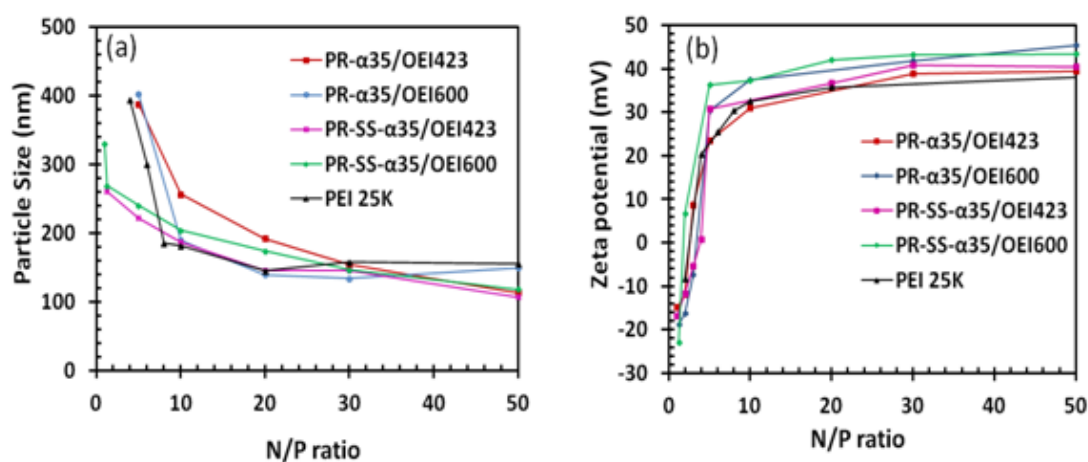
Fig. 5.4 Particle size (a) and zeta potential (b) of polyplexes formed by PR-SS-α35/OEI, PR-α35/OEI and pDNA at various N/P ratios, in comparison with PEI (25k)

It is generally believed that the particle size and surface charge of polyplexes are crucial to endocytosis and gene transfer [23]. Fig. 5.4 shows the particle size and zeta potential measurements of cationic polyrotaxane/DNA complexes in comparison with PEI (25 kDa) at various N/P ratios. Generally, in Fig. 5.4(a), all polyrotaxanes could efficiently condense pDNA into small nanoparticles and the particle size of polyplex decreased with an increase of N/P ratio. Their diameters changed

dramatically from 300~400 nm to 200 nm as N/P ratio increase from 1 to 10, which is similar with the PEI25k/DNA complexes. With further increasing the N/P ratios, their particle size changed slightly and remained in the 100–200 nm range.

Zeta potential is an indicator of the surface charge of polymer/DNA nanoparticles, and a positive surface potential of polyplexes is crucial for the attachment of anionic cell surface and endocytosis [40]. As shown in Fig. 5.4(b), the surface net charge of the complexes of pDNA with cationic polyrotaxanes increased sharply from negative to positive as the N/P ratio increased from 1 to 3, and reached a plateau at an N/P ratio of 10 and above. The phenomenon is in accordance with the results obtained from gel retardation assay, and particle size as discussed earlier. When N/P ratio is higher than 10, the zeta potential of the complexes stabilized at 30-40mV, which could result in a similar affinity to the cell surface.

5.3.5 Biodegradation behavior of polymer/DNA complexes

In last two decades, disulfide bond has been highly investigated as a crucial linkage for gene delivery vectors due to the rapid disulfide bond cleavage upon the interaction with reducing molecules such as, glutathione (GSH), cystein and so forth in living cells [41]. This rapid cleavage of disulfide linkage will ensure DNA release from complexes efficiently leading to facilitating nuclear import, gene transcription and gene expression [42], and also lowering the cytotoxicity of the system.
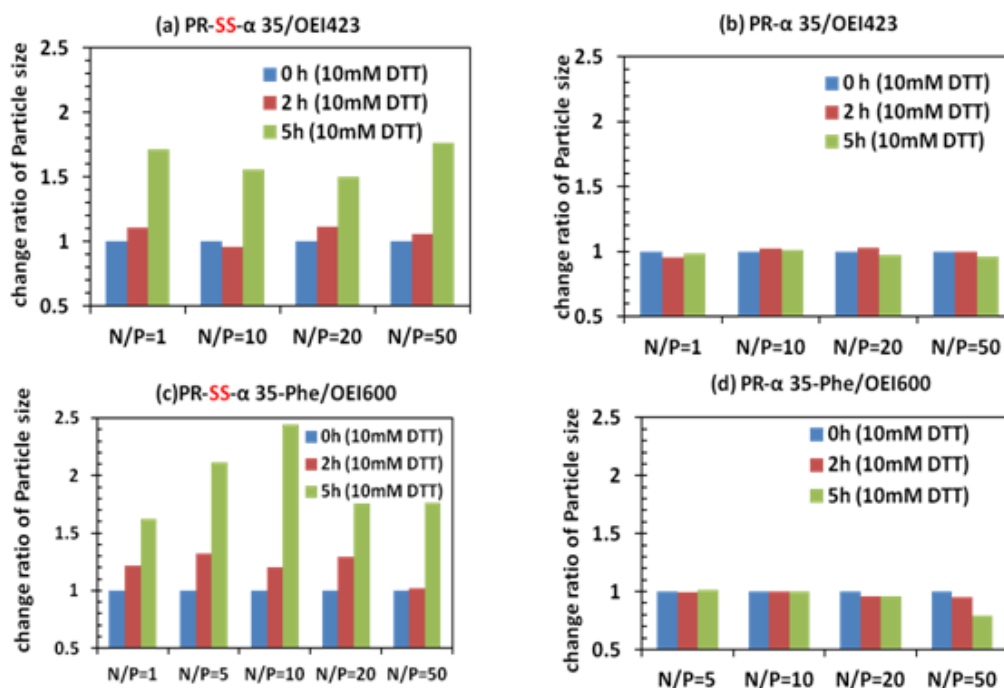
Fig 5.5 Particle size change ratio of polyplexes formed by (a) PR-SS-α35/OEI423, (b) PR-α35/OEI423, (c)PR-SS-α35/OEI600, (d) PR-α35/OEI600 and pDNA in the presence of 10 mM DTT after 0h, 2h and 5h.

In order to confirm the degradation and dissociation of our disulfide-containing systems, the bioreductive cleavage of the disulfide bond in the polyrotaxane was mimicked by treating with reducing agent DTT (10mM), which is analogous to the intracellular environment such as cytosol. And the particle size change of the polyplex with different N/P ratios in response to DTT was determined by DLS (Fig. 5.5). The responsive reductive polyplexes PR-SS-α35/OEI were stable in physiological solution during 24 h incubation in PBS (part 5.3.11). However, as shown in Fig. 5.5, when these complexes were treated with reductive agent, 10 mM DTT, the particle size of PR-SS-α35/OEI markedly increased and the increased ratio is varied from 1.5 to 2.5 (Fig. 5.5a and 5.5c). Notably, at N/P ratio of 10, after incubation with DTT for 5h, the size of polyplex formed by PR-SS-α35/OEI423 and PR-SS-α35/OEI600 markedly increased from 186 nm to 291 nm (change ratio=1.6) and 90 nm to 221 nm (change ratio=2.5), respectively. In contrast, non-reductive

polyplex PR-α35/OEI were sufficiently stable in the presence of DTT and no change in particle size was observed (Fig. 5.5b and 5.5c). The increased of particle sizes were probably due to the cleavage of the disulfide-bond in the presence of DTT, which led to decreased DNA binding ability. This phenomenon is good agreement with other disulfide bond based bioreductive gene systems [41, 43, 44]. Therefore, the above result confirms the dissociation behavior of the supramolecular structure by cleavage of the disulfide linkages upon a reductive intracellular environment.

5.3.6 DNA release ability
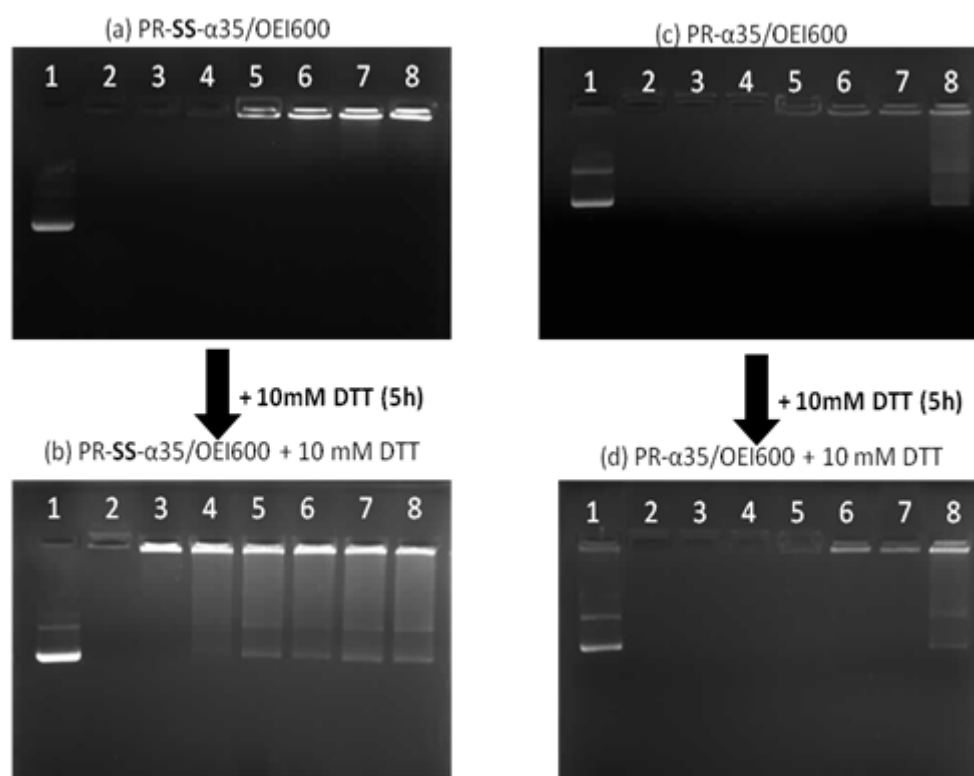
Fig. 5.6 Agarose gel electrophoretic images of the polyplexes (N/P=50) of PR-SS-α35/OEI600 (a,b) and PR-α35/OEI600 (c,d) with (b,d) or without (a,c) 10 mM DTT. *(Line 1 shows the bands of control pDNA. Concentrations of heparin at lines 2, 3, 4, 5, 6, 7, and 8 were 0, 200, 300, 400, 450, 500 and 600 μg/mL, respectively.)*

To further examine the DNA release ability in the reductive condition, condensed polyplexes were subjected to gel retardation and a heparin competitive displacement assay was performed in the absence or presence of 10 mM DTT. Fig.

5.6(a)-(b) show the gel electrophoretic images of PR-SS-α35/OEI600 before or after incubating with DTT for 5h. In the absence of DTT, the critical concentration of heparin, at the point of pDNA release, for PR-SS-α35/OEI600 is higher than 600 μg/mL(Fig. 5.6a), confirming that DNA were compacted tightly by the tested cationic polymer. Remarkably, after incubating with DTT for 5h, free DNA bands were observed at much lower concentration of heparin (200 μg/mL) (Fig. 5.6b). The results suggest that in PR-SS-α35/OEI systems, effective pDNA release was observed in the reductive condition, indicating the DNA binding ability of polyrotaxane decreased after incubating with DTT. In contrast, no obvious pDNA release was observed on the reduction insensitive control under the same condition (Fig. 5.6c-d). In the case of PR-α35/OEI600, DNA release ability was not enhanced with DTT and the DNA release occurs only when concentration of heparin is 600 μg/mL. These results indicate that the pDNA release from PR-SS-α35/OEI polyplexes was induced by the SS cleavage, followed by a dissociation of the supramolecular structure of polyrotaxanes [31]. Similar results were also found by other groups [44]. These findings were thus in accordance with the particle sizes results discussed earlier. Similarly, polyplexes formed by PR-SS-α35/OEI423 also exhibited the same results (Fig. 5.7). In summary, it is predicted that PR-SS-α35/OEI/DNA system was stable extracellularly and could rapid release DNA from the system intracellularly by rapid disulfide bond cleavage.
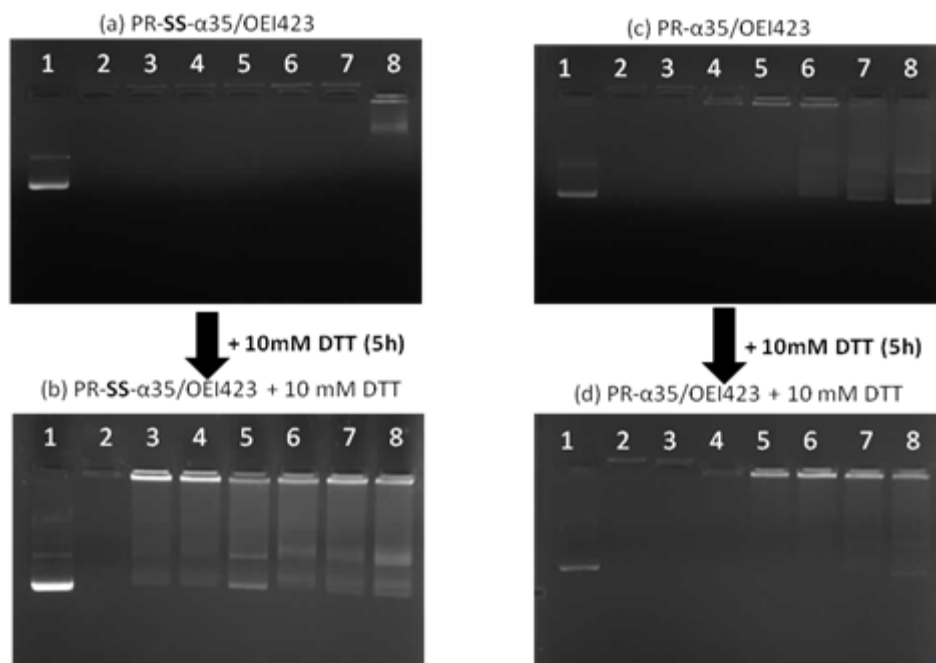
Fig. 5.7 Agarose gel electrophoretic images of the polyplexes (N/P=50) of PR-SS-α35/OEI423 (a,b) and PR-α35/OEI423 (c,d) with (b,d) or without (a,c) 10 mM DTT. *(Line 1 shows the bands of control pDNA. Concentrations of heparin at lines 2, 3, 4, 5, 6, 7, and 8 were 0, 200, 300, 400, 450, 500 and 600 µg/mL, respectively.)*

5.3.7 Cytotoxicity of the cationic polyrotaxanes

Based on the pioneer findings, we modified our PEI based polyrotaxane with the purpose of lowering cytotoxicity using the following strategies: (1) Conjugation of low molecular weight PEI chain (OEI423 and OEI600) to CD rings in the polyrotaxane to form a large molecular weight star shaped and flexible polymer; (2) Introduction of disulfide linkage to polyrotaxane chain to ensure CD dethreading, DNA release and lower toxicity; (3) Introduction of PEG hydrophilic shell which could decrease cytotoxicity due to its shielding effect on the surface charge of particles [23-25].
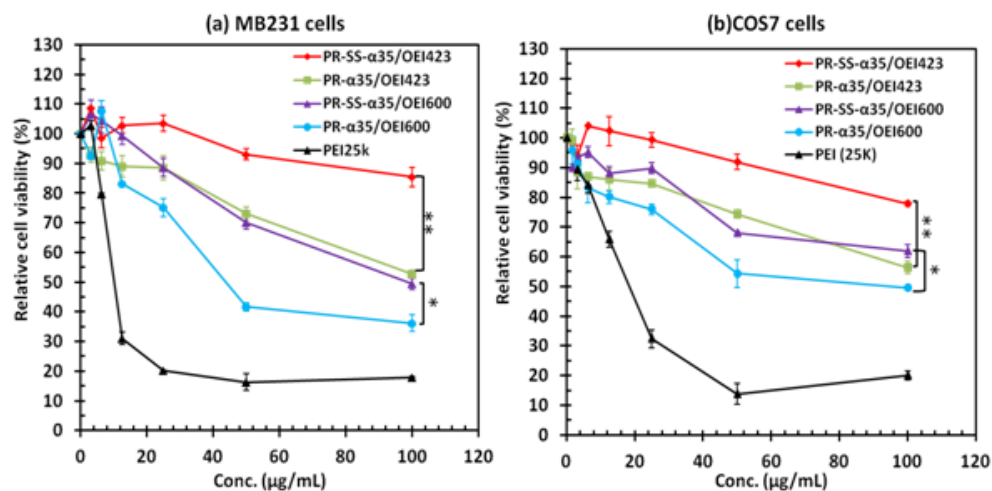
Fig. 5.8 Cell viability assay with various concentrations of PR-(SS)-α 35-OEI systems compared with bPEI (25k) in (a) MB231 and (b) COS 7 cells for 24 h in a serum-containing medium (n=6). *p<0.01, **p<0.001

The *in vitro* cell cytotoxicity of our cationic polyrotaxane systems was evaluated by MTT assays in MB231 and COS 7 cell lines, using commercial available PEI25k and non-reducible polyrotaxane as control (Fig. 5.8). As shown in Fig. 5.8, all investigated polymers exhibited a dose-dependent toxicity effect on both cell lines. It is worth noting that all four cationic polyrotaxanes exhibited markedly less toxicity in both cultured MB231 and COS7 cells than the PEI control. One possible reason is that the introduction of polyrotaxane and lower molecular PEI results in the lower density of amino groups and the high density of amino groups in PEI is always considered as an important factor leading to high cytotoxicity [45]. Likewise, the cytotoxicity of OEI600 based polyrotaxane is higher than that with linear OEI423, which could also be attributed to its higher density of amino group.

More importantly, by comparing the cytotoxicity of disulfide bond contained polymer with the non-reductive control, it was valuable to found that polyrotaxane with SS linkage showed a remarkable decrease in cytotoxicity over PR-α35/OEI, which is the PR-SS-α35/OEI analogue lacking a reductively cleavable disulfide bond. The dramatically decreased cytotoxicity is believed to be a direct consequence of the

intracellular degradation of the disulfide bond of PR-SS-α35/OEI systems leading to CD dethreading with smaller fragments, which results in reduced binding affinity of polymers with cellular membranes and reduced interference with cellular signal transduction pathway. It is evident that introduction of disulfide linkage is benefit for enhancing polymer biocompatibility. Such findings are in accordance with the previous reports, demonstrating that the incorporation of bioreductive disulfide bond could lower cytotoxicity [18, 46, 47]. From the above cytotoxicity result, we could safely come to the conclusion that our modification strategies including conjugation of low MW PEI chain to CD rings and introduction of disulfide linkage into the polyrotaxane systems are succeed in improving cell viability of PEI.

5.3.8 In vitro transfection and luciferase assay
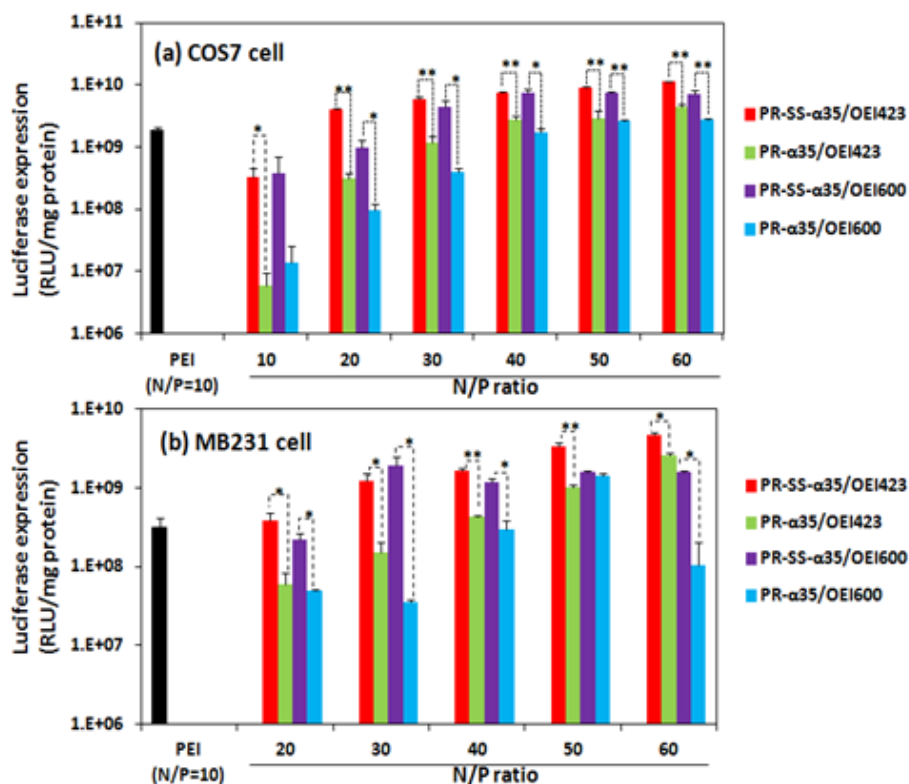
Fig. 5.9 Gene transfection efficiency of the polyplexes formed by PR-(SS)-α35/OEI and 25K PEI in (a) COS7 and (b) MB231 cells in the presence of serum. Luciferase was measured at 24h after transfection. Data represent mean±SD (n=3, *p<0.05, **p<0.01).

In vitro gene transfection efficiency of the cleavable cationic polyrotaxane was assessed using luciferase as a marker gene in MB231 and COS7 cells in the presence of serum. Fig. 5.9 shows the luciferase protein expression of the bioreductive polyrotaxane PR-SS-α35/OEI compared with non-reductive analogue PR-α35/OEI and PEI25k. As presented in Fig. 5.9, it could be seen that the luciferase expression mediated by cationic polyrotaxane was greatly dependent on the N/P ratios. Generally, the transfection efficiency increased with the increasing of N/P ratios and the optimal N/P ratio for the most efficient transfection is around 50. Remarkably, all polyrotaxanes showed excellent *in vitro* gene transfection efficiency, comparable to or even higher than that of branched PEI (25 K) at their optimal N/P ratios. In particular, the transfection efficiency mediated by PR-SS-α35/OEI423 (N/P=60) was 15 times higher than that of PEI (25K) (N/P=10) in MB231 cells (Fig. 5.9b). Furthermore, it is worth of note that the reductive polyrotaxane PR-SS-α35/OEI exhibited significant higher luciferase expression than the non-biodegradable polyrotaxane control (PR-α35/OEI). They have significant difference in most N/P ratios. It is hypothesized that cytotoxicity was related to gene transfection ability and might be caused by electrostatic interactions with negatively charged glycocalyx of the cell surface [4]. Since the bioreducible cationic polyrotaxane showed a remarkable decrease in cytotoxicity over the non-degradable control (Fig. 5.8), the higher luciferase expression of degradable polyrotaxane may have benefited from their lower toxicity inside cells, which might enable to enhance the transfection efficiency.
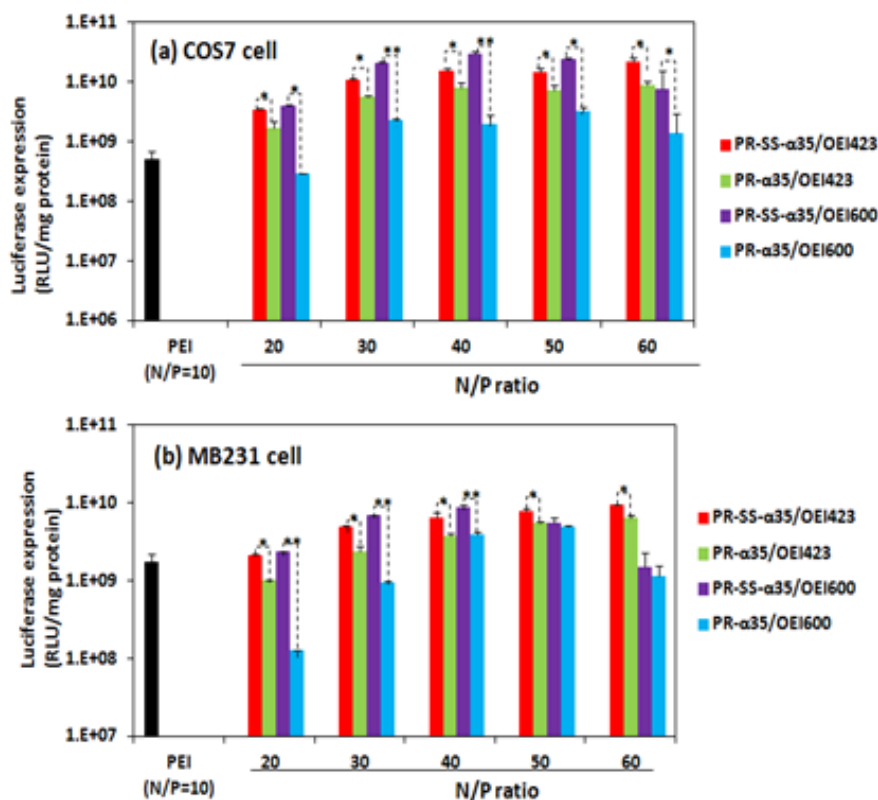
Fig. 5.10 Gene transfection efficiency of the polyplexes formed by PR-(SS)-α35/OEI and 25K PEI in (a) COS7 and (b) MB231 cells in the presence of serum. Luciferase was measured at 48h after transfection. Data represent mean±SD (n=3, *p<0.05, **p<0.01).

We also investigated the luciferase expression level mediated by our cationic polyrotaxane after longer transfection time (Fig. 5.10). It was found that the polyrotaxane exhibit much better transfection efficiency than PEI, especially after long time incubation. It is probably because the transfection efficiency of PEI decreased when increasing transfection time, which might be caused by the cumulative cytotoxicity of PEI inside cells [28]. While the transfection ability of cationic polyrotaxane increased with the increased of incubation time, owing to their low cytotoxicity, which may enable them to stay within the cells long enough and slowly release the pDNA to enhance luciferase expression.

5.3.9 In vitro Green fluorescence protein expression
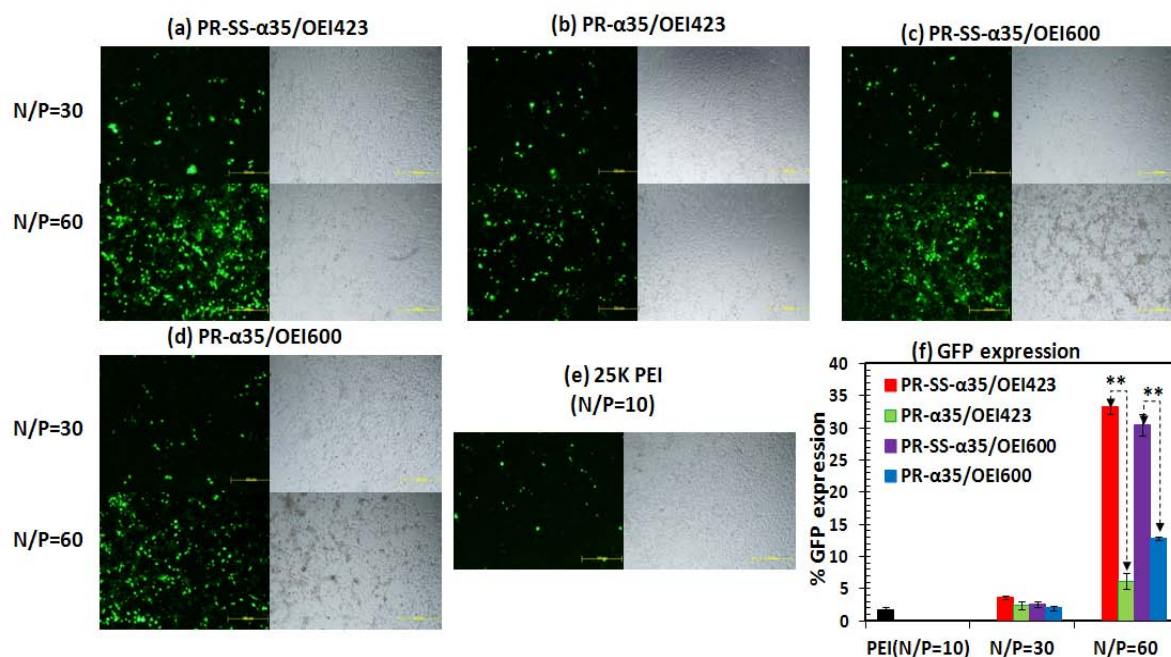
Fig. 5.11 The fluorescence microscopy images of transfected COS 7 cells mediated by pEGFP-N1 complexes form by (a) PR-SS-α35/OEI423, (b) PR-α35/OEI423, (c) PR-SS-α35/OEI600 and (d) PR-α35/OEI600 at N/P ratio of 30 and 60, comparing with PEI 25K at N/P=10. (f) Quantitative comparison of the percentage of cells expressing GFP. Student's unpaired t-test (**p<0.005). (left: fluorescence light; right: bright light).

We employ another reporter gene pEGFP-N1 plasmid DNA encoding green fluorescence protein (GFP) to further visualize transgenetic efficacies of the PR-SS-α35/OEI carriers with its non-reductive analogue PR-α35/OEI as control. As shown in Fig. 5.11, strong fluorescence signal could be observed in delivering EGFP-pDNA when transfections were mediated by polyrotaxane systems, exhibiting high levels of vector internalization and gene expression. Fluorescence signal increased by the increasing of N/P ratio. Both PR-SS-α35-OEI and PR-α35-OEI showed significantly higher fluorescence than PEI, indicating higher gene GFP expression efficiency (Fig. 5.11f). It is in line with the results of luciferase assay. Furthermore, by comparing PR-SS-α35-OEI and PR-α35-OEI at N/P ratio of 60, a stronger GFP fluorescence emission was observed for the bio-reductive vector. As a result, GFP transfection

assay showed higher gene transfection efficiencies for PR-SS-α35-OEI systems, and this trend agrees well with that measured by luciferase assay (Fig. 5.9).

5.3.10 GSH inhibition
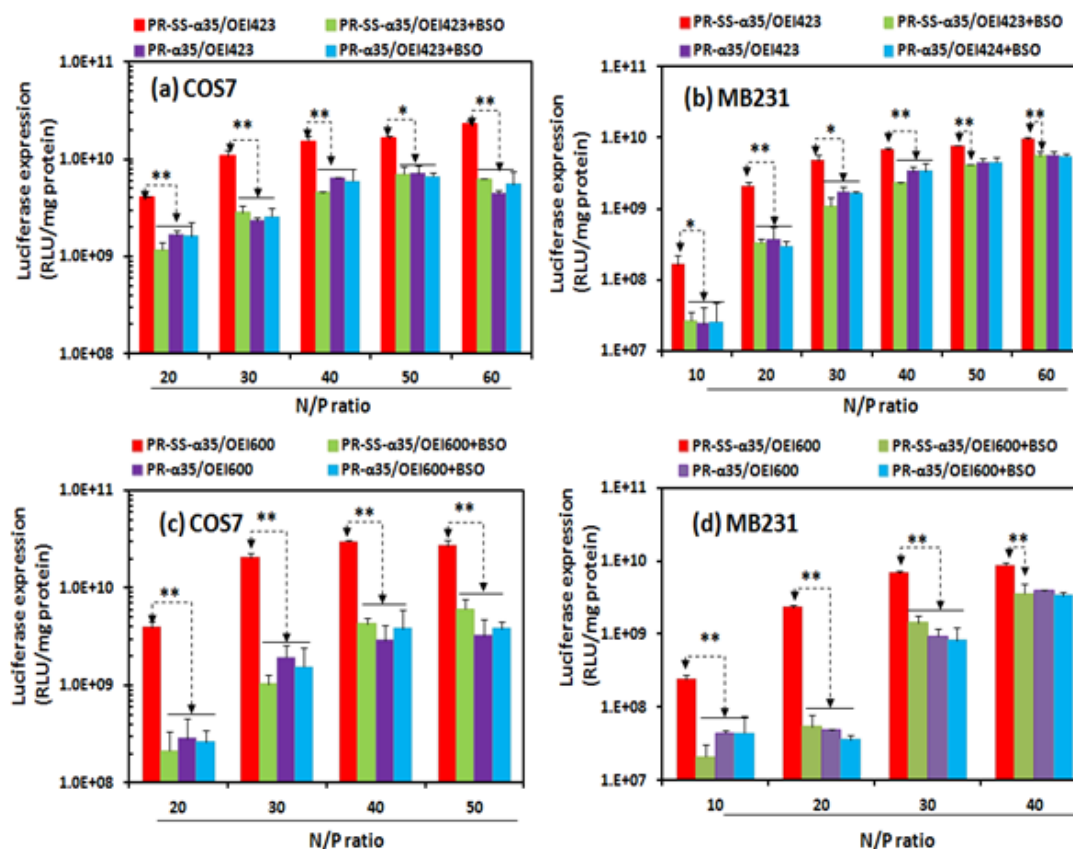
Fig. 5.12 Effects of BSO (300μM) on luciferase expression levels in COS7 and MB231 cells. Polyplex formed by PR-(SS)-α35/OEI423 (a,b) and PR-(SS)-α35/OEI600 (c,b) were transfected in the presence of serum with/without BSO. Data represent mean±SD (n=3). *p<0.05, **p<0.01

In previous research, we confirmed the degradation behavior and DNA release ability of bioreductive polyrotaxane in response to DTT, due to the cleavage of disulfide linkage (Fig. 5.5-5.7). And the transfection results and MTT assay further showed that the cell viability and gene transfer ability of PR-SS-α35/OEI systems were noticeably stronger than the non-reductive analogue PR-α35/OEI control (Fig. 5.8-5.11). However, we still not sure whether the degradation of the complexes occurred intracellularly reducing by glutathione (GSH), and whether the degradation

and intracellular reductive environment GSH are responsive for the low cytotoxicity and high transfection efficiency. Therefore, in order to further determine the role of disulfide linkage of our system in improvement of gene transfection, D,L-Buthionine sulfoxamine (BSO), a known GSH inhibitor resulting in depletion of intracellular GSH, was used [37, 48]. Fig. 5.12 shows the effects of BSO (300μM) on luciferase expression levels in COS7 and MB231 cells. The results showed that when cells were pre-incubated with BSO prior to transfection, the transfection efficiency of disulfide-linkage containing PR-SS-α35/OEI423 (Fig. 5.12a-b) and PR-SS-α35/OEI600 (Fig.5.12c-d) sharply decreased as compared to the same polyplex without the treatment of GSH inhibitor (p<0.01). In contrast, the luciferase expression level of non-degradable analogue PR-α35/OEI was not affected by BSO (p>0.05). Therefore, it is evident that the observed inhibitions of transfection were not caused by cytotoxicity of BSO and the disulfide linkages were cleaved by intracellular GSH. It suggests that the degradation did play a role in reductive polyrotaxane transfection, presumably through the efficient unpacking of DNA. Furthermore, after treating with BSO, no significant differences were observed in the transfection efficiency of PR-SS-α35/OEI and PR-α35/OEI (p>0.05). This is in consistent with the previous report [48, 49], which indicating the intracellular cleavage of the disulfide bond in the PR-SS-α35/OEI systems by GSH is responsible for their higher transfection efficiency observed previous in compared with PR-α35/OEI systems (Fig. 5.9 and 5.10).
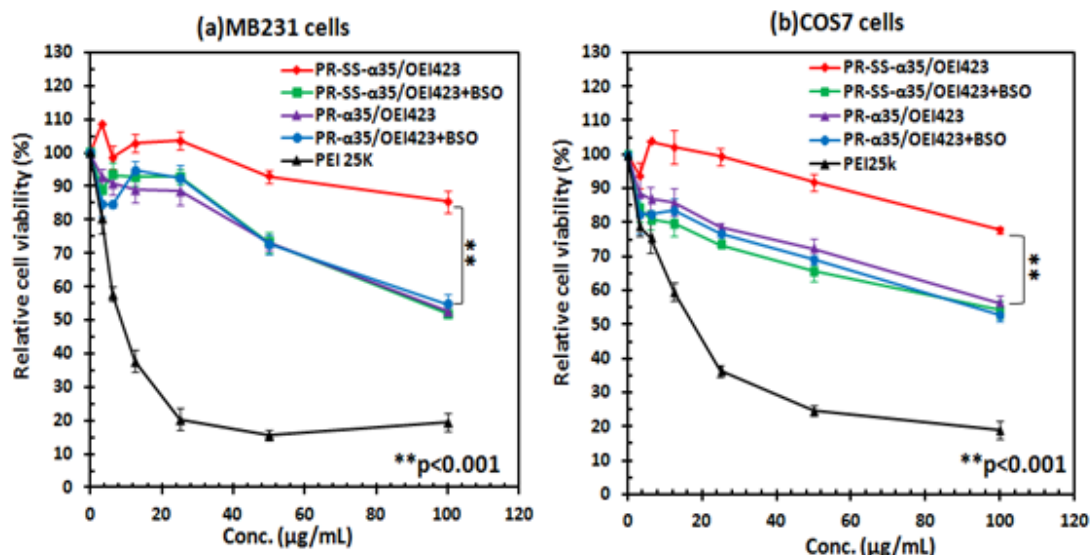
Fig. 5.13 Effects of BSO (300μM) on cytotoxicity of PR-SS-α35/OEI423 in (a) MB231 and (b) COS7 cells. Data represent mean ± SD (n=6). **p<0.001

Since we originally hypothesized that the reductive polyrotaxane would facilitate DNA release triggered by the intracellular degradation in response to GSH, we expected that the cytotoxicity of the biodegradable polyrotaxane would also be affected by the level of intracellular GSH level, which causes the degradation. To test this point, cell viabilities were compared between the cells treated with and without BSO. As shown in Fig. 5.13, in both cell lines, the cytotoxicity of PR-SS-α35/OEI423 system significantly increased to the level of its non-degradable analogue PR-α35/OEI423 upon treatment with BSO (p<0.001). It should also be noted that the decreased of cell viability should not be associated with toxicity of BSO, because the cytotoxicity of non-reductive PR-α35/OEI423 was not affected by BSO treatment (p>0.05). The results showed that the GSH inhibitor led to the inability of polyplex to completely degradation, resulting limited DNA release and higher cytotoxicity. Evidently, lower the cytotoxicity of complexes is the one of the major contributions of disulfide linkage to gene transfection. The results are in accordance with our previous hypothesis.

5.3.11 Stability of polymer/DNA complexes

Serum stability is one of the most important barriers for gene delivery. In the case of *in vivo* gene delivery, the polyplex particles could prone rapid aggregation due to the negatively charged plasma proteins in the serum or blood, which affect the stability of the positively charged polyplexes [50]. In our system, due to the unique supramolecular structure of star PEG with partial threaded CDs, the naked PEG arms could form a sheddable hydrophilic shell by self-assembly, which could stabilize the polyplex. This is one of the major advantages of our systems in contrast to other cationic polyrotaxanes formed by linear polymers and cyclodextrins [19, 27]. Furthermore, unlike traditional PEGylation via covalent or non-covalent attachment, the PEG shell was formed naturally and no more modification is needed, which could prevent the drawbacks due to the traditional PEG modification, such as lower transfection efficiency and reduced internalization of untargeted polyplexes [51], degradation of DNA by nucleases [52], and lower DNA binding ability [53].

We studied the aggregation behaviors of the polyplex formed by cationic polyrotaxane with PEG shell under physiological salt condition (N/P=50) (Fig. 5.14). In order to verify the importance of naked PEG arms in our unique PR core-shell structure, three control systems are used: PEI25k, α-CD-OEI600 without PEG and polyrotaxane based on almost fully threaded 8-arm PEG and cationic α-CD (PR-SS-α65/OEI600). The last two of which are synthesized with the same procedures as our test polyrotaxanes and their structures are confirmed by ^{1}H NMR. The NMR result showed that in PR-SS-α65/OEI600 systems, 65 α-CDs are threaded on each polymer (~7 PEG arms threaded, 1 arm naked) and the grafted ratio of OEI/CD is two,

confirming it as the PR-SS-α35/OEI600 (~3.5 PEG arms threaded, 4.5 arm naked) analogue but threading with more CDs.
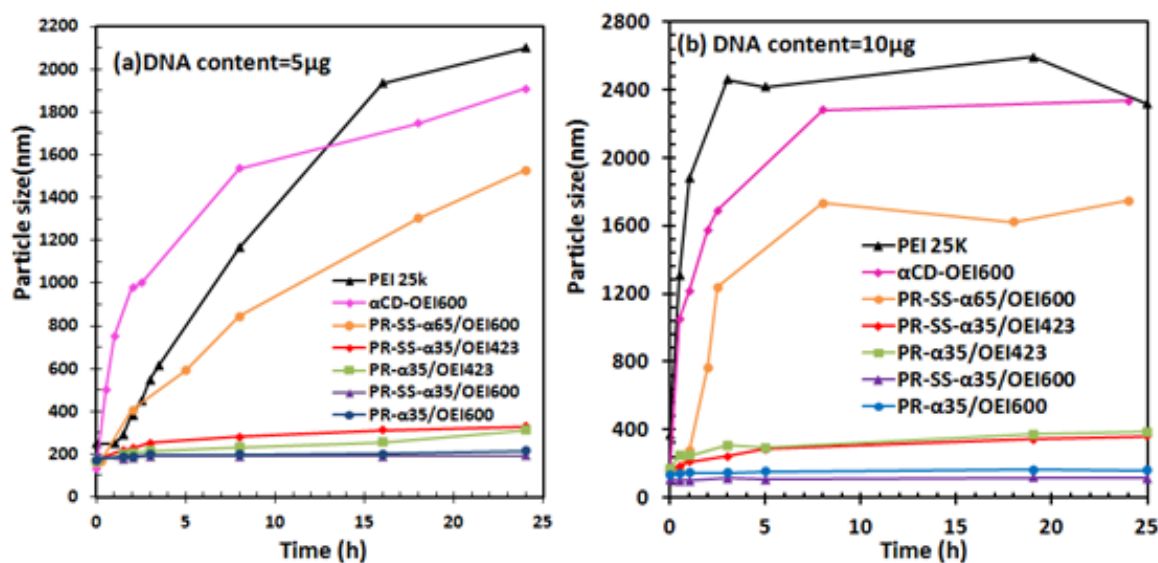
Fig.5.14 Hydrodynamic size of polyplex formed by PEI, αCD-OEI, PR-SS-α65-OEI and PR-(SS)-α35-OEI systems at N/P ratio of 50 with different DNA content as a function of time in the presence of 150 mM PBS. (a) DNA content=5μg; (b) DNA content=10μg

As shown in Fig. 5.14, in the presence of PBS, the hydrodynamic diameters of our four test cationic polyrotaxanes remained relatively stable within 24hrs, but the complexes formed by polymer without PEG (α-CD-OEI600) or with less naked PEG (PR-SS-α65/OEI600) and PEI25k aggregated rapidly in PBS. In particular, the size of polyplexes formed by PR-SS-α35/OEI600 with 10 μg DNA increased from 101.3 nm to 113.8 nm in 24 hours with PBS incubation, and the size change ratio was 1.13 (Fig. 5.14b). In contrast, with the increase of CD threaded number and decrease of naked PEG arms, the trend of size changes of both α-CD-OEI600 and PR-SS-α65/OEI600 system were much steeper. The diameters of PR-SS-α65/OEI600 complexes increased from 164.5 nm to 1749 nm in 24 hours and the size change ratio was 10.63. These results demonstrates that the naked PEG in PR-(SS)-α35/OEI contributes to the formation of exterior surface with hydrophilic PEG brush layer,

171

which could stabilize the polyplex and prevent aggregation of particles under physiological salt conditions.
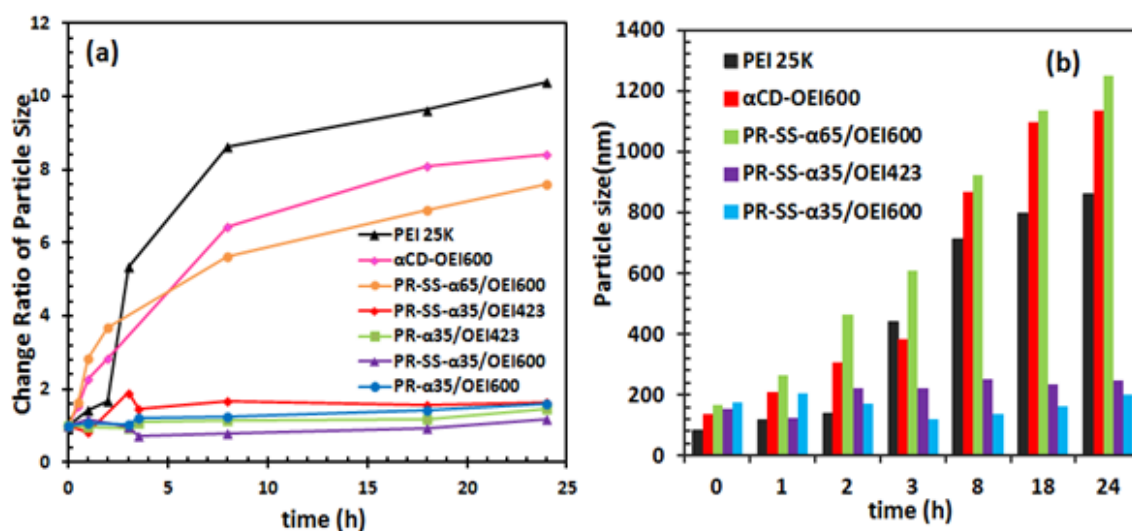
Fig. 5.15 Evaluation of the change in particle size of polyplexes in PBS that contains 5wt% of BSA at 37 °C, as determined by dynamic light scattering: (a) size change ratio (b) particle size. (All the N/P ratio of the polymer/DNA complex was fixed at 50.)

In this chapter, bovine serum albumin (BSA) was selected as the model protein to simulate the serum condition. We investigate the stability of the polymer/DNA complexes in BSA containing PBS. Fig. 5.15 shows the ratio of size change (a) and the size of polyplexes (b) in 5% BSA solution as a function of time. Similar with the investigation of salt stability, the particle size of PR-(SS)-α35/OEI/DNA complex was compared to 3 systems: PEI25k, α-CD-OEI600 without PEG and PR-SS-α65/OEI600 (7 arms threaded with CDs). As expected, it was found that all the four tested polyrotaxanes with 4.5 naked PEG arms (PR-(SS)-α35/OEI) could prevent particle aggregation for 24h in the presence BSA. The sizes of PR-SS-α35/OEI600 /DNA complexes increased from 173.7 nm to 202.1 nm in 24 hours, and the size change ratio was 1.16. And the size change ratio of other three polyrotaxane are all lower than 2. However, without the modification of PEG, the trend of size changes of both PEI/DNA and α-CD-OEI/DNA system were much steeper. The ratios

of size change at 24 h were 10.4 and 8.4, respectively. Furthermore, there is a trend that polyrotaxane with less naked PEG arms is less effective to alleviate BSA-induced aggregation. By comparing with polyrotaxanes with 4.5 naked PEG arms, the diameter of PR-SS-α65/OEI600 (1 naked arm) complexes increased from 164.5 nm to 1248 nm in 24 hours and the size change ratio was 7.59. The results are in line with the previous salt stability studies. It is confirmed that the shielding effect of PEG could hinder the interaction with protein and aggregation of particles. Our polyrotaxanes with core-shell nanostructures may be more stable and resistant to serum system than other polycationic gene systems, which is important for *in vivo* applications.

5.3.12 Serum tolerance capacity investigations
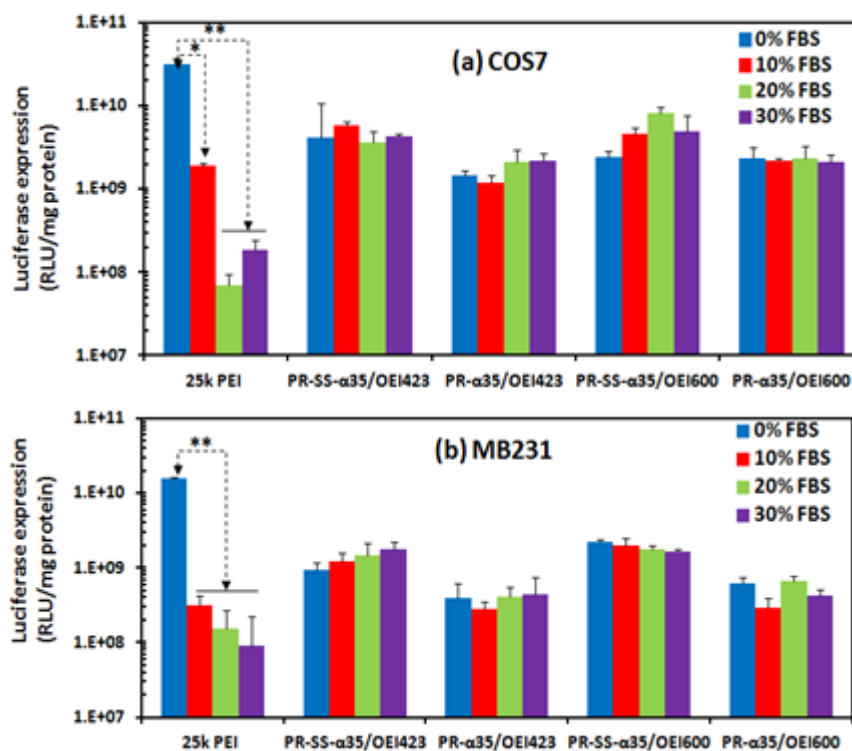
Fig. 5.16 Effect of serum contents on the luciferase activities of polymer/DNA complexes in (a) COS-7 and (b) MB231 cells. All polyrotaxane were tested at its optimal N/P ratio in presence of serum, PEI25k at N/P 10 and polyrotaxane at N/P=30. Data represent mean±SD (n=3, *p<0.01, **p<0.001).

We have confirmed that the PEG shell could prevent aggregation upon salt and protein conditions (part 5.3.11). However, we still do not know whether the hydrophilic shell could intracellularly weak the inhibitory effect of serum to transfection. To achieve that point, serum tolerance capacity of PR-(SS)-α35/OEI systems was investigated. The luciferase gene expression mediated by PR/DNA was studied in the medium containing various concentrations of FBS and compared with PEI25k (Fig. 5.16). As shown in Fig. 5.16, the increased FBS concentrations exert negative effect on gene transfection by PEI25k. In the presence of 30% FBS, transfection efficacies were drastically decreased to be less than 1% of those values assayed in serum-free medium ($p<0.001$) in both COS7 and MB231 cells. The low transfection efficiencies were possible caused by aggregation of the particles in response to serum contained medium, which was verified in the stability studies in BSA (Fig. 5.15). In contrast, the polyplex mediated by our four test polyrotaxanes with PEG shell interestingly remained high luciferase protein expression level eve in 30% of FBS ($p>0.05$), indicated its high serum-resistance capability during transfection. The serum tolerance capacity of polyrotaxane system was probably because of the particles formed by PR-(SS)-α35/OEI were covered with naked PEG, which is hydrophilic and hinder the non-specific interaction of the negative charged serum. This property of PEG possibly allows lower binding affinity to serum constitutes. This is in consistent with the stability studies.

5.4 CONCLUSIONS

Aiming to increase the serum stability and achieving optimal DNA release to maximize transfection, a novel reduction-sensitive gene delivery system was

successfully developed based on cationic polyrotaxanes with core-shell nanostructures, which consists of partially threaded α-CD, star PEG, end blocking polymer with disulfide-linkage and multiple OEI arms by conjugating onto α-CD rings. The resulted cationic supramolecular structure demonstrated good ability to condense DNA into nanoparticles. DLS and gel retardation experiment confirmed their degradability and DNA release ability in response to DTT. Remarkably, the results of MTT assay and luciferase expression confirmed that the biodegradable polyrotaxane with disulfide linkage exhibited significant lower cytotoxicity and higher gene transfection efficiency in contrast to reduction insensitive control and polyethylenimine (PEI) 25k. They showed excellent *in vitro* transfection efficiency which was comparable to or even higher than that of PEI 25k. Furthermore, in according to the glutathione (GSH) inhibition experiment, it was found that cell viability and transfection was markedly decreased, confirming that introduction of disulfide linkage to the system result in fast intracellular degradation and disassociation, efficient DNA release, decreased cytotoxicity and enhanced transfection. More importantly, the hindrance effect of PEG shell allows the system to be stable in salt and protein solution, and inhibits non-specific protein absorption on the particle surface. Moreover, high serum concentration exerts neglect effect on the transfection efficiency of this polyrotaxane system, further verifying the PEG shell enhances the serum stability of the system. Taken together, our cationic nanostructures boast many favorable properties as gene carriers, which include good DNA binding ability, reduction-sensitive biodegradability, intracellular DNA release, low cytotoxicity, high gene transfection efficiency and high stability in biological fluids.

5.5 REFERENCES

1. Rideout WM, 3rd, Hochedlinger K, Kyba M, Daley GQ, Jaenisch R. Correction of a genetic defect by nuclear transplantation and combined cell and gene therapy. Cell 2002 Apr 5;109(1):17-27.

2. Cavazzana-Calvo M, Hacein-Bey S, de Saint Basile G, Gross F, Yvon E, Nusbaum P, et al. Gene therapy of human severe combined immunodeficiency (SCID)-X1 disease. Science 2000 Apr 28;288(5466):669-672.

3. Kaplitt MG, Feigin A, Tang C, Fitzsimons HL, Mattis P, Lawlor PA, et al. Safety and tolerability of gene therapy with an adeno-associated virus (AAV) borne GAD gene for Parkinson's disease: an open label, phase I trial. Lancet 2007 Jun 23;369(9579):2097-2105.

4. Fischer D, Li Y, Ahlemeyer B, Krieglstein J, Kissel T. In vitro cytotoxicity testing of polycations: influence of polymer structure on cell viability and hemolysis. Biomaterials 2003 Mar;24(7):1121-1131.

5. Godbey WT, Wu KK, Mikos AG. Size matters: molecular weight affects the efficiency of poly(ethylenimine) as a gene delivery vehicle. J Biomed Mater Res 1999 Jun 5;45(3):268-275.

6. Godbey WT, Wu KK, Mikos AG. Poly(ethylenimine)-mediated gene delivery affects endothelial cell function and viability. Biomaterials 2001 Mar;22(5):471-480.

7. Fischer D, Bieber T, Li Y, Elsässer H, Kissel T. A novel non-viral vector for DNA delivery based on low molecular weight, branched polyethylenimine: effect of molecular weight on transfection efficiency and cytotoxicity. Pharm Res 1999 Aug;16(8):1273-1279.

8. Fischer D, Bieber T, Li Y, Elsasser HP, Kissel T. A novel non-viral vector for DNA delivery based on low molecular weight, branched polyethylenimine: effect of molecular weight on transfection efficiency and cytotoxicity. Pharm Res 1999 Aug;16(8):1273-1279.

9. Li J, Yang C, Li HZ, Wang X, Goh SH, Ding JL, et al. Cationic supramolecules composed of multiple oligoethylenimine-grafted beta-cyclodextrins threaded on a polymer chain for efficient gene delivery. Advanced Materials 2006 Nov;18(22):2969-+.

10. Yang CA, Li HZ, Wang X, Li J. Cationic supramolecules consisting of oligoethylenimine-grafted alpha-cyclodextrins threaded on poly(ethylene oxide) for gene delivery. Journal of Biomedical Materials Research Part A 2009 Apr;89A(1):13-23.

11. Yang C, Wang X, Li HZ, Goh SH, Li J. Synthesis and characterization of polyrotaxanes consisting of cationic alpha-cyclodextrins threaded on poly[(ethylene oxide)-ran-(propylene oxide)] as gene carriers. Biomacromolecules 2007 Nov;8(11):3365-3374.

12. Shuai XT, Merdan T, Unger F, Kissel T. Supramolecular gene delivery vectors showing enhanced transgene expression and good biocompatibility. Bioconjugate Chemistry 2005;16(2):322-329.

13. Grigsby CL, Leong KW. Balancing protection and release of DNA: tools to address a bottleneck of non-viral gene delivery. J R Soc Interface 2010 Feb 6;7 Suppl 1:S67-82.

14. Kim TI, Kim SW. Bioreducible polymers for gene delivery. React Funct Polym 2011 Mar 1;71(3):344-349.

15. Xia W, Wang PJ, Lin C, Li ZQ, Gao XL, Wang GL, et al. Bioreducible polyethylenimine-delivered siRNA targeting human telomerase reverse transcriptase inhibits HepG2 cell growth in vitro and in vivo. Journal of Controlled Release 2012 Feb;157(3):427-436.

16. Ruiz J, Ceroni M, Quinzani OV, Riera V, Piro OE. Reversible S-S bond breaking and bond formation in disulfide-containing dinuclear complexes of Mn. Angewandte Chemie-International Edition 2001;40(1):220-222.

17. Go YM, Jones DP. Redox compartmentalization in eukaryotic cells. Biochim Biophys Acta-Gen Subj 2008 Nov;1780(11):1271-1290.

18. Cheng R, Feng F, Meng F, Deng C, Feijen J, Zhong Z. Glutathione-responsive nano-vehicles as a promising platform for targeted intracellular drug and gene delivery. J Control Release 2011 May 30;152(1):2-12.

19. Ooya T, Choi HS, Yamashita A, Yui N, Sugaya Y, Kano A, et al. Biocleavable polyrotaxane - Plasmid DNA polyplex for enhanced gene delivery. Journal of the American Chemical Society 2006;128(12):3852-3853.

20. Yamashita A, Yui N, Ooya T, Kano A, Maruyama A, Akita H, et al. Synthesis of a biocleavable polyrotaxane-plasmid DNA (pDNA) polyplex and its use for the rapid nonviral delivery of pDNA to cell nuclei. Nature Protocols 2006;1(6):2861-2869.

21. Roux E, Passirani C, Scheffold S, Benoit JP, Leroux JC. Serum-stable and long-circulating, PEGylated, pH-sensitive liposomes. Journal of Controlled Release 2004 Feb;94(2-3):447-451.

22. Gref R, Minamitake Y, Peracchia MT, Trubetskoy V, Torchilin V, Langer R. Biodegradable long-circulating polymeric nanospheres. Science 1994 Mar;263(5153):1600-1603.

23. Wen Y, Pan S, Luo X, Zhang W, Shen Y, Feng M. PEG- and PDMAEG-graft-modified branched PEI as novel gene vector: synthesis, characterization and gene transfection. J Biomater Sci Polym Ed 2010;21(8-9):1103-1126.

24. Wen Y, Pan S, Luo X, Zhang X, Zhang W, Feng M. A biodegradable low molecular weight polyethylenimine derivative as low toxicity and efficient gene vector. Bioconjug Chem 2009 Feb;20(2):322-332.

25. Lin S, Du FS, Wang Y, Ji SP, Liang DH, Yu L, et al. An acid-labile block copolymer of PDMAEMA and PEG as potential carrier for intelligent gene delivery systems. Biomacromolecules 2008 Jan;9(1):109-115.

26. Yang C, Li H, Wang X, Li J. Cationic supramolecules consisting of oligoethylenimine-grafted alpha-cyclodextrins threaded on poly(ethylene oxide) for gene delivery. J Biomed Mater Res A 2009 Apr;89(1):13-23.

27. Yang C, Wang X, Li HZ, Tan E, Lim CT, Li J. Cationic Polyrotaxanes as Gene Carriers: Physicochemical Properties and Real-Time Observation of DNA Complexation, and Gene Transfection in Cancer Cells. Journal of Physical Chemistry B 2009 Jun;113(22):7903-7911.

28. Ping Y, Liu CD, Zhang ZX, Liu KL, Chen JH, Li J. Chitosan-graft-(PEI-beta-cyclodextrin) copolymers and their supramolecular PEGylation for DNA and siRNA delivery. Biomaterials 2011 Nov;32(32):8328-8341.

29.   Lo CL, Huang CK, Lin KM, Hsiue GH. Mixed micelles formed from graft and diblock copolymers for application in intracellular drug delivery. Biomaterials 2007 Feb;28(6):1225-1235.

30.   Ooya T, Choi HS, Yamashita A, Yui N, Sugaya Y, Kano A, et al. Biocleavable polyrotaxane-plasmid DNA polyplex for enhanced gene delivery. J Am Chem Soc 2006 Mar 29;128(12):3852-3853.

31.   Yamada Y, Nomura T, Harashima H, Yamashita A, Katoono R, Yui N. Intranuclear DNA Release Is a Determinant of Transfection Activity for a Non-viral Vector: Biocleavable Polyrotaxane as a Supramolecularly Dissociative Condenser for Efficient Intranuclear DNA Release. Biological & Pharmaceutical Bulletin 2010 Jul;33(7):1218-1222.

32.   Yamashita A, Kanda D, Katoono R, Yui N, Ooya T, Maruyama A, et al. Supramolecular control of polyplex dissociation and cell transfection: Efficacy of amino groups and threading cyclodextrins in biocleavable polyrotaxanes. Journal of Controlled Release 2008 Oct;131(2):137-144.

33.   Loh XJ, Colin Sng KB, Li J. Synthesis and water-swelling of thermo-responsive poly(ester urethane)s containing poly(epsilon-caprolactone), poly(ethylene glycol) and poly(propylene glycol). Biomaterials 2008 Aug;29(22):3185-3194.

34.   Chiera JM, Lindbo JA, Finer JJ. Quantification and extension of transient GFP expression by the co-introduction of a suppressor of silencing. Transgenic Res. 2008;17:1143-54.

35.   Tan PHS, Aung KZ, Toh SL, Goh JCH, Nathan SS. Three-dimensional porous silk tumor constructs in the approximation of in vivo osteosarcoma physiology. Biomaterials. 2011;32:6131-7.

36.   Kelei Chen PS, Thomas Kok Hiong Teh, Siew Lok Toh and James CH Goh. In vitro generation of a multilayered osteochondral construct with an osteochondral interface using rabbit bone marrow stromal cells and a silk peptide-based scaffold. J Tissue Eng Regen Med. 2013;doi: 10.1002/term.1708.

37.   Christensen LV, Chang CW, Yockman JW, Conners R, Jackson H, Zhong ZY, et al. Reducible poly(amido ethylenediamine) for hypoxia-inducible VEGF delivery. Journal of Controlled Release 2007 Apr;118(2):254-261.

38.   Harada A, Kamachi M. Complex-formation between poly(thylene glycol) and alpha-cyclodextrin. Macromolecules 1990 May;23(10):2821-2823.

39.   Yang C, Wang X, Li H, Goh SH, Li J. Synthesis and characterization of polyrotaxanes consisting of cationic alpha-cyclodextrins threaded on poly[(ethylene oxide)-ran-(propylene oxide)] as gene carriers. Biomacromolecules 2007 Nov;8(11):3365-3374.

40.   Mansouri S, Cuie Y, Winnik F, Shi Q, Lavigne P, Benderdour M, et al. Characterization of folate-chitosan-DNA nanoparticles for gene therapy. Biomaterials 2006 Mar;27(9):2060-2065.

41.   Oumzil K, Khiati S, Grinstaff MW, Barthelemy P. Reduction-triggered delivery using nucleoside-lipid based carriers possessing a cleavable PEG coating. J Control Release 2011 Apr 30;151(2):123-130.

42.   Nounou MI, Emmanouil K, Chung S, Pham T, Lu Z, Bikram M. Novel reducible linear L-lysine-modified copolymers as efficient nonviral vectors. J Control Release 2010 May 10;143(3):326-334.

43. Piest M, Lin C, Mateos-Timoneda MA, Lok MC, Hennink WE, Feijen J, et al. Novel poly(amido amine)s with bioreducible disulfide linkages in their diamino-units: structure effects and in vitro gene transfer properties. J Control Release 2008 Aug 25;130(1):38-45.

44. Zhang GY, Liu J, Yang QZ, Zhuo RX, Jiang XL. Disulfide-Containing Brushed Polyethylenimine Derivative Synthesized by Click Chemistry for Nonviral Gene Delivery. Bioconjugate Chemistry 2012 Jun;23(6):1290-1299.

45. Merdan T, Kopecek J, Kissel T. Prospects for cationic polymers in gene and oligonucleotide therapy against cancer. Adv Drug Deliv Rev 2002 Sep 13;54(5):715-758.

46. Zhu CH, Jung S, Meng FH, Zhu XL, Park TG, Zhong ZY. Reduction-responsive cationic biodegradable micelles based on PDMAEMA-SS-PCL-SS-PDMAEMA triblock copolymers for gene delivery. Journal of Controlled Release 2011 Nov;152:E188-E190.

47. Dai FY, Sun P, Liu YJ, Liu WG. Redox-cleavable star cationic PDMAEMA by arm-first approach of ATRP as a nonviral vector for gene delivery. Biomaterials 2010 Jan;31(3):559-569.

48. Xu PS, Quick GK, Yeo Y. Gene delivery through the use of a hyaluronate-associated intracellularly degradable crosslinked polyethyleneimine. Biomaterials 2009 Oct;30(29):5834-5843.

49. Breunig M, Lungwitz U, Liebl R, Goepferich A. Breaking up the correlation between efficacy and toxicity for nonviral gene delivery. Proc Natl Acad Sci U S A 2007 Sep 4;104(36):14454-14459.

50. Wang Y, Ke CY, Weijie Beh C, Liu SQ, Goh SH, Yang YY. The self-assembly of biodegradable cationic polymer micelles as vectors for gene transfection. Biomaterials 2007 Dec;28(35):5358-5368.

51. Lomas H, Massignani M, Abdullah KA, Canton I, Lo Presti C, MacNeil S, et al. Non-cytotoxic polymer vesicles for rapid and efficient intracellular delivery. Faraday Discuss 2008;139:143-159; discussion 213-128, 419-120.

52. Pathak A, Patnaik S, Gupta KC. Recent trends in non-viral vector-mediated gene delivery. Biotechnol J 2009 Nov;4(11):1559-1572.

53. Fernandez CA, Rice KG. Engineered nanoscaled polyplex gene delivery systems. Mol Pharm 2009 Sep-Oct;6(5):1277-1289.

CHAPTER 6   SHELL DETACHABLE AND BIOCLEAVABLE NANOSTRUCTURES BASED ON STAR POLYROTAXANE WITH PDMAEMA FOR REDOX-RESPONSIVE GENE DELIVERY

6.1 INTRODUCTION

pDMAEMA is a synthetic polymer with tertiary amino groups on the side chain. It is water soluble and owning to its positive charged surface, it could compact DNA into small particles by electrostatic interaction [1] and show higher transfection efficiency [2, 3]. Cytotoxicity, lack of cell specificity and serum-induced aggregation are the major obstacles for pDMAEMA-based polyplexes to apply in gene delivery [4]. Similar with PEI, the molecular weight of the polymer plays an important role to the cytotoxicity [5]. Generally, the cytotoxicity of polymer appears to increase with the increasing of molecular weight. Membrane disruption, apoptosis and cytotoxicity of PDMAEMA increased with their chain length [6]. Therefore, it was suggested that one of the most rational ways to decrease cytotoxicity and enhance gene transfection efficiency could be achieved by combining low molecular weight transfection segments with degradable linkages and forming a combined large molecular weight transfection polymer. In addition, because it was reported that higher zeta potential of

polyplexes could lead significant cytotoxicity [7], PEGlyation is a well verified method to decrease cytotoxicity due to its shielding effect on the surface charge of particles [8-10].

Recently, a group of reduction-responsive polymer and conjugates was synthesized based on PDMAEMA for gene delivery [11-13]. Generally, they contain disulfide-linkage, which is prone to rapid degradation in reductive intracellular environment and cell nucleus [14, 15]. So they showed distinct feature from the normally hydrolytically degradable counterparts: on the one hand they could lead to polyplex dissociation and efficient intracellular release of DNA or siRNA [16, 17], on the other hand, they may result in low toxicity by avoiding accumulation of high molecular weight polycations inside cells, and finally increasing the transfection efficiency [18, 19]. Serum stability is another barrier for gene delivery. In the case of *in vivo* gene delivery, the polyplex particles could prone rapid aggregation due to the negatively charged plasma proteins in the serum or blood, which affect the stability of the positively charged polyplexes. PEG shell layer, could stabilize the aggregation in the interior of micelles and at the same time provide a "stealth" layer on the surface which could resist protein adsorption and cellular adhesion [20, 21].

In spite of many studies on the pDMAEMA-based polycations as gene vectors reported so far [11-13], little is known about the star pDMAEMA based on reduction-sensitive polyrotaxanes, not to mention of their dual self-assembly behavior, which leads to the formation of core-shell nanostructure and their applications to redox-responsive gene delivery. In this chapter, we exploit a novel redox-responsive and shell detachable nanostructure with hydrophilic PEG shell and cyclodextrin core for effective and reductive gene delivery (Scheme 6.1). This nanostructure is derived

from star polyrotaxanes based on partially threaded α-CD, star PEG, and end blocking cationic polymer pDMAEMA with disulfide linkage, which was prepared via Cu(I)-mediated ATRP. Uniquely, low molecular weight pDMAEMA segments was linked to star PEG and formed a combined large MW transfection polymer with disulfide linkages, which would allow the system sensitive to reduction environment, resulting in sufficiently DNA protection extracellularly, rapid degradation and DNA release intracellular, decreased cytotoxicity and enhanced transfection efficiency. Furthermore, owning to the unique supramolecular structure of 8-arm PEG with partial threaded CDs, the naked PEG arms would form a sheddable hydrophilic shell, which could stabilize the polyplex, enhance their serum tolerant ability. More importantly, due to the presence of polyrotaxanes, the star pDMAEMA based polyrotaxane could further self-assembled into core-shell nanostructures in water, which would be very promising for drug/gene codelivery (Charpter 7).
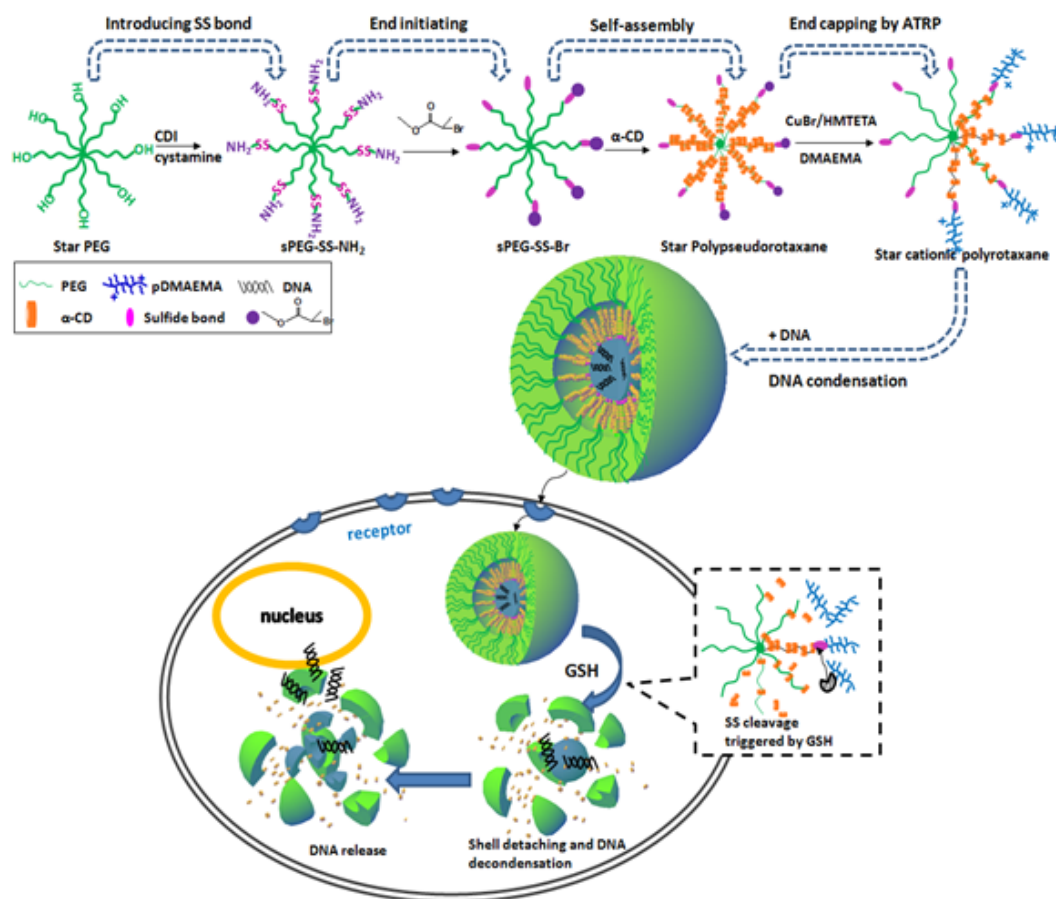
Scheme 6.1 Illustration of star polyrotaxanes based on PDMAEMA and intracellular DNA release

6.2 MATERIALS AND METHODS

6.2.1 Materials

Star PEG (Mn=9468) were purchased from Fluka. α-CD was purchased from TCI. DMAEMA monomer, 2-bromopropionyl bromide, Cu(I)Br, 1,1,4,7,10,10-Hexamethyltriethylenetetramine (HMTETA), ethylenediamine, cystamine dihychloride, TEA, CDI, DTT, were received from Sigma-Aldrich and used as received. Diethyl ether, methanol, tetrahydrofuran (THF), *n*-hexane and DMSO were purchased from Merck. Penicillin, streptomycin and MTT were obtained from Sigma.

6.2.2 Synthesis Methods
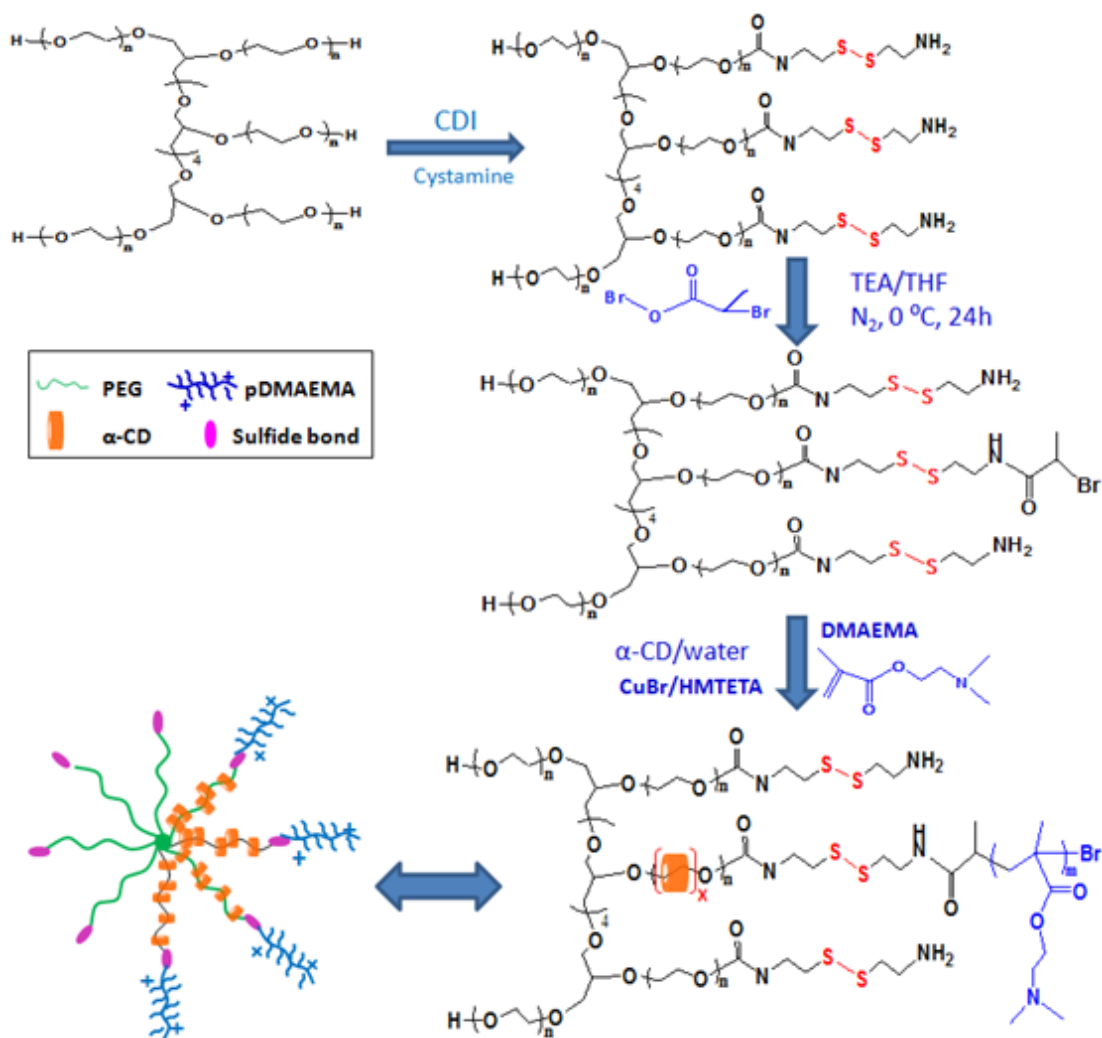
Scheme 6.2 Synthesis procedure for the star polyrotaxanes

6.2.2.1 Synthesis of PEG-SS-NH$_2$ and PEG-NH$_2$

The synthesis procedures of PEG-SS-NH$_2$ and PEG-NH$_2$ are the same with the methods we presented before. (4.2.2.1)

6.2.2.2 Synthesis of initiator (PEG-SS-Br and PEG-Br)

8 arm PEG was converted to the corresponding ATRP macroinitiator by the end capping reaction with 2-bromopropionyl bromide in THF [22, 23]. In brief, 8-

arm-PEG-SS-NH$_2$/PEG-NH$_2$ (1g, 0.1056 mmol) was dissolved in 20 mL anhydrous THF. Then TEA (118μL, 0.8114 mmol), DMAP (103mg, 0.8114 mmol) and 5 mL dry THF containing 2-bromopropionyl bromide (0.18g, 0.8114 mmol) were added dropwise during 1h under nitrogen. The reaction was continued for 2h at 0 °C and for another 24h at room temperature. After the reaction stopped, the mixture was filtered to remove the resultant triethylamine hydrobromide. The solution was precipitated in *n*-hexane and the crude product was dissolved in water and extracted using chloroform, following by precipitated in hexane again, centrifuged and dried under vacuum to give the purified product (Yield, 0.8g (80%)).

6.2.2.3 Synthesis of polyrotaxane copolymer via ATRP (PR-SS-PDMAEMA and PR-PDMAEMA)

A typical protocol for amphiphilic PR-based copolymer synthesis via the ATRP of PDMAEMA was as follows [22, 24]. In a sealable reactor, 8 arm PEG-SS-Br (0.25g, 0.0264 mmol) was added to 6.9 mL of α-CD (1g, 1mmol) saturated aqueous solution (0.145 g/mL), followed by vigorously stirring at room temperature for 24h to form PPR. Then DMAEMA (0.67g, 4.224 mmol) and HMTETA (37 mg, 0.158 mmol) were added to the resulting PPR suspension. After purged with dry nitrogen for 50 min to degas the reaction solution, CuBr (15 mg, 0.1056 mmol) was added, followed by three times of degassing using a nitrogen purge. The [PPR-SS-Br]:[DMAEMA]:[HMTETA]:[CuBr] relative molar ratios were 1:40:1.5:1 and 1:50:1.5:1, respectively. The reactor was sealed and the polymerization was carried out at 25 °C for 6h. The experiment was stopped by opening the flask and exposing the catalyst to air, and the crude product was directly freeze-dried. Then they were dissolved in 15 mL DMSO and dialyzed against water for 5 days (MWCO=6000) and freeze-dried.

The crude product was again dissolved in water and further purified by column chromatography on a Sephadex G-75 column with water as eluent. Finally, the purified product was lyophilized and characterized by ^{1}H NMR. Yeild, 0.48g (45%). The Synthesis of Polyrotaxane without disulfide-linkage (PR-PDMAEMA) was based on 8-arm PEG-Br with the similar procedure as above.

6.2.3 Measurements and Characterization

6.2.3.1 Proton Nuclear Magnetic Resonance (^{1}H-NMR)

The details were described in section 3.2.3.1 of Chapter 3.

6.2.3.2 Elemental analysis

The details were described in section 5.2.3.2 of Chapter 5.

6.2.3.3 Plasmid amplification

The details were described in section 5.2.3.3 of Chapter 5.

6.2.3.4 Cells and media

The details were described in section 5.2.3.4 of Chapter 5. Four cells were used: COS7, MB231, Hela and MCF-7 cells.

6.2.3.5 Gel retardation experiment

The methods of electrophoretic mobility of polymer/DNA complex were described in section 5.2.3.5 of Chapter 5.

6.2.3.6 Particle size and zeta-potential measurements

The details of particle size and zeta potential measurements are described in section 5.2.3.6 of Chapter 5.

6.2.3.7 Stability of polymer/DNA complexes

The methods of salt stability and protein stability (BSA) studies of polyplexes were described in section 5.2.3.7 of Chapter 5.

6.2.3.8 Biodegradation behavior of polymer/DNA complexes

Polymer/DNA complexes containing 3 µg of pDNA were prepared at N/P ratios of 50. After 30 min, polymer/DNA polyplexes were treated with same volume of 20 mM DTT solution or water. The mixture was incubated at 37 °C and determined at time interval, defined as t_i. The average diameter and zeta potential of particles in water before DTT treatment, t_o, was also measured by dynamic light scattering. The change ratio of particle size and zeta potential was calculated as t_i/t_o.

6.2.3.9 DNA release ability

The procedures of DNA release studies were described in section 5.2.3.9 of Chapter 5.

6.2.3.10 Cell viability assay

The methods of measuring cell cytotoxicity of cationic polymers on MB231, Hela, COS7 and MCF7 cells were described in section 5.2.3.10 of chapter 5.

The cytotoxicity of the polymer/DNA complexes at various N/P ratios were also measured against different cell lines with the DNA amount of 0.25 µg per well in 96-well plate. Polymer/DNA complexes were freshly prepared as previously

described. The MTT assay was performed according to the protocol as described in the previous section.

6.2.3.11 *In vitro* transfection and luciferase assay

4 cell lines (MB231, Hela, COS7 and MCF7) were seeded onto 24-well plate at a density of 5×10^4 per well in 500 μL DMEM medium with 10% FBS 24h prior to transfection. Then the culture medium was replaced with 300 μL fresh complete medium with 10% FBS. Polyplexes with different N/P ratios containing 1 μg pDNA were added to each well and were further incubated with cells for 4h. Then 200 μL medium containing 10% FBS was added and cells are incubated for further 20 hours. The measuring method of luciferase expression levels are as the same with the protocols described in section 5.2.3.11 of chapter 5.

6.2.3.12 *In vitro* GFP expression

The methods of observing in vitro GFP expression of polyplexes on COS7 cells were described in section 5.2.3.12 of chapter 5. ImageJ (NIH) was used for comparative analysis and quantifying the transfection efficiency. The cells with GFP Expression above threshold levels were automatically counted from the threshold green channel image series using the Analyze Particles function in ImageJ. The GFP expression was obtained by dividing the pixel area within the threshold set for the chromogen by the total pixel area of the region.

6.2.3.13 GSH inhibition

The methods of investigation of cell viability and transfection efficiency changed after treating with BSO were described in section 5.2.3.13 of chapter 5.

6.3 RESULTS AND DISCUSSION

6.3.1 Synthesis of cationic polyrotaxane via ATRP (PRSSP and PRP)

Scheme 6.1 (b) shows the synthesis procedures of partial cationic polyrotaxane based on ATRP of PDMAEMA, which includes 4 steps. (1) Firstly, 8-arm PEG-SS-NH$_2$/PEG-NH$_2$ was synthesized by the CDI reaction. Specifically, the hydroxyl groups at the end of 8-arm PEG were activated with CDI, followed by reaction with large excess of cystamine/ethylenediamine to give terminal amino groups. (2) Next, 2-bromopropionyl bromide was grafted on the end of PEG arm to form corresponding ATRP macroinitiator (PEG-SS-Br). By controlling the feeding ratio of 2-bromopropionyl bromide/PEG, partially terminated initiator could be achieved (eg. 4 arm grafted). (3) The PPR initiator (PPR-SS-Br) for ATRP was obtained by threading α-CDs onto PEG-SS-Br chain, and it was used to polymerize DMA. (4) Finally, star polyrotaxane PRSSP was prepared via ATPR of DMAEMA using PPR-SS-Br as macroinitiator and the flanking chains of pDMAEMA were introduced as the stoppers to prevent CD dethreading. During the end capping process, water was used as ATRP solvent to avoid the α-CD rings dethreading [22, 23]. Furthermore, according to references regarding polyrotaxane ATRP, the reaction was controlled to proceed at room temperature due to the fact that higher temperature would cause severe dethreading of α-CDs from the polymeric axle [24, 25].

6.3.2 Characterization of cationic polyrotaxanes
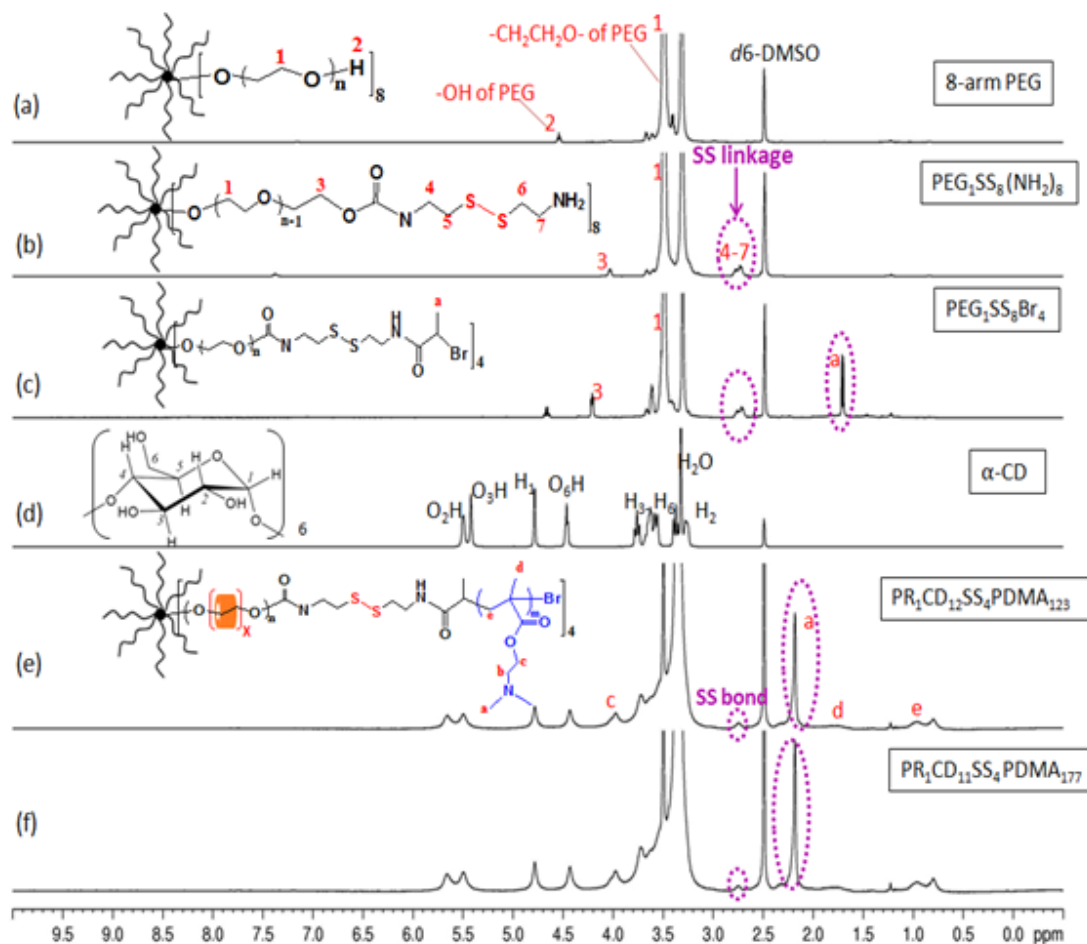
Fig. 6.1 [1]**H-NMR spectrum of (a) 8-arm PEG (Mw=9468, n=25), (b) PEG$_1$-(SS-NH$_2$)$_8$, (c) PEG$_1$-SS$_8$-Br$_4$, (d) α-CD, (e) PR$_1$-CD$_{12}$-SS$_4$-PDMA$_{123}$ and (f) PR$_1$-CD$_{11}$-SS$_4$-PDMA$_{177}$ in d$_6$-DMSO.** *(In PR$_x$CD$_y$SS$_z$PDMA$_n$, in where x are number of PEG, y are the number of threaded CD, z are number of SS linkage, and n are number of DMA repeat units, calculated by* [1]*H NMR)*

Fig 6.1(a)-(b) show the ^{1}H NMR result of 8-arm PEG-SS-NH$_2$ in comparison with pure 8-arm PEG. In the spectrum, the peaks for the original PEG and cystamine are shown. The peak of δ=2.7~2.8 was attributed to the SS-linkage. Due to the end grafting of cystamine, the chemical shift of H$_3$ in PEG was change from 3.5 ppm (in pure PEG) to 4.05 ppm (in the product, Fig. 6.1b). The results confirm the successful conjugation of 8-arm PEG with cystamine. Quantitative comparisons between the integral intensities of peaks H$_3$ and peak H$_2$ were used to derive the grafted ratio of

the polymer. It was found that the grafted degree for PEG-SS-NH$_2$ is 96%, suggesting

that all 8 arms of PEG are grafted with cystamine.

Fig. 6.1(c) shows the ^{1}H NMR of macroinitiator PEG-SS-Br. The signal at

1.78 ppm was attributed to the methyl group of bromopropionyl-terminated PEG. By

comparing the integration of the signals for the methyl protons Ha (-CH(CH$_3$)Br, 1.78

ppm) of the initiation group to those for the H$_1$ of 8 arm PEG in the region of 3.5 ppm,

the degree of substitution was estimated. The value was calculated to be 4 for the

purified macroinitiator PEG-SS-Br.

Fig 6.1 (a), (d), (e) and (f) show the ^{1}H NMR of polyrotaxane in comparison

with pristine α-CD and 8-arm PEG-SS-NH$_2$. In Fig. 6.1(e) and (f), the signals for α-

CD, the threading 8-arm PEG (δ=3.5) and the end capping polymer PDMAEMA ((-

N(CH$_3$)$_2$, δ=2.21 ppm) were all observed. Furthermore, it was found that the peaks of

α-CDs in Fig. 6.1(d) were clearly sharp, but those of polyrotaxanes were broadened

(Fig. 6.1e and f). These results suggest that the mobility of α-CDs in polyrotaxane is

restricted by the PEG chain after forming the supramolecular structure. These results

provide us clear evidence for the physically interlocked supramolecular structure of 8

arm PEG covered by α-CDs ended with PDMAEMA [26, 27]. In Fig. 6.1(f), a higher

intensities on Ha (δ=2.21 ppm) of PDMAEMA was observed in contrast to Fig. 6.1(e),

indicating a higher polymerization degree is obtained with increasing the feedings of

DMA. The CD threaded number could be derived by quantitative comparison

between the value for the area of the resonance peak due to H$_1$ of α-CD (δ=4.79) and

the peak due to the PEG (δ=3.50). Moreover, by comparing the integration of the

signals for the pDMAEMA (-N(CH$_3$)$_2$, around 2.21 ppm) to those for the peak of PEG,

the degree of polymerization was calculated. By calculation, it was found that about

12 CD rings, on average, were threaded on each 8-arm PEG and about 123 (Fig. 6.1e) or 177 (Fig. 6.1f) DMA repeat units were formed on the end of PEG (4 arm initiated) (Table 6.1). The structure of polyrotaxane without disulfide linkage was also confirmed in Fig. 6.2. The resulted cationic polymers exhibited similar peaks with the degradable analogue in Fig. 6.1 expecting the peak around 2.7~2.8, which is attributed to the disulfide bond. Therefore, it could be concludes that the synthesized polymer in Fig. 6.2 is the analogue of PRSSP (Fig. 6.1) lacking disulfide linkage.
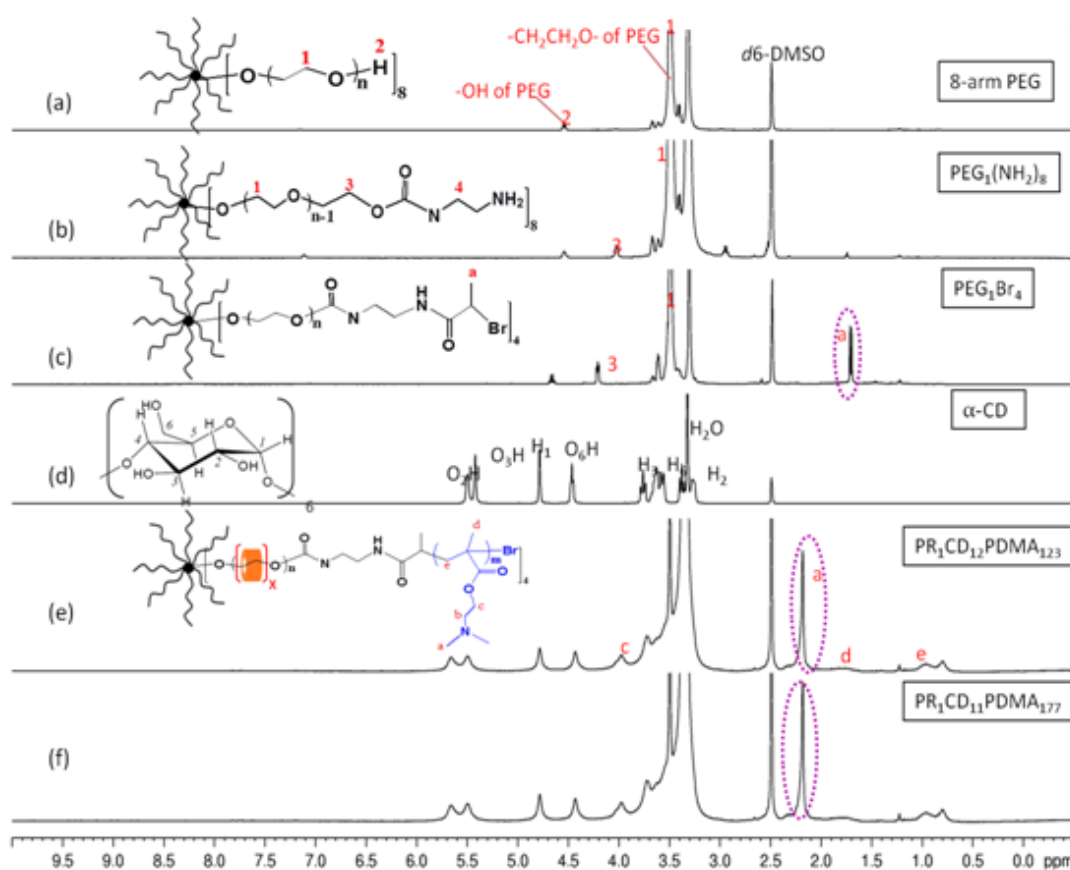
Fig. 6.2 ^{1}H-NMR spectrum of (a) 8-arm PEG, (b) PEG$_1$-(NH$_2$)$_8$, (c) PEG$_1$-Br$_4$, (d) α-CD, (e) PR$_1$-CD$_{12}$-PDMA$_{123}$ and (f) PR$_1$-CD$_{11}$-PDMA$_{177}$ in d_6-DMSO.

Table 6.1 shows the compositions of PR-based cationic polymer synthesized via ATRP of PDMAEMA. According to references about PEG based polyrotaxane [28], α-CD will form an inclusion complex with ratio EO/CD of 2. However, in our case, though the feed molar ratio of CD/PEG is 40, only 12 CDs were obtained. It is

probably because only 4 arm of PEG was initiated, and the steric hindrance of 8-arm

PEG limited the CD threaded number. In addition, with the increasing of molar ratio

of DMA in feed, more DMA repeats units are found in the product.

Table 6.1 The cationic polyrotaxane compositions with PDMAEMA

sample	Feeding molar ratio[a] [PEG]:[CD]:[DMA]	Found molar ratio[b] [PEG]:[CD]:[DMA]	Initiated PEG arms[b] (CD threaded arms)	DMAEMA repeat unit per arm
PRSSP123	1:40:160	1:12:123	4 arms	31
PRSSP177	1:40:200	1:11:176	4 arms	44
PRP123	1:40:130	1:12:123	4 arms	31
PRP177	1:40:180	1:11:177	4 arms	45

[a]Molar ratio in feed= [8 arm PEG-Br$_4$]:[α-CD]:[DMAEMA]
[b]Data was all calculated on the basis of ^{1}H NMR in DMSO-D$_6$

The elemental analysis of the synthesized cationic polyrotaxane was presented

in Table 6.2. By calculation, the compositions of the cationic polyrotaxane, which

determined based on ^{1}H NMR results (Table 6.1), are also in good agreement with the

elemental analysis results. Therefore, from the results of ^{1}H NMR and elemental

analysis, it could be conclude that the cationic 8-arm polyrotaxane threaded with OEI

grafted α-CD and end blocked with disulfide-linkage were successful synthesized.

Table 6.2 Elemental analysis of the cationic polyrotaxanes with PDMAEMA

sample	composition[a]	Anal.calcd[b]				Found[c]			
		N%	C%	H%	S%	N%	C%	H%	S%
PRSSP123	PEG$_1$CD$_{12}$SS$_4$Br$_4$PD$_{123}$	4.25	49.07	8.35	1.26	4.27	49.00	8.39	1.38
PRSSP177	PEG$_1$CD$_{11}$SS$_4$Br$_4$PD$_{177}$	5.22	57.87	8.02	1.12	5.17	57.95	7.98	1.08
PRP123	PEG$_1$CD$_{12}$Br$_4$PD$_{123}$	4.27	49.40	8.45	—	4.29	49.45	8.47	—
PRP177	PEG$_1$CD$_{11}$Br$_4$PD$_{177}$	5.17	59.85	7.71	—	5.20	59.9	7.73	—

[a] The compounds are denoted PEG$_x$CD$_y$(SS$_z$)Br$_m$PD$_n$, in where x are number of PEG, y are the number of threaded CD, z are number of SS linkage, m are the number of Br and n are number of DMA repeat units, calculated by ^{1}H NMR (Table 6.1).
[b] Theoretical elemental analysis calculated for the corresponding compound.
[c] Elemental analysis found.

6.3.3 Gel retardation experiment
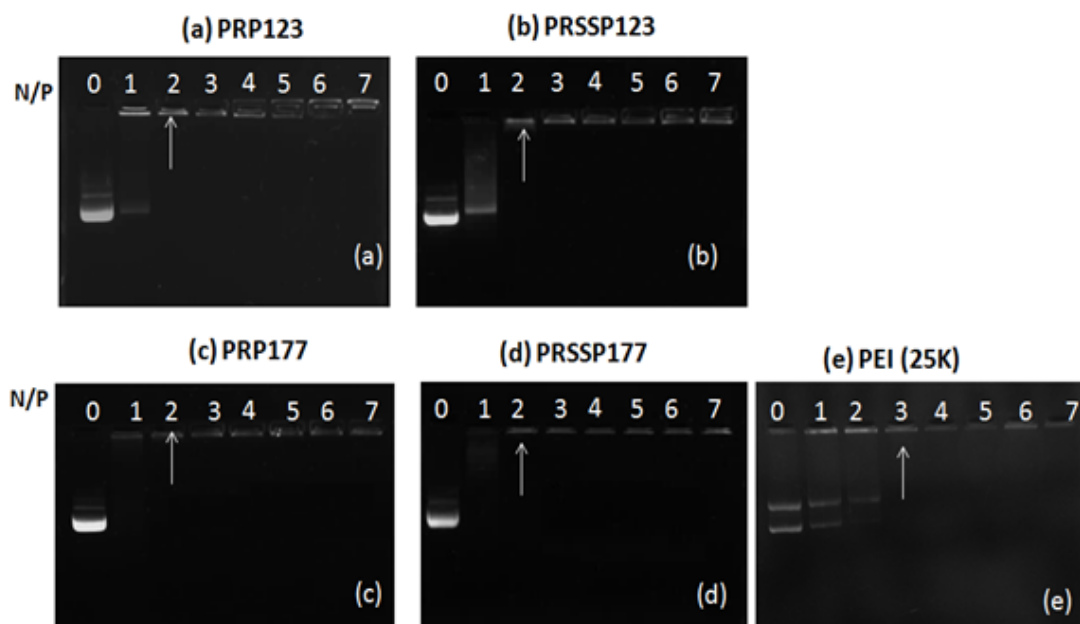
Fig. 6.3 Electrophoretic mobility of plasmid DNA in the polyplexes formed by (a) PRP123, (b) PRSSP123, (c) PRP177, (d) PRSSP177 and (e)25KPEI at different N/P ratio

In this chapter, gel retardation assay was performed to investigate the DNA binding ability of the PDMAEMA based cationic polyrotaxanes. Before gel electrophoresis, positively charged polyrotaxane was mixed with negatively charged pDNA to form complexes at various N/P ratios via electrostatic interaction. As shown in Fig. 6.3, all cationic polyrotaxane exhibited good DNA binding at N/P ratio of 2, where total DNA retardation was detected. Particularly, PEI25k (Fig. 6.3e) could inhibit the migration of the pDNA at N/P ratio of 3 and above, while the four test polyrotaxane can retard DNA efficiently at N/P ratio of 2. The results exhibit better DNA condensation capability of the PDMAEMA based polyrotaxane than PEI25k. Furthermore, no obvious difference in DNA retardation was observed between the polyrotaxane PRP (Fig. 6.3a and 6.3c) and PRSSP (Fig. 6.3b and 6.3b), indicating the introduction of disulfide bond will not affect the DNA binding ability of the polyrotaxane.

6.3.4 Particle size and Zeta potential
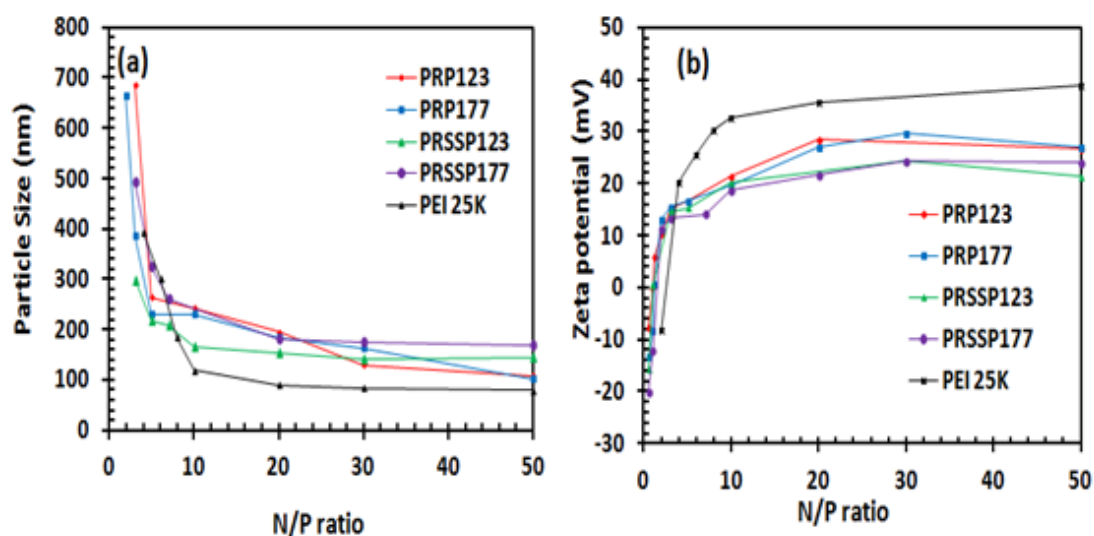
Fig. 6.4 Particle size (a) and zeta potential (b) of polyplexes formed by PRP, PRSSP and pDNA at various N/P ratios, in comparison with PEI (25K)

It is generally believed that the particle size and surface charge of polyplexes are crucial to endocytosis and gene transfer [8]. Formation of nanoparticles could facilitate polyplex diffusion, extravasation through vascular fenestration, and cellular uptake. Fig. 6.4 shows the particle size and zeta potential measurements of PRSSP/DNA and PRP/DNA complexes in comparison with PEI (25 kDa) at various N/P ratios. Generally, in Fig. 6.4(a), all polyrotaxanes could efficiently condense pDNA into small nanoparticles and the particle size of polyplex decreased with an increase of N/P ratio. Their diameters changed dramatically from 400~700 nm to 200 nm as N/P ratio increase from 1 to 10, which is similar with the PEI25k/DNA complexes. With further increasing the N/P ratios, their particle size changed slightly and remained in the 100–200 nm range. Furthermore, PRSSP and PRP yielded significant larger particles at all N/P ratios as compared to 25kPEI, probably due to a looser PEG shell formed by naked PEG arms in the polyrotaxane.

As shown in Fig.6.4 (b), the surface net charge of the complexes of pDNA with cationic polyrotaxanes increased sharply from negative to positive as the N/P ratio increased from 1 to 3, and reached a plateau at an N/P ratio of 10 and above. The phenomenon is in accordance with the results obtained from gel retardation assay, and particle size as discussed earlier. When N/P ratio is higher than 10, the zeta potential of the complexes stabilized at 20mV, which could result in a similar affinity to the cell surface. It must be pointed out here that all the four polyrotaxanes with PEG shell showed significant lower surface charge of complexes than that of PEI. It may be because that the PEG shell led to lower surface charge and exhibited shielding effect of polyplex, indicating that the naked PEG arms in the polyrotaxane should be preferentially located at the outer layer of complex as the larger particle size and lower zeta potential of PRP/DNA or PRSSP/DNA compared with that of PEI. These results are also supported by the findings of others [29, 30]. Therefore, the core-shell nanostructures self-assembled from our cationic polyrotaxanes could be confirmed.

6.3.5 Biodegradation behavior of polymer/DNA complexes

In last two decades, disulfide bond has been highly investigated as a crucial linkage for gene delivery vectors due to the rapid disulfide bond cleavage upon the interaction with reducing molecules such as, glutathione (GSH), cystein and so forth in living cells [31]. This rapid cleavage of disulfide linkage will ensure DNA release from complexes efficiently leading to facilitating nuclear import, gene transcription and gene expression [32], and also lowering the cytotoxicity of the system.
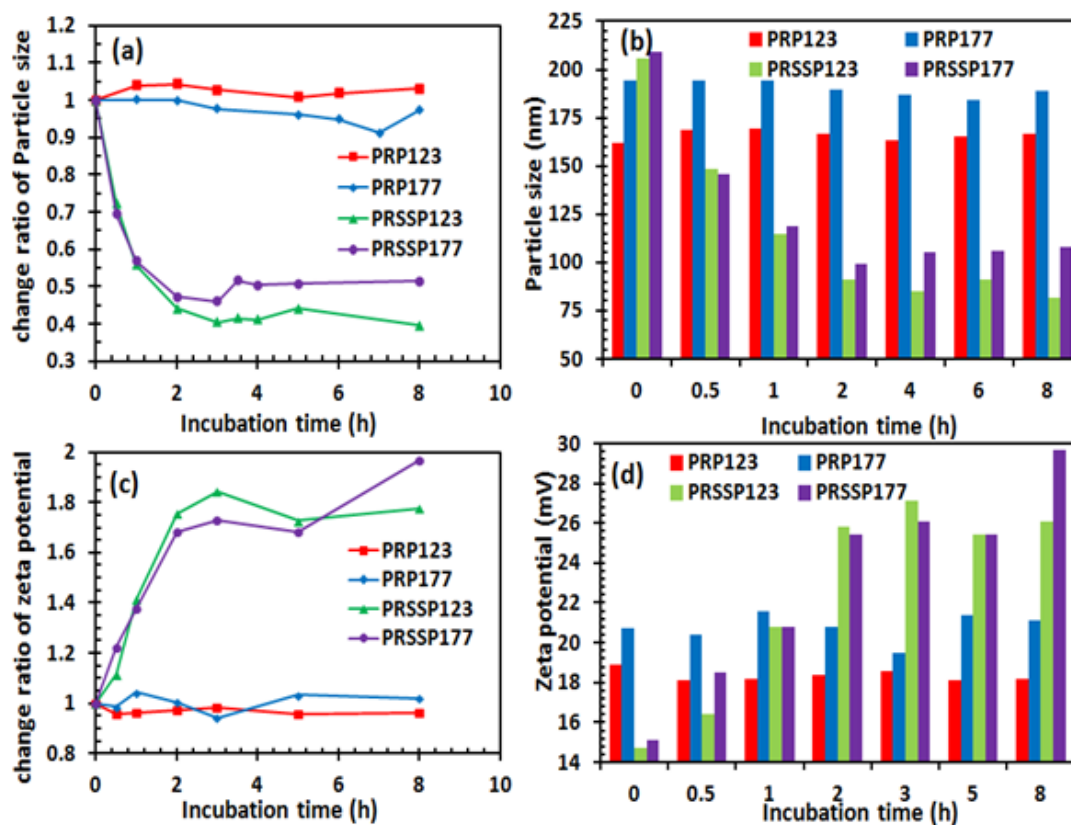
Fig. 6.5 Particle size and zeta potential at various determined time in 10 mM of DTT solution at 37 ^{0}C. (a) Change ratio of particle size; (b) particle size of polymer/DNA complexes ; (c) change ratio of zeta potential and (d) zeta potential of polyplex. (N/P=50)

In order to confirm the degradation and shell detachment property of our disulfide-containing systems, the bioreductive cleavage of the disulfide bond in the nanostructures was mimicked by treating with reducing agent DTT (10mM), which is analogous to the intracellular environment such as cytosol. And the particle size and zeta potential change of the polyplex with different N/P ratios in response to DTT was determined by DLS (Fig. 6.5). The responsive reductive polyplexes PRSSP123 and PRSSP177 were stable in physiological solution during 24 h incubation in PBS (part 6.3.11). However, as shown in Fig. 6.5, when these complexes were treated with reductive agent, 10 mM DTT for 8h, the size of polyplex formed by PRSSP123 and PRSSP177 markedly decreased from 205.6 nm to 81.44 nm (change ratio=0.39) and 209.2 nm to 107.8 nm (change ratio=0.51), respectively (Fig. 6.5a-b). Zeta potentials

also significantly increased from 14.7 mV to 26.1 mV (change ratio=1.78) and 15.1 mV to 29.7 mV (change ratio=1.96), respectively (Fig. 6.5c-d). In contrast, non-reductive polyplex PRP123 and PRP177 were sufficiently stable in the presence of DTT and no change in particle size or zeta potential was observed. The decreased particle sizes of disulfide linkage contained complexes were probably due to cleavage of disulfide bond and detachment of PEG shell segment. And it also led to the increased zeta potentials because the shielding effect of the PEG layer disappeared due to the cleavage of disulfide linkage. This phenomenon is in good agreement with other disulfide bond based bioreductive gene systems [12, 30]. Therefore, the above result confirms the degradation and shell detachment behavior of our core-shell nanostructure based on polyrotaxanes by the cleavage of disulfide linkages upon a reductive intracellular environment.

6.3.6 DNA release ability
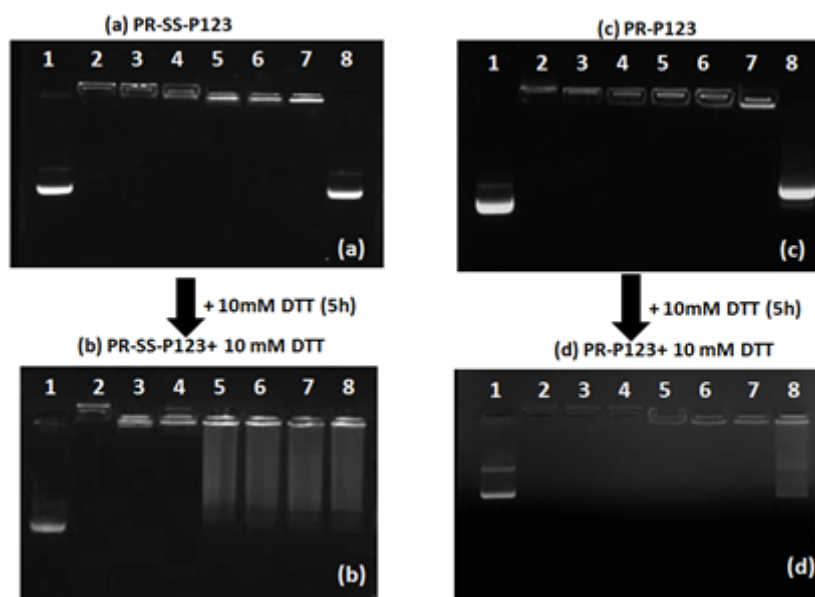
Fig. 6.6 Agarose gel electrophoretic images of the polyplexes (N/P=50) of PRSSP123 (a,b) and PRP123 (c,d) with (b,d) or without (a,c) 10 mM DTT. *(Line 1 shows the bands of control pDNA. Concentrations of heparin at lines 2, 3, 4, 5, 6, 7, and 8 were 0, 200, 300, 400, 500, 600 and 800 μg/mL, respectively.)*

To further examine the DNA release ability in the reductive condition, condensed polyplexes were subjected to gel retardation and a heparin competitive displacement assay was performed in the absence or presence of 10 mM DTT. Fig. 6.6(a) and 6.6(b) show the gel electrophoretic images of PRSSP123 before or after incubating with DTT for 5h. In the absence of DTT, the critical concentration of heparin, at the point of pDNA release, for PRSSP123 is 800 µg/mL (Fig. 6.6a), confirming that DNA were compacted tightly by the tested cationic polymer. Remarkably, after incubating with DTT for 5h, free DNA bands were observed at much lower concentration of heparin (400 µg/mL) (Fig. 6.6b). The results suggest that in PRSSP123 systems, effective pDNA release was observed in the reductive condition, indicating the DNA binding ability of polyrotaxane decreased and large part of DNA was released after incubating with DTT. In contrast, no obvious pDNA release was observed on the reduction insensitive control under the same condition (Fig. 6.6c-6.6d). These results confirmed that the pDNA release from PRSSP123 polyplexes was induced by the SS cleavage, followed by a dissociation and shell detachment of the polyrotaxanes nanoaggregates [33]. These findings were thus in accordance with the particle sizes results we discussed earlier. Furthermore, polyplexes formed by PRSSP177 also exhibited the same results. In summary, it is predicted that PRSSP/DNA system was stable extracellularly and could rapid release DNA from the system intracellularly by rapid disulfide bond cleavage.

6.3.7 Cytotoxicity of the cationic polyrotaxanes

It was reported that linear PDMAEMA only with high molecular weight exhibited high transgene expression but it could also lead to significant cytotoxicity. In contrast, low molecular weight PDMAEMA was less toxic but exhibit poor

transfection efficiency [3, 6, 34]. Based on the findings, we modified our PDMAEMA based polyrotaxane with the purpose of lowering cytotoxicity using the following strategies: (1) Conjugation of low molecular weight PDMAEMA chain to the end of star PEG, which was threaded on CDs, to form a large molecular weight star polymer; (2) Introduction of disulfide linkage to polyrotaxane chain to ensure the PDMAEMA was intracellularly degraded into small segments, resulting in DNA release and lower toxicity; (3) Introduction of PEG hydrophilic shell which could decrease cytotoxicity due to its shielding effect on the surface charge of particles [8-10].
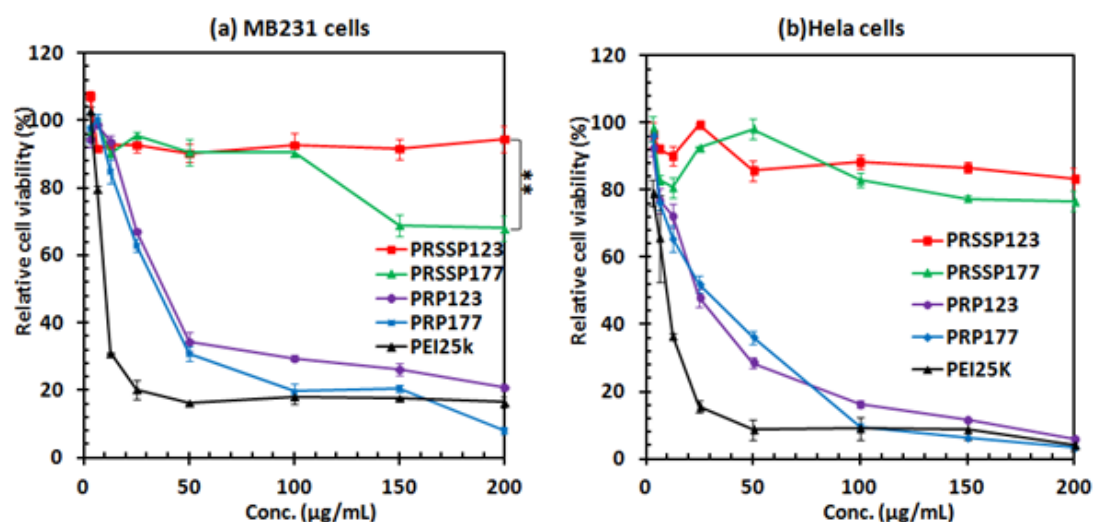
Fig. 6.7 Cell viability assay in (a) MB231 and (b) Hela cells with various concentrations of tested polymers in serum -containing medium for 24h, compared with bPEI (25k). Mean value ± SD (n=5). **$p<0.01$

The *in vitro* cell cytotoxicity of the bioreductive polyrotaxane was evaluated by MTT assays in MB231 and Hela cell lines, using commercial available PEI25k and non-reducible polyrotaxane as control (Fig. 6.7). As shown in Fig. 6.7, all investigated polymers exhibited a dose-dependent toxicity effect on both cell lines. It is worth noting that the polyrotaxane with disulfide linkage PRSSP exhibited markedly less toxicity in both cultured MB231 and Hela cells than non-degradable control PRSSP and PEI. Generally, cell viability of reductive polymer PRSSP (PRSSP123 and

PRSSP177) are above 70% when the concentration increased to 200 μg/mL, while viability of PRP, which is the analogue of PRSSP lacking a reductively cleavable disulfide bond, markedly decreased to lower than 20% at the same polymer concentration. The dramatically decreased cytotoxicity is believed to be a direct consequence of the intracellular cleavage of disulfide bond of PRSSP systems leading to polyrotaxane degradation with smaller PDMAEMA fragments (MW<7k Da), which results in reduced binding affinity of polymers with cellular membranes and reduced interference with cellular signal transduction pathway. It is evident that introduction of disulfide linkage is benefit for enhancing polymer biocompatibility.

Moreover, in MB231, it was found that the cytotoxicity of PRSSP177 is higher than that of PRSSP123 in high concentration. Since the molecular weight is always considered as an important factor for PDMAEMA leading to high cytotoxicity, the higher cytotoxicity of PRSSP177 could be attributed to the higher density of amino groups in polyrotaxane with higher molecular weight PDMAEMA in contrast to PRSSP123. Such findings are in accordance with the previous reports, demonstrating that the incorporation of bioreductive disulfide bond could lower cytotoxicity of PDMAEMA [11, 12, 19].
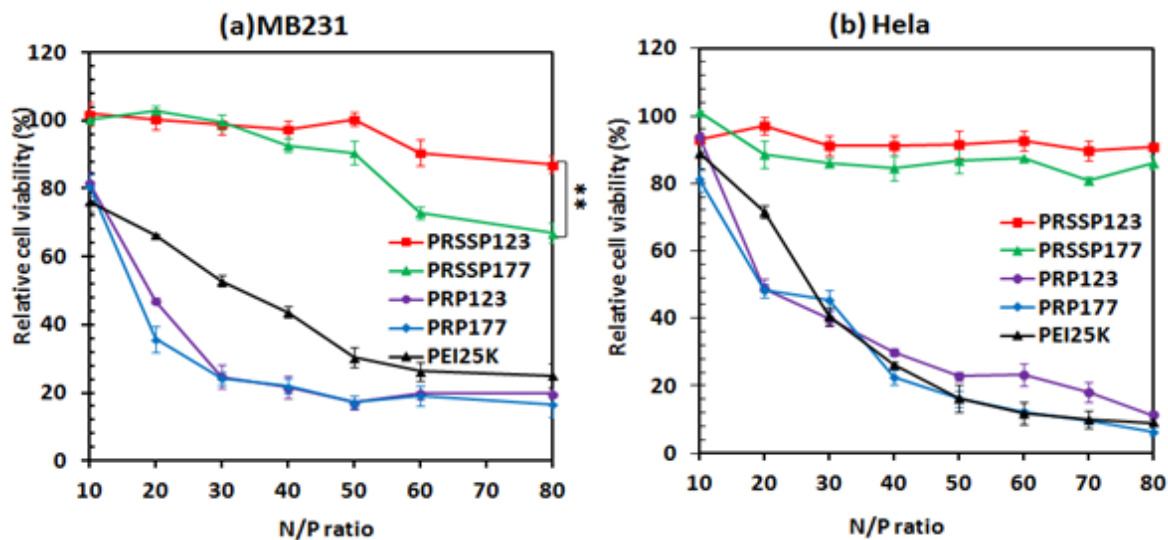
Fig. 6.8 Cell viability assay in (a) MB231 and (b) Hela cells with various N/P ratios of tested polymer/DNA complexes. Cell viability was expressed as a percentage of the control cell culture. Mean value ± SD (n=5), **p<0.01

In order to determine the non-lethal N/P ratios of the various polyplexes and further investigate the effect of disulfide bond on the cytotoxicity of polyplexes after interacting with DNA, cytotoxicity of polymer/DNA complexes were evaluated by MTT assay. Fig. 6.8 showed the cytotoxicity of polyplex formed by PRP and PRSSP at various N/P ratios, by comparing with PEI25k. It was found that at N/P ratio of 10, cell viabilities of all tested polyplexes were above 80% with no appreciable cytotoxicity and the effect of disulfide bond is the least. However, with the increase of N/P ratios, N/P-dependent toxicity effect was observed and the influence of disulfide-linkage largely increased. Notably, as the N/P ratio increased from 10 to 80, the cell viability of polyplex formed by PEI25k and non-biodegradable control PRP sharply decreased from 80% to less than 20%. In contrast, cell viability stays near 85% up to N/P ratio of 80 for PRSSP123/DNA and PRSS177/DNA complex (expect PRSSP177 in MB231, which is near 70%). Considering that the only different component in the formation between PRSSP/DNA and PRP/DNA polyplexes is the disulfide bond, it is evident that the remarkable decreased cytotoxicity of PRSSP systems is mainly due to

the reductive of disulfide linkage, leading to polyrotaxane degradation with smaller and less-toxic PDMAEMA segments. Furthermore, due to the higher amino density of PRSSP177, it showed a higher cytotoxicity in contrast to PRSSP123 (Fig. 6.8a). The above results are in line with the cell viability curve of the pure polymer (Fig. 6.7). From the above cytotoxicity result, we could safely come to the conclusion that our modification strategies including conjugation of low MW PDMAEMA chain to PEG arms and introduction of disulfide linkage into the polyrotaxane systems are succeed in improving cell viability of PDMAEMA, and resulting a dramatically decreased in cytotoxicity over important commercially available reagents PEI25k.

6.3.8 In vitro transfection and luciferase assay
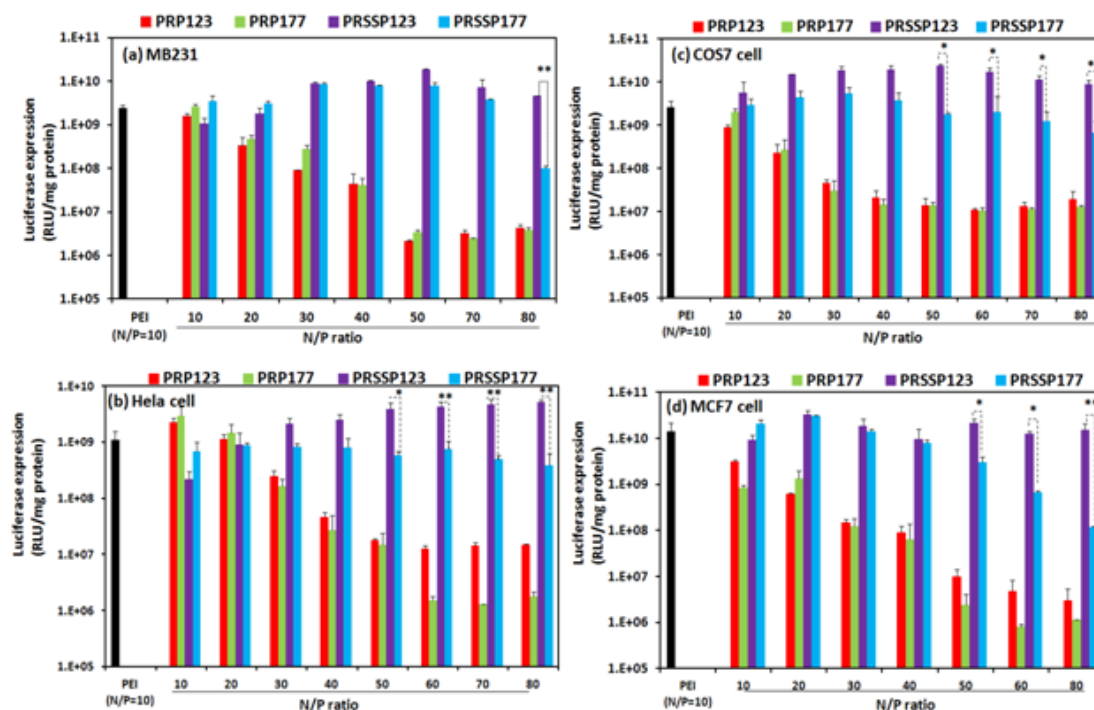
Fig. 6.9 Gene transfection efficiency of the polyplexes formed by PRSSP, PRP and 25K PEI in (a) MB231, (b) Hela, (c)COS7 and (d) MCF7 cells in the presence of serum. Data represent mean±SD (n=3, *p<0.05, **p<0.01).

In vitro gene transfection efficiency of the biocleavable cationic polyrotaxane was assessed using luciferase as a marker gene in 4 cell lines (MB231, Hela, COS7

and MCF7) in the presence of serum. Fig. 6.9 shows the luciferase protein expression of the bioreductive polyrotaxane PRSSP123 and PRSSP177 compared with non-reductive analogue PRP123, PRP177 and gold standard PEI25k at various N/P ratios. As presented in Fig. 6.9, it could be seen that the luciferase expression mediated by cationic polyrotaxanes was greatly dependent on the N/P ratios. Remarkably, all polyrotaxanes showed excellent *in vitro* gene transfection efficiency, comparable to or even higher than that of branched PEI (25 K) at their optimal N/P ratios. In particular, the transfection efficiency mediated by PRSSP123 (N/P=50) was 9 times higher than that of PEI (25K) (N/P=10) in COS7 cells (Fig. 6.9c).

Most importantly, it is worth of note that the reductive polyrotaxane PRSSP exhibited dramatically higher luciferase expression than the non-biodegradable polyrotaxane control (PRP). Generally, in four cell lines, non-cleavable PRP123 and PRP177 led to the highest luciferase protein expression at N/P ratio of 10. However, their gene transfection levels sharply decreased with the increase of N/P ratios, probably due to the significant cytotoxicity of the polyplexes (Fig. 6.8). Surprisingly, the luciferase expression of bioreducible polyrotaxane PRSSP123 and PRSSP177 could maintain their highest transfection levels from N/P ratio of 10 to 70. In comparison, at N/P ratio of 50, the transfection ability mediated by PRSSP123 was observed about 1000 times higher than that of the non-reductive analogue PRP123 in all cell lines. It is hypothesized that cytotoxicity was related to gene transfection ability and might be caused by electrostatic interactions with negatively charged glycocalyx of the cell surface [35]. Since the bioreducible cationic polyrotaxane showed a remarkable decrease in cytotoxicity over the non-degradable control (Fig. 6.8), the higher luciferase expression of degradable polyrotaxane may have benefited

from their lower toxicity inside cells, which might enable to enhance the transfection efficiency. Likewise, due to the higher cytotoxicity of PRSSP177 in contrast to PRSSP123, a lower gene expression levels were observed in PRSSP177/DNA complex, especially at high N/P ratios

From the above results, we could conclude that the transfection efficiency of PDMAEMA was largely enhanced by the introduction of disulfide linkage. Evidently, the therapy windows of degradable PRSSP systems are noticeably wider comparing to the non-degradable analogue PRP, which is highly desirable for *in vivo* gene therapy.

6.3.9 In vitro Green fluorescence protein expression
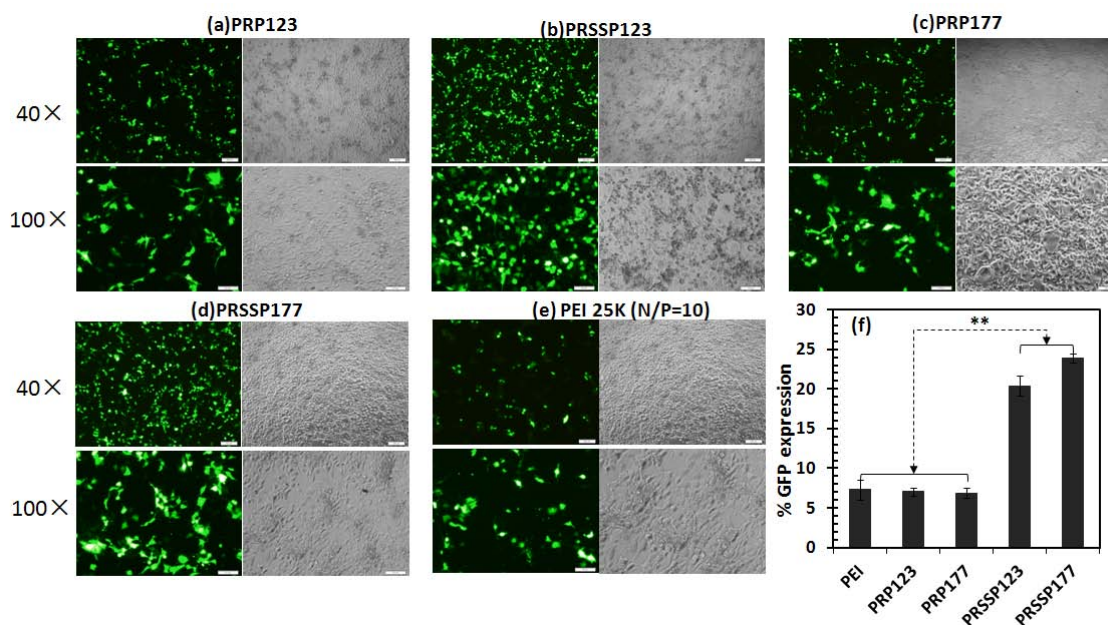
Fig. 6.10 The fluorescence microscopy images of transfected COS 7 cells mediated by pEGFP-N1 complexes form by (a) PRP123, (b) PRSSP123, (c) PRP177 and (d) PRSSP177 at their optimal N/P ratios, comparing with PEI 25K at N/P=10. (40× and 100 ×) (f) Quantitative comparison of the percentage of cells expressing GFP (40×). Student's unpaired t-test (**p<0.001).. (left: fluorescence light; right: bright light).

We employ another reporter gene pEGFP-N1 plasmid DNA encoding green fluorescence protein (GFP) to further visualize transgenetic efficacies of the PRSSP carriers with its non-reductive analogue PRP as control. As shown in Fig. 6.10, strong

fluorescence signal could be observed in delivering EGFP-pDNA when transfections were mediated by the polyrotaxanes, exhibiting high levels of vector internalization and gene expression. Both PRSSP123 and PRSSP177 showed higher fluorescence than PEI, indicating higher gene GFP expression (Fig. 6.10b and 6.10d). It is in line with the results of luciferase assay. Furthermore, by comparing PRSSP and PRP at their optimal N/P ratios, a much stronger GFP fluorescence emission was observed for the bio-reductive vector. As a result of Fig. 6.10 (f), GFP transfection assay showed higher gene transfection efficiencies for PRSSP123 and PRSSP177 systems, and this trend agrees well with that measured by luciferase assay (Fig. 6.9).

6.3.10 GSH inhibition
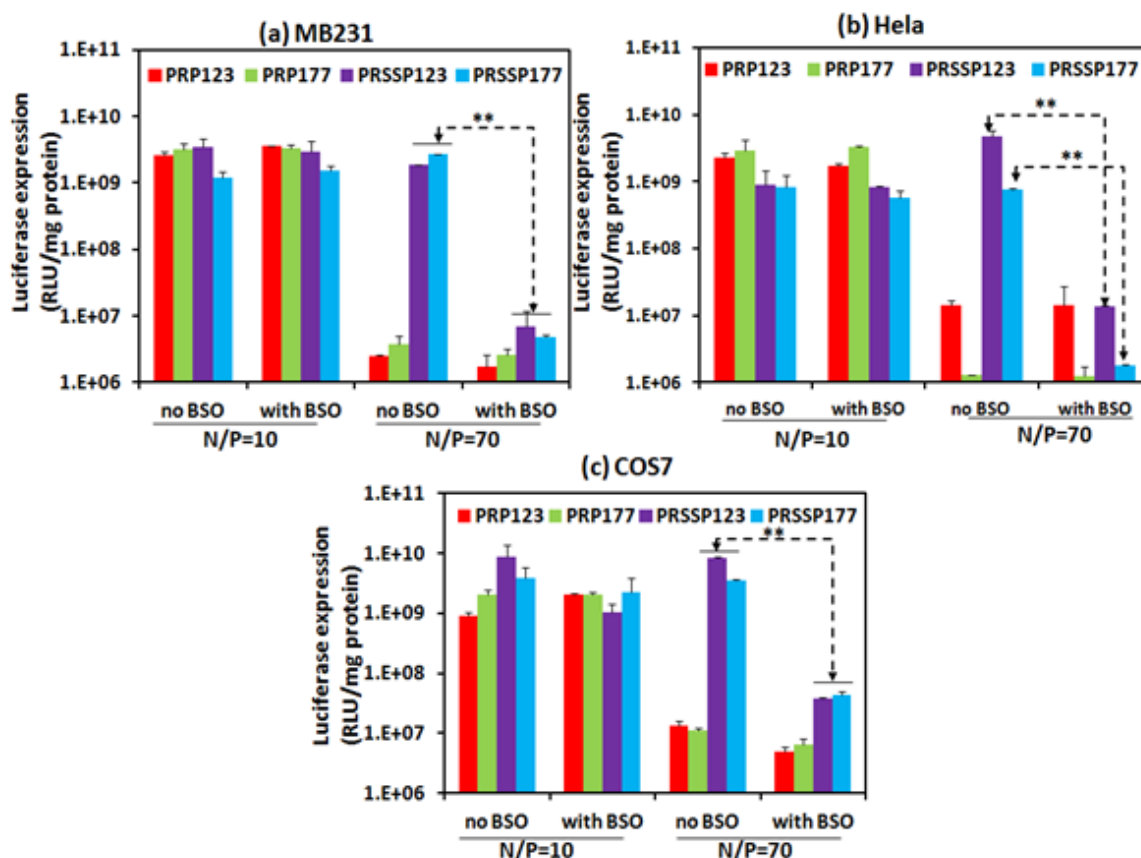
Fig. 6.11 Effects of BSO (300μM) on luciferase expression levels in (a)MB231, (b)Hela and (c)COS7 cells at N/P ratio of 10 and 70. Polyplex formed by PRP and PRSSP were transfected in the presence of serum with/without BSO (300μM). Data represent mean ±SD (n=3). **p<0.01

In previous research, we confirmed the degradation behavior and DNA release ability of bioreductive cationic polyrotaxane in response to DTT, due to the cleavage of disulfide linkage (Fig. 6.5-6.6). And the transfection results and MTT assay further showed that the cell viability and gene transfer ability of biodegradable PRSSP systems were noticeably stronger than that of the non-reductive analogue PRP control (Fig. 6.7-6.10). However, we still not sure whether the degradation of the complexes occurred intracellularly reducing by glutathione (GSH), and whether the degradation and intracellular reductive environment GSH are responsive for the low cytotoxicity and high transfection efficiency. Therefore, in order to further determine the role of disulfide linkage of our system in improvement of gene transfection, D,L-Buthionine sulfoxamine (BSO), a known GSH inhibitor resulting in depletion of intracellular GSH, was used [36, 37]. Fig. 6.11 shows the effects of BSO (300μM) on luciferase expression levels in MB231, Hela and COS7 cells. The results showed that at low N/P ratios (N/P=10), no significant difference was observed for all polyrotaxanes before or after BSO treatment, probably because no appreciable cytotoxicity of all the test polyplexes at this N/P ratios and the effect of disulfide bond is the least, which is confirmed by our previous research (Fig. 6.8). However, at N/P ratio of 70, when cells were pre-incubated with BSO prior to transfection, the transfection efficiency of disulfide-linkage containing PRSSP123 and PRSSP177 sharply decreased as compared to the same polyplex without the treatment of GSH inhibitor (p<0.01). In contrast, the luciferase expression level of non-degradable analogue PRSSP was not affected by BSO (p>0.05). Therefore, it is evident that the observed inhibitions of transfection were not caused by cytotoxicity of BSO and the disulfide linkages were cleaved by intracellular GSH. It suggests that the degradation did play a role in reductive polyrotaxane transfection, presumably through the efficient unpacking of

DNA. Furthermore, after treating with BSO, no significant differences were observed in the transfection efficiency of PRSSP and PRP (p>0.05). This is in consistent with the research reported by other groups [36, 38], which indicating the intracellular cleavage of the disulfide bond in the PRSSP systems by GSH is responsible for their higher transfection efficiency observed previous in compared with PRP systems.
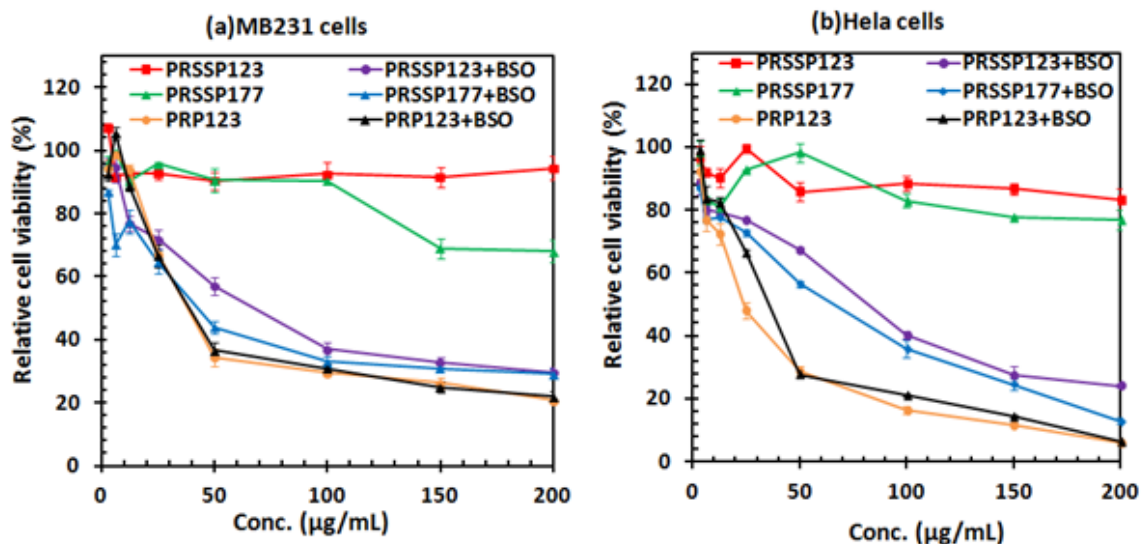
Fig. 6.12 Effects of BSO (300μM) on cytotoxicity of polymers in (a) MB231 and (b) Hela cells. Cell viability was compared with various concentrations of polymers with/without BSO in the presence of serum. Data represent mean ± SD (n=5).
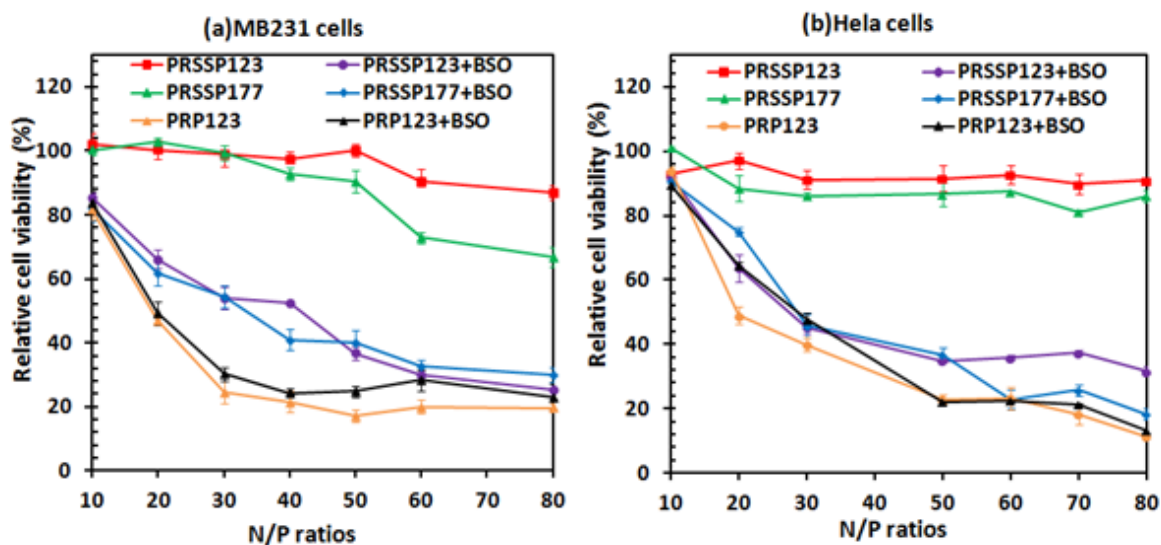
Fig. 6.13 Effects of BSO (300μM) on cytotoxicity of polymer/DNA complex in (a) MB231 and (b) Hela cells. Cell viability was compared with various N/P ratios with/without BSO in the presence of serum. Data represent mean ± SD (n=5).

Since we originally hypothesized that the reductive polyrotaxane would facilitate DNA release triggered by the intracellular degradation in response to GSH, we expected that the cytotoxicity of the biodegradable polyrotaxane would also be affected by the level of intracellular GSH level, which causes the degradation. To test this point, cell viabilities were compared between the cells treated with and without BSO. Treatment with BSO, an inhibitor of g-glutamylcysteine synthetase, would result in depletion of intracellular GSH. As shown in Fig. 6.12 and Fig. 6.13, in both cell lines, the cytotoxicity of PRSSP system significantly increased to the level of its non-degradable analogue PRP upon treatment with BSO ($p<0.001$). It should also be noted that the decreased of cell viability should not be associated with toxicity of BSO, because the cytotoxicity of non-reductive PRP123 was not affected by BSO treatment ($p>0.05$). The results showed that the GSH inhibitor led to the inability of polyplex to completely degradation, resulting limited DNA release and higher cytotoxicity. Evidently, lower the cytotoxicity of complexes is the one of the major contributions of disulfide bonds to gene transfection. The results are in accordance with our previous hypothesis.

6.3.11 Stability of polymer/DNA complexes

Serum stability is one of the most important barriers for gene delivery. PEGylation is a well studied method to stabilize the polyplexes by providing a steric hydrophilic shell around particles. Polyplexes with PEG shell could prevent the aggregation of particles, resist protein adsorption and cell adhesion, lower cytotoxicity and improve anti-serum ability [20, 21]. In our system, due to the unique self-assembly behavior of star polyrotaxanes based on star PEG and partial threaded CDs, the naked PEG arms could form a sheddable hydrophilic shell by self-assembly,

which could stabilize the polyplex. This is another major advantage of our systems in contrast to other PDMAEMA based gene vectors [11, 39]. The 8 arm PEG not only can offer rotating backbone and moving axle for α-CD; more importantly they could also provide a hydrophilic shell with naked PEG brush layer. Furthermore, unlike traditional PEGylation via covalent or non-covalent attachment, the PEG shell was formed naturally and no more modification is needed, which could prevent the drawbacks due to the traditional PEG modification, such as lower transfection efficiency and reduced internalization of untargeted polyplexes [40], degradation of DNA by nucleases [41], and lower DNA binding ability [42].
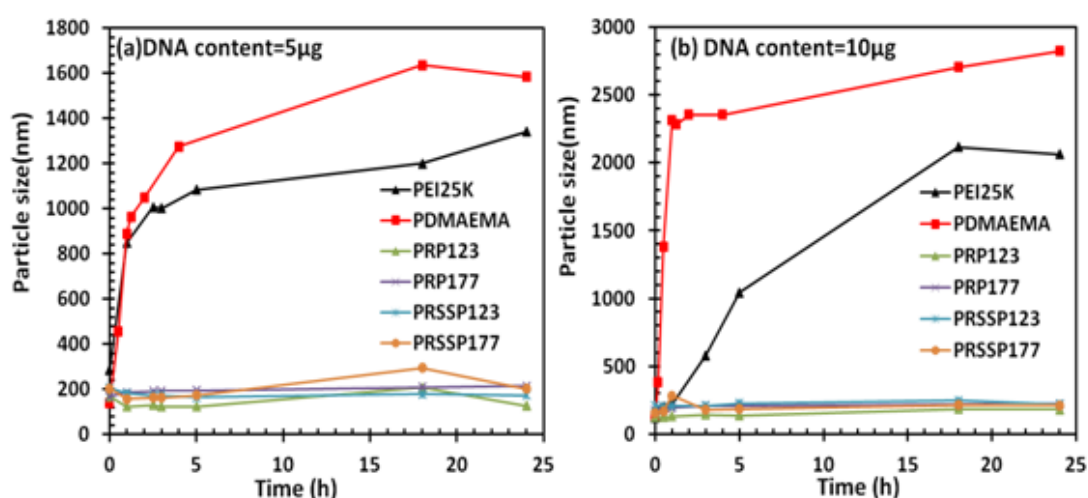
Fig. 6.14 Hydrodynamic size of polyplex formed by PEI25k, PDMAEMA-177, PRSSP and PRP systems at N/P ratio of 50 with different DNA content as a function of time in the presence of 150 mM PBS. (a) DNA content=5μg; (b) DNA content=10μg

We studied the aggregation behaviors of the polyplex formed by polyrotaxane PRSSP and PRP with PEG shell under physiological salt condition (150 mM) (Fig. 6.14). In order to verify the importance of PEG chain on the stability of polyplex, two control systems are used: PEI25k and PDMAEMA without PEG. PDMAEMA was synthesized via ATPR of DMAEMA with the same procedures as our test polyrotaxane and their structures are confirmed by ^{1}H NMR, which showed that about

177 DMA repeat units were polymerized. As shown in Fig. 6.14, in the presence of PBS, the hydrodynamic diameters of our four test core-shell structures (PRSSP and PRP systems) remained sufficiently stable within 24hrs, but the complexes formed by pure PDMAEMA without PEG and PEI25k aggregated rapidly in PBS. For example, the size of polyplexes formed by PRP177 with 10 μg DNA increased from 174 nm to 222.2 nm in 24 hours with PBS incubation, and the size change ratio was 1.27 (Fig. 6.14b). In contrast, without naked PEG shell, the trend of size changes of both PEI25k and PRDMAEMA-177 system were much steeper. The diameters of PEI25K/DNA and PDMAEMA/DNA complexes increased from 119.7 nm to 2063 nm and from 132.9 nm to 2822 nm, respectively in 24 hours. Their size change ratio was 17.23 and 21.23 respectively. These results demonstrates that the naked PEG in partial polyrotaxane PRSSP and PRP contributes to the formation of core-shell nanostructure with hydrophilic PEG brush layer in the exterior surface, which could stabilize the polyplex and prevent aggregation of particles under physiological salt conditions.
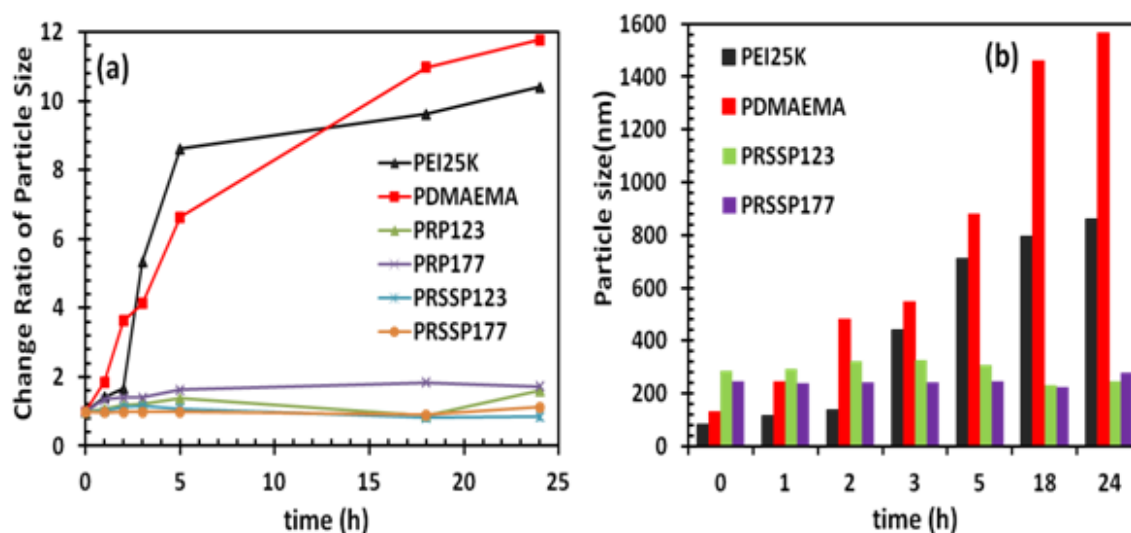
Fig. 6.15 Evaluation of the change in particle size of polyplexes in PBS that contains 5% w/w of BSA at 37 °C, as determined by dynamic light scattering: (a) size change ratio (b) particle size. (All the N/P ratio of the polymer/DNA complex was fixed at 50.)

Ingredients in serum especially the proteins may affect the stability of the particles. In the case of *in vivo* gene delivery, the negatively charged plasma proteins in the blood may cause aggregation of the positively charged polymer/DNA complexes. Thus, many polyplexes are not likely to maintain their colloidal stability upon intravenous injection, like PEI25k, Lipofectamine 2000 et.al, and their applications in vivo are compromised [43]. Therefore, it is necessary to evaluate the stability of our polyrotaxane self-assembled nanostructures with PEG shell upon proteins. In this chapter, bovine serum albumin (BSA) was selected as the model protein to simulate the serum condition. We investigate the stability of the polymer/DNA complexes in BSA containing PBS. Fig. 6.15 showed the ratio of size change (a) and the size of polyplexes (b) in 5% BSA solution as a function of incubation time, with fixed N/P ratio of 50. Similar with the investigation of salt stability, the particle size of PRSSP/DNA and PRP/DNA complex was compared to PEI25k and PDMAEMA177 without PEG. As expected, it was found that all the four tested core-shell nanostructures (PRSSP and PRP) could prevent particle aggregation for 24h in the presence BSA. The sizes of PRSSP177/DNA complexes increased from 245.6 nm to 279.4 nm in 24 hours, and the size change ratio was 1.14. All the other three polyrotaxane showed the similar phenomena and the size change ratio are all lower than 2. However, without the modification of PEG, the trend of size changes of both PEI/DNA and PDMAEMA/DNA system were much steeper. The ratios of size change at 24 h were 10.4 and 11.8, respectively. The diameter of PDMAEMA177/DNA complexes increased from 132.9 nm to 1565 nm in 24 hours and the size change ratio was 11.8. The results are in line with the previous salt stability studies. It is confirmed that the shielding effect of PEG could hinder the interaction with protein and aggregation of particles. Our polyrotaxane system based

on PDMAEMA in this chapter may be more stable and resistant to serum system than other polycationic gene systems, which is important for *in vivo* applications.

6.4 CONCLUSIONS

Aiming to increase the serum stability and improve the transfection efficiency of PDMAEMA systems with optimal DNA release and decreasing cytotoxicity, a novel reduction-sensitive and shell detachable gene delivery system was successfully developed based on star polyrotaxanes, which consists of partially threaded α-cyclodextrin (α-CD), 8-arm PEG and low molecular weight PDMAEMA segments linked to the end of PEG arms with disulfide linkage. The resulted star supramolecular structure demonstrated good ability to condense DNA into nanoparticles. Particle size, zeta potential and gel retardation experiment confirmed their degradability and DNA release ability in response to DTT, a reductive environment analogous to that of the intracellular compartments such as cytosol and the cell nucleus. Remarkably, the results of MTT assay and luciferase expression confirmed that the biodegradable star polyrotaxane with disulfide linkage exhibited remarkable lower cytotoxicity and higher gene transfection efficiency in contrast to reduction insensitive control and polyethylenimine (PEI) 25k. They showed excellent *in vitro* transfection efficiency and noticeably wider therapy window than that of PEI 25k and non-degradable control. Furthermore, in according to the glutathione (GSH) inhibition experiment, it was found that cell viability and transfection was markedly decreased, confirming that introduction of disulfide linkage to the system result in fast intracellular degradation and disassociation, efficient DNA release, decreased cytotoxicity and enhanced transfection.

More importantly, the hindrance effect of PEG shell allows the system to be stable and prevent aggregation in salt and protein solution. Taken together, our supramolecular self-assembled nanostructure boast many favorable properties as gene carriers, which include good DNA binding ability, reduction-sensitive biodegradability, intracellular DNA release, low cytotoxicity, high gene transfection efficiency and high stability in biological fluids. Moreover, due to the dual self-assembly behavior of the polyrotaxane, the star polymer could also be very promising for the application of drug/gene codelivery.

6.5 REFERENCES

1.   van de Wetering P, Cherng JY, Talsma H, Crommelin DJ, Hennink WE. 2-(Dimethylamino)ethyl methacrylate based (co)polymers as gene transfer agents. J Control Release 1998 Apr 30;53(1-3):145-153.

2.   Layman JM, Ramirez SM, Green MD, Long TE. Influence of polycation molecular weight on poly(2-dimethylaminoethyl methacrylate)-mediated DNA delivery in vitro. Biomacromolecules 2009 May 11;10(5):1244-1252.

3.   Schallon A, Jerome V, Walther A, Synatschke CV, Muller AHE, Freitag R. Performance of three PDMAEMA-based polycation architectures as gene delivery agents in comparison to linear and branched PEI. Reactive & Functional Polymers 2010 Jan;70(1):1-10.

4.   Grigsby CL, Leong KW. Balancing protection and release of DNA: tools to address a bottleneck of non-viral gene delivery. J R Soc Interface 2010 Feb 6;7 Suppl 1:S67-82.

5.   Fischer D, Bieber T, Li Y, Elsasser HP, Kissel T. A novel non-viral vector for DNA delivery based on low molecular weight, branched polyethylenimine: effect of molecular weight on transfection efficiency and cytotoxicity. Pharm Res 1999 Aug;16(8):1273-1279.

6.   Cai JG, Yue YA, Rui D, Zhang YF, Liu SY, Wu C. Effect of Chain Length on Cytotoxicity and Endocytosis of Cationic Polymers. Macromolecules 2011 Apr;44(7):2050-2057.

7.   Jevprasesphant R, Penny J, Jalal R, Attwood D, McKeown NB, D'Emanuele A. The influence of surface modification on the cytotoxicity of PAMAM dendrimers. Int J Pharm 2003 Feb 18;252(1-2):263-266.

8.   Wen Y, Pan S, Luo X, Zhang W, Shen Y, Feng M. PEG- and PDMAEG-graft-modified branched PEI as novel gene vector: synthesis, characterization and gene transfection. J Biomater Sci Polym Ed 2010;21(8-9):1103-1126.

9.   Wen Y, Pan S, Luo X, Zhang X, Zhang W, Feng M. A biodegradable low molecular weight polyethylenimine derivative as low toxicity and efficient gene vector. Bioconjug Chem 2009 Feb;20(2):322-332.

10.   Lin S, Du FS, Wang Y, Ji SP, Liang DH, Yu L, et al. An acid-labile block copolymer of PDMAEMA and PEG as potential carrier for intelligent gene delivery systems. Biomacromolecules 2008 Jan;9(1):109-115.

11.   Zhu CH, Jung S, Meng FH, Zhu XL, Park TG, Zhong ZY. Reduction-responsive cationic biodegradable micelles based on PDMAEMA-SS-PCL-SS-PDMAEMA triblock copolymers for gene delivery. Journal of Controlled Release 2011 Nov;152:E188-E190.

12.   Dai FY, Sun P, Liu YJ, Liu WG. Redox-cleavable star cationic PDMAEMA by arm-first approach of ATRP as a nonviral vector for gene delivery. Biomaterials 2010 Jan;31(3):559-569.

13.   Jiang X, Lok MC, Hennink WE. Degradable-brushed pHEMA-pDMAEMA synthesized via ATRP and click chemistry for gene delivery. Bioconjugate Chemistry 2007 Nov-Dec;18(6):2077-2084.

14.   Kim TI, Kim SW. Bioreducible polymers for gene delivery. React Funct Polym 2011 Mar 1;71(3):344-349.

15. Xia W, Wang PJ, Lin C, Li ZQ, Gao XL, Wang GL, et al. Bioreducible polyethylenimine-delivered siRNA targeting human telomerase reverse transcriptase inhibits HepG2 cell growth in vitro and in vivo. Journal of Controlled Release 2012 Feb;157(3):427-436.

16. Ruiz J, Ceroni M, Quinzani OV, Riera V, Piro OE. Reversible S-S bond breaking and bond formation in disulfide-containing dinuclear complexes of Mn. Angewandte Chemie-International Edition 2001;40(1):220-222.

17. Go YM, Jones DP. Redox compartmentalization in eukaryotic cells. Biochim Biophys Acta-Gen Subj 2008 Nov;1780(11):1271-1290.

18. Meng F, Hennink WE, Zhong Z. Reduction-sensitive polymers and bioconjugates for biomedical applications. Biomaterials 2009 Apr;30(12):2180-2198.

19. Cheng R, Feng F, Meng F, Deng C, Feijen J, Zhong Z. Glutathione-responsive nano-vehicles as a promising platform for targeted intracellular drug and gene delivery. J Control Release 2011 May 30;152(1):2-12.

20. Roux E, Passirani C, Scheffold S, Benoit JP, Leroux JC. Serum-stable and long-circulating, PEGylated, pH-sensitive liposomes. Journal of Controlled Release 2004 Feb;94(2-3):447-451.

21. Gref R, Minamitake Y, Peracchia MT, Trubetskoy V, Torchilin V, Langer R. Biodegrable long-circulating polymeric nanospheres. Science 1994 Mar;263(5153):1600-1603.

22. Zhang XW, Zhu XQ, Ke FY, Ye L, Chen EQ, Zhang AY, et al. Preparation and self-assembly of amphiphilic triblock copolymers with polyrotaxane as a middle block and their application as carrier for the controlled release of Amphotericin B. Polymer 2009 Aug;50(18):4343-4351.

23. Ren LX, Ke FY, Chen YM, Liang DH, Huang J. Supramolecular ABA triblock copolymer with polyrotaxane as B block and its hierarchical self-assembly. Macromolecules 2008 Jul;41(14):5295-5300.

24. Tong XM, Zhang XW, Ye L, Zhang AY, Feng ZG. Synthesis and characterization of block copolymers comprising a polyrotaxane middle block flanked by two brush-like PCL blocks. Soft Matter 2009;5(9):1848-1855.

25. Liu J, Sondjaja HR, Tam KC. Alpha-cyclodextrin-induced self-assembly of a double-hydrophilic block copolymer in aqueous solution. Langmuir 2007 Apr 24;23(9):5106-5109.

26. Li J, Yang C, Li HZ, Wang X, Goh SH, Ding JL, et al. Cationic supramolecules composed of multiple oligoethylenimine-grafted beta-cyclodextrins threaded on a polymer chain for efficient gene delivery. Advanced Materials 2006 Nov;18(22):2969-+.

27. Yang C, Li J. Thermoresponsive Behavior of Cationic Polyrotaxane Composed of Multiple Pentaethylenehexamine-grafted alpha-Cyclodextrins Threaded on Poly(propylene oxide)-Poly(ethylene oxide)-Poly(propylene oxide) Triblock Copolymer. Journal of Physical Chemistry B 2009 Jan;113(3):682-690.

28. Li JJ, Zhao F, Li J. Polyrotaxanes for applications in life science and biotechnology. Appl Microbiol Biotechnol 2011 Apr;90(2):427-443.

29. Ping Y, Liu CD, Zhang ZX, Liu KL, Chen JH, Li J. Chitosan-graft-(PEI-beta-cyclodextrin) copolymers and their supramolecular PEGylation for DNA and siRNA delivery. Biomaterials 2011 Nov;32(32):8328-8341.

30. Kim HJ, Oba M, Pittella F, Nomoto T, Cabral H, Matsumoto Y, et al. PEG-detachable cationic polyaspartamide derivatives bearing stearoyl moieties for systemic siRNA delivery toward subcutaneous BxPC3 pancreatic tumor. Journal of Drug Targeting 2012 Jan;20(1):33-42.

31. Oumzil K, Khiati S, Grinstaff MW, Barthelemy P. Reduction-triggered delivery using nucleoside-lipid based carriers possessing a cleavable PEG coating. J Control Release 2011 Apr 30;151(2):123-130.

32. Nounou MI, Emmanouil K, Chung S, Pham T, Lu Z, Bikram M. Novel reducible linear L-lysine-modified copolymers as efficient nonviral vectors. J Control Release 2010 May 10;143(3):326-334.

33. Yamada Y, Nomura T, Harashima H, Yamashita A, Katoono R, Yui N. Intranuclear DNA Release Is a Determinant of Transfection Activity for a Non-viral Vector: Biocleavable Polyrotaxane as a Supramolecularly Dissociative Condenser for Efficient Intranuclear DNA Release. Biological & Pharmaceutical Bulletin 2010 Jul;33(7):1218-1222.

34. Nemoto Y, Borovkov A, Zhou YM, Takewa Y, Tatsumi E, Nakayama Y. Impact of molecular weight in four-branched star vectors with narrow molecular weight distribution on gene delivery efficiency. Bioconjug Chem 2009 Dec;20(12):2293-2299.

35. Fischer D, Li Y, Ahlemeyer B, Krieglstein J, Kissel T. In vitro cytotoxicity testing of polycations: influence of polymer structure on cell viability and hemolysis. Biomaterials 2003 Mar;24(7):1121-1131.

36. Xu PS, Quick GK, Yeo Y. Gene delivery through the use of a hyaluronate-associated intracellularly degradable crosslinked polyethyleneimine. Biomaterials 2009 Oct;30(29):5834-5843.

37. Christensen LV, Chang CW, Yockman JW, Conners R, Jackson H, Zhong ZY, et al. Reducible poly(amido ethylenediamine) for hypoxia-inducible VEGF delivery. Journal of Controlled Release 2007 Apr;118(2):254-261.

38. Breunig M, Lungwitz U, Liebl R, Goepferich A. Breaking up the correlation between efficacy and toxicity for nonviral gene delivery. Proc Natl Acad Sci U S A 2007 Sep 4;104(36):14454-14459.

39. Zhu C, Jung S, Luo S, Meng F, Zhu X, Park TG, et al. Co-delivery of siRNA and paclitaxel into cancer cells by biodegradable cationic micelles based on PDMAEMA-PCL-PDMAEMA triblock copolymers. Biomaterials 2010 Mar;31(8):2408-2416.

40. Lomas H, Massignani M, Abdullah KA, Canton I, Lo Presti C, MacNeil S, et al. Non-cytotoxic polymer vesicles for rapid and efficient intracellular delivery. Faraday Discuss 2008;139:143-159; discussion 213-128, 419-120.

41. Pathak A, Patnaik S, Gupta KC. Recent trends in non-viral vector-mediated gene delivery. Biotechnol J 2009 Nov;4(11):1559-1572.

42. Fernandez CA, Rice KG. Engineered nanoscaled polyplex gene delivery systems. Mol Pharm 2009 Sep-Oct;6(5):1277-1289.

43. Wang Y, Ke CY, Weijie Beh C, Liu SQ, Goh SH, Yang YY. The self-assembly of biodegradable cationic polymer micelles as vectors for gene transfection. Biomaterials 2007 Dec;28(35):5358-5368.

CHAPTER 7   SELF-ASSEMBLED NANOSTRUCTURES BASED ON STAR POLYROTAXANE FOR CO-DELIVERY OF DRUG AND GENE

7.1 INTRODUCTION

In cancer therapy, one of the major issues associated with current chemotherapy is multiple drug resistance (MDR), which is mainly due to the gene malfunction. [1] Combination therapy of gene and drug may provide a solution to this problem by correcting malfunctioned gene and sensitizing cancer cells to anticancer drugs.[2, 3] Furthermore, codelivery of gene and drug with one delivery system may take the advantages of enhanced gene transfection efficiency by achieving the synergistic effects because the therapeutic agents are delivered into target cells simultaneously.[4-6] Over the past few years, many designs of novel co-delivery vectors have attracted much attention in delivery systems, including cationic micelles,[6-8], cationic liposomes, [9-11] and cationic supramolecular polymers [12]. For example, micelles capable of dual delivery of DNA and other therapeutics have also have been designed [6, 13, 14]. Specially, poly N-methyldietheneamine sebacate and (cholesteryl oxocarbonylamido ethyl) methyl bisethylene ammonium bromide sebacate (PMDS-co CES) form micelles with an inner hydrophobic core composed of

cholesterol surrounded by polycationic polymer. The co-delivery of the micelle containing paclitaxel and the plasmid DNA suppresses tumor growth in a 4T1 mouse breast cancer model more effectively than the delivery of micelles with either therapeutic alone [6]. In addition, biodegradable PDMAEMA-PCL-PDMAEMA triblock copolymer was also prepared for siRNA and paclitaxel codelivery. Significant enhanced gene silencing efficiency of the polycations micelles was observed as compared to 20K PDMAEMA or 25K PEI. Moreover, due to the improved cellular uptake, micelle loaded with paclitaxel displayed higher drug efficacy than free drug. These results suggested that cationic biodegradable micelles are highly promising for the combinatorial delivery of siRNA and lipophilic anticancer drugs [8].

DOX is one of the most potent anticancer drugs and used widely in the treatment of different types of solid malignant tumors [15, 16]. DOX is known to interact with DNA by intercalation and inhibition of macromolecular biosynthesis. It is crucial, therefore, to deliver and release DOX in the cytoplasm and/or right into the cell nucleus. However, the cardiotoxicity of this drug limits its direct administration and cumulative storage [17, 18]. In order to minimize the cardiotoxicity, reduction of DOX dose would be necessary in the future research. But low dose of anticancer drugs will be less effective to the treatment of cancers, especially to drug resistant cancers [19]. Therefore, it would be very useful to explore the combination therapy and achieve a high anticancer efficacy in low DOX dose.

Our previous studies present a novel redox-responsive and shell detachable star shaped polyrotaxane nanostructure based on pDMAEMA, which could be very promising in reduction-sensitive intracellular gene delivery with the advantages of

biodegradability, intracellular DNA release, low cytotoxicity, high gene transfection efficiency and high stability in biological fluids. In this work, we are interested in designing a series of these star shaped cationic polyrotaxanes based on pDMAEMA with different threading numbers of CDs (Scheme 7.1). Their self-assembly formations with PEG shell and polyrotaxane core would be confirmed. Furthermore, by taking the advantages of the core-shell structure, the cationic polyrotaxanes are expected to encapsulate DOX into the CD core and applied in drug delivery with high drug loading efficiency, higher cell uptake and improved drug efficacy. More importantly, in this star polyrotaxane, cationic PDMAEMA arms are expected to condense DNA efficiently into nanoparticles and this new cationic polyrotaxane nanostructure could be very promising in co-delivery therapeutics by combing the advantages of core-shell structures as drug vectors and reductive star polyrotaxanes as gene vectors.
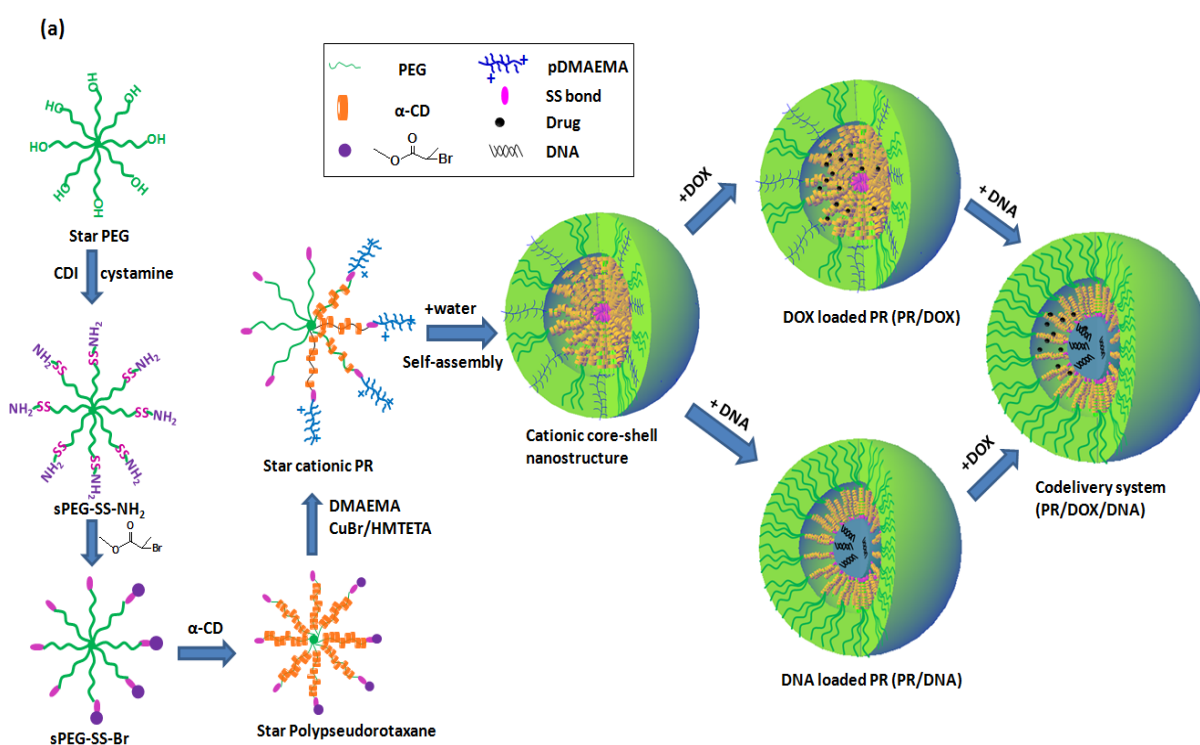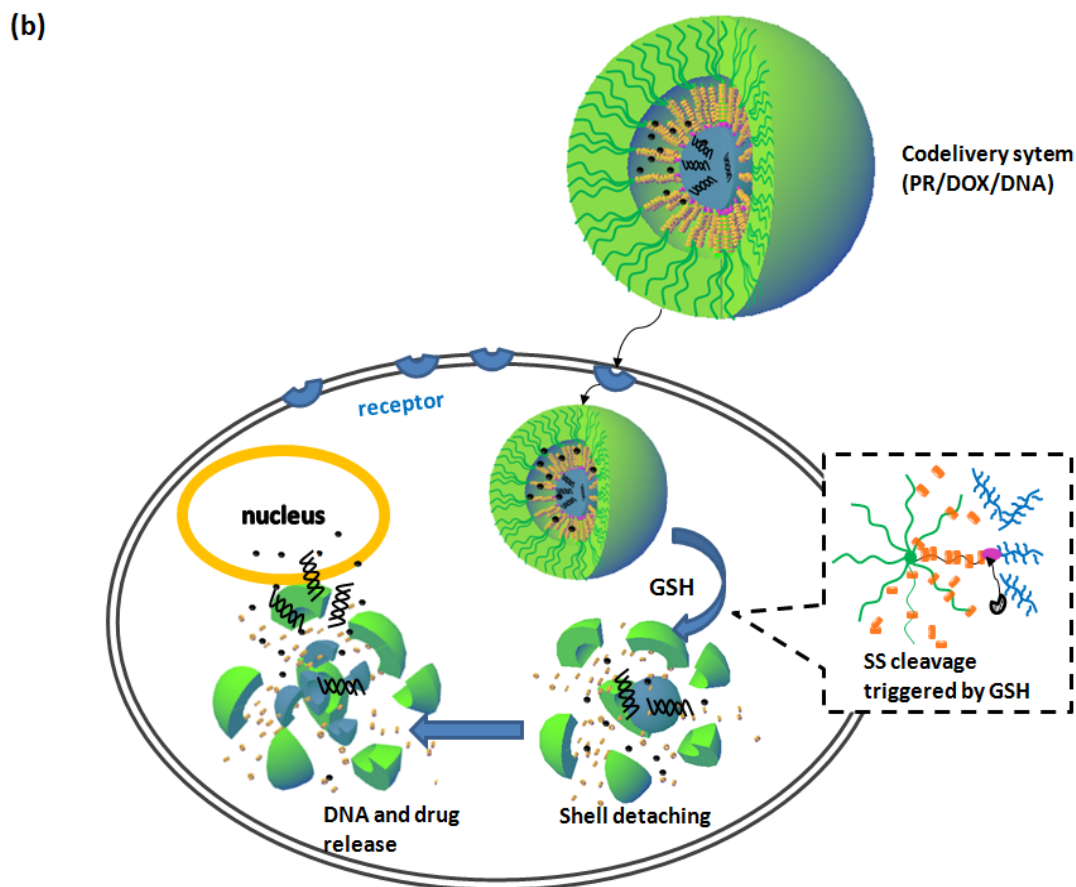
Scheme 7.1 Illustration of (a) the preparation of bioreductive codelivery systems and (b) the intracellular drug and gene release

7.2 MATERIALS AND METHODS

7.2.1 Materials

Star PEG (Mn=9468) were purchased from Fluka. α-CD was purchased from TCI. DMAEMA monomer, 2-bromopropionyl bromide, Cu(I)Br, HMTETA were supplied by Aldrich. Ethylenediamine, cystamine dihychloride, triethylamine (TEA), 1,1'-Carbonyldiimidazole (CDI), dithiothreitol (DTT), doxorubincin (DOX) were received from Sigma-Aldrich and used as received. Diethyl ether, methanol, tetrahydrofuran (THF), *n*-hexane and dimethyl sulfoxide (DMSO) were purchased from Merck. Penicillin, streptomycin and MTT were obtained from Sigma.

7.2.2 Synthesis Methods

The synthesis of partial cationic polyrotaxane based on PDMAEMA is as the same with the synthesis methods of star polyrotaxane PR-SS-PDMAEMA described in section 6.2.2.1~6.2.2.3 of chapter 6.

7.2.3 Measurements and Characterization

7.2.3.1 Proton Nuclear Magnetic Resonance (^{1}H-NMR)

The details were described in section 3.2.3.1 of Chapter 3.

7.2.3.2 Elemental analysis

The details were described in section 5.2.3.2 of Chapter 5.

7.2.3.3 Self-assembly and Critical aggregation concentration (CAC) determination

The resulted polyrotaxanes are soluble in water, and the core-shell nanostrucutres could be prepared by directly dissolving the polymer in water and allowing it to stay overnight to ensure complete dissolution [20]. The resulted solution was then diluted to the desired concentration with proper amount of water. For TEM and particle size measurements, the solution was filtered through a 0.45 μm Whatman PVDF filter into a dust-free vial.

The CAC values were determined by the dye solubilization method [21]. The hydrophobic dye 1,6-diphenyl-1,3,4-hexatriene (DPH) was dissolved in methanol with a stock concentration of 0.6mM. Star polyrotaxanes were dissolved in water with variable concentration in the range of 0.0001 to 10 mg/mL, while keeping the concentration of DPH constant. 1 mL of polyotaxane aqueous solution was mixed

with 10 µL DPH stock solution and equilibrated at room temperature overnight. A UV-vis spectra in the range of 330-430 nm were recorded at room temperature. And the CAC values were determined by the plot of the difference in absorbance at 378 nm and at 400 nm (A378-A400) versus logarithmic concentration.

7.2.3.4 Transmission Electron Microscopy (TEM) and Dynamic light scattering (DLS)

The morphology of the formed core-shell nanostructures was conducted by TEM and DLS. The procedures described in section 3.2.3.4 and 3.2.3.5 of chapter 3.

7.2.3.5 DOX encapsulation and drug content determination

DOX was loaded into the star polyrotaxane followed by the method reported before [22]. 20 mg soluble polyrotaxane was added to 1 mg Doxorubicin hydrochloride (DOX·HCl) and dissolved together with 1 mL DI water, and the solution was stirred overnight at room temperature. Solution of sodium hydroxide (NaOH) was added to the solution to adjust the pH to 8~9 and stirred for 3 h. Because DOX is insoluble in basic condition, the unloaded DOX molecular were precipitated and removed by ultracentrifugation. The obtained solution with loaded DOX was then lyophilized (Yield, 11 mg).

The amount of DOX encapsulated in the nanoaggregates was analyzed by fluorescence measurement. For determination of drug loading content, 1 mL DMSO was added into 1mg DOX-loaded polyrotaxane, the core-shell structure were broken up and the DOX was dissolved in the solution. The characteristic emission absorbance of DOX at 588 nm was recorded and compared with a standard curve generated DOX/DMSO solutions with different DOX concentrations varying from 0 to 60

µg/mL. Drug loading content (DLC) and drug loading efficiency (DLE) were calculated according to the following formula:

DLC (wt%) = (weight of loaded drug/weight of polymer) $\times$ 100%

DLE (wt%) = (weight of loaded drug /weight of drug in feed) $\times$ 100%

7.2.3.6 Cell viability assay

The methods of measuring the anticancer efficacy of the DOX loaded polyrotaxanes were described in section 3.2.3.9 of chapter 3.

7.2.3.7 Intracellular cell uptake and distribution

The methods of measuring the cell uptake and distribution of the DOX loaded polyrotaxanes were described in section 3.2.3.10 of chapter 3.

7.2.3.8 In vitro transfection and luciferase assay

MB231 and Hela cells were seeded onto 24-well plate at a density of 5×10^4 per well in 500 µL DMEM medium with 10% FBS 24h prior to transfection. After the confluence of the cells reaching to 70-80%, the culture medium was replaced with 500 µL fresh complete medium with 10% FBS. Polyplexes with different N/P ratios containing 1 µg pDNA were added to each well and were further incubated with cells for 4h. Then the culture medium were changed to 500 µL medium containing 10% FBS and cells are incubated for further 20 hours. At the end of transfection, the cells were washed with PBS three times and the measuring method of luciferase expression levels are as the same with the protocols described in section 5.2.3.11 of chapter 5.

7.2.3.9 Co-delivery of p53-encoding plasmid with DOX

Co-delivery of p53 (a therapeutic gene) and DOX was used to test the synergy in the anti-cancer abilities in MB231 cells. Cells were seeded onto 6-well plate at a density of 2×10^5 per well in 2 mL of culture medium with 10% FBS 24h prior to transfection. At the time of transfection, polyplexes containing 4 μg p53 were added to each well and were further incubated with cells for 4h. Then the culture media were changed to 2 mL medium containing 10% FBS. After 72 h of transfection, total RNA was isolated from the cells by using RNA Maxiprep Kit (Axygen). The RNA was reverse transcribed with OligodT (Promega) according to the manufacturer's protocol. Real-time PCR was performed on 1μL of cDNA with the Brillian SYBR Green PCR Kit (Stratagene) according to the manufacturer's recommended instruction. The sequences of p53 primers, β-actin primer and amplification conditions used for the RT-PCR experiment were the same as described elsewhere [7]. β-actin was used as an internal standard. Data were analyzed for relative mRNA expression using $\Delta\Delta C_T$ method, and normalized against β-actin expression profile.

7.3 RESULTS AND DISCUSSION

7.3.1 Synthesis of cationic polyrotaxane via ATRP

Scheme 7.1 shows the synthesis procedures of partial cationic polyrotaxane based on ATRP of PDMAEMA, which includes 4 steps. (1) Firstly, 8-arm PEG-SS-NH$_2$ was synthesized by the CDI reaction. Specifically, the hydroxyl groups at the end of 8-arm PEG were activated with CDI, followed by reaction with large excess of cystamine to give terminal amino groups. The reaction was completed in anhydrous DMF under nitrogen because the polarity of the reaction solvent has a strong influence on the conversion. To minimize intermolecular crosslinking, the molar ratio

of cystamine/ethylenediamine to PEG was more than 50 times in the conjugate reaction. (2) Next, 2-bromopropionyl bromide was grafted on the end of PEG arm to form corresponding ATRP macroinitriator (PEG-SS-Br). By controlling the feeding ratio of 2-bromopropionyl bromide/PEG, partially terminated initiator could be achieved (eg. 4 arm grafted). (3) The PPR initiator (PPR-SS-Br) for ATRP was obtained by threading different amounts of α-CDs onto PEG-SS-Br chain, and it was used to polymerize DMA. (4) Finally, star shaped polyrotaxane PRSSP was prepared via ATPR of DMAEMA using PPR-SS-Br as macroinitiator and the flanking chains of pDMAEMA were introduced as the stoppers to prevent CD dethreading. During the end capping process, water was used as ATRP solvent to avoid the α-CD rings dethreading [20, 23]. Furthermore, according to references regarding polyrtoaxane ATRP, the reaction was controlled to proceed at room temperature due to the fact that higher temperature would cause severe dethreading of α-CDs from the polymeric axle [24, 25]. In order to obtain polyrotaxanes with different CD threaded number, different molar ratios of CD/sPEG in feed was used varying from 20 to 160.

7.3.2 Characterization of cationic polyrotaxanes
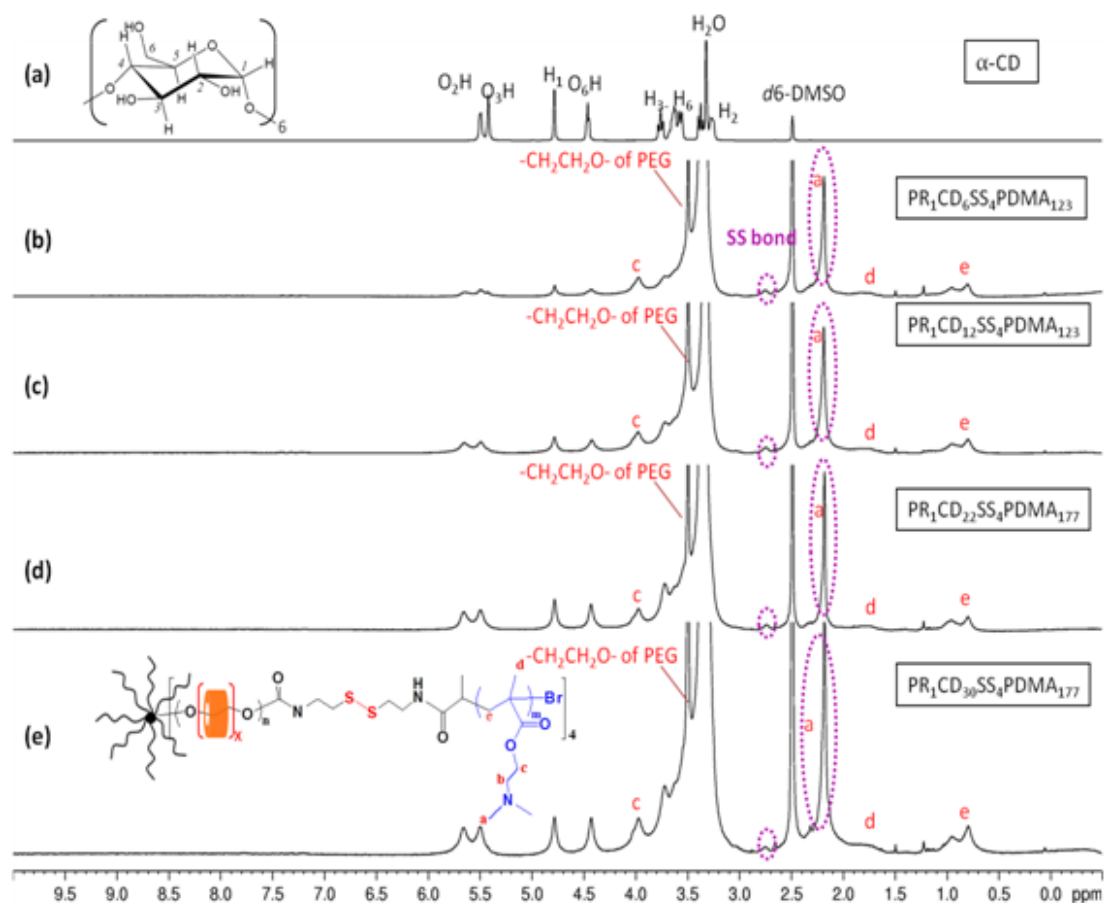
Fig. 7.1 ^{1}H-NMR spectrum of (a) α-CD, (b) PR_1-CD_6-SS_4-$PDMA_{123}$, (c) PR_1-CD_{12}-SS_4-$PDMA_{123}$, (d) PR_1-CD_{22}-SS_4-$PDMA_{177}$ and (e) PR_1-CD_{30}-SS_4-$PDMA_{177}$ in d_6-DMSO. (*In PRxCDySSzPDMAn, in where x are number of PEG, y are the number of threaded CD, z are number of SS linkage, and n are number of DMA repeat units, calculated by ^{1}H NMR*)

Fig.7.1 shows the ^{1}H NMR of polyrotaxane in comparison with pristine α-CD. The peak of δ=2.7~2.8 was attributed to the SS-linkage. In Fig. 7.1(b)-7.1(e), the signals for α-CD, the threading 8-arm PEG (δ=3.5) and the end capping polymer PDMAEMA ((-N(CH₃)₂, δ=2.21 ppm) were all observed. Furthermore, it was found that the peaks of α-CDs in Fig. 7.1(a) were clearly sharp, but those of polyrotaxanes were broadened (Fig. 7.1b-7.1e). These results suggest that the mobility of α-CDs in polyrotaxane is restricted by the PEG chain after forming the supramolecular structure. These results provide us clear evidence for the physically interlocked supramolecular

227

structure of 8 arm PEG covered by α-CDs ended with PDMAEMA [26, 27]. The CD threaded number could be derived by quantitative comparison between the value for the area of the resonance peak due to H_1 of α-CD (δ=4.79) and the peak due to the PEG (δ=3.50). Moreover, by comparing the integration of the signals for the pDMAEMA (-N(CH$_3$)$_2$, around 2.21 ppm) to those for the peak of PEG in the region of 3.50 ppm, the degree of polymerization was calculated. By calculation, the structure of the star polyrotaxanes is confirmed (Table 7.1). It was found that different numbers of CD rings, on average, were threaded on each molecule of 8-arm PEG and about 123 or 177 DMA repeat units were formed on the end of PEG (4-arm initiated).

Table 7.1 The cationic polyrotaxane compositions with PDMAEMA

sample	Feeding molar ratio[a] [PEG]:[CD]:[DMA]	Found molar ratio[b] [PEG]:[CD]:[DMA]	Initiated PEG arms[b] (CD threaded arm)	DMAEMA repeat unit per arm
PRCD6P123	1:20:160	1:6:123	4 arms	31
PRCD12P123	1:40:160	1:12:123	4 arms	31
PRCD12P177	1:40:200	1:12:177	4 arms	45
PRCD22P177	1:80:200	1:22:177	4 arms	45
PRCD30P177	1:160:200	1:30:177	4 arms	45

[a]Molar ratio in feed= [8 arm PEG-Br$_4$]:[α-CD]:[DMAEMA]

[b]Data was all calculated on the basis of ^{1}H NMR in DMSO-D$_6$

The elemental analysis of the synthesized cationic polyrotaxane was presented in Table 7.2. By calculation, the compositions of the cationic polyrotaxane, which determined based on ^{1}H NMR results (Table 7.1), are also in good agreement with the elemental analysis results. Therefore, from the results of ^{1}H NMR and elemental analysis, it could be conclude that the cationic 8-arm polyrotaxane threaded with OEI grafted α-CD and end blocked with disulfide-linkage were successful synthesized.

Table 7.2 Elemental analysis of the cationic polyrotaxanes with PDMAEMA

sample	composition [a]	Anal.calcd [b]				Found [c]			
		N%	C%	H%	S%	N%	C%	H%	S%
PRCD6P123	$PEG_1CD_6SS_4PD_{123}$	4.27	49.40	7.96	0.91	4.26	49.5	7.84	0.95
PRCD12P123	$PEG_1CD_{12}SS_4PD_{123}$	4.25	49.07	8.35	1.26	4.27	49.00	8.39	1.38
PRCD12P177	$PEG_1CD_{12}SS_4PD_{177}$	5.22	57.87	8.02	1.12	5.17	57.95	7.98	1.08
PRCD22P177	$PEG_1CD_{22}SS_4PD_{177}$	3.46	47.23	7.01	0.79	3.75	46.18	6.96	0.82
PRCD30P177	$PEG_1CD_{30}SS_4PD_{177}$	3.02	48.98	7.63	0.79	3.17	49.91	7.73	0.75

[a] The compounds are denoted PEGxCDySSzPDn, in where x are number of PEG, y are the number of threaded CD, z are number of SS linkage and n are number of DMA repeat units, calculated by ^{1}H NMR (Table 7.1).

[b] Theoretical elemental analysis calculated for the corresponding compound.

[c] Elemental analysis found.

7.3.3 Self-assembly behavior and CAC determination
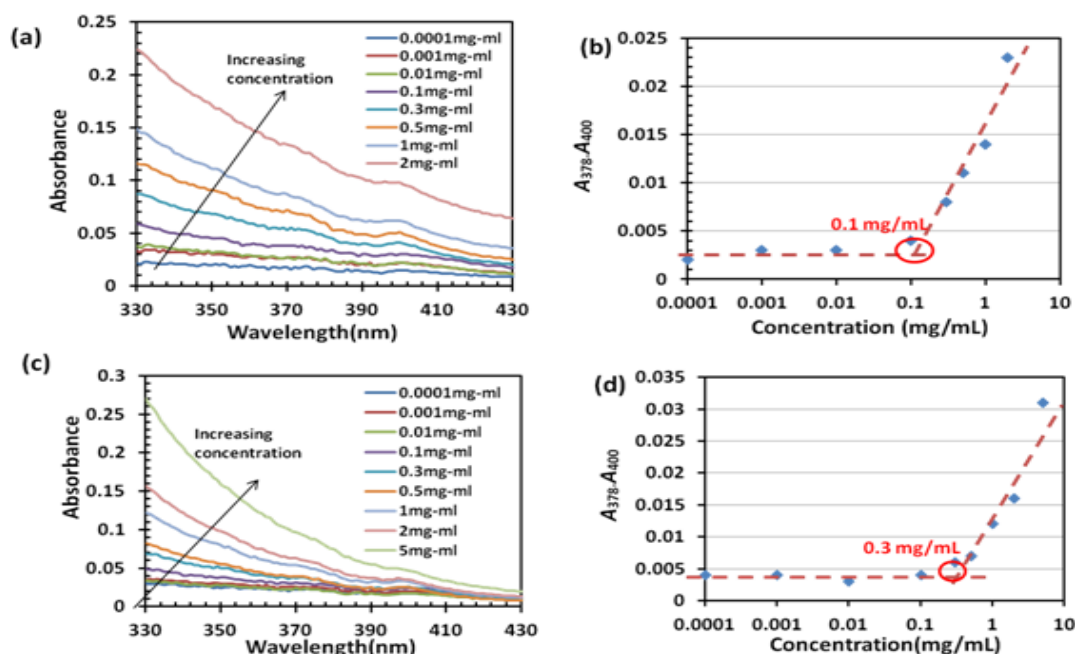
Fig. 7.2 (a) and (c) UV-vis spectra changes of DPH with increasing PRCD22P177 and PRCD30P177 concentration in water at 25 °C. DPH concentration was fixed at 6 mM. (b) and (d) CAC determination by extrapolation of the difference in absorbance at 378 nm and 400 nm

The star polyrotaxanes were soluble and the core-shell nanoaggregates were

formed by directly dissolving in water. Their CAC were determined by DPH method

[28, 29]. This experiment was conducted by varying the aqueous polymer concentration in the range of 0.00001 mg/mL to 5 mg/mL, while keeping the concentration of DPH constant. DPH shows a higher absorption coefficient in a hydrophobic environment than in water. Thus, with increasing polymer concentration, the absorbance at 344, 358 and 378 nm increased (Fig. 7.2a). The point where the absorbance suddenly increases corresponds to the concentration at which nanoaggregates are formed. When the core-shell structure is formed, DPH partitions preferentially into the hydrophobic core formed in the aqueous solution [28, 29]. The CAC was determined by extrapolating the absorbance at 378 nm minus the absorbance at 400 nm (A_{378}-A_{400}) versus logarithmic concentration (Fig. 7.2b). It was found that the CAC values for PRCD22P177 are 0.1 mg/mL. Similarly, PRCD30P177 showed a CAC of 0.3 mg/mL (Fig. 7.2c-d).

7.3.4 TEM and Particle Size of the self-assembly
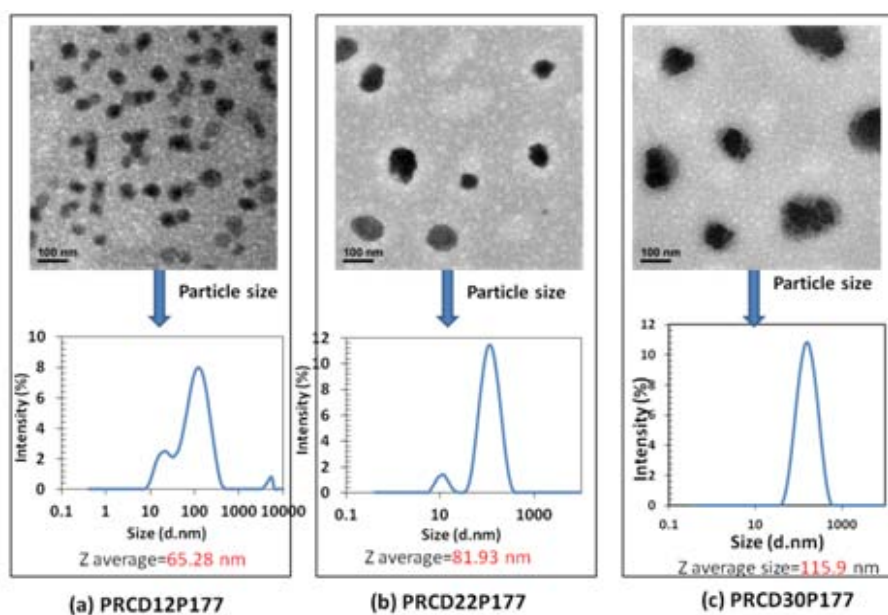
Fig. 7.3 Particle size distribution (intensity distribution) and TEM images of the self-assembly nanoaggregates of PRCD12P177 (a), PRCD22P177 (b) and PRCD30P177 (c). (conc.=1 mg/mL)

To convince the self-assembly and characterize the size and morphology of the polyrotaxane nanoaggregates, TEM and DLS experiments were conducted. These nano-scaled particles were imaged with staining of the polymer shell with sodium salt of phosphotungstic acid. As shown in Fig. 7.3, spherical particles were observed in the three kinds of polyrotaxanes, and the average size was confirmed by particle size with DLS measurement. It was found that all three polyrotaxane assembly exhibited very small size (<120 nm), and the small sizes of particles may enable them to prolong circulation in blood and slower elimination by the reticuloendothelium system (RES) [30]. Specifically, in Fig. 7.3 (a), DLS measurements showed that PRCD12P177 formed nanoaggregates with sizes of 65 nm and TEM micrograph revealed that these particles had a spherical morphology with an average size of ~60 nm. The smaller size observed by TEM as compared to that determined by DLS is most likely due to shrinkage of the PEG shell. With increased number of CDs, the size distribution became monomodal due to the increase of hydrophobic segments. Furthermore, by comparison Fig. 7.3a, b and c, it could be found that with increase in the number of threaded α-CDs, the formed particles tend to be larger (from 65 nm to 116 nm), showing that the presence of more CDs as hydrophobic segment in the CD core increases particle volume.

Therefore, given the CAC, TEM and DLS analytical data as mentioned above, the self-assembly behavior of the synthesized star polyrotaxanes can be confirmed. Furthermore, by comparison with the DLS of 8 arm PEG-PDMAEMA without CDs (z average=5 nm), it can be concluded that the threading of α-CD into the PEG chain not only affects the chain conformation, but also attributes to the aggregation and self-assembly of the novel polyrotaxane.

7.3.5 Drug loading and loading efficiency

In this chapter, we use DOX as the model molecule and try to decrease the limitations and achieve high drug efficacy in low drug dose. The potential application of our star cationic polyrotaxane as anti-cancer drug carrier was evaluated.

Table 7.3 Drug loading content and loading efficiency for DOX loaded polyrotaxanes

sample	Final drug concentration (μg/1 mg polymer)	Loading content [a] (wt.%)	Theory loading content (wt.%)	Loading efficiency [b] (%)
PRCD6P123	7.56 μg	0.76 %	5%	16.6%
PRCD12P123	16.6μg	1.66%	5%	39.9%
PRCD12P177	19.1μg	1.91%	5%	42.1%
PRCD22P177	26.9 μg	2.69%	5%	59.2%
PRCD30P177	32.1μg	3.21%	5%	70.6%
Pure DOX (control)	47.14 μg	-	-	4.7%

[a] Drug loading content (wt%) = (weight of loaded drug/weight of polymer) $\times$ 100%

[b] Drug loading efficiency (wt%) = (weight of loaded drug / drug in feed) $\times$ 100%

Table 7.3 shows the drug loading contents and efficiency of the star polyrotaxanes. The theoretical drug loading content was set at 5 wt% and fluorescence was used to determine the DOX content in the polymer. The results showed that the drug loading efficiencies for the star polyrotaxanes with PDMAEMA were around 16%~70%. The loading content markedly increased with increasing of threading CDs. This can be explained that the more hydrophobic part in the polymer chain makes it possible to have more hydrophobic interaction points in the formed nanoaggregates, giving rise to a higher loading content [31, 32]. Pure DOX was used as control to further verify the drug loading ability of the polyrotaxanes. With the same procedure in the absence of polyrotaxanes, only 4.71 wt% free DOX were found in the final product. In contrast, in the presence of polyrotaxane, approximately 70 wt% DOX was observed. The result confirms the high drug load efficiency and capacity of the polyrotaxane nanostructures. In addition to the hydrophobic interaction, the high drug load efficiency may be attributed to the hydrogen-bond interaction between

hydroxyl group of CDs and amide group of DOX under neutral and basic conditions [22]. The results indicate that the threading of CDs into sPEG chains not only contributes to the self-assembly, but also to the drug loading ability of the polyrotaxane nanoaggregates. Therefore, a controllable drug loading efficiency could be achieved by controlling the threaded number of CDs in the polyrotaxanes.

7.3.6 *In vitro* cytotoxicity
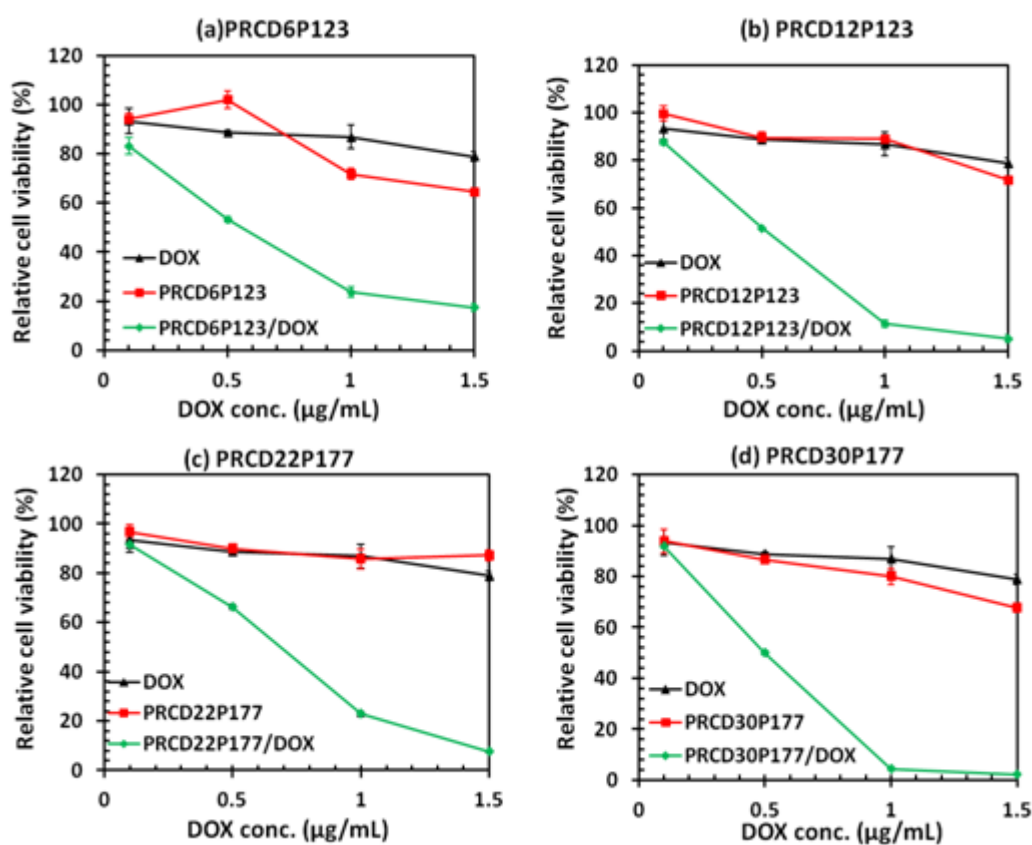
Fig. 7.4 The cytotoxicity of DOX loaded (a) PRCD6P123, (b) PRCD12P123, (c) PRCD22P177 and (d) PRCD30P177 against MB231 after 24h incubation. Free DOX and polymer without DOX was set as control. Data represent mean ± standard deviation (n=3).
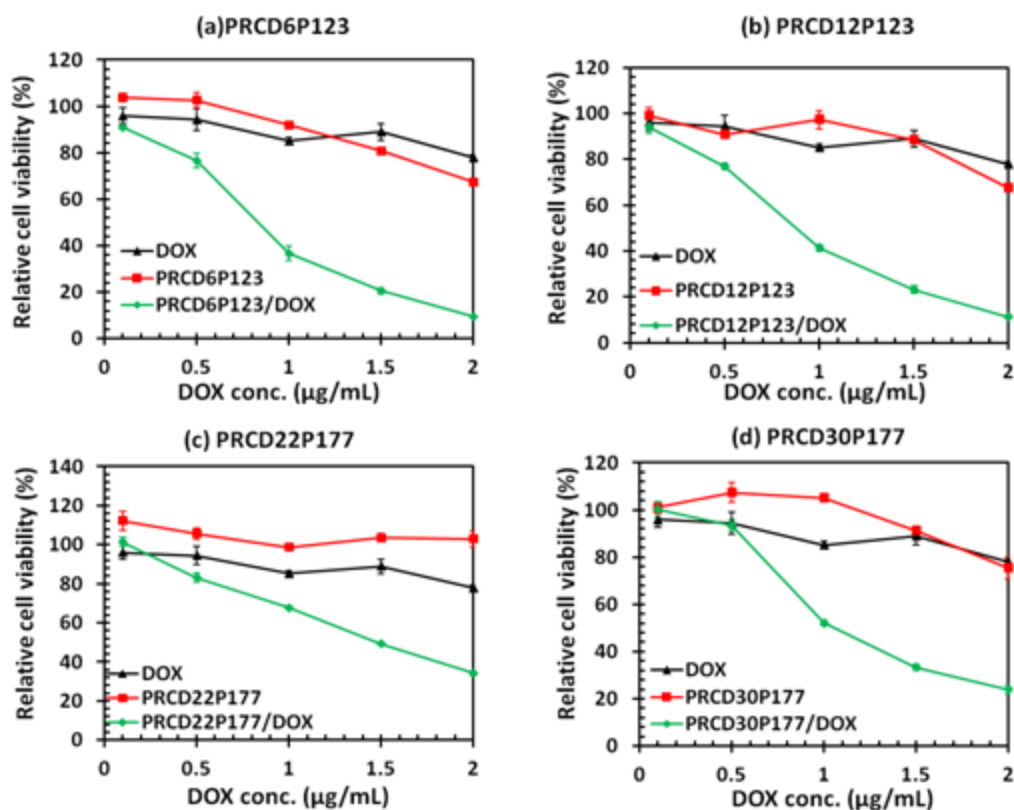
Fig. 7.5 The cytotoxicity of DOX loaded (a) PRCD6P123, (b) PRCD12P123, (c) PRCD22P177 and (d) PRCD30P177 against Hela after 24h incubation. Free DOX and polymer without DOX was set as control. Data represent mean ± standard deviation (n=3).

Table 7.4 IC$_{50}$ values (μg/mL) for DOX loaded PRP

	MB231	Hela
PRCD6P123/DOX	0.56	0.83
PRCD12P123/DOX	0.52	0.87
PRCD22P177/DOX	0.69	1.48
PRCD30P177/DOX	0.49	1.06
DOX	9.82	6.62

The *in vitro* anticancer activity of the DOX loaded polyrotaxane was performed on MB231 and HeLa cancer cells using MTT assay (Fig. 7.4 and Fig. 7.5). As shown in Fig. 7.4 and Fig. 7.5, similar dose-response viability was observed in both cells for all DOX formulas, suggesting our polyrotaxane nano-aggregates could successfully delivery DOX into the cancer cell. It fitted with other researches based on the cytotoxicity of free DOX.[33, 34] Remarkably, all four tested DOX loaded star polyrotaxane showed much more cytotoxicity and higher potent in killing cancer cells

in comparison with free DOX in the low dose range from 0.1 to 2 μg/mL, and their IC_{50} was much lower than free DOX in two cancer cells (Table 7.4). The high cytotoxicity could be attributed to higher cell uptake when delivered by the core-shell aggregates (detail showed in Fig. 7.6-7.7). Additionally, there was no obvious cellular toxicity caused by the blank polyrotaxanes (without DOX) (Fig. 7.4-7,5) at the studied DOX concentration range, eliminating the possibility that polymer themselves were responsible for the cytotoxicity. From the above results, we could conclude that the encapsulation of DOX into our star polyrotaxane could result in a significant higher antitumor efficacy than equivalent free DOX, especially in low DOX dose. This unique property of our star polyrotaxane could be highly beneficial to reduce cardiotoxicity, which is a serious drawback for DOX as anti-cancer therapy.[17, 18]

7.3.7 Intracellular uptake of DOX
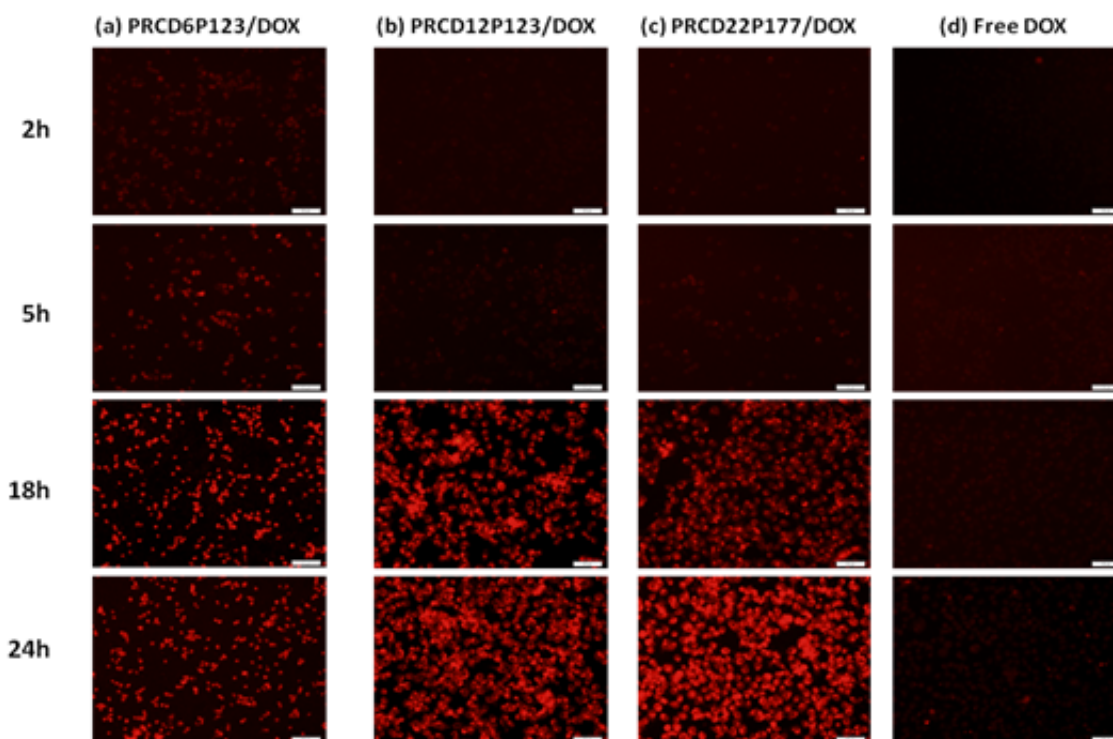
Fig. 7.6 Cellular uptake and internalization of (a) PRCD6P123/DOX, (b) PRCD12P123/DOX, (c) PRCD22P177/DOX and (d) Free DOX in MB231 cells at 2 h, 5 h, 18h and 24 h followed by fluorescence microscopy. (DOX conc.=1 μg/mL).
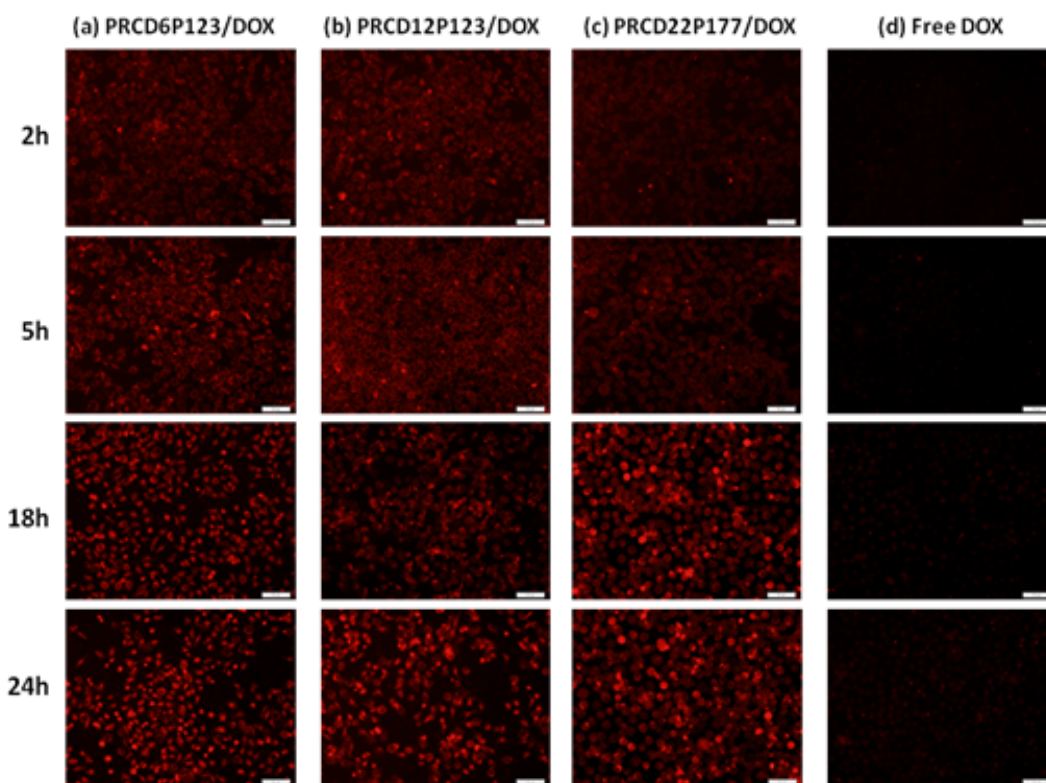
Fig. 7.7 Cellular uptake and internalization of (a) PRCD6P123/DOX, (b) PRCD12P123/DOX, (c) PRCD22P177/DOX and (d) Free DOX in Hela cells at 2 h, 5 h, 18h and 24 h followed by fluorescence microscopy. (DOX conc.=1 μg/mL). Scale length=100μm.

Cellular uptake of DOX may play an important role in the contribution to its antitumor ability. DOX exhibits its own fluorescence with an excitation and emission wavelengths of 480 and 580 nm, respectively. Therefore, fluorescence microscopy was used to evaluate the cellular uptake and internalization behaviour of DOX loaded PRP using MB231 and Hela cell line (Fig. 7.6-7.7). As shown in Fig. 7.6-7.7, DOX loaded polyrotaxane could be rapidly uptaken by the cells and the uptake efficiency increased with time. Notably, in contrast to free DOX without transport carriers (Fig. 7.6d), the PRP/DOX complexes exhibited a much faster and higher cell uptake, as reflected by the higher intensity of fluorescence within the exposed cells. The high internalization and cell uptake of our core-shell carriers may be due to the small size and water soluble PEG shell, which increased the cell-impermeability and stability of DOX.[30] Since it has been reported that fluorescence is observed only when DOX is

released due to the self-quenching effect of DOX in nanoparticles,[35, 36] it is clear from these fluorescence images that DOX has been efficiently released from star polyrotaxane nanoaggregates.

7.3.8 Co-delivery of DOX and luciferase-encoding plasmid
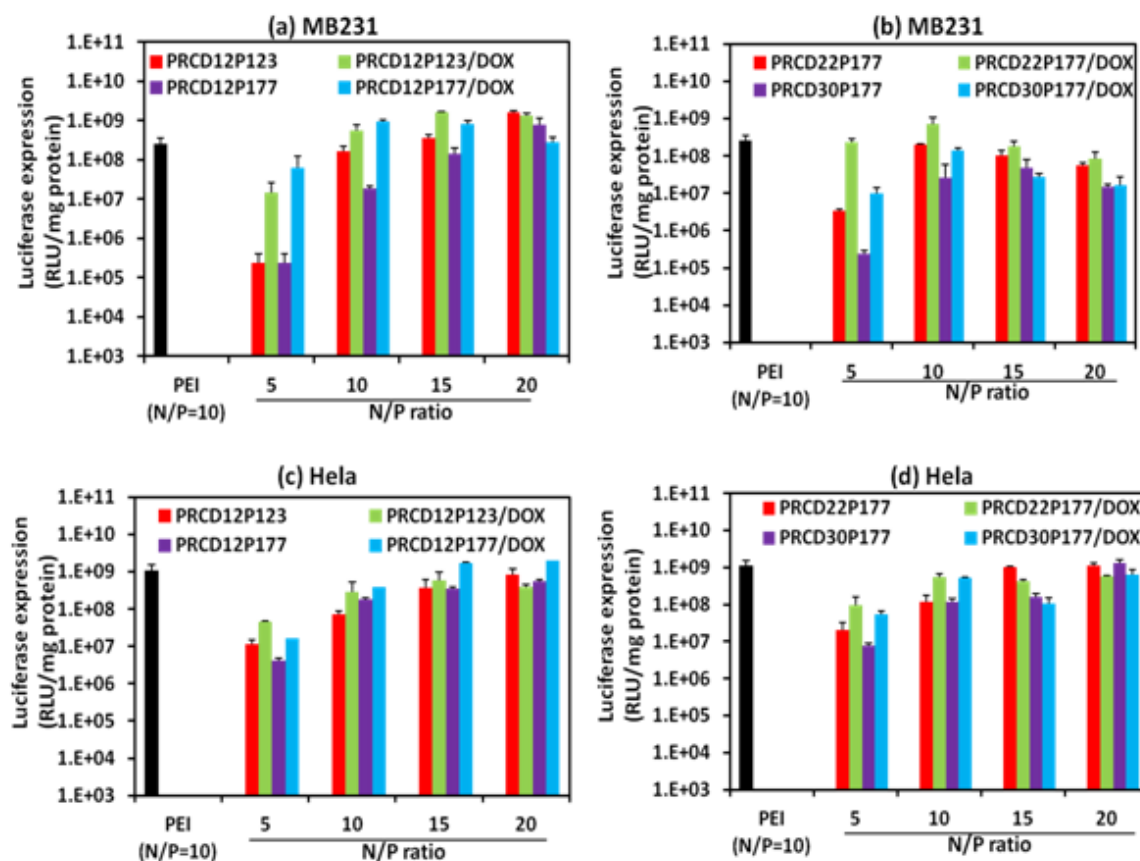
Fig. 7.8 Gene transfection efficiency of the polyplexes formed by PRCDP, PRCDP/DOX and 25K PEI in (a, b) MB231 and (c, d) Hela cells in the presence of serum. Data represent mean$\pm$SD (n=3). DOX concentration (μg/mL) in transfection medium (N/P=10): 1.24 (PRCD12P123); 0.53 (PRCD12P177); 0.79 (PRCD22P177) and 0.83 (PRCD30P177)

Based on the previous researches, reduction-sensitive star polyrotaxanes PRCDP are found to exhibit excellent gene transfection efficiency (chapter 6). Structure similarly with star polyrotaxane we studied before, PRCDP/DOX is also expected to mediate efficient gene delivery. *In vitro* gene transfection efficiency of the DOX loaded polyrotaxanes was assessed using luciferase as a marker gene in MB231 and Hela cells in the presence of serum (Fig. 7.8). 25k PEI and PRCDP

without DOX loading was set as control. As shown in Fig. 7.8, PRCDP/DOX still exhibited excellent gene transfection efficiency, which is comparable or even better than PEI 25k. At lower N/P ratios, the co-delivery of DOX into the polyrotaxane showed a slightly higher gene expression by comparing with single gene delivery system of PRCDP. However, when the N/P ratio increased, their transfection level appeared to be reduced. The reduced luciferase expression could be attributed to the cytotoxicity of DOX, which may inhibit macromolecular biosynthesis. This phenomenon was also reported by other groups.[7, 19] The results confirmed that drug encapsulation in the cyclodextrin core would not hamper gene transfection. Moreover, it seems that the endocytosis of the vector and gene expression was implemented quickly before DOX exerted endocellular function, which could probably resulted in enhanced transfection ability at lower N/P ratios.[37]

7.3.9 Co-delivery of DOX and p53-encoding plasmid

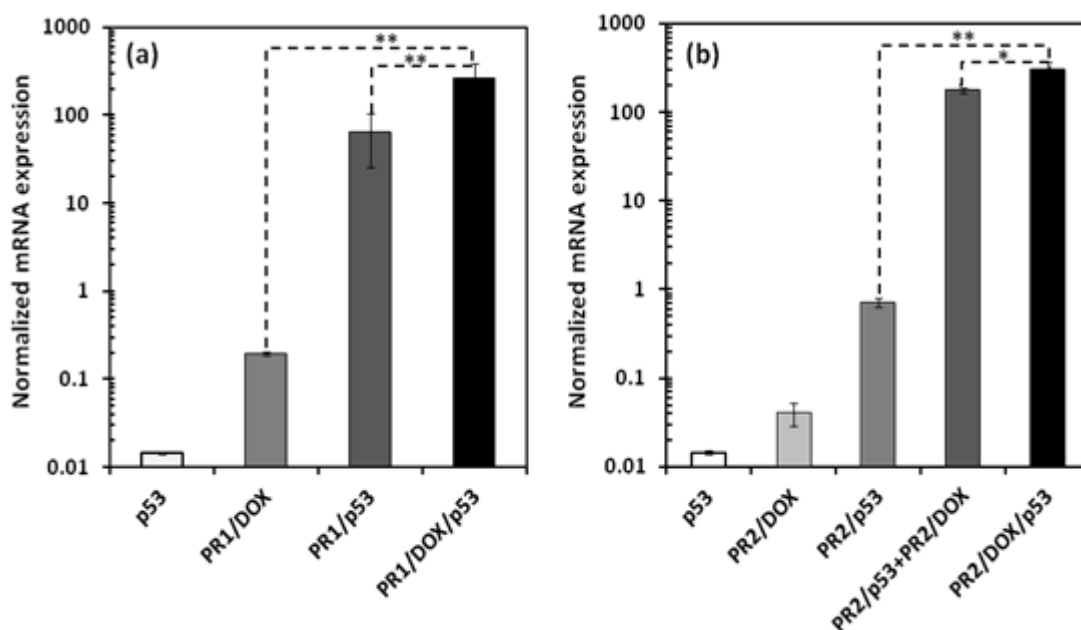**Fig. 7.9 RT-PCR detection of p53 mRNA expression levels in MB231 cells transfected with naked p53, PR/DOX, PR/p53, PR/DOX+PR/P53, and PR/DOX/p53 complexes at N/P of 10. (PR1 refers to PRCD12P123 and PR2 denotes PRCD12P177, **p<0.01, *p<0.05, n=3)**

The p53 gene is a tumor suppressor gene, which can inhibit cell proliferation and affect various cellular pathways, such as DNA repair, cell cycle regulation and apoptosis [38]. It is also the most frequently mutated gene occurring mutations in around half of all human tumors, such as breast, liver and ovarian tumors [39]. The mutant p53 gene cannot suppress tumor growth and also results in drug resistance. Therefore, the reintroduction of wild-type p53 is crucial in tumor inhibition by inducing apoptosis and G1-cell cycle arrest in various carcinoma cells [40]. In this chapter, based on the above transfection results mediated by pRL-CMV, we further evaluated the synergistic cancer therapeutic effects of drug/gene co-delivery using wild-type p53. Because the p53 protein has a shorter half-life, mRNA levels were used as an indicator of gene expression and detected by RT-PCR. Fig. 7.9 shows the mRNA expression levels of p53 in MB231 transfected with DOX loaded star polyrotaxanes: PR1/DOX/p53 (Fig. 7.9a) and PR2/DOX/p53 (Fig. 7.9b). Their expressions were compared with various control groups, such as naked p53 plasmid, PR/DOX without p53, PR/p53 without DOX and physical mixture of PR/DOX and PR/p53 (PR/p53+PR/DOX). As shown in Fig. 7.9, the p53 mRNA expressions of both DOX load polyrotaxanes (PR/DOX/p53) were significantly higher than the control groups, indicating their excellent transfection efficiency. Importantly, by comparing PR/p53 and PR/DOX/p53, it can be seen that the presence of DOX made the vectors much more effective in causing p53 upregulation. For example, in Fig. 7.9a, the PR1/DOX/p53 exhibited 4 times higher p53 transfection abilities than that without DOX (PR1/p53). The results suggested that the synergy between drug and gene therapeutics was supported by the increased p53 expression levels in the presence of DOX. Similar results were also found in other DOX based codelivery systems.[7, 19] The synergistic effect between p53 gene and DOX could be explained

by the mechanism of DOX antitumor activity. It was reported that p53 protein could be positively in response to some stress signals such as DNA damages caused by drugs, like DOX.[41, 42] Wang et al. further found that DOX induced apoptosis of tumor cells through the activation of p53-dependent apoptosis pathways.[43]

Additionally, physical mixture of gene and drug is another therapeutic system. In Fig. 7.9b, the p53 mRNA expression with PR2/p53+PR2/DOX was found higher than those of p53, PR2/p53 and PR2/DOX, but the levels are still 50% lower than that of PR2/DOX/p53. It is probably because that the codelivery system PR2/DOX/p53 can ensure both gene and drug to be delivered into the same cancer cells. However, the physical mixture may cause separated delivery pathways and result in incompletely or less effectively synergistic effects of drug and gene.[19] Therefore, it could be concluded that our design of star polyrotaxane nanoaggregates for co-delivery of DOX and gene into one system did present the gene expression enhancement and higher anti-tumor ability.

7.4 CONCLUSIONS

In this chapter, a novel gene/drug co-delivery system was successfully designed and synthesized based on star cationic polyrotaxane, which consists of controlled threaded α-CD, star PEG and low molecular weight PDMAEMA segments linked to the end of PEG arms with disulfide linkage. This unique polyrotaxane could easily self-assembled in water to form cationic nanostructures with PEG/PDMAEMA shell and CD core. After encapsulating DOX, the nano-sized particles showed high drug loading efficiency around 16%~70% and the loading ability increased with the increase of CD threaded numbers in the core. Intracellularly, the core-shell structures

were capable of faster internalization, higher intracellular uptake and higher anticancer efficacy as compared to free DOX, especially in low drug dose. It could be helpful to reduce cardiotoxicity, which is a serious drawback for DOX as anti-cancer therapy. In addition, owning to the cationic end group PDMAEMA, the polyrotaxanes were capable of condensing and delivering DNA with high efficiency. More importantly, the co-delivery of DOX and p53 using the cationic nanostructures achieved a synergistic effects in suppressing the proliferation of cancer cells, which is much more effective than the single delivery systems. Therefore, given to the above results, our multifunctional PR/DOX/DNA delivery system should be very promising in delivering anticancer drug and gene simultaneously for improved cancer therapy.

7.5 REFERENCES

1. Marchisone C, Pfeffer U, Del Grosso F, Noonan DM, Santi L, Albini A. Progress towards gene therapy for cancer. J Exp Clin Cancer Res 2000 Sep;19(3):261-270.

2. Kishida T, Asada H, Itokawa Y, Yasutomi K, Shin-Ya M, Gojo S, et al. Electrochemo-gene therapy of cancer: intratumoral delivery of interleukin-12 gene and bleomycin synergistically induced therapeutic immunity and suppressed subcutaneous and metastatic melanomas in mice. Mol Ther 2003 Nov;8(5):738-745.

3. Aszalos A, Ladanyi A, Bocsi J, Szende B. Induction of apoptosis in MDR1 expressing cells by daunorubicin with combinations of suboptimal concentrations of P-glycoprotein modulators. Cancer Lett 2001 Jun 26;167(2):157-162.

4. Kaneshiro TL, Lu ZR. Targeted intracellular codelivery of chemotherapeutics and nucleic acid with a well-defined dendrimer-based nanoglobular carrier. Biomaterials 2009 Oct;30(29):5660-5666.

5. Cheng H, Li YY, Zeng X, Sun YX, Zhang XZ, Zhuo RX. Protamine sulfate/poly(L-aspartic acid) polyionic complexes self-assembled via electrostatic attractions for combined delivery of drug and gene. Biomaterials 2009 Feb;30(6):1246-1253.

6. Wang Y, Gao SJ, Ye WH, Yoon HS, Yang YY. Co-delivery of drugs and DNA from cationic core-shell nanoparticles self-assembled from a biodegradable copolymer. Nature Materials 2006 Oct;5(10):791-796.

7. Wiradharma N, Tong YW, Yang YY. Self-assembled oligopeptide nanostructures for co-delivery of drug and gene with synergistic therapeutic effect. Biomaterials 2009 Jun;30(17):3100-3109.

8. Zhu C, Jung S, Luo S, Meng F, Zhu X, Park TG, et al. Co-delivery of siRNA and paclitaxel into cancer cells by biodegradable cationic micelles based on PDMAEMA-PCL-PDMAEMA triblock copolymers. Biomaterials 2010 Mar;31(8):2408-2416.

9. Xiao W, Chen X, Yang L, Mao Y, Wei Y, Chen L. Co-delivery of doxorubicin and plasmid by a novel FGFR-mediated cationic liposome. Int J Pharm 2010 Jun 30;393(1-2):119-126.

10. Liu F, Shollenberger LM, Huang L. Non-immunostimulatory nonviral vectors. FASEB J 2004 Nov;18(14):1779-1781.

11. Xu Z, Zhang Z, Chen Y, Chen L, Lin L, Li Y. The characteristics and performance of a multifunctional nanoassembly system for the co-delivery of docetaxel and iSur-pDNA in a mouse hepatocellular carcinoma model. Biomaterials 2010 Feb;31(5):916-922.

12. Hu QD, Fan H, Ping Y, Liang WQ, Tang GP, Li J. Cationic supramolecular nanoparticles for co-delivery of gene and anticancer drug. Chem Commun (Camb) 2011 May 21;47(19):5572-5574.

13. Wang Y, Ke CY, Beh CW, Liu SQ, Goh SH, Yang YY. The self-assembly of biodegradable cationic polymer micelles as vectors for gene transfection. Biomaterials 2007 Dec;28(35):5358-5368.

14. Wang Y, Wang LS, Goh SH, Yang YY. Synthesis and characterization of cationic micelles self-assembled from a biodegradable copolymer for gene delivery. Biomacromolecules 2007 Mar;8(3):1028-1037.

15. Akinc A, Anderson DG, Lynn DM, Langer R. Synthesis of poly(beta-amino ester)s optimized for highly effective gene delivery. Bioconjugate Chemistry 2003 Sep-Oct;14(5):979-988.

16. Adams ML, Lavasanifar A, Kwon GS. Amphiphilic block copolymers for drug delivery. Journal of Pharmaceutical Sciences 2003 Jul;92(7):1343-1355.

17. Brown MD, Schatzlein A, Brownlie A, Jack V, Wang W, Tetley L, et al. Preliminary characterization of novel amino acid based polymeric vesicles as gene and drug delivery agents. Bioconjugate Chemistry 2000 Nov-Dec;11(6):880-891.

18. Son YJ, Jang JS, Cho YW, Chung H, Park RW, Kwon IC, et al. Biodistribution and anti-tumor efficacy of doxorubicin loaded glycol-chitosan nanoaggregates by EPR effect. Journal of Controlled Release 2003 Aug;91(1-2):135-145.

19. Lu X, Wang QQ, Xu FJ, Tang GP, Yang WT. A cationic prodrug/therapeutic gene nanocomplex for the synergistic treatment of tumors. Biomaterials 2011 Jul;32(21):4849-4856.

20. Zhang XW, Zhu XQ, Ke FY, Ye L, Chen EQ, Zhang AY, et al. Preparation and self-assembly of amphiphilic triblock copolymers with polyrotaxane as a middle block and their application as carrier for the controlled release of Amphotericin B. Polymer 2009 Aug;50(18):4343-4351.

21. Loh XJ, Goh SH, Li J. New biodegradable thermogelling copolymers having very low gelation concentrations. Biomacromolecules 2007 Feb;8(2):585-593.

22. Yang XY, Chen LT, Huang B, Bai F, Yang XL. Synthesis of pH-sensitive hollow polymer microspheres and their application as drug carriers. Polymer 2009 Jul;50(15):3556-3563.

23. Ren LX, Ke FY, Chen YM, Liang DH, Huang J. Supramolecular ABA triblock copolymer with polyrotaxane as B block and its hierarchical self-assembly. Macromolecules 2008 Jul;41(14):5295-5300.

24. Liu J, Sondjaja HR, Tam KC. Alpha-cyclodextrin-induced self-assembly of a double-hydrophilic block copolymer in aqueous solution. Langmuir 2007 Apr 24;23(9):5106-5109.

25. Tong XM, Zhang XW, Ye L, Zhang AY, Feng ZG. Synthesis and characterization of block copolymers comprising a polyrotaxane middle block flanked by two brush-like PCL blocks. Soft Matter 2009;5(9):1848-1855.

26. Li J, Yang C, Li HZ, Wang X, Goh SH, Ding JL, et al. Cationic supramolecules composed of multiple oligoethylenimine-grafted beta-cyclodextrins threaded on a polymer chain for efficient gene delivery. Advanced Materials 2006 Nov;18(22):2969-+.

27. Yang C, Li J. Thermoresponsive Behavior of Cationic Polyrotaxane Composed of Multiple Pentaethylenehexamine-grafted alpha-Cyclodextrins Threaded on Poly(propylene oxide)-Poly(ethylene oxide)-Poly(propylene oxide) Triblock Copolymer. Journal of Physical Chemistry B 2009 Jan;113(3):682-690.

28. Bae SJ, Suh JM, Sohn YS, Bae YH, Kim SW, Jeong B. Thermogelling poly(caprolactone-b-ethylene glycol-b-caprolactone) aqueous solutions. Macromolecules 2005 Jun;38(12):5260-5265.

29. Hwang MJ, Suh JM, Bae YH, Kim SW, Jeong B. Caprolactonic poloxamer analog: PEG-PCL-PEG. Biomacromolecules 2005 Mar-Apr;6(2):885-890.

30. Lee ALZ, Wang Y, Cheng HY, Pervaiz S, Yang YY. The co-delivery of paclitaxel and Herceptin using cationic micellar nanoparticles. Biomaterials 2009 Feb;30(5):919-927.

31. Lin JP, Zhang SN, Chen T, Lin SL, Jin HT. Micelle formation and drug release behavior of polypeptide graft copolymer and its mixture with polypeptide block copolymer. International Journal of Pharmaceutics 2007 May;336(1):49-57.

32. Oh I, Lee K, Kwon HY, Lee YB, Shin SC, Cho CS, et al. Release of adriamycin from poly(gamma-benzyl-L-glutamate)/poly(ethylene oxide) nanoparticles. International Journal of Pharmaceutics 1999 Apr;181(1):107-115.

33. Chen YC, Liao LC, Lu PL, Lo CL, Tsai HC, Huang CY, et al. The accumulation of dual pH and temperature responsive micelles in tumors. Biomaterials 2012 Jun;33(18):4576-4588.

34. Li YL, Zhu L, Liu Z, Cheng R, Meng F, Cui JH, et al. Reversibly stabilized multifunctional dextran nanoparticles efficiently deliver doxorubicin into the nuclei of cancer cells. Angew Chem Int Ed Engl 2009;48(52):9914-9918.

35. Bae Y, Fukushima S, Harada A, Kataoka K. Design of environment-sensitive supramolecular assemblies for intracellular drug delivery: polymeric micelles that are responsive to intracellular pH change. Angew Chem Int Ed Engl 2003 Oct 6;42(38):4640-4643.

36. Sun HL, Guo BN, Li XQ, Cheng R, Meng FH, Liu HY, et al. Shell-Sheddable Micelles Based on Dextran-SS-Poly(epsilon-caprolactone) Diblock Copolymer for Efficient Intracellular Release of Doxorubicin. Biomacromolecules 2010;11(4):848-854.

37. Qiu LY, Bae YH. Self-assembled polyethylenimine-graft-poly(epsilon-caprolactone) micelles as potential dual carriers of genes and anticancer drugs. Biomaterials 2007 Oct;28(28):4132-4142.

38. Yoshida K, Miki Y. The cell death machinery governed by the p53 tumor suppressor in response to DNA damage. Cancer Sci 2010 Apr;101(4):831-835.

39. Hollstein M, Sidransky D, Vogelstein B, Harris CC. p53 mutations in human cancers. Science 1991 Jul 5;253(5015):49-53.

40. Shen Y, White E. p53-dependent apoptosis pathways. Adv Cancer Res 2001;82:55-84.

41. Fornari FA, Jr., Jarvis DW, Grant S, Orr MS, Randolph JK, White FK, et al. Growth arrest and non-apoptotic cell death associated with the suppression of c-myc expression in MCF-7 breast tumor cells following acute exposure to doxorubicin. Biochem Pharmacol 1996 Apr 12;51(7):931-940.

42. Fornari FA, Randolph JK, Yalowich JC, Ritke MK, Gewirtz DA. Interference by doxorubicin with DNA unwinding in MCF-7 breast tumor cells. Mol Pharmacol 1994 Apr;45(4):649-656.

43. Wang S, Konorev EA, Kotamraju S, Joseph J, Kalivendi S, Kalyanaraman B. Doxorubicin induces apoptosis in normal and tumor cells via distinctly different mechanisms. intermediacy of H(2)O(2)- and p53-dependent pathways. J Biol Chem 2004 Jun 11;279(24):25535-25543.

CHAPTER 8 CONCLUSIONS AND FUTURE RESEARCH

8.1 SUMMARY OF RESULTS AND CONCLUSION

This research studied the synthesis of novel core-shell nanostructures self-assembled from star polyrotaxane, based on star PEG, α-CD, triggered biodegradable linkage and cationic polymers (such as OEI or PDMAEMA), and investigated their applications to biomedical areas such as drug delivery and gene delivery.

Firstly, a series of novel star polyrotaxanes is successful synthesized by controlled threading of α-CD on star PEG, and blocking the end of the polymer with both enzymatic biodegradable linkage. The SPR could further self-assembled into nanostructures in water with polyrotaxane core and hydrophilic PEG shell. Their self-assembly behavior and enzymatic-triggered biodegradability was confirmed by CAC, TEM and particle size. The nano-sized particles provide high capacity for DOX loading with sustained *in vitro* release for more than 2 months. Furthermore, PR-phe/DOX exhibited a faster release, suggesting their stimuli-responsible properties, which would be benefic to the controlled drug delivery. Intracellularly, the PR/DOX was capable of fast cell internalization and cell uptake to yield significantly enhanced

drug efficacy as compared to free DOX. And the DOX-loaded polyrotaxane which present a hydrophilic coating would be great interest *in vivo* due to the long-circulating properties as compared to other structures.

In order to meet the conflicting requirements of an ideal drug delivery system, we further developed a reduction-sensitive biodegradable system for rapid intracellular drug release based on the similar polyrotaxane self-assembled nanostructures. Disulfide linkage was introduced to the end of star PEG, which was threaded with α-CD. Similarly, this unique polyrotaxane could self-assembled into nanostructures with PR core and PEG shell. The biodegradability of polyrotaxane with disulfide bond in response to DTT was confirmed by TEM and particle size. After encapsulating DOX, the nano-sized particles exhibited sustained and reduction-sensitive *in vitro* release profile within 30 days even in the presence of DTT. It is much longer than the *in vitro* release results reported by Sun and coworkers [1]**.** The unique property could be important for intravenous delivery in order to prolong the therapeutic effect and reduce cardiotoxicity, which is a serious drawback for DOX as an anti-cancer therapy. Furthermore, the core-shell nanostructures were capable of faster internalization, rapid intracellular uptake and higher anticancer efficacy as compared to reduction insensitive control and free DOX. Taken together, our SPR nanostructures boast many favorable properties as a drug carries, which include excellent biocompatibility and reduction-sensitive biodegradability, adequate drug loading capacity, sustained drug release, higher cell uptake and highly drug efficacy.

Besides drug delivery, this research also developed a series of disulfide-containing cationic polyrotaxanes as reduction-sensitive gene carriers and investigated their applications in gene delivery. Multiple OEI arms of different chain length were
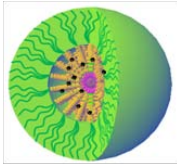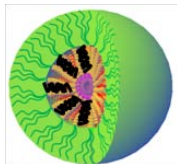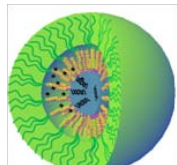
conjugated onto α-CD rings in the polyrotaxane, which is end blocked with disulfide linkage. The cationic polyrotaxane displayed degradability and DNA release capability in response to DTT. Importantly, due to the introduction of low MW OEI with α-CD and disulfide linkage into the polyrotaxane, significant lower *in vitro* cytotoxicity and higher gene transfection were achieved in contrast to reduction insensitive control and polyethylenimine (PEI) 25k. They showed excellent *in vitro* transfection efficiency which was comparable to or even higher than that of PEI 25k. Furthermore, the hindrance effect of PEG shell allows the system to be stable in salt and protein solution, and thus improve their serum stability. This research is helpful as it creates a new approach to design a reduction-sensitive delivery system by introducing disulfide linkage into polyrotaxane, which achieves rapid intracellular release, effective unpacking ability, low cytotoxicity, high transfection efficiency and high stability in biological fluids.

Cytotoxicity, lack of cell specificity and serum-induced aggregation are the major obstacles for pDMAEMA-based polyplexes in application in gene delivery [2]. Aiming to increase the serum stability and improve the transfection efficiency of PDMAEMA systems with optimal DNA release and decreasing cytotoxicity, a novel reduction-sensitive and shell detachable gene delivery system was successfully developed based on star polyrotaxanes, which consists of partially threaded α-cyclodextrin (α-CD), 8-arm PEG and low molecular weight PDMAEMA segments linked to the end of PEG arms with disulfide linkage. Their degradability and DNA release ability in response to DTT was confirmed. Remarkably, the biodegradable star polyrotaxane with disulfide linkage exhibited remarkable lower cytotoxicity and higher gene transfection efficiency in contrast to reduction insensitive control and PEI

25k with noticeably wider therapy window, which is highly desirable for *in vivo* gene therapy. More importantly, owning to the shell sheddable effect of hydrophilic PEG shell, the system could prevent aggregation in salt and protein solution.

Based on the similar structures with above star cationic polyrotaxanes, a novel gene/drug co-delivery system was further designed, which consists of controlled threaded α-CD, star PEG and low molecular weight PDMAEMA segments linked to the end of PEG arms with disulfide linkage. This unique polyrotaxane could easily self-assembled in water to form cationic nanostructures with PEG/PDMAEMA shell and CD core. After encapsulating DOX, the nano-sized particles showed high drug loading efficiency around 16%~70% and the loading ability increased with the increase of CD threaded numbers in the core. Intracellularly, the core-shell structures were capable of faster internalization, higher intracellular uptake and higher anticancer efficacy as compared to free DOX, especially in low drug dose. In addition, owning to the cationic end group PDMAEMA, the polyrotaxanes were capable of condensing and delivering DNA with high efficiency. More importantly, the co-delivery of DOX and p53 using the cationic nanostructures achieved a synergistic effects in suppressing the proliferation of cancer cells, which is much more effective than the single delivery systems. Therefore, given to the above results, our multifunctional PR/DOX/DNA delivery system should be very promising in delivering anticancer drug and gene simultaneously for improved cancer therapy.

Table 8.1 Comparison and summary of different polyrotaxanes

Systems	Similarity	Difference application	Difference characteristics
SPR/DOX	(1) SPR consist of 8 arm PEG and α-CD	Drug delivery	(1) High drug loading efficiency (2) Stability in biological fluids (3) Stimuli-responsive and sustained intracellular release (4) High cell uptake and drug efficacy
SPR-OEI/DNA	(2) Core-shell nanostructure with hydrophilic PEG shell (high stability in biological fluids)	Gene delivery	(1) Good DNA binding ability (2) Stability in biological fluids (3) Biodegradation and DNA intracellular release (4) Low cytotoxicity and enhanced transfection efficiency
SPR-PDMAEMA /DNA/DOX	(3) Reduction sensitive SS linkage (intracellular release)	Gene delivery /codelivery	(1) Combined advantages of core-shell structures as drug vectors and reductive SPR as gene vectors (2) Co-delivery system achieved a synergistic effects

The different versions of polymers were compared in Table 8.1. In short, the result of the present study exploited the applications of supramolecular self-assembled core-shell nanostructures based on star PEG and CDs to the field of drug delivery and gene therapy. This research is helpful in creating a new approach to design of reduction-sensitive delivery system by introducing disulfide linkage into polyrotaxane, which could achieve rapid intracellular release, low cytotoxicity, high transfection efficiency and effective unpacking ability.

8.2 POSSIBLE FUTURE RESEARCH

The work presented in this thesis opens new avenues for the development of core-shell nanostructures derived from star polyrotaxanes and it can be utilized for effective drug and gene delivery due to the "smart design" and flexibility of the

polyrotaxane. However, this study did not explore the application of the biodegradable nanostructures as drug and gene carriers through *in vivo* tests since the *in vivo* animal tests are very complicated and involve many biological issues. Further research is therefore needed to investigate their advantages as drug and gene carriers by using *in-vivo* animal tests, which can be better suited for observing the overall effects of a novel material on a living subject.

In addition, our unique core-shell nanostructures could also be applied in target drug/gene delivery. In the future, owning to the flexibility and easy modification of the supramolecular systems, the possible modifications, such as conjugating folic acid and peptide will be introduced to the CD rings in polyrotaxane to obtain targeting carriers. The proposed functional nanoparticels would show higher tumor uptake and concomitant enhanced tumor reduction. Furthermore, when folic acid is conjugated to the exterior of PEG shell, the nanostructures are targeted to cancer cells, and upon binding to the receptor, the particles will be endocytosed [3-5].

Another possible avenue of future work is drug/gene codelivery. We have reported a strategy of gene/drug codelivery by combing the advantages of core-shell systems as drug carriers and cationic bioreductive polyrotaxane systems as gene carrier. The strategy was developed in our shell detachable core-shell nanostructures self-assembled from star polyrotaxanes with PDMAEMA. DOX was encapsulated in this system and some preliminary results were obtained. In the future research, based on the similar principles of drug delivery with core-shell nanostructures, our cationic polyrotaxane nanoaggregates could be utilized in co-delivery of other anticancer drugs (e.g. PTX, DTX) and therapeutic genes (e.g. siRNA), which could enhance gene transfection and antitumor efficacy in both *in vitro* and *in vivo* studies [6-10].

8.3 REFERENCES

1. Sun H, Guo B, Cheng R, Meng F, Liu H, Zhong Z. Biodegradable micelles with sheddable poly(ethylene glycol) shells for triggered intracellular release of doxorubicin. Biomaterials 2009 Oct;30(31):6358-6366.
2. Grigsby CL, Leong KW. Balancing protection and release of DNA: tools to address a bottleneck of non-viral gene delivery. J R Soc Interface 2010 Feb 6;7 Suppl 1:S67-82.
3. Torchilin VP. Micellar nanocarriers: pharmaceutical perspectives. Pharm Res 2007 Jan;24(1):1-16.
4. Croy SR, Kwon GS. Polymeric micelles for drug delivery. Curr Pharm Des 2006;12(36):4669-4684.
5. Bae Y, Jang WD, Nishiyama N, Fukushima S, Kataoka K. Multifunctional polymeric micelles with folate-mediated cancer cell targeting and pH-triggered drug releasing properties for active intracellular drug delivery. Mol Biosyst 2005 Sep;1(3):242-250.
6. Wang Y, Gao SJ, Ye WH, Yoon HS, Yang YY. Co-delivery of drugs and DNA from cationic core-shell nanoparticles self-assembled from a biodegradable copolymer. Nature Materials 2006 Oct;5(10):791-796.
7. Wang Y, Wang LS, Goh SH, Yang YY. Synthesis and characterization of cationic micelles self-assembled from a biodegradable copolymer for gene delivery. Biomacromolecules 2007 Mar;8(3):1028-1037.
8. Wang Y, Ke CY, Beh CW, Liu SQ, Goh SH, Yang YY. The self-assembly of biodegradable cationic polymer micelles as vectors for gene transfection. Biomaterials 2007 Dec;28(35):5358-5368.
9. Wen J, Mao HQ, Li W, Lin KY, Leong KW. Biodegradable polyphosphoester micelles for gene delivery. J Pharm Sci 2004 Aug;93(8):2142-2157.
10. Zhu C, Jung S, Luo S, Meng F, Zhu X, Park TG, et al. Co-delivery of siRNA and paclitaxel into cancer cells by biodegradable cationic micelles based on PDMAEMA-PCL-PDMAEMA triblock copolymers. Biomaterials 2010 Mar;31(8):2408-2416.